TUNING THE PNA BACKBONE CONFORMATION: SYNTHESIS AND BIOPHYSICAL STUDIES OF DIALKYL SUBSTITUTED PEPTIDE NUCLEIC ACIDS

A Thesis Submitted to

Savitribai Phule Pune University for the degree of

Doctor of Philosophy

In

Chemistry

By

PRADNYA BOKIL-KULKARNI

Under guidance of

Prof. K. N. Ganesh

DIVISION OF ORGANIC CHEMISTRY

CSIR – NATIONAL CHEMICAL LABORATORY

PUNE-411008, INDIA

SEPTEMBER, 2015

राष्ट्रीय रासायनिक प्रयोगशाला

(वैज्ञानिक तथा औद्योगिक अनुसंधान परिषद्)

डॉ. होमी भाभा मार्ग पुणे – 411 008. भारत

NATIONAL CHEMICAL LABORATORY

(Council of Scientific & Industrial Research)

Dr. Homi Bhabha Road, Pune - 411 008. India.

NCL

CERTIFICATE

This is to certify that the work presented in the thesis entitled **"Tuning the PNA backbone conformation: Synthesis and Biophysical studies of Dialkyl substituted peptide nucleic acids"** submitted by Pradnya Bokil-Kulkarni, was carried out by the candidate at the National Chemical Laboratory, Pune, under my supervision. Such materials as obtained from other sources have been acknowledged in the thesis.

PROF. KRISHNA N. GANESH

(Research Supervisor)

Professor and Coordinator, Chemistry

Director, IISER Pune

J. C. Bose Fellow (DST)

Formerly at National Chemical Laboratory

PUNE-411008

INDIA   **SEPTEMBER 2015**

Communication Channels

☎
NCL Level DID : 2590
NCL Board No. : +91-20-25902000
EPABX : +91-20-25893300
          +91-20-25893400

FAX
Director's Office : +91-20-25893355
COA's Office : +91-20-25893619
COS&P's Office : +91-20-25893008

WEBSITE
www.ncl-india.org

CANDIDATE'S DECLARATION

I hereby declare that the thesis entitled "**Tuning the PNA backbone conformation: Synthesis and Biophysical studies of Dialkyl substituted peptide nucleic acids**" submitted for the award of degree of *Doctor of Philosophy* in Chemistry to the University of Pune has not been submitted by me to any other university or institution. This work was carried out by me at CSIR – National Chemical Laboratory, Pune, India. Such materials as obtained from other sources have been duly acknowledged in the thesis.

Pradnya Bokil-Kulkarni

CSIR – National Chemical Laboratory

Pune-411008   **September, 2015**

DEDICATED TO ALL MY FAMILY MEMBERS
& MY MENTOR PROF. K.N. GANESH....

Acknowledgements

Pursuing a Ph.D. project is a both painful and enjoyable experience. It's just like climbing a high peak, step by step, accompanied with bitterness, hardships, frustration, encouragement and trust and with so many people's kind help. Though it will not be enough to express my gratitude in words to all those people who helped me, I would still like to give my many, many thanks to all these people.

First of all, I'd like to express my special appreciation and thanks to my Research Supervisor Prof. K. N. Ganesh. His patience, flexibility, genuine caring and concern, and faith in me during the process enabled me to attend to life while also earning my Ph.D. He's been motivating, encouraging, and enlightening. He has never judged nor pushed when he knew I needed to juggle priorities. It's only because of his belief in me that I could re-initiate the Research work after a gap of 4 years and take it to completion. I've learned a lot from him, without his help I could not have finished this Ph.D successfully.

I'd like to give special thanks, beginning with Prof. D D Dhavale. His efforts made it possible for me to complete this degree.

Thirdly, I am very grateful to chairperson of my Research committee Dr. Vaijayanti A. Kumar. Her academic support and input and personal cheering are greatly appreciated.

I'd also like to thank all of my friends who supported me in writing, and incented me to strive towards my goal. I thank V. Madhuri and Gitali for their motivation. I thank Vrushali for all the help related to NCL formalities.

I also admire the full support and co-operation of my colleagues who have taught me many things. My special thanks to Vijay Kadam, Satish E and Madan Gopal for their co-operation and extending their help when needed.

I thank Dr. Chugh and Nitin for helping me out with NMR experiments at last moment. I thank Abhik for his help in biology experiments.

I thank Prabhakar, Shahaji, Manoj, Pramod, Dr. Dhrub, Nitin for their support and help, who made workplace fun, lively. I thank my seniors and colleagues from Lab 209 in NCL. I thank Raman, Umashankara, Sridhar, Ashwini, Mahesh, Manaswini, Roopa.

I'd also like to thank all my family members for motivating me to pursue this course and always being there for my support, appreciation, for giving me their unconditional love and pushing me hard to achieve my goal!

And Finally, I thank my Almighty, for letting me through all the difficulties. I have experienced your guidance day by day. You are the one who let me finish my degree. I will keep on trusting you for my future. Thank you.

Pradnya.

Table of Contents

Chapter 1: Introduction to Peptide Nucleic Acids

Chapter 2 - Design and synthesis of gem-dialkyl substituted PNA monomers and their oligomerization

Chapter 3 - Biophysical Studies of PNA Oligomers (UV-Tm and CD)

Abbreviations

A	Adenine
Abs.	Absolute
Ac$_2$O	Acetic anhydride
AcOH	Acetic acid (glacial)
ACN	Acetonitrile
aeg	Aminoethylglycine
aep	Aminoethylprolyl
ap	Antiparallel
APS	Ammonium persulphate
aq.	Aqueous
azb	Azidobutylene
azm	Azidomethylene
(Boc)$_2$O	Boc anhydride
BPB	Bromophenol blue
Bz	Benzoyl
C	Cytosine
Calcd	Calculated
Cbz	Benzyloxycarbonyl
CD	Circular Dichroism
CF/5(6)-CF	5(6)-Carboxyfluorescein
ch	Cyclohexyl
CHCA	α-cyano-4-hydroxycinnamic acid
cp	Cyclopentyl
CuAAC	Copper mediated azide-alkyne cycloaddition
DCC	Dicyclohexylcarbodiimide
DCM	Dichloromethane
DCU	Dicyclohexyl urea
DHB	2,5-dihydroxybenzoic acid
DIC	N,N'-diisopropylcarbodiimide
DIPEA/DIEA	N,N-Diisopropylethylamine
DMAP	N,N-Dimethyl-4-aminopyridine
DMEM	Dulbecco's Modified Eagle Medium
DMF	N,N-dimethylformamide
DMSO	N,N-Dimethyl sulfoxide
DNA	2'-deoxyribonucleic acid
ds	Double stranded
eam	Ethyleneamino
EBA	Ethylbromo acetate

EDTA	Ethylene diamine tetraacetic acid
Egd	Ethyleneguanidino
EMSA	Electrophoretic mobility shift assay
Et	Ethyl
EtBr	Ethidium Bromide
EtOAc	Ethyl acetate
FACS	Fluorescence Activated Cell Sorter
FBS	Fetal bovine serum
Fmoc	9-Fluorenylmethoxycarbonyl
g	gram
G	Guanine
gly	Glycine
h	Hours
his	Histidine
HBTU	2-(1H-Benzotriazole-1-yl)-1,1,3,3 tetramethyluronum-hexafluoro-phosphate
HIV	Human Immuno Difficiency Virus
HOBt	N-Hydroxybenzotriazole
HPLC	High Performance Liquid Chromatography
in situ	In the reaction mixture
in vivo	Within the living
IR	Infrared
KBrO$_3$	Potassium bromate
L-	Levo-
LC-MS	Liquid Chromatography-Mass Spectrometry
Lys	Lysine
MALDI-TOF	Matrix Assisted Laser Desorption Ionisation-Time of Flight
MBHA	4-Methyl benzhydryl amine
mg	milligram
MHz	Megahertz
min	minutes
Ni	Nickel
µL	Microliter
µM	Micromolar
mL	milliliter
mM	millimolar
mmol	millimoles
mp	melting point
MS	Mass spectrometry
MsCl	Mesyl Chloride

MW	Molecular weight
N	Normal
nm	Nanometer
NMR	Nuclear Magnetic Resonance
ODNs	Oligonucleotides
p	Parallel
PAGE	Polyacrylamide Gel Electrophoresis
PCR	Polymerase chain reaction
Pd	Palladium
PIDA	iodosobenzene diacetate (phenyliodonium diacetate)
ppm	Parts per million
PNA	Peptide Nucleic Acid
PS-oligo	Phosphorothioate-oligo
R	Rectus
R$_f$	Retention factor
RNA	Ribonucleic Acid
RP	Reverse Phase (-HPLC)
rt	Room temperature
RT	Retention time
S	Sinister
SAR	Structure Activity Relationship
SPPS	Solid Phase Peptide Synthesis
ss	Single strand/single stranded
T	Thymine
TEA/Et$_3$N	Triethylamine
TEMED	Tetramethylethylenediamine
TFA	Trifluoroacetic acid
TFMSA	Trifluoromethane sulfonic acid
THF	Tetrahydrofuran
TLC	Thin layer chromatography
T$_m$	Melting temperature
UV-Vis	Ultraviolet-Visible

Abstract of Thesis

The Thesis entitled **"Tuning the PNA Backbone Conformation: Synthesis and Biophysical Studies of Dialkyl Substituted Peptide Nucleic Acids"** is comprised of studies towards the design, synthesis, biophysical and biological evaluation of modified peptide nucleic acids (PNA) analogs. The modifications consist of incorporation of gem dialkyl group in the PNA backbone. The PNA oligomers obtained by solid phase peptide synthesis were investigated for their binding to target DNA/RNA by various biophysical techniques. The work also describes the self-assembling ability of modified PNAs and cell permeation properties of synthesized PNA oligomers.

The thesis is presented as 4 chapters:

Chapter 1:   Introduction to Peptide Nucleic Acids

Chapter 2:   Design and synthesis of *gem*-dialkyl substituted PNA monomers and their oligomerization.

Chapter 3:   Biophysical Studies of PNA Oligomers (UV-Tm and CD)

Chapter 4:   Self-assembly and Cell uptake studies of PNA analogues.

Chapter 1: Introduction to peptide nucleic acids

This chapter gives an overview on the background literature for undertaking the research work emphasizing recent advancements in the field of peptide nucleic acids and their applications.

Oligonucleotides (ONs) capable of sequence specific recognition of nucleic acids (DNA / RNA) are becoming more important for research, diagnosis and therapy. This is vital to make antisense or antigene based inhibition as practical approach to therapeutics. Sequence specific binding of oligodeoxynucleotides (ODNs) to single stranded RNA or duplex DNA through triple helix formation provides a way to modulate gene expression. The specific inhibition is based on the Watson-Crick base pairing between heterocyclic bases of the antisense ONs and the target nucleic acids. In order to meet all the requirements of a successful medicinal agent, it is necessary for natural ONs to be chemically modified in a suitable manner. The chemical modifications of ONs have resulted in the synthesis and analysis of a large variety of oligonucleotide derivatives

with modification of the phosphate, the ribose or the nucleobase. This chapter presents a survey of the literature relevant to the area of nucleic acid therapeutics.

Peptide Nucleic Acids (PNA) (Figure **1**), first introduced by Nielsen *et al*, have emerged as novel development in the field of oligonucleotide analogs. A brief introduction to the word PNA is presented in this chapter followed by discussion on the recent trends in this area of research.
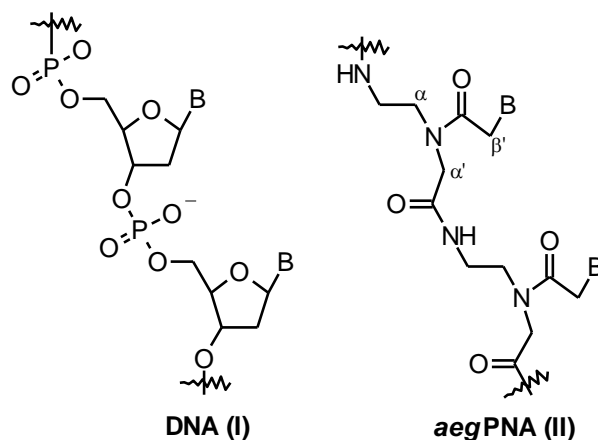

DNA (I)   *aeg* PNA (II)

Figure 1: Structures of DNA and *aeg*-PNA

The replacement of sugar-phosphate backbone of DNAby *N*-2-aminoethyl-glycyl backbone carrying nucleobases through methyl-carbonyl linker leads to PNA. The charge-neutral and achiral peptide nucleic acids were originally designed as oligonucleotide analogs that could be used for sequence-specific targeting of double-stranded DNA. PNAs bind with higher affinity to complementary DNA/RNA than their natural counterparts obeying Watson-Crick base pairing rule. PNAs and their analogs are resistant to hydrolytic enzymes like proteases and nucleases. Due to these exceptional properties PNAs have major applications as a tool in molecular biology, as lead compounds for the development of gene targeted drugs via antigene/antisense technology, for diagnostics and biosensors. Peptide nucleic acids suffer from few drawbacks like poor water solubility, lack of efficient cell permeability and ambiguity in binding (parallel v/s antiparallel) orientation. These limitations are being systematically addressed by various rationally designed PNA analogs that have improved PNA properties to different extents. The effect of the different structural modifications on

biophysical and biochemical properties of PNA is overviewed to draw directions for the present work, aiming towards exploring new pathways of PNA-design and applications.

Chapter 2: Design and synthesis of *gem*-dialkyl substituted PNA monomers and their oligomerization

The α-amino isobutyric acid, α, α-disubstituted glycine is a naturally occurring amino acid. The α-amino isobutyric acid (Aib) residues in peptides are known to stabilize helix structures. The stereochemical consequences of introducing Aib into peptide chains limits the range of accessible conformations; nucleates helical structures and facilitates crystallization presumably by restricting conformational flexibility in solution. Also α, α-dialkylated amino acids possess significant steric bulk which makes their incorporation into peptides is difficult. Peptides containing these hindered residues are of significant biological importance. Hence the objective was to incorporate *gem*-dimethyl groups into aminoethylglycyl- and aminopropylglycyl- PNA backbone as conformational constrain elements.

Through the incorporation of gem dialkyl group, the conformational constraint is conferred on the classical PNA backbone to influence the orientation of binding, strike a balance between entropy and enthalpy and more importantly to introduce discrimination in binding to RNA and DNA. These properties will influence the overall physicochemical and biological properties of the so derived PNAs.Recently it is reported from our laboratory that the incorporation of gem-dimethyl substituent at α carbon of aeg-PNA backbone preferentially increased the T_m of the derived complexes with DNA as compared with RNA.[1]

This is interesting since the earlier study from our group has shown that the cyclic cyclohexanyl PNA show strong preference for RNA binding.[2] In view of this, the present work demonstrates the incorporation of gem dialkyl functionality at γ and β position of aminoethylglycyl and aminoprolylglycyl PNA in order to investigate its hybridization properties.
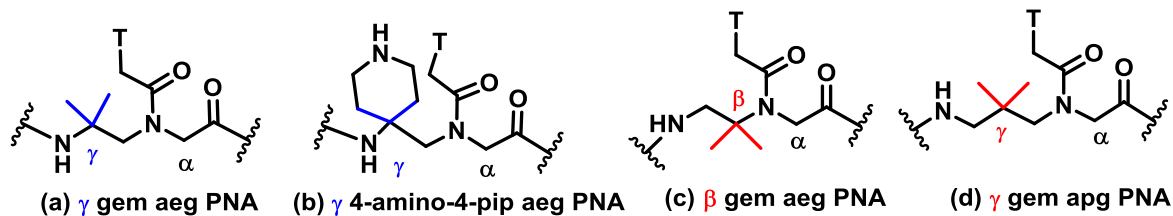
Figure 2: Target Molecules

(a) γ gem aeg PNA   (b) γ 4-amino-4-pip aeg PNA   (c) β gem aeg PNA   (d) γ gem apg PNA

Section (1): Synthesis and characterisation of *gem*-dialkyl substituted PNA monomers

SCHEME 1: Schematic representation of synthesis of β gem aeg PNA monomer
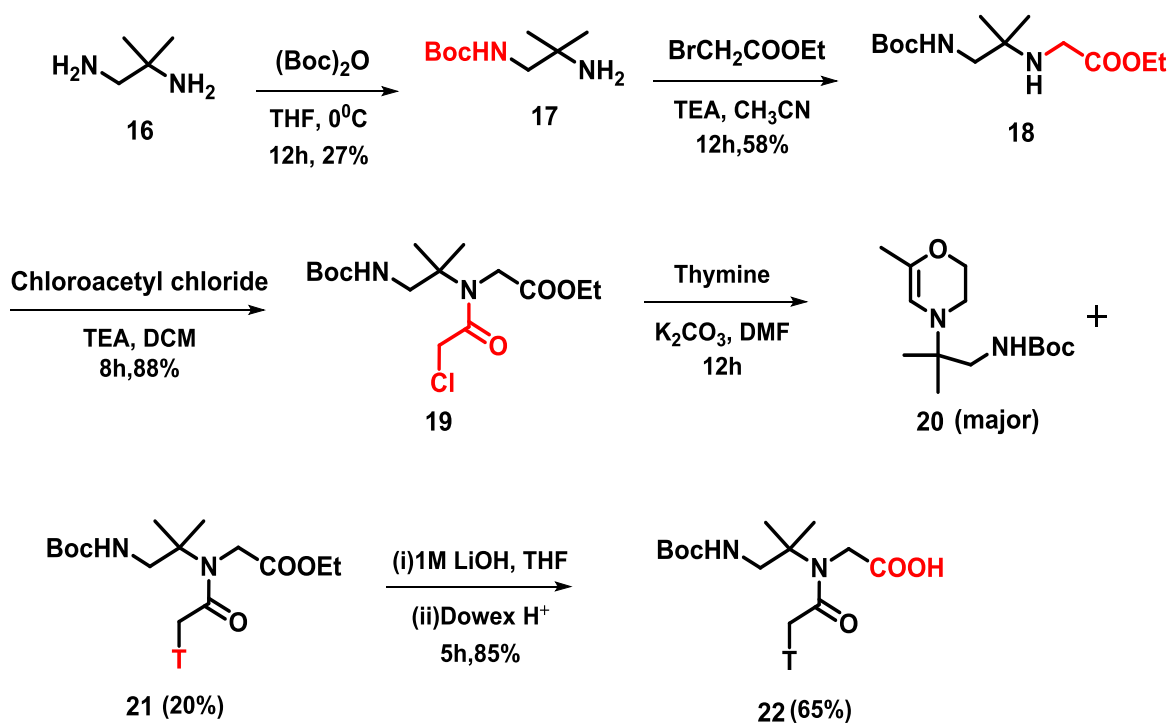
In an attempt towards the synthesis of target β gem aeg PNA monomer, the commercially available 1,2-Diamino-2-methylpropane **1** was treated with di-tert-butyl dicarbonate (Boc)$_2$O to obtain Boc-protected amine 2 which on alkyalation with ethyl bromo acetate to give **3.** Acylation of **3** with chloroacetyl chloride gave product 4. Chloro-derivative **4**

was then converted to its thymine derivative **5** (15%). The chloro-derivative in presence of K_2CO_3 gets cyclized to give cyclised compound **6**.

The thymine derivative **5** was hydrolysed using lithium hydroxide inTHF to give final acid monomer **7** which is used for solid phase peptide synthesis.

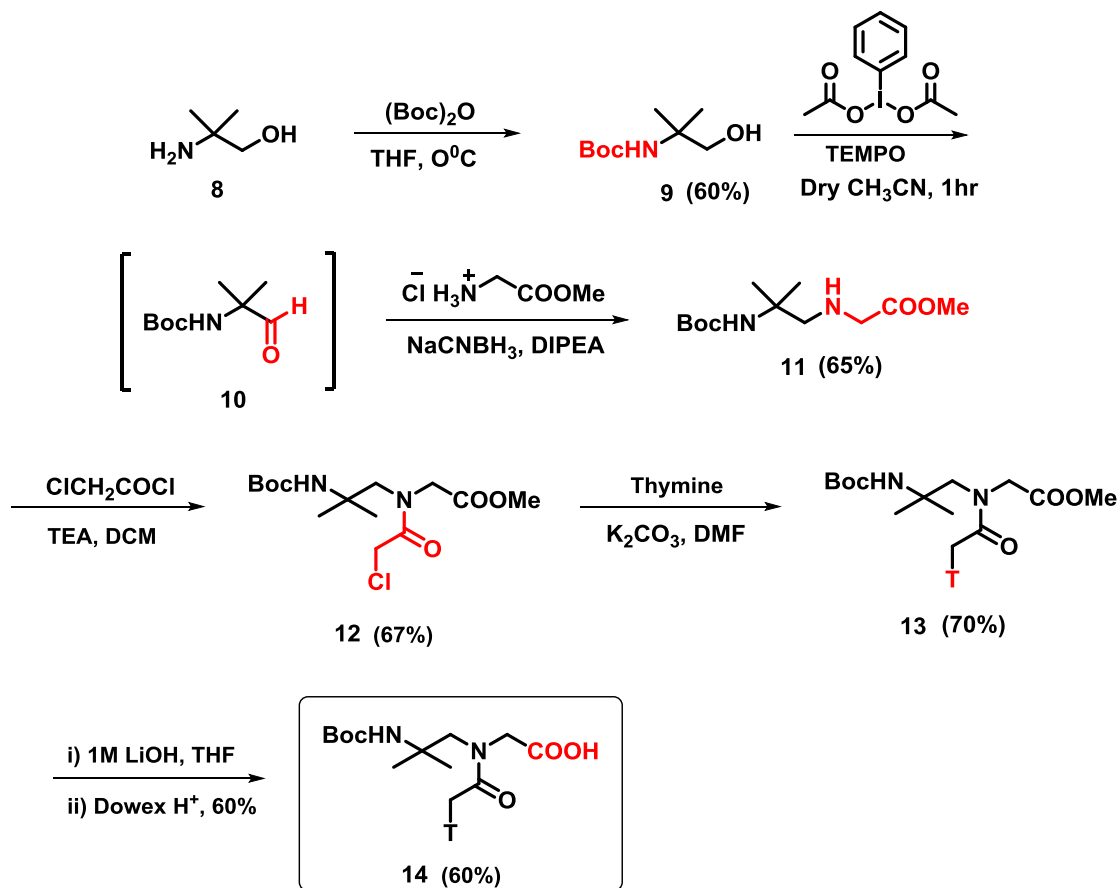**SCHEME 2: Schematic representation of synthesis of γ gem aeg PNA monomer**

To synthesise γ gem aeg PNA monomer, amine group of commercially available 2-amino-2-methylpropan-1-ol **8** was protected with di-tert-butyl dicarbonate (Boc)$_2$O to obtain Boc-protected amine **9**. The protected amino alcohol was then subjected to oxidation with (Diacetoxyiodo)benzene in presence of catalytic amount of TEMPO in dry CH$_3$CN. The aldehyde **10** insitu reacted with Glycine ester to give **11.** Acylation with chloroacetyl chloride gave product **12** which on alkylation with Thymine gave ester

monomer **13**. Thymine ester 13 on hydrolysis with lithium hydroxide in THF gave final acid monomer **14** for solid phase peptide synthesis.

SCHEME 3: Schematic representation of synthesis of Synthesis of *γ 4-amino-4-pip aeg* PNA monomer
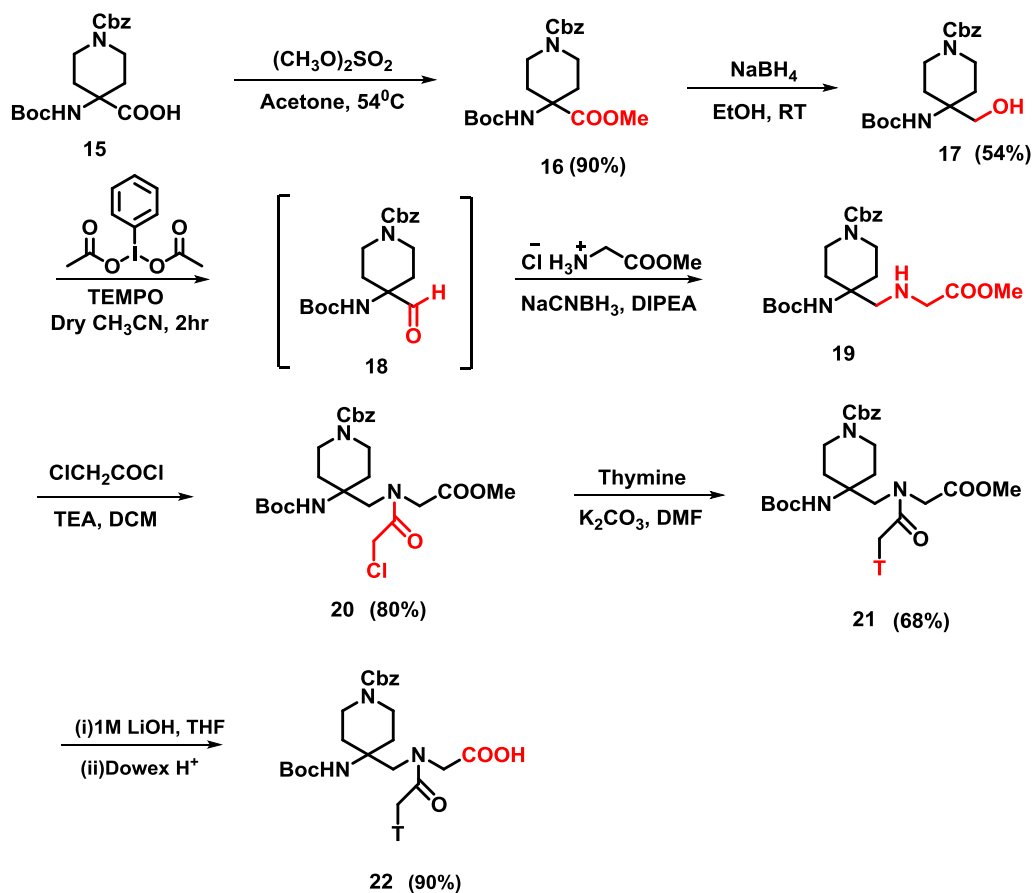
Synthesis of *γ 4-amino-4-pip* aeg PNA Monomer started with commercially available 4-(Boc-amino)-1-Cbz-piperidine-4-carboxylic Acid **15.** Amino acid **15** was converted to methyl ester **16** using dimethyl sulfate and activated K_2CO_3. The methyl ester was reduced to give alcohol **17** using sodium borohydride in absolute ethanol. The alcohol **17** was then oxidized to aldehyde **18** which in situ reacts with glycine ester to give alkylated product **19**. This was then acylated with chloroacetyl chloride to yield chloro compound **20**. The condensation of **20** with nucleobase thymine afforded the γ 4-amino-4-pip aeg

ester. The ester **20** was hydrolysed with aq.LiOH to get γ 4-amino-4-pip aeg acid which was then used for incorporation in desired PNA sequences.

SCHEME 4: Synthesis of γ *gemdimethyl apg* PNA Monomer
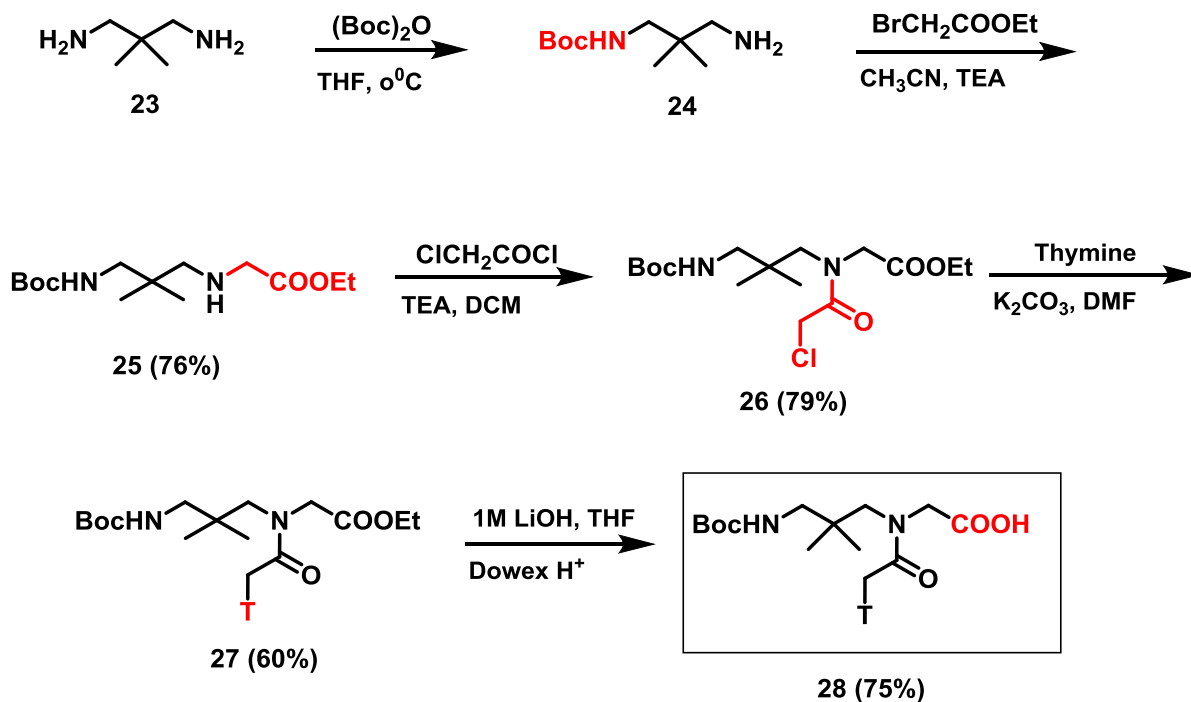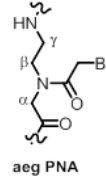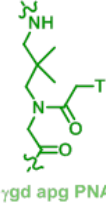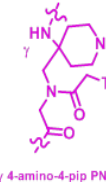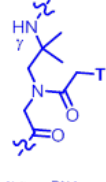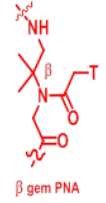
Synthesis of γ *gemdimethyl apg* PNA Monomer started with Monoboc protection of commercially available 2,2-Dimethyl-1,3-propanediamine **23** with di-tert-butyl dicarbonate, (Boc)$_2$O.

Monoboc protected amine **23** was treated with ethyl bromoacetate to give alkylated product **25.** Product 25 was the acylated with chloro acetyl chloride to give chloro compound **26.** Thymine N-alkylation with **26** gave Thymine ester **27.** Thymine ester **27** was then hydrolysed with aq.LiOH to give γ *gemdimethyl apg* PNA acid monomer for PNA oligomer synthesis.

Section (2): Solid phase synthesis, purification and characterisation of PNA oligomers

The PNA oligomers were synthesised by solid phase peptide synthesis protocol using Boc strategy. The modified PNA monomers **7, 14, 22, 28** were incorporated at desired positions in the unmodified aeg PNA sequence using MBHA (4-methyl-Benzhydryl amine) resin as solid support (Table **1**).

Table 1: PNA Oligomers with modified / unmodified monomers at various positions

No	Sequences	Monomer	HPLC (rt)(min)	Mole. formula	Calc. Mass	Obs. Mass
1	H G T A G A T C A C T Lys	aeg PNA	16.0	$C_{114}H_{149}N_{60}O_{31}$	2854.1927	2854.6863
2	H G T A G A t C A C T Lys		17.2	$C_{117}H_{155}N_{60}O_{31}$	2896.2397	2896.4778
3	H G t A G A T C A C T Lys		17.6	$C_{117}H_{155}N_{60}O_{31}$	2896.2397	2896.5830
4	H G t A G A t C A C T Lys		18.8	$C_{120}H_{161}N_{60}O_{31}$	2938.2866	2938.7803
5	H G t A G A t C A C t Lys	γgd apg PNA	19.5	$C_{123}H_{167}N_{60}O_{31}$	2980.3336	2980.5967
6	H G T A G A t C A C T Lys		15.2	$C_{118}H_{156}N_{61}O_{31}$	2923.2506	2923.6196
7	H G t A G A T C A C T Lys	γ 4-amino-4-pip PNA	15.7	$C_{118}H_{156}N_{61}O_{31}$	2923.2506	2923.2092 (2614.1152)
8	H G T A G A t C A C T Lys		17.3	$C_{116}H_{153}N_{60}O_{31}$	2882.2240	2882.2756
9	H G t A G A T C A C T Lys		17.6	$C_{116}H_{153}N_{60}O_{31}$	2882.2240	2882.4302
10	H G t A G A t C A C T Lys		18	$C_{118}H_{157}N_{60}O_{31}$	2910.2553	2910.64
11	H G t A G A t C A C t Lys	γ gem PNA	19.2	$C_{120}H_{161}N_{60}O_{31}$	2938.2866	2938.4849
12	H G T A G A t C A C T Lys		16.8	$C_{116}H_{153}N_{60}O_{31}$	2882.2240	2882.0698
13	H G t A G A T C A C T Lys		17.3	$C_{116}H_{153}N_{60}O_{31}$	2882.2240	2882.1616
14	H G t A G A t C A C T Lys		18.4	$C_{118}H_{157}N_{60}O_{31}$	2910.2553	2910.8999
15	H G T A G A t C A C t Lys	β gem PNA	18.2	$C_{118}H_{157}N_{60}O_{31}$	2910.2553	2910.1594

To investigate the binding selectivity, specificity and discrimination of gem dialkyl substituted PNAs towards complementary DNA and RNA the mixed purine pyrimidine sequences were synthesised.
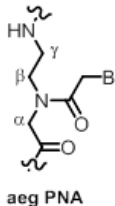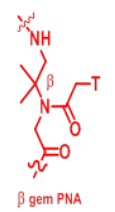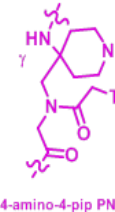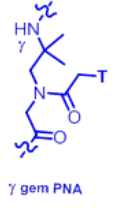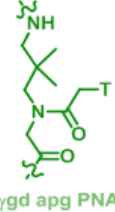
All the modified PNA oligomers were purified by RP-HPLC and characterized by MALDI-TOF mass spectroscopy. These purified PNA oligomers were used for biophysical studies discussed in the next chapter.

Chapter 3: Biophysical Studies of PNA Oligomers (UV-Tm and CD)

This chapter deals with the temperature dependent UV-spectroscopic studies to determine the thermal stability of all modified PNA oligomers with complementary antiparallel **DNA1** and parallel **DNA2**. The results of thermal stabilities for all PNA oligomers are tabulated in Table **2**. The specificity of these PNA oligomers was also investigated by challenging them to bind to complementary antiparallel and parallel **RNA1** and **RNA2** respectively.

All the modified PNAs preferably show specificity for complementary DNA as compared to RNA.

Table 2: UV-T_m and ΔTm(°C) values of duplexes of modified PNA oligomers with complimentary DNA1 and DNA2

Entry	Sequences	Monomer	DNA1 3'CATCTAGTGA5'	DNA2 5'CATCTAGTG3'
			UV-T_m(ΔTm)	
aeg PNA **1**	H G T AG A T CAC T Lys	aeg PNA	49.1	41.1
γgem PNA **2**	H G t AG A T CAC T Lys		41.8(-7.3)	43(+1.9)
γgem PNA **3**	H G T AG A t CAC T Lys		47.3(-1.8)	45.3(+4.2)
γgem PNA **4**	H G T AG A t CAC t Lys		40.4(-8.7)	46.1(+5.0)
γgem PNA **5**	H G t AG A t CAC t Lys	β gem PNA	38.2(-10.9)	48.3(+7.2)
γ pip PNA **6**	H G T AG A t CAC T Lys		48.6(-0.5)	43.3(+2.2)
γ pip PNA **7**	H G t AG A T CAC T Lys	γ 4-amino-4-pip PNA	39.8(-9.3)	42.6(+1.5)
βgem PNA **8**	H G t AG A T CAC T Lys		47.6(-1.5)	46.2(+5.1)
βgem PNA **9**	H G T AG A t CAC T Lys		36.6(-12.5)	52.8(+11.7)
βgem PNA **10**	H G t AG A t CAC T Lys		45.5(-3.6)	51.9(+10.8)
βgem PNA **11**	H G T AG A t CAC t Lys	γ gem PNA	38.6(-10.5)	43.9(+2.8)
γgem apg PNA **12**	H G t AG A T CAC T Lys		47.8(-1.3)	52.4(+11.3)
γgem gem PNA **13**	H G T AG A t CAC T Lys		35.9(-13.2)	45.8(+4.7)
γgem gem PNA **14**	H G t AG A t CAC T Lys		29.4(-19.7)	38.8(-2.3)
γgem gem PNA **15**	H G t AG A t CAC t Lys	γgd apg PNA	27.4(-21.7)	30.5(-10.6)

ΔTm = indicates the difference in Tm with control *aeg* PNA, nb = not binding, Δ Tm values are accurate to ±0.5 °C

Chapter 4, Section A: Self-assembly of PNA analogues:

Molecular self-assembly is the spontaneous organisation of molecules under thermodynamically favoured conditions into structurally well-defined and stable arrangements through non-covalent interactions i.e. hydrogen bonding, electrostatic attraction, hydrophobic force and van der Waals interactions. Among the many self-assembly systems (DNA, protein/peptide, lipid and surfactant), peptides have drawn much attention in nanoscience and nanotechnology due to their desirable chemical/physical properties and biological functionalities. The morphology of self assembled peptide nanostructures depends on various factors like pH, temperature, solvent etc. PNAs comprising the peptide backbone and nucleobases of oligonucleotides, may exhibit different nanostructures. With this idea we thought of studying the ability of dialkyl substituted PNA's to form nanostructures in single strand and duplex form with complementary DNA using FESEM.

Figure 3: Self-assembled nanostructures of PNA7:DNA duplex

Self-assembling properties for single stranded PNAs and in duplex form with complementary DNA were investigated.

Chapter 4, Section B: Cell uptake studies of PNA analogues

In order to gain insight on cellular uptake properties, PNA oligomers were tagged with 5(6)-carboxyfluorescein at the N-terminus for visualization in the cells. (Figure **4**, Table **3**).
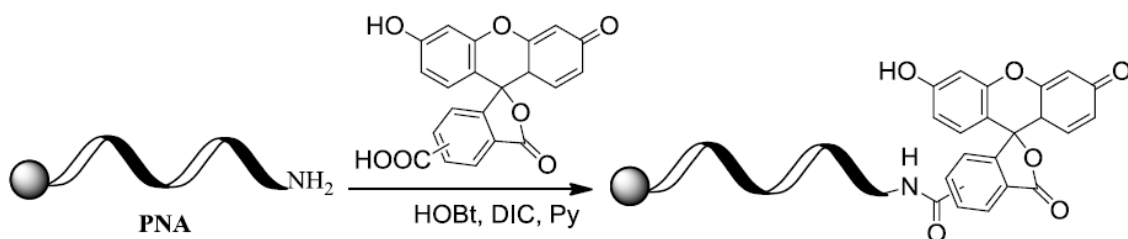
Figure 4: Synthesis of 5(6)-carboxyfluorescein fluorescein tagged PNA oligomers

Table 3: 5(6)-carboxyfluorescein fluorescein tagged PNA oligomers

Entry	Sequences												Monomer	Exp mass	Obs mass
1	Cf	G	T	A	G	A	T	C	A	C	T	Lys	aegPNA	2854.78	2854.68
2	Cf	G	*t*	A	G	A	*t*	C	A	C	*t*	Lys	γ – genapg	2882.78	2882.06
3	Cf	G	*t*	A	G	A	*t*	C	A	C	*t*	Lys	γ – genaeg	2882.78	2882.16
4	Cf	G	T	A	G	A	*t*	C	A	C	T	Lys	*γ 4-amino-4-pip* PNA	2910.78	2910.89

The cell permeation ability of these PNA oligomers was studied by live cell imaging in MCF-7cell line using confocal microscopy.
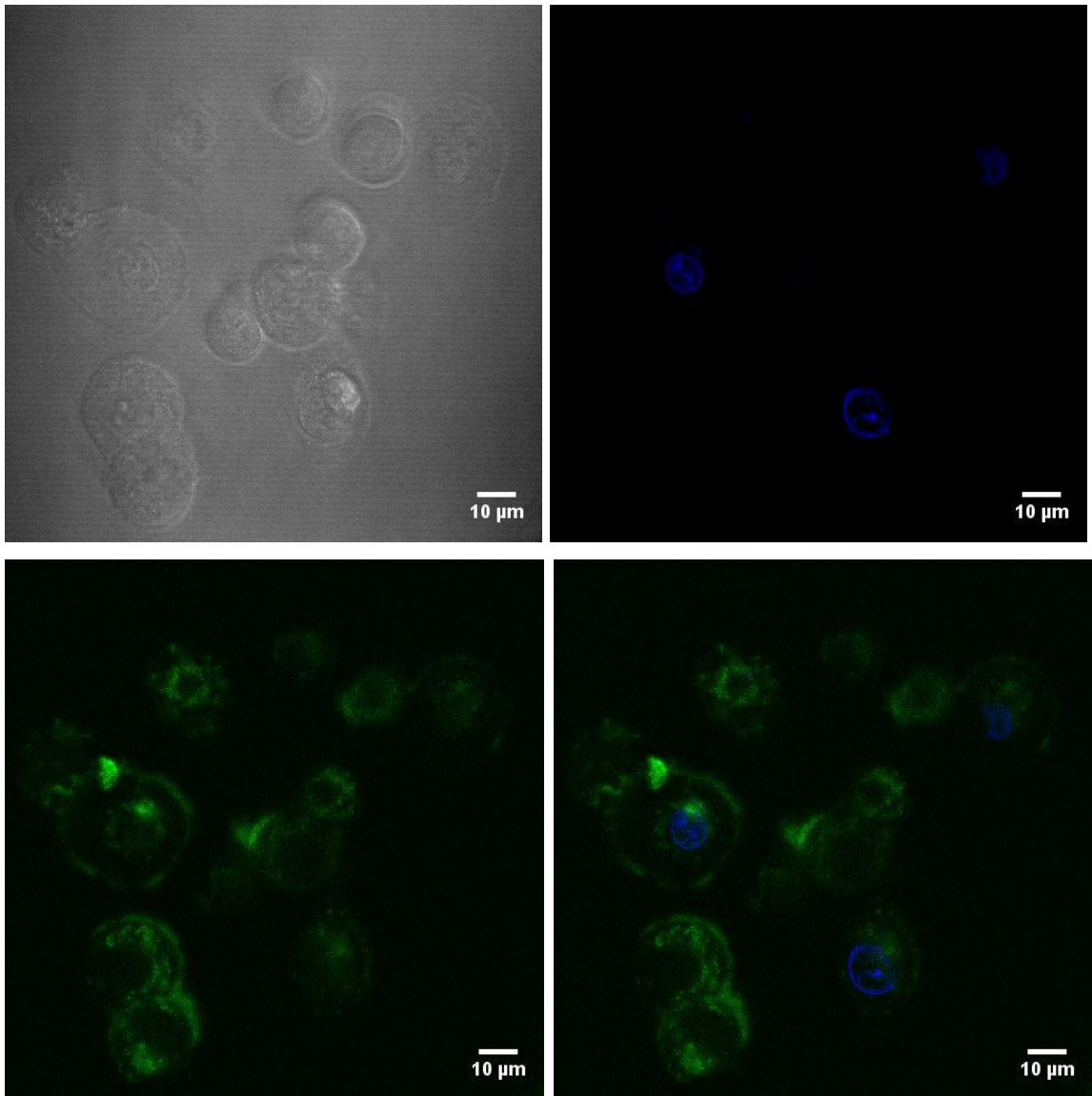
Figure 5: Confocal microscopy images for γ pip PNA7CF (a) Bright field image of MCF-7 cells (b) DAPI stained image (c) Green fluorescent image and (d) Superimposed image of images (a), (b) and (c)

The images showed that PNAs were able to enter the cells and got localized near the nuclear membrane of the cell.

Summary of Thesis

Rationally designed γ and β gem dialkyl substituted control PNA monomers have been synthesized.

The modified PNA monomers were incorporated into aeg PNA sequence at desired positions by solid phase peptide synthesis using Boc strategy.The synthesized PNA oligomers were purified by RP-HPLC and characterized by MALDITOFspectrometry.

- The thermal stability of γ and β dialkyl substituted PNA oligomers with complementary DNA and RNA was investigated by temperature dependent UV-visible spectroscopy. The specificity of these PNA oligomers was also investigated by challenging them to mismatch DNA and RNA carrying a single base mismatch in the middle of the sequence.

- The effect of γ and β dialkyl substituents in the PNA on the conformation of PNA:DNA/RNA duplexes was studied by CD spectroscopy.

- The self-assembling properties of the PNA:DNA duplexes were studied using FESEM .

- The cell permeation ability of 5(6)-carboxyfluorescein labelled PNA oligomers was investigated by live cell imaging using confocal microscopy.

- The quantification of cell penetration of modified PNA oligomers by fluorescence activated cell sorter (FACS) analysis is in progress.

References:

1. Ganesh *et al*, *Art DNA:PNA&XNA*, **2012**, *3*, 5-13
2. Govindaraju, T.; Madhuri, V.; Kumar, V.A.; Ganesh, K.N. *J. Org. Chem.,* **2006**, *71*, 14-21.

CHAPTER 1

Introduction to

Peptide Nucleic acids

A brief introduction to nucleic acids especially peptide nucleic acids followed by the recent literature trends are presented in this chapter. Important PNA properties and its structural features are discussed to understand the various functions of PNA. The different structural modifications to overcome the drawbacks of PNA has been overviewed to draw directions for the present work, targeted towards exploring new pathways of PNA design and applications.

1.1   Introduction to Nucleic Acids

The nucleic acids are the building blocks of living organisms. These biopolymers and proteins together ultimately govern the metabolic activities of the cell and in turn control the fate of organism. These macromolecules 2'-deoxyribonucleic acids (DNA) and ribonucleic acids (RNA) are made up of repeating units called nucleotides. The three components – a nitrogenous heterocyclic base (nucleobase), which is either a purine or pyrimidine, a pentose sugar and a phosphate group together make a nucleotide. Nucleobases are connected to the pentose sugar via a β-glycosidic linkage to give rise to nucleoside,[1] that upon phosphorylation becomes a nucleotide. RNA is made up of ribonucleotides whereas 2'-deoxyribonucleotides are the monomers of DNA (Figure **1.1**).
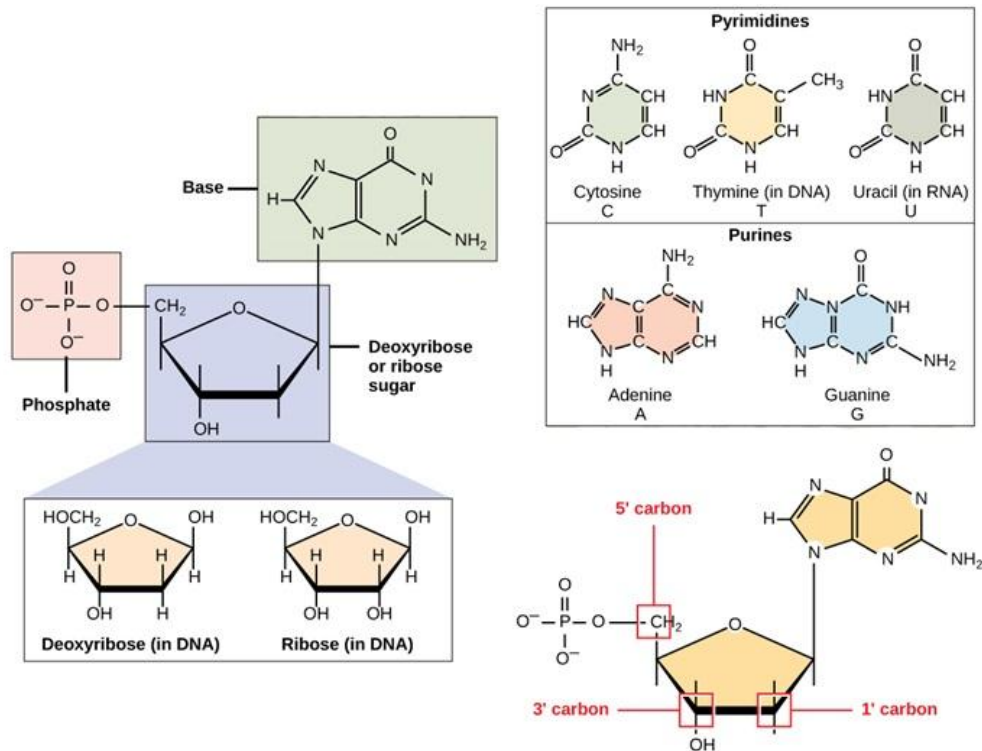

Figure 1.1: Chemical constituents of DNA and RNA

In 1953, Watson and Crick proposed that DNA exists as a double helix, in what two helical chains are coiled round the same axis with a right handed twist.[2] The phosphodiester group connect two β-D-deoxyribofuranose residues through 3'-5'

linkages forming helical chain where-in they are pointed outside the helix. The other main constituents of DNA are nucleobases adenine (A), thymine (T), guanine (G) and cytosine (C) pointing towards centre of helix. The backbone is highly negatively charged as a result of the phosphate groups. Two antiparallel strands of double helical DNA are held together by hydrogen bonds (Watson-Crick base pair[2]) between complementary base pairs (A:T, G:C). In RNA 2'-deoxyribose sugar is replaced by ribose sugar and the nucleobase composition remaining the same except thymine which is replaced by uracil.

1.2   Hydrogen bonding in DNA

The N-H groups of the bases are potent hydrogen bond donors, while the sp^2-hybridised electron pairs on the oxygen of the C=O groups and on the ring nitrogens are hydrogen bond acceptors, better than the oxygens of either the phosphate or the pentose sugar. In **Watson-Crick pairing** there are two hydrogen bonds in A:T base pair and three hydrogen bonds in a G:C base pair (Figure **1.2**).

A·T base pair   G·C base pair
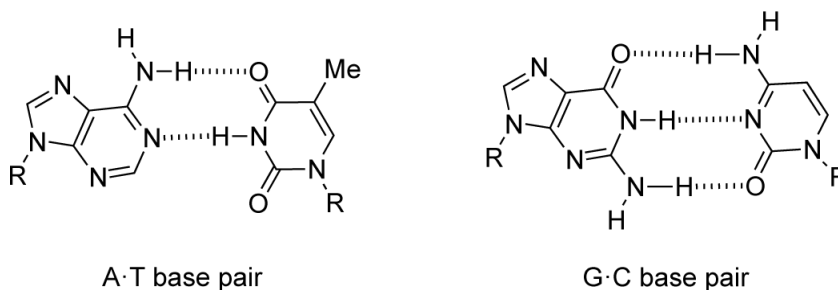
Figure 1.2: Watson-Crick hydrogen bonding for A: T and G: C base pair

Other significant hydrogen bonds present in nucleotides are **Hoogsteen**[3] (HG) and **Wobble base pairs**[4] (Figure **1.3**). Hoogsteen base pairing is not isomorphous with Watson-Crick base pairing and is important in triple helix formation. In Wobble base pairing, a single purine base is able to recognize a non-complementary pyrimidine (e.g. G:U) through wobble base pairing which has importance in the interaction of messenger RNA (m-RNA) with transfer RNA (t-RNA) on the ribosome for codon-anticodon interactions during protein synthesis. Several anomalous hydrogen bonding patterns have been seen in X-ray studies of synthetic oligodeoxynucleotides.[5]

Figure 1.3: Hoogsteen base pairing (**a** & **b**), Wobble base pairing (**c** & **d**)

1.3   Secondary Structures of Nucleic acids

(i)   Secondary structure of DNA

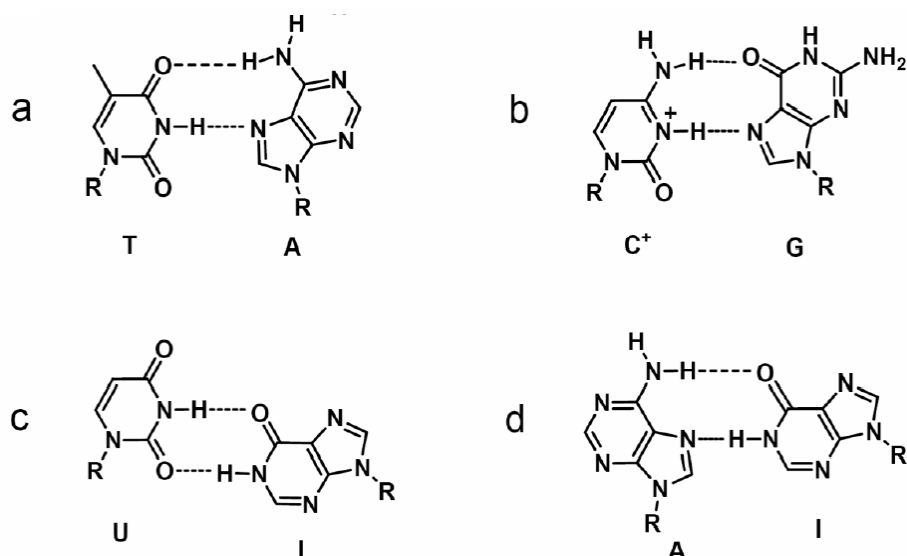Diffraction studies on heterogeneous DNA fibres showed two distinct conformations for double helical DNA,[6] A and B. Both A and B DNA are right handed double helices. B-DNA has a wide and deep major-groove with a narrow and shallow minor-groove, where the bases lie perpendicular to the helical axis. A-DNA has major groove which is deep and narrow while the minor groove is broad and shallow. In both A and B forms of DNA (Figure **1.4**), the Watson-Crick base pairing is maintained along with anti-glycosidic conformation however they differ in sugar conformation, B-DNA shows C2'-endo puckering while A-DNA exhibit *C3'-endo* sugar-pucker. Z-DNA (Figure **1.4**) is a left-handed double-helical structure and is favoured for alternating G-C sequences. Purines adopt the syn-glycoside conformation and the C3'-endo sugar pucker maintaining Watson-Crick pairing. The phosphate backbone has a zig-zag appearance. The minor groove is narrow and very deep and major groove is very shallow exposing otherwise inaccessible parts of C and G bases.
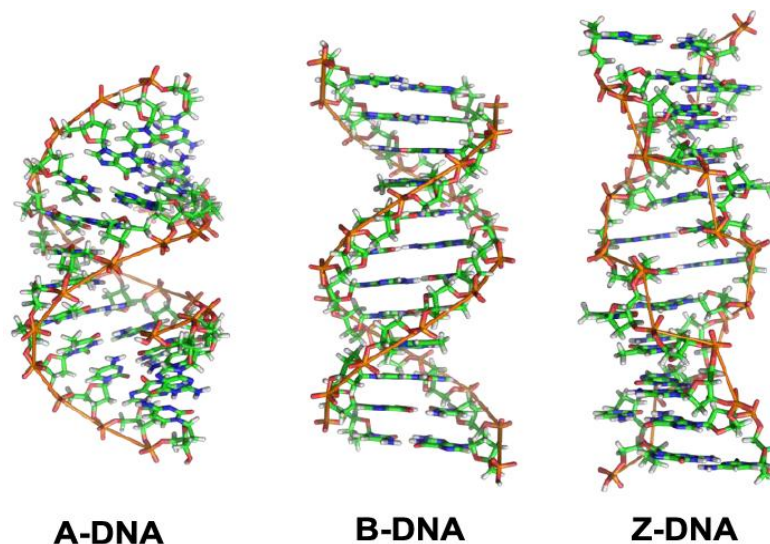
Figure 1.4 Molecular models of A, B, and Z-forms of DNA

(ii) Secondary structure of RNA

The scientific view of RNA has transformed over the past few decades. Earlier, most RNAs involved in translation were otherwise thought to be relatively uninteresting, but now, it is realized that RNAs serve many other essential functions: they help in protein synthesis, control gene activity and modify other RNAs. At least 85% of the human genome is transcribed into RNA. Unlike DNA, which forms a predictable double helix, RNAs comprise of a single strand that folds up into elaborate loops, bulges, pseudo-knots, hammerheads, hairpins and other 3D motifs (Figure **1.5**). These structures flip and twist between different forms, and are thought to be central to the operation of RNA, albeit in ways that are not yet known.

Primary structure of RNA is built on 3'→5'phosphodiester linkage. While RNA sequences vary in size from 65 nucleotides upwards, their helical structures are restricted to A-form duplexes with 11-12 residues per turn. The presence of the 2'-hydroxyl group in RNA hinders the formation of a B-type helix. A-type heteroduplexes with one RNA and one DNA strand can be formed; they have higher self-melting temperature than their double-stranded DNA equivalents.

Single stranded RNAs form stable secondary structures like thermodynamically favored hairpin loops, bulges, and interior loops.
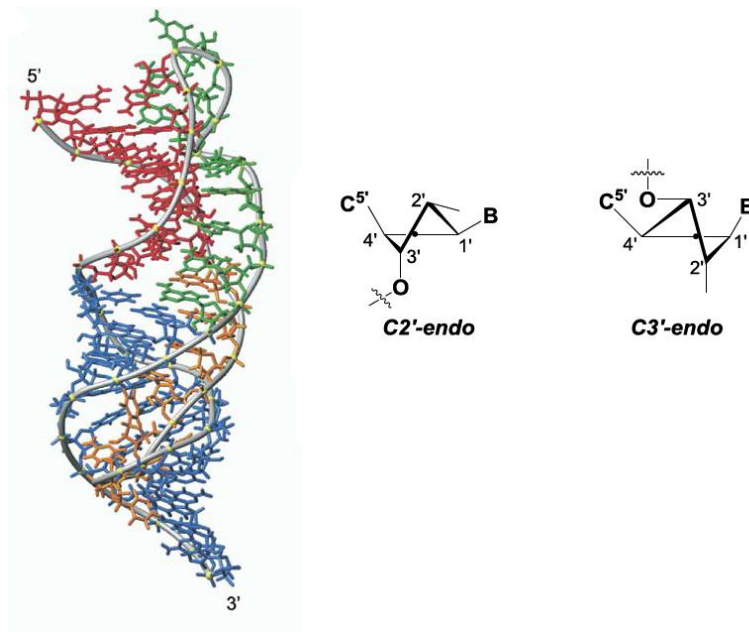

Figure 1.5: Molecular model of RNA[7] & Structures of *C2'*-endo and *C3'*-endo sugar puckering

1.4   Applications of Nucleic Acids

After 63 years of elucidation of double helical DNA by Watson and Crick, it is slowly emerging as to how the molecular and supramolecular structure of DNA would lead to design of future drugs, diagnostics, and new materials through explorations of chemical space in both modified DNA and RNA structures accompanied by expanded functionality. The recent decades have seen DNA evolve from just "genetic" material to a "generic" material for several applications from the intention of antisense activity of nucleic acid analogues, covalent conjugation of functional ligands and the explosion of DNA as a nanoscale construction material.

1) **Nucleic acid Nanotechnology**

Inspired by nature, researchers over the past four decades have explored nucleic acids as convenient building blocks to assemble novel nanodevices.[8] Nucleic acid nanotechnology has come a long way since its inception a quarter century ago. In

1982, Seeman first proposed using branched DNA building blocks to construct ordered arrays, which dramatically accelerated progress in nucleic acid nanotechnology by increasing the simplicity, precision, and fidelity of the design principles available for generating spatially addressable nanoscale structures.[9] Nucleic acid scaffolds are nanostructures that may be functionalized for ordering and arraying materials with nanometer precision. Scaffolds were originally formed by combining different short double-stranded DNA domains joined in a programmable fashion using single-stranded DNA overhangs known as 'sticky ends'.[10] These 'sticky ends' can be used as molecular walkers or as an adhesive to bring other macromolecules like proteins or lipids to form nucleic acid hybrids.

Reduction in errors in self-assembly, extension of two-dimensional self-assembly to three dimensional, and scale up in self-assembly will help in construction of nucleic acid based molecular devices and patterned superstructures on nanometer-scale.

2) **Disease Diagnosis**

Nucleic acids are natural biomarkers that can be used as probes for disease diagnosis based on the fact that they reorganize and bind to specific complementary sequences of nucleic acids (i.e. DNA or RNA). Nucleic acid-based diagnostics detect the presence of a pathogen either by directly detecting the presence of DNA or RNA nucleic acids in the host or by first amplifying the pathogen DNA or RNA. In the case of infectious diseases, nucleic acid-based diagnostics detect DNA or RNA from the infecting organism. For non-infectious diseases, nucleic acid-based diagnostics may be used to detect a specific gene or the expression of a gene associated with disease. Nucleic acid-based diagnostics are used to diagnose a wide range of conditions, including cancer, genetic markers associated with a high risk of cancer, and genetic diseases (e.g. cystic fibrosis). Common nucleic-acid based diagnostic techniques used to diagnose infectious diseases are PCR/RT-PCR, Isothermal amplification, hybridization, sequencing.[11] Nucleic acid-based diagnostics are also used to detect infectious diseases, such as anthrax, *Clostridium difficile* (a common hospital

acquired bacterial infection), chlamydia, and gonorrhea and are useful for diagnosis of leishmaniasis, tuberculosis, and HIV.

3) Therapeutics

Nucleic acid therapeutics include antisense oligonucleotides, aptamers and small interfering RNAs, and are typically considered in cases where specific inhibition of the function of a particular gene involved in disease is thought to be therapeutically desirable. Several steps in the process of gene expression may be modulated, including the transcription, RNA splicing and translation by various mechanisms. In the last two decades, therapeutic nucleic acid technology has developed as a promising tool to fight human diseases without secondary effects often observed with nucleoside and nucleotide analogues. This novel approach to drug design was more promising than rational drug design in the sense that it can be used for specific control of gene expression at the level of nucleic acid with increased specificity against malignant cells or viral entities and reduced side effects. Traditional small molecule therapeutic agents, such as nucleoside and nucleotide analogues work by interfering or modulating the function of enzymes, receptors, transport or structural proteins, whereas the therapeutic oligonucleotides alter the flow of genetic information at the DNA, mRNA or even protein level, and in many cases stimulate immune responses resulting in the suppression of disease-associated gene products.[12]

3.1) **Plasmids**: Plasmids are high molecular weight, double-stranded DNA constructs containing transgenes, which encode specific proteins. Upon cellular internalization plasmid DNAs exploit the transcription and translation apparatus in the cell to biosynthesize the therapeutic entity, the protein.[13] The action of these plasmids, requires entry into the nucleus through cytoplasm. Along with disease treatment, plasmids can be used as DNA vaccines for genetic immunization.[14]

3.2) **DNAzymes:** DNAzymes are a catalytically active class of antisense reagents discovered in the 1990s. These are single stranded DNA molecules that bind to their target mRNA by Watson–Crick base pairing and cleave the link between an

unpaired purine (A or G) and a paired pyrimidine (C or U) in the RNA by the cation-dependent domain of the DNAzyme.[15] DNAzymes are relatively small and inexpensive to synthesize and are resistant to nuclease degradation. DNAzymes have been used as inhibitory agents in a variety of experimental disease settings, suggesting their possible clinical utility. The first demonstration of DNAzyme activity in animals was in 1999 when a DNAzyme against the zinc finger transcription factor Egr-1 inhibited restenosis in balloon-injured rat carotid arteries.[16] DNAzyme directed against vascular endothelial growth factor receptor 2 was confirmed to be capable of tumor suppression by blocking angiogenesis upon intratumoral injections in mice.[17] Thus DNAzymes may be useful potentially as interventional tools in common disorders.

3.3) **Gene therapy:** Gene therapy is an experimental technique that uses genes to treat or prevent diseases and allow doctors in future to treat a disorder by inserting a gene into a patient's cells instead of using drugs or surgery. Researchers are testing several approaches to gene therapy, including:

- Replacing a mutated gene that causes disease with a healthy copy of the gene.
- Inactivating, or "knocking out," a mutated gene that is functioning improperly.
- Introducing a new gene into the body to help fight a disease.

Although gene therapy is a promising treatment option for a number of diseases, the technique remains risky and is under development to make sure that it is safe and effective.

3.4) **RNA interference (RNAi):** RNA interference (RNAi) is an evolutionarily conserved mechanism by which small non-coding double-stranded RNA (dsRNA) silences gene expression, either by inducing the sequence specific degradation of complementary mRNA or by inhibiting translation via endogenous cellular machinery. The concept of RNAi introduced in 1998 and employed dsRNA molecules to inhibit expression of homologue genes in *C. elegans*.[18]
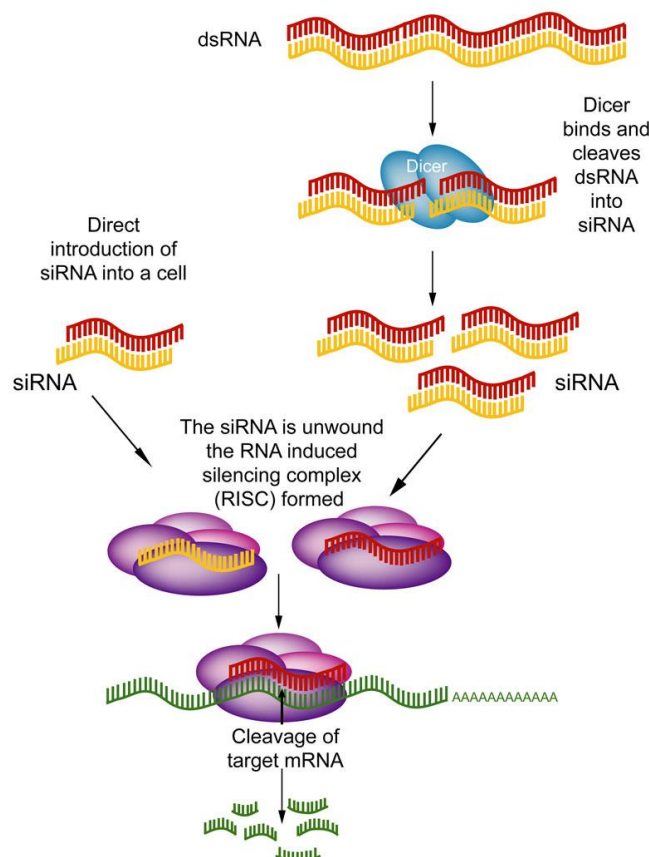
Figure 1.6: gene silencing by RNA interference[19]

RNAi effect is triggered by long pieces of dsRNA, which are cleaved into fragments known as siRNA (21–23 nucleotides long) by the enzyme Dicer.[20] In the cytoplasm of the cell, siRNA is incorporated into a protein complex called the RNA induced silencing complex (RISC), which unwinds the siRNA, after which the sense strand (or passenger strand) of the siRNA is cleaved.[21] The activated RISC containing the antisense strand (or guide strand) of the siRNA then selectively degrades mRNA that is complementary to the antisense strand.[22] The cleavage of mRNA occurs at a position between nucleotides 10 and 11 on the complementary antisense strand, relative to the 5-end.[23] The activated RISC complex can further move on to destroy additional mRNA targets. (Figure **1.6**)

MicroRNAs:

MicroRNAs (miRNAs) are another class of small non-coding RNAs that have been found to regulate gene expression at the post-transcriptional level. Mature

miRNAs originate from longer transcripts, called primary miRNAs (pri-miRNAs) that are transcribed in the cell nucleus by polymerase II.[24] In the nucleus, pri-miRNAs are processed into pre-miRNAs by the microprocessor complex, which consists of the RNAse III enzyme Drosha.[25] The pre-miRNAs are then transported from the nucleus to the cytoplasm via Exportin 5 complex.[26] These pre-miRNAs are additionally processed by the RNAse III enzyme Dicer to generate miRNA.[27] These miRNA are incorporated into a RISC-like complex which can either lead to mRNA cleavage or translational repression.[28] Hence, a single miRNA can regulate multiple genes due to its successful gene silencing ability even with partial complementarity between the miRNA and its target.

3.5) **Catalytically active RNA molecules (ribozymes):** Another strategy for drug development is by targeting the transcriptional process using ribozymes, a unique class of RNA molecules that not only store information but also possess catalytic activity.[29] In the early 1980s, Cech and coworkers discovered that RNA molecules are capable of catalysing reactions even in the absence of any protein component[30] and were named ribozymes. The hammer-head and hairpin ribozymes, among various ribozymes, have been extensively studied due to their small size and high cleavage efficiency.[31] Chemical modification of the RNA molecules is required to withstand nucleolytic degradation. Various clinical trials are in progress to evaluate the potential of ribozymes to fight cancer, e.g. angiozyme, is in phase II trial for treatment of metastatic colorectal cancer,[32a] while herzyme (Zinzyme) is in phase I clinical trial for treatment of breast and ovarian cancer.[32b]

3.6) **Decoy oligonucleotides:** Expression of almost every gene is regulated at the transcription level by a complex biological process which includes transcription factor-DNA interaction, which initiates gene transcription.[33] DNA sequences, generally of 6-10 base pairs in length, bind to transcription factor proteins which in turn bind to promoter regions of target genes whose expression gets regulated thereafter.
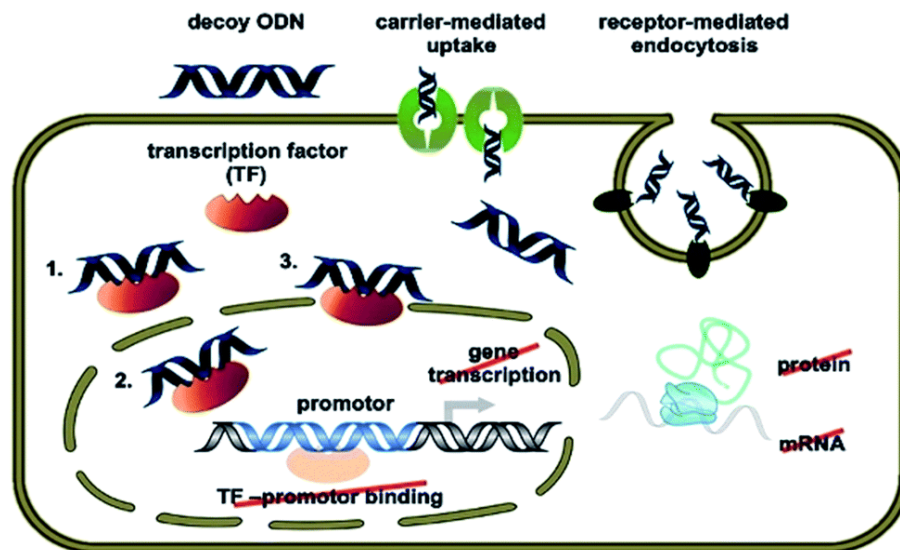
Figure 1.7: Schematic representation of mechanism of a decoy ODN's action

Chemically modified decoy oligodeoxynucleotides (ODNs) and different delivery systems have been investigated in order to use the therapeutic potential of the decoy ODNs, which have poor bioavailability and short half-life.[34] Phosphorothioate (PS) modified double-stranded ODNs which bind specifically to transcription nuclear factor kappa beta (NF-kB) have increased serum stability and regulate gene expression in a specific manner.[35]

3.7) **Aptamers:** Aptamers are single stranded ODNs whose three-dimensional structure allows it to bind to a variety of molecular targets such as proteins with high affinity and specificity. Nucleic acid aptamers are selected from a library of random sequences by an in vitro selection procedure called SELEX (systematic evolution of ligands by exponential enrichment) to bind to the chosen ligands with high specificity and affinity.[36] Aptamers are prone to degradation by serum nucleases and quick renal filtration. Unmodified aptamers may have half-lives in the blood as short as 2 minutes.[37] This can be overcome by capping ODNs at the 3'-terminus[38] or by 'Spiegelmer' concept[39] where enantioselective action of nucleases is used to overcome the degradation. The rate of renal filtration can be dropped by the conjugation of high molecular mass poly (ethyleneglycol) (PEG) etc.[40] Aptamers can also be used as cargo to disease targets (DNA or protein).[41]

FDA in December 2004 approved **Macugen™** [42] (pegaptanib sodium), an anti-VEGF RNA aptamer for the treatment of all types of neovascular age-related macular degeneration.

Aptamer technology is proving to be versatile and adaptable with the potential to become an attractive tool for diagnostic and therapeutic applications.

3.8) **Antisense and Antigene oligonucleotides:** An antisense oligonucleotide (ASO) is a short strand of oligonucleotide analogue that hybridizes with the complementary mRNA in a sequence-specific manner via Watson-Crick base pairing and downregulates the target protein expression. Antisense technology was first reported by Zamecnik and Stephenson in 1978 in Rous sarcoma virus (RSV).[43] On the basis of mechanism of action, two classes of antisense oligonucleotide can be discerned: (*a*) the RNase H-dependent oligonucleotides, which induce the degradation of mRNA; and (*b*) the steric-blocker oligonucleotides, which physically prevent or inhibit the progression of splicing or the translational machinery. RNase H is a ubiquitous enzyme that hydrolyzes the RNA strand of an RNA/DNA duplex.

Oligonucleotide-assisted RNase H-dependent reduction of targeted RNA expression can be quite efficient, reaching 80–95% down-regulation of protein and mRNA expression. RNase H-dependent oligonucleotides can inhibit protein expression when targeted to virtually any region of the mRNA.

An antigene drug is a triplex-forming oligonucleotide that recognizes and attaches directly to a specific DNA sequence and prevents transcription of the blocked DNA sequence into mRNA.[44] The strategy of blocking transcription and inducing specific mutations, both in vitro and in vivo has been successfully reported.[45]

There are pre-requisites to be an effective and successful therapeutic oligonucleotide candidate, like (i) easy synthesis in ample amounts (ii) in vivo

stability towards cellular degrading enzymes (iii) ability to penetrate into cells (iv) retention by the target cell (v) ability to interact with their cellular targets (DNA/RNA) (vi) No non-specific interaction with other macromolecules. Naturally occurring DNA or RNA can act as therapeutic agents but they lack binding affinity and get degraded by nucleases. Numerous chemical modifications have been developed to overcome meet limitations and to make these oligonucleotides successful therapeutic agents.

1.5 Chemical modifications of DNA and RNA

In quest of successful therapeutic oligonucleotides,[46] several modifications have been attempted (Figure **1.8**). These include chemical modifications of backbone,[47a] base,[47b] and/or sugar.[47c]
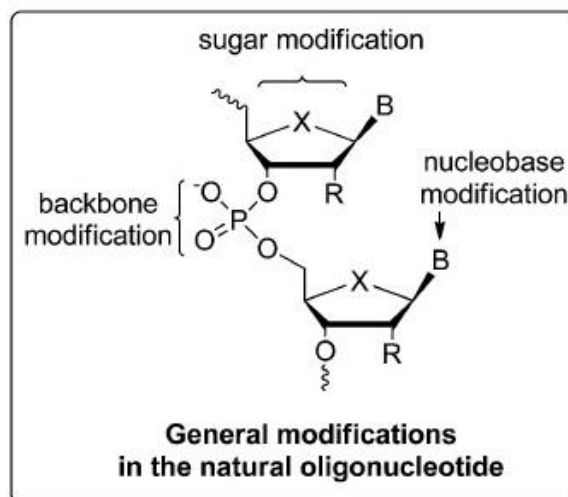

Figure 1.8: Different sites of modifications for oligonucleotides

1.5.1 Backbone modifications: First generation ODNs with backbone modified have backbone with 5'-N-carbamate, methylene-methylimine(MMI), amide, triazole phosphorothioate (PS), phoshorodithioate, thioether, methylphosphonate, boranophosphate, N-3'-phosphoramidate(NP), S-methylthiourea and guanidinium linkages. The modifications can be broadly divided into neutral, anionic or cationic internucleoside linkages. (Figure **1.9**)
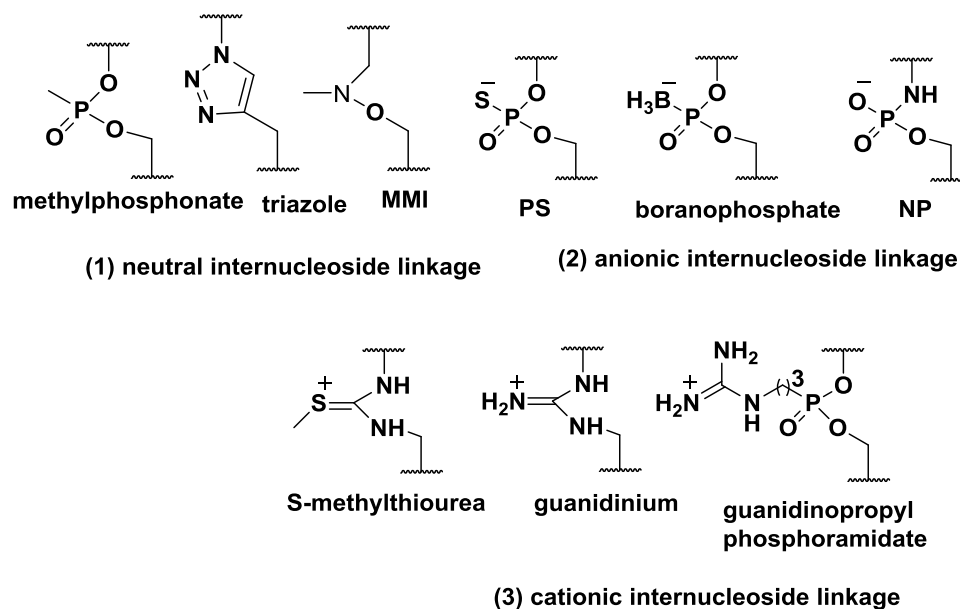
Figure 1.9: Modified internucleoside phosphate backbone

Major representatives of these first generation modified ODNs are Phosphorothioate oligonucleotides (PS-ODNs) and they have been used most successfully for gene silencing. Replacement of non-bridging oxygen atom by sulfur makes ODNs sufficiently resistant to nuclease degradation. Also PS-ODNs by regular Watson-Crick pairing activates RNase H, the negative charge helps cell delivery. These have increased binding to plasma proteins and other receptor sites as compared to natural phosphodiesters[48] which improves their cell uptake.

The binding of PS-ODNs to proteins, which interact with polyanions such as hairpin-binding proteins, prove to be their major drawback.[49] Despite of these disadvantages, the FDA approved first antisense drug Vitravene in 1998, which is a PS ON used for the treatment of AIDS-related cytomegalovirus (CMV) retinitis.

Other backbone modified ODNs (methylphosphonate, phosphoroamidates etc.) proved to be less successful at improving the ODNs properties. For example neutral methylphosphonates, although provide high nuclease resistance, does not induce RNase H activity. Increased number of methylphosphonate units lead to loss of affinity towards the target mRNA and poor water solubility.

1.5.2 Sugar modifications: Nucleoside analogues derived from modification of sugar include: (i) introducing electronegative atom in nucleoside analogues or introducing substituent at the 2'-position of sugar.[50] (ii) introducing an extra ring fused to the sugar moiety[51] (iii) nucleoside analogues with different sugar-rings.[52] (iv) introducing spirocyclic ring at different positions of sugar ring.[53] (Figure **1.10**)
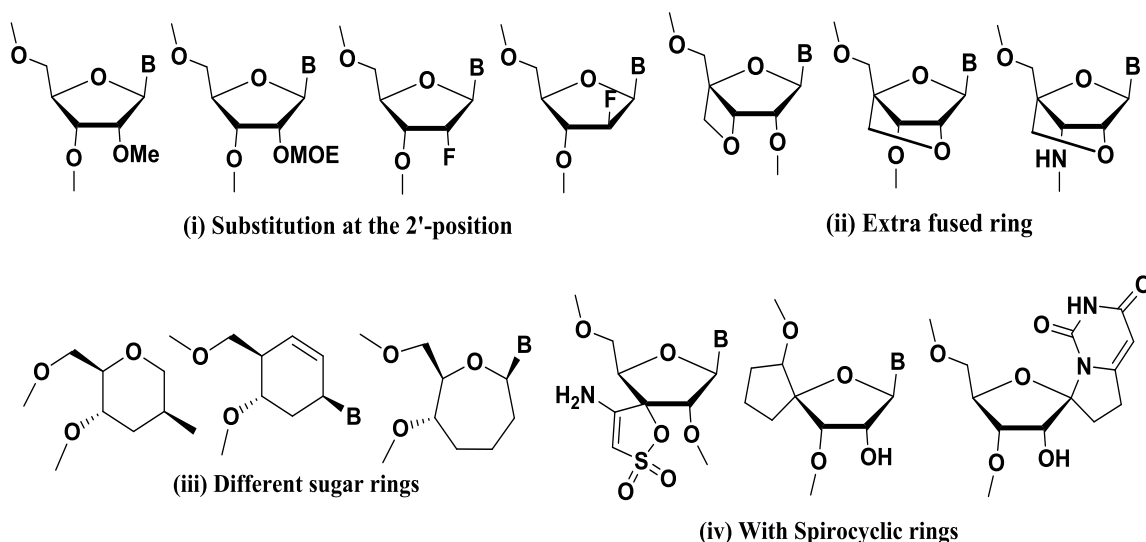

(i) Substitution at the 2'-position   **(ii) Extra fused ring**

(iii) Different sugar rings

(iv) With Spirocyclic rings

Figure 1.10: Structures of different types of sugar-modified nucleoside analogues

The most important members of these second generation class molecules (2'-OMe, 2'-OMOE, and locked nucleic acid) have helped to improve specificity and cellular uptake, and are less toxic than PS-ODNs, however they are not efficient to induce RNase H cleavage of the target.[54]

Gapmer ODNs consist of a central 'gap' of deoxynucleotides, just sufficient to induce RNase H cleavage, and terminal 'wings' that possess modifications to protect central gap from degradation. Kynamro[TM][55] approved recentlya (January 2013) as an antisense drug has 2'-OMOE sugar modified nucleosides and phosphorothioate-linkage (PS).

Substitution of electronegative atom like fluorine and oxygen influence the furanose sugar to adopt RNA like C_3'-endo conformation,[56] which is exclusively present in A-type duplexes. The conformationally restricted sugar moiety and extensive hydration of the 2'-substituent gives ODNs a high metabolic stability and high affinity to target mRNA. FDA

approved RNA aptamer macugen for the treatment of macular degeneration, consists of 2'-F and 2'-OMe substituted sugar moieties.

1.5.3 Nucleobase modifications: Fastidious selectivity of natural nucleobases in recognizing complementary bases as given by Watson-Crick rules, confines the scope of nucleobase modifications. Nucleobase modification can improve the binding affinity for the complementary ON but not the nuclease resistance.[57] Subtle change in nucleobase can have dramatic effect on binding because of the electronic distribution (H-bond capacity), tautomeric structures or functional group pKa values. Some of the modified nucleobases are shown in Figure **1.11**. The stacking interactions between the planar nucleobases contribute significantly to stability of duplexes, and hence chemical modifications can influence the stability to duplexes.[58] The most inviting sites of substitution in a nucleobase are the positions exposed to solvents in the major groove, which includes the 4- and 5-positions of pyrimidines and the 6- and 7- positions of purines. These substituted positions neither interfere with base pairing nor induce steric hindrance and do not influence the general geometry of the double helix.[59]
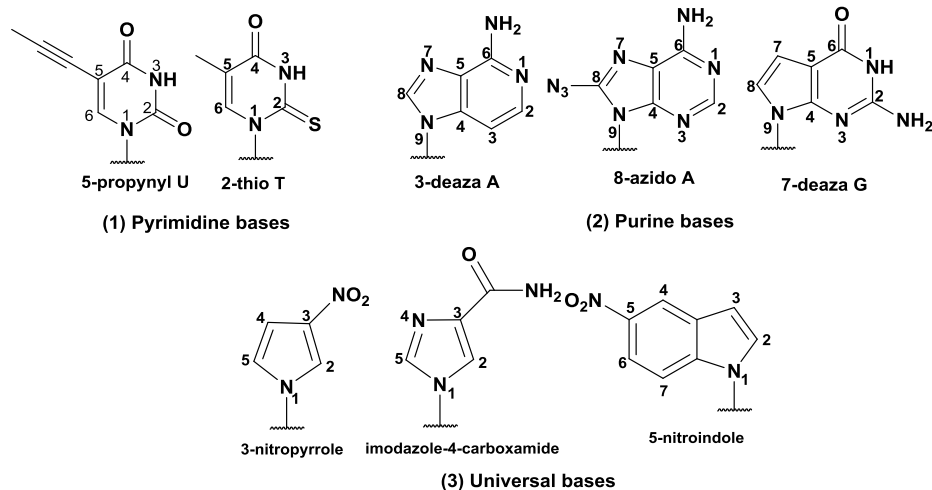

Figure 1.11: Structures of different types of nucleobase modified nucleoside analogues

1.5.4 Sugar-phosphate backbone modifications: The third generation of ODNs with modified isosteric structures obtained by replacing sugar and phosphate backbone has lead to enhance target affinity, nuclease resistance, biostability and pharmacokinetics. Some of the modifications are described below:

Locked nucleic acid (LNA) Locked nucleic acid (LNA) introduced in 1998 by Imanishi and Wengel group[60] is a novel oligonucleotide analogue in which 2'-O and 4'-C positions in the β-D-ribofuranosyl ring are joined via an O-methylene, S-methylene or amino-methylene moiety, and furanose conformation is locked in a C3'-endo (Figure **1.12**).
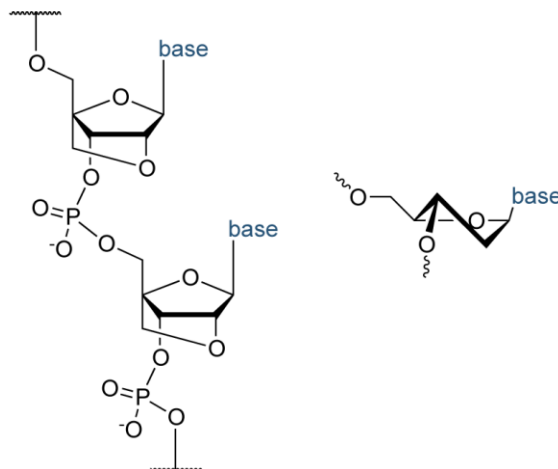

Figure 1.12: LNA (Locked Nucleic Acid)

 LNAs have high hybridization affinities for complementary DNA/RNA sequences, remarkable antisense activity, nuclease resistance, good aqueous solubility and non-detectable toxicity. Like other 2'-O ribose modifications, but LNA is unable to activate RNase H. To overcome this limitation the chimeric LNA-DNA-LNA gapmer have been designed with 7-10 PS-modified DNA central gaps flanked by three to four LNA nucleotides on both sides. LNA offers one of the most promising analogues for the development of diagnostics and therapeutics.

Morpholino oligonucleotides (MF): Morpholino ONs are uncharged agents in which ribose sugar is replaced by a six-membered morpholino ring and the phosphodiester bond is replaced by a phosphorodiamidate linkage[61] (Figure **1.13**).

Non-ionic Morpholino ODNs are devoid of unwanted electrostatic interactions with nucleic acid binding proteins. MF ODNs are stable against nucleases and have similar target affinity to that of the isosequential unmodified ODNs. However, uncharged backbone affects their cellular uptake and then do not activate RNase H. They can be used as a steric blocker to inhibit gene expression.[62]
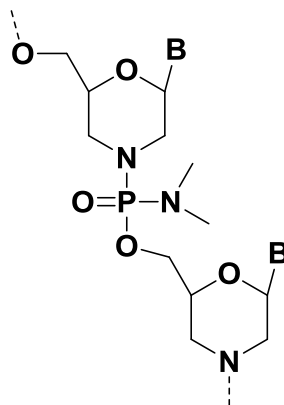
Figure 1.13: Morpholino oligonucleotide (MF)

Cyclohexene nucleic acids (CeNA): Cyclohexene nucleic acids (CeNA) have five membered sugar furanose ring replaced by a six membered cyclohexene ring, which imparts more comformational rigidity to oligomers (Figure **1.14**).
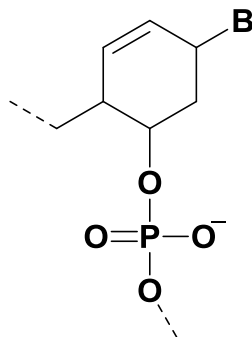

Figure 1.14: cyclohexene nucleic acid (CeNA)

They are known to form stable duplexes with complementary ODNs and are resistant to nucleases,[63] also CeNA:RNA hybrids have been reported to activate RNase H.[64]

Peptide nucleic acids (PNA) Peptide nucleic acids are a class of ODNs where the phosphodiester backbone is replaced with a flexible pseudopeptide backbone. PNA first introduced by Nielsen *et al.*[65] in 1991, consists of repeating N-(2-aminoethyl) glycine units linked by amide bonds and nucleobases are attached to backbone via a methylenecarbonyl linker (Figure **1.15**).
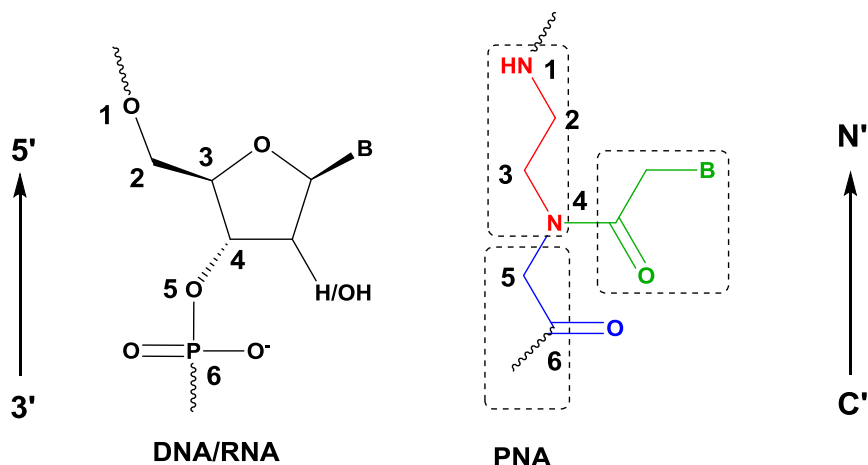
Figure 1.15: Structures of DNA/RNA and PNA

PNAs thus possess a rare structural combination of peptides and nucleic acids. They do not have any sugar moieties or phosphate groups non-ionic, but still surprisingly mimic the DNA behavior in many aspects. An antiparallel duplex of PNA: DNA/RNA is represented with N-terminus of PNA facing 3'-end of DNA/RNA and C-terminus of PNA facing 5'-end of DNA/RNA. PNA, a non-charged ON analogue, hybridizes with complementary DNA or RNA with high affinity and specificity than DNA-DNA and DNA-RNA duplexes. Also they have higher mismatch discrimination, resistant to both proteases and nucleases. High chemical and bio-stability, favourable hybridization makes PNA a promising tool in medicinal chemistry and biosupramolecular chemistry.

1.6 PNA structure:

PNA recognizes specific with complementary nucleic acid sequences forming Watson-Crick base rules.[66] The three dimensional structure of a PNA-RNA duplex,[67a] a PNA-DNA duplex[67b] was solved by NMR methods, while PNA_2-DNA triplex[67c] and PNA-PNA duplex[67d] structure was solved by X-ray crystallography (Figure **1.18**). These structures demonstrated that PNA preferred structure of its own termed the 'P-form' helix that is slightly different from other nucleic acid helices. This P-form conformation dominating in the PNA_2-DNA triplex and PNA-PNA duplex is a very wide helix (28 Å diameter) with a large pitch (18 base pairs per turn). The DNA duplexes have B-form helix with 20Å diameter and a pitch of 10 base pairs per turn and RNA duplexes have

20Å diameter but a pitch of 11 base pairs per turn, with base pairs tilted 20° relative to the helix axis. Also just like in P-form the base pairs are displaced away from helix. Thus PNA is able to structurally adapt well to its nucleic acid partner.

Chemical and physical properties of PNA: PNA has two unique properties – (1) ability to hybridize complementary nucleic acid in both parallel and antiparallel fashion, and (2) ability to invade DNA duplexes to give PNA_2-DNA or higher order complexes. These abilities together with remarkable chemical and biological properties such as stability to harsh acidic or basic conditions, stability to nucleases and proteases, high specificity and selectivity of binding to complementary ON, makes PNA a promising tool for interfering gene expression as antigene and antisense molecules. It is also generally useful for all applications based on the hybridization of PNA to DNA/RNA.

Duplex formation with complementary oligonucleotides Watson-Crick base pairing rules are obeyed for PNA hybridization to complementary ON. In DNA-DNA duplex, the two strands run in antiparallel direction while in PNA-DNA duplex, the two strands may adopt parallel or antiparallel orientation (Figure **1.16**), preferring antiparallel orientation.[68] This allows PNA to bind to two DNA strands of opposite sequence.
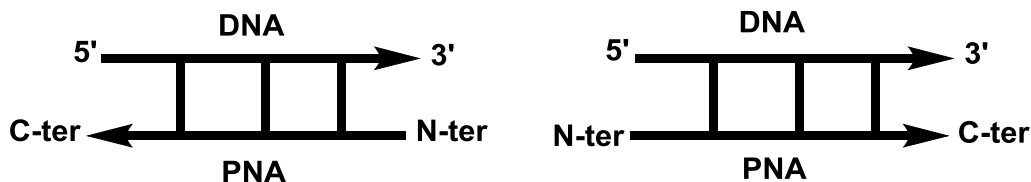

Figure 1.16: Antiparallel and parallel mode of orientation

Triplex formation of PNA: Polypyrimidine PNAs can form PNA_2-DNA triplexes[69] via Watson-Crick (Figure **1.2**) and Hoogsteen hydrogen bonds (Figure **1.3**). In the triplex with only one type of PNA, both strands are necessarily either antiparallel or parallel to DNA strand. While in the triplex with two different PNAs, one strand is oriented antiparallel which follows Watson-Crick base rules and the other strand which is parallel to DNA strand follows Hoogsteen base rules. The sequence specificity of triple helix formation is based on the selectivity of formation of the intermediate PNA-DNA duplex, whereas binding of the third strand contributes only slightly to selectivity.

Strand invasion by PNA: PNAs have unique property to displace one of the DNA strand in a DNA-DNA duplex,[70] which makes them good antigene agents. PNAs can target DNA duplex in a sequence specific manner by four modes (Figure **1.17**), three of which involve invasion of the duplex by PNA strands.
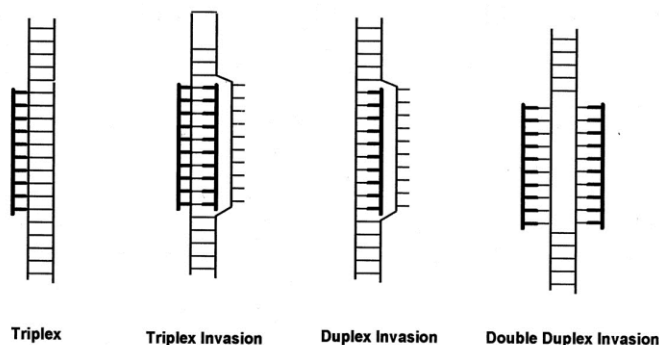

Triplex   Triplex Invasion   Duplex Invasion   Double Duplex Invasion

Figure 1.17: Various modes of binding of PNA to ds DNA

It is possible for PNA (homopurine) single strand to either invade (duplex invasion) via Watson-Crick base pairing. Alternatively, invasion may be accomplished by two pseudo-complementary PNA strands, each of which binds to one of the DNA strands of the target (double duplex invasion). These pseudo-complementary PNAs contain modified adenine and thymine nucleobases[71] (Figure **1.18**) that do not allow stable hybridization between the two complementary sequence PNAs, but does permit good binding to the DNA.
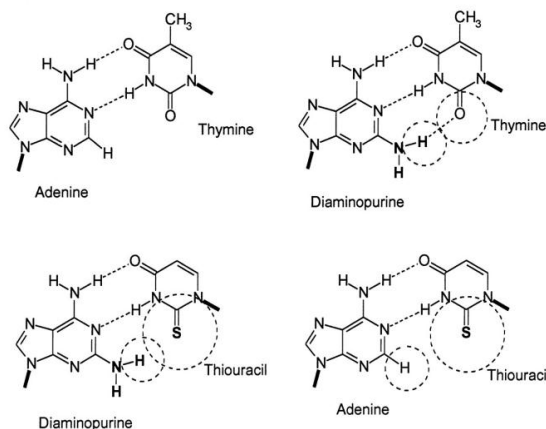

Figure 1.18: Schematic representation of extra hydrogen bonding between diamnopurine and thymine; and steric clash between diaminopurine and thiouracil[71]

In triplex invasion homopyrimidine PNAs binds to complementary homopurine DNA throughWatson-Crick-Hoogsteen base pairing and forms very stable PNA_2-DNA triplex.

Quadruplex formation by PNA: The novel supramolecular architecture of G-quartets has led to the development of interesting and functional noncovalent assemblies such as G-wires,[72] ion-channels[73] and self-assembled ionophores[74] PNAs have been developed to mimic Watson-Crick and Hoogsteen base-pairing and they are expected to participate in G-tetrad formation as well. In an attempt to use this mode of molecular recognition, homologous G-rich PNA and DNA oligomers hybridise to form a PNA_2-DNA_2 quadruplex. The hybrid quadruplex exhibits high thermodynamic stability and expands the range of molecular recognition motifs for PNA beyond duplex and triplex formation.

Specificity and binding of PNA to complementary nucleic acid: PNA binds to complementary nucleic acid with high specificity. Mismatch in PNA-DNA duplex is more destabilizing than a mismatch in a DNA-DNA duplex. T_m of a PNA-DNA duplex (15-mer) is lowered by 8-20°C (15°C on average) by introduction of a single mismatch base pair. Whereas, in the corresponding DNA-DNA duplex, a single mismatch destabilizes the duplex by 4-16°C (11°C on average).[75]

The T_m values of PNA-DNA duplex are independent of salt concentration, whereas the T_m values of DNA-DNA duplex are highly dependent on ionic strength,[76] this can be attributed to neutral backbone of PNA.

Solubility of PNA: Uncharged PNAs have limited water solubility as compared to DNA, and tend to aggregate to a degree dependent on oligomer sequence. PNA solubility is dependent on length of the oligomer and the purine/pyrimidine ratio.[77] Solubility of PNA can be improved by incorporation of lysine or arginine, a positively charged residues, or making PNA inherently charged by modifying backbone of PNA itself.

Cellular uptake of PNA: Poor cellular uptake of PNA hamperes its exploration as an antisense/antigene agents in spite of having other advantages like high specificity binding to complementary ON and stability in biological fluids. A number of transfection

protocols for PNA have been established like microinjection, electroporation, co-transfection with DNA, conjugation to lipophilic moieties, conjugation to cell penetrating peptides etc.[78]

PNA-peptide or nucleic acid conjugates show a significant improvement in the solubility and cellular uptake as compared to unconjugated molecules, however their use is hampered by their high cost.[79] To improve PNA solubility in aqueous media, the cellular uptake, the binding selectivity towards RNA versus DNA, or to stabilize duplex or triplex structure, several modified PNA analogues have been synthesized over years.

1.7 Chemical modifications of PNA:

The high affinity and selectivity towards natural nucleic acids render PNAs very potent tools in analytical and biotechnological applications. Their ability to bind to interior or structured regions of mRNA makes PNA superior to DNA in the antisense approach. Still the number of *in vivo* applications is very limited, due to their low solubility in aqueous environment and their low cellular uptake. Furthermore, their lack of charge and hydrogen bond donors/acceptors inhibits their use in applications involving the recognition of molecules mediated by hydrogen bond formation and charge–charge interactions. To improve PNA solubility in aqueous media, the cellular uptake, the binding selectivity towards RNA versus DNA, or to stabilise duplex or triplex structures, several analogues have been synthesised over the years.

Structure activity relationships showed that the original design containing a 6-atom repeating unit and a 2-atom spacer between backbone and the nucleobase was optimal for DNA recognition.[80] Introduction of different functional groups with different charges/polarity/flexibility have been described and are extensively reviewed.[81] These studies showed that a "constrained flexibility" was necessary to have good DNA binding. Modified PNAs have been constantly improved during these years, using the concept of "preorganization", i.e. the ability to adopt a conformation which is most suitable for DNA or RNA binding, thus minimizing the entropy loss of the binding process. Preorganization was achieved either by cyclization of the PNA backbone (in the

aminoethyl side or in the glycine side), by adding substituents in the C2 or C5 carbon of the monomer or by inserting the aminoethyl group into cyclic structures. The addition of substituents at C2 or C5 carbon of the monomers can also in principle preorganize the PNA strand, but mainly it has the effect of shifting the PNA preference towards a right-handed or left-handed helical conformation, according to the configuration of the new stereogenic centers, in turn affecting the stability of the PNA-DNA duplex through a control of the helix handedness.

Preorganization of acyclic PNAs: Using the linear *N*-(2-aminoethyl)glycine as a starting point, several PNA derivatives were obtained by insertion of side chains either at the C2 (α) or C5 (γ) or C4(β) carbon atoms (Figure 1.**19**). These modifications have the effect of shifting PNA "natural" constrained flexibility towards more constraints and less flexibility. If the constraint is appropriate for the conformation required for DNA binding, this can actually result in improved DNA binding properties, otherwise, a detrimental effect is obtained.

$R_1=R_2=R_3=H$
$R_1=$side chain, $R_2=H$, $R_3=H$
$R_1=H$, $R_2=$side chain, $R_3=H$
$R_1=H$, $R_2=H$, $R_3=$side chain

aeg-PNA
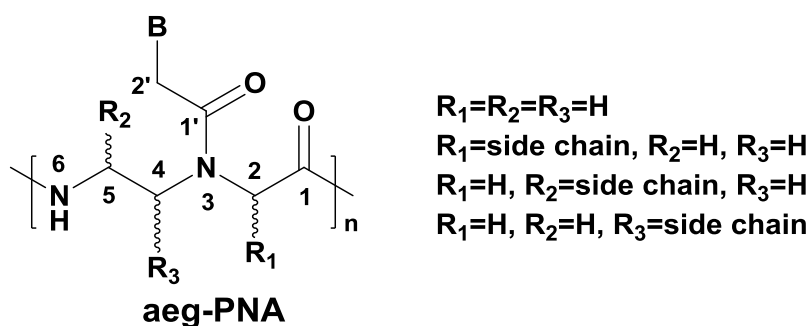
Figure 1.19: Schematic representation of achiral and chiral acyclic PNAs

α-PNAs: Nielsen *et al*. reported the first α-chiral PNA in 1994, in which glycine moiety of the PNA backbone was substituted by alanine.[82]

Both the L- and D-forms of the chiral monomers derived from L- or D-alanine were incorporated into oligomers. Thermal stability of PNA-DNA duplex containing D-form monomers was similar to that of the original PNA with a glycine backbone, whereas L-form monomers showed reduced stability.

When the relative binding affinities of chiral PNAs including L and D-alanine, L- and D-lysine, L- and D-serine, D-glutamic acid, L-aspartic acid, L- and D-leucine were considered,[83] the PNA:DNA duplex stability was found to be dependent on stereochemistry: PNAs carrying the D-amino acid derived monomers bound complementary antiparallel DNA strands with higher affinity than the corresponding L-monomers. Therefore, the affinity of chiral PNAs for complementary DNA emerged to be a contribution of different factors: electrostatic interactions, steric hindrance and, most interestingly, enantioselectivity, with a preference for the D-configuration.

From CD spectroscopy it could be demonstrated that PNAs containing D-monomers with the stereogenic center in position 2 induced a preference for a right-handed conformation in PNA-PNA duplexes, whereas PNAs containing L-monomers with the stereogenic center in the same position induced an opposite preference for a left handed double helix.[84] This shows that PNAs preferring a right-handed helical conformation would have higher DNA binding affinity than their mirror images. Chiral PNAs derived from alanine or from arginine and lysine side chains showed the best affinity for DNA on account, of the small steric hindrance and of the electrostatic interaction respectively with the negatively charged DNA strand. The poor affinity for DNA was displayed by PNAs bearing side chains derived from bulky apolar amino acids, such as valine, tryptophan or phenylalanine. Thus steric hindrance was clearly responsible for the destabilization of these PNA-DNA duplexes.

D-Arginine in place of glycine leads to α-guanidium PNAs (GPNAs), which showed the destabilization of derived PNA:DNA duplex. However incorporation of multiple α-guanidium PNA units in PNA decamer improved the binding affinity, partly from electrostatic interaction between guanidium group and phosphate groups.[85]

Interestingly incorporation of PNA monomers derived from substitution of glycine moiety of aeg-PNA (C_2, position) by achiral amino isobutyric acid (α,α-disubstituted methyl groups), into PNA oligomers increases the Tm of PNA-DNA duplexes (Figure 1.**20**).[86]

Also incorporation of the homologous aminopropyl-(α,α-dimethyl)glycyl (*apdmg*)-PNA monomers also improved DNA binding. Introduction of appropriate rigidity without any chirality improved DNA binding properties of PNA. Another interesting feature of dimethyl PNAs is their preferential binding to DNA than to RNA.
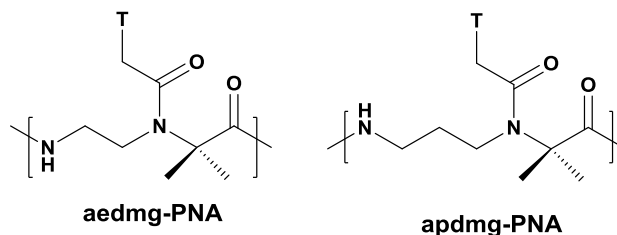

aedmg-PNA   **apdmg-PNA**

Figure 1.20: Structures of α,α-dimethyl PNAs

β -PNAs: Though Cyclic PNA analogues containing a chiral center at the β-position have been reported,[87] substitution of a single substituent β-position alone has not been explored much.

Since the β-position of the PNA backbone corresponds to the C4' of the deoxyribose moiety of DNA and the C4' is a chiral carbon atom, the incorporation of a substituent at the β-position was expected to significantly affect the conformation and the DNA binding properties of PNA oligomers.

In 2011, Sugiyama *et al*. reported the first β-PNA bearing a methyl group at the β-position.[88] A PNA monomer possessing a methyl group at the β-position was designed and both enantiomers, β-(*S*)- and β-(*R*)-configurations, were synthesized and incorporated into PNA oligomer. PNA oligomer containing three β(S)-PNA monomers and unmodified PNA showed similar T_m values, in contrast, PNA oligomer containing three β(R)-PNA monomers did not bind to DNA. Thus in contrast to α-PNAs, the stereochemistry of the β-carbon of the PNA backbone plays a critical role towards the hybridization ability of PNA and strictly limited to *S*-configuration.

γ –PNAs: Although the first γ-chiral PNA monomer was reported in 1994,[89] incorporation into a PNA oligomer appeared only in 2005.[90]

Incorporation of Cγ-(L)-Lys -modified PNA slightly stabilized PNA-DNA duplexes relative to the unmodified duplex. Moreover, the ability of Cγ-(L)-Lys -PNA to discriminate single-base mismatches was superior to that of the corresponding unmodified PNA.[91]

PNA oligomers carrying the Cysteine-base γ-PNAs at the *N*-terminus could be used for native chemical PNA ligation with thioesters of PNAs to yield long chain PNAs γ-PNA bearing a sulfate group aimed at making PNAs more DNA-like in terms of polarity and charge have been reported by Romanelli *et al*.[92] PNA2•DNA triplex formed by homopyrimidine PNA nonamer containing three sulfate monomers was less stable (ΔT_m −5.6 °C) than the standard PNA hybrid. This destabilization was explained by electrostatic repulsion between the negatively charged phosphate of DNA and sulphate of the modified PNA. The modified PNA could be lipofected into human breast cancer (SKB3) cells due to its negative charge and exhibited antigene activity against *ErbB2* gene Ly *et al*.[93] reported that a simple γ-backbone modification preorganized single-stranded PNA oligomers into a right-handed helical structure that was very similar to that of PNA-DNA duplex.

The γ-PNAs bound to DNA with very high affinity and high sequence selectivity. Helical induction was sterically driven and stabilized by base stacking.

In contrast to α-PNA, which is sensitive to steric hindrance arising from side chains at the α-position Ly *et al*.[94] have demonstrated that the γ-position could accommodate various hindered side chains without inducing adverse effects on the hybridization properties of PNAs Ly *et al*.[95] have reported the synthesis of γ-GPNA, the second-generation GPNA, which was prepared from inexpensive Boc-L-Lysine (selected based purely on cost) and had a homo-arginine side chain at the γ-position (Figure **1.21**)

A fully alternate γ-GPNA decamer was taken up by HeLa cells and the uptake efficiency was comparable to that of the TAT transduction domain. Recently, inhibition of micro-RNA by GPNAs has been reported by Manicardi *et al*.[96] Anti-miR-210 activity of PNAs

in leukemic K562 cells was examined using a series of 18-mer PNAs: unmodified PNAs, PNAs conjugated with arginine octamer and modified PNAs containing eight units of α- or γ-GPNA monomers. It is noteworthy that uptake of α-GPNAs was resistant to serum. The best anti-miR-210 activity was exhibited by γ-GPNA with consecutive placement.
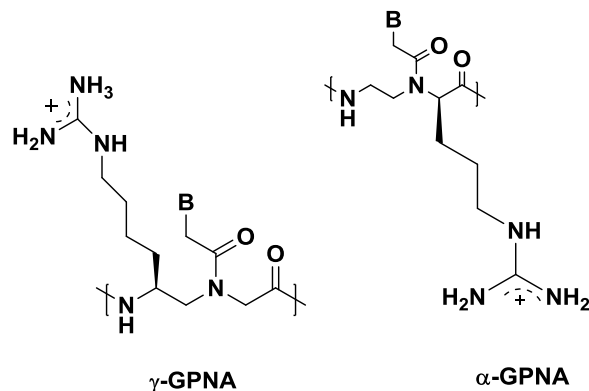

Figure 1.21: Structures of γ-GPNAs

Ganesh *et al*.[97] reported the synthesis of chiral PNAs (*am*-PNAs) with cationic aminomethyl groups at the α- or γ-position of the PNA backbone (Figure **1.22**). The *am*-PNAs formed more stable PNA-DNA duplexes than the unmodified PNA and the order of stabilization was γ-(*S*)-*am* PNA > α-(*R*)-*am* PNA > α-(*S*)-*am* PNA. The *am*-PNAs could traverse the cell membrane of HeLa cells and localized into the nucleus. The order of cellular uptake efficiency of *am*-PNAs was again γ-(*S*) > α-(*R*) > α-(*S*).
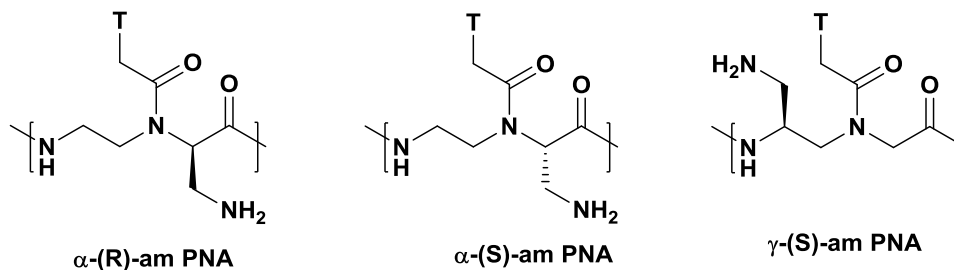
Figure 1.22: Structures of aminomethyl-PNAs

Recently it was shown that length of side chain in γ-GPNA and γ-azido PNA is important for hybridization with DNA (Figure 1.**23**).

The guanidium PNAs with shorter spacer chain increases the PNA:DNA duplex stability. These PNAs taken up in 3T3 and HeLa cells were visualized by confocal microscopy and

quantified using fluorescence assisted cell sorter (FACS).[98] Methylene/ butylene azido group at Cγ of PNA enable the attachment of multisite labeling and introduction of fluorophores in a single step through click reaction without any protection/deprotection steps. The azido substituted PNAs are seen to accumulate around the nuclear membrane in 3T3 cells.[99]
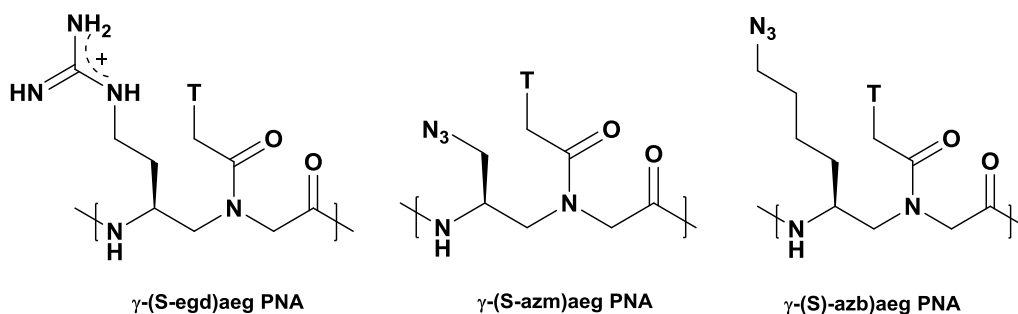
Figure 1.23: Structure of γ-GPNA and γ-azido

Preorganization through cyclic PNAs: Unmodified aminoethylglycine PNAs (aegPNA) have several conformational degrees of freedom which allow them to be considered as rather flexible molecules. When cyclic structures are used in the PNA backbone, some of the dihedral angles depicted in Figure **1.24** are mainly determined by the stereochemistry and by ring puckering.
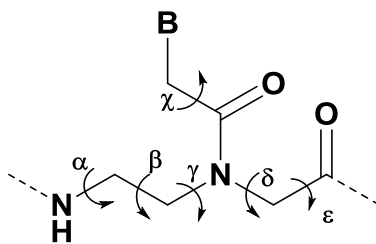
Figure 1.24: Rotatable bonds defining the torsion angles in the unmodified aegPNA structure

As a rule of thumb, stereochemical requirements can be derived from the model described in Figure **1.25**, which is based on the disposition of the 5', 3' and nucleobase groups in the DNA structure. In some cases, however, the role of terminal groups (whether 3' equivalent or 5' equivalent) is ambiguous and some of the derivatives can

present inverted orientation. However this is a simplified model and conformational properties of the cyclic structures should be also taken into account.
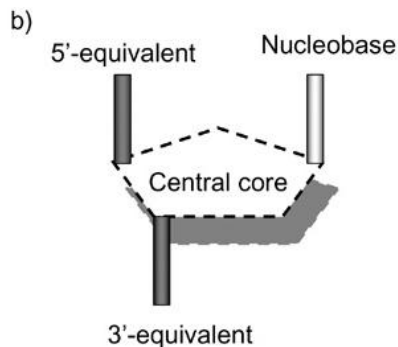
Figure 1.25: Stereochemical model of an appropriate group arrangement for DNA-mimics

The conformational properties also influence the preference for binding DNA over RNA or vice-versa. In fact, due to the different conformation of DNA (C2'endo) and of RNA (C3' endo), the dihedral angles of PNA can induce a conformation more suitable for the binding of either of the two classes of nucleic acids. Ganesh *et. al.* have recently proposed a model, based on available structural data, in which the preference for DNA/RNA is affected by the β-dihedral angle (Figure **1.26**); the 65° angle was proposed to be favouring the preference for RNA over DNA, while the 25° angle, if inserted in a five-membered ring, allowing binding of both RNA and DNA,[100] while widening this angle resulted in inappropriate binding.
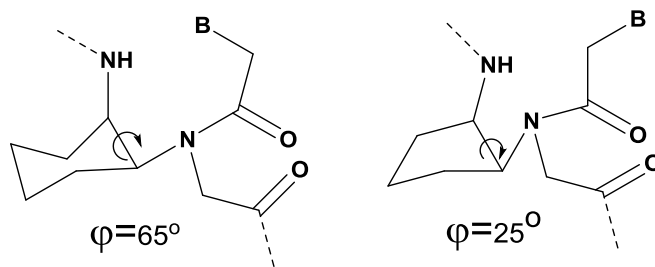
Figure 1.26: β-torsion angle bias obtained by means of a rigid core constraint in the 2-aminoethyl group

One major contribution to the DNA:PNA duplex stability is the occurrence of attractive electrostatic interactions. Therefore cyclic structures with amino groups, which are

protonated at neutral pH usually have higher affinities than neutral analogues. Another very important issue is stereochemistry and conformation imposed by the cyclic moieties. One of the most interesting class is that of rigid PNAs containing cyclic structures of five membered rings, some of which resulted in improved DNA affinity, or six membered rings, most of which gave poorer results.[101] The cyclic structure induces a "preorganization" of the PNA conformation, therefore in this case, if the cyclic structure induces the correct preorganization an entropic advantage in DNA or RNA binding is more likely to be expected than in the case of acyclic derivatives.

Cyclic PNA analogues containing five-membered rings: The naturally occuring amino acid *trans*-4-hydroxy-L-proline, a five-membered nitrogen heterocycle, is a versatile, commercially available starting material for creating structural diversity to mimic DNA/PNA structures. From this amino acid, a wide variety of chiral constrained and structurally pre-organized PNAs have been synthesized. Depending on the synthetic approach and on the presence of the tertiary amine group in the monomers, the modifications afford either positively charged or uncharged cyclic PNA analogs. The different cyclic PNAs proposed showed that the right stereochemistry and conformation is really determinant for binding abilities towards nucleic acids and in some cases even discriminate between RNA and DNA.

All steroisomers of cyclic PNA analogue *N*- (thymin-1-ylacetyl)-4-aminoproline were synthesized (Figure **1.27**).

(2S,4R)-aminoprolyl-PNA   (2R,4S)-aep-PNA
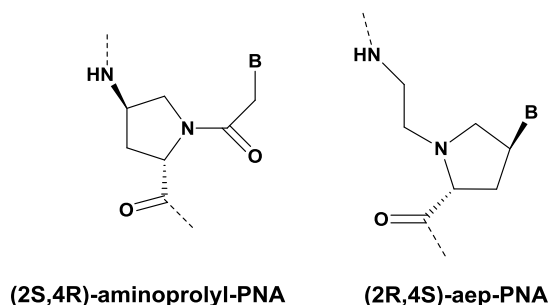
Figure 1.27: Cyclic PNA analogues containing five-membered rings

L-*trans*-4-aminoprolyl isomer was shown to bind to DNA with higher affinity, while the L-*cis* isomer and the D-*trans*, which could not adopt the same spatial arrangement, showed reduced performances.[102]
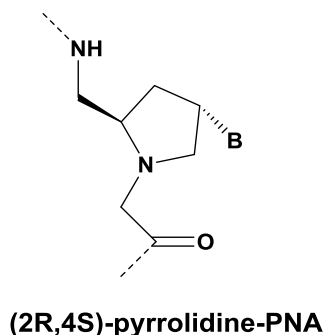

(2R,4S)-pyrrolidine-PNA

Figure 1.28: Cyclic PNA analogues containing five-membered rings

The synthesis of pyrrolidine-based chiral positively charged PNAs (Figure **1.28**), the derived (2*R*,4*S*) stereomeric homoadenylate oligomer formed a stable complex with both DNA and RNA.[103] PNAs containing the other pyrrolidine stereoisomers are reported but they do not show any considerable improvement in binding affinity.[104]

A model, has been proposed by Micklefield[105] using a *cis* stereochemistry between the nucleobase and the methylamino unit, creating units which were called pyrrolidine amide oligonucleotide mimics POM, (Figure **1.29**).

(2R, 4R) pyrrolidine PNA
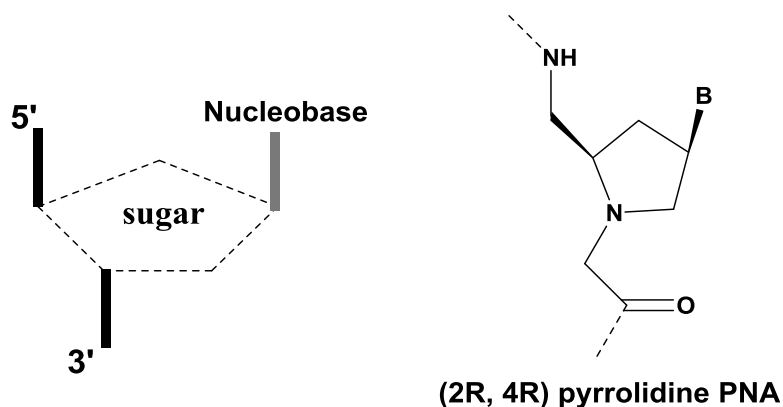
Figure 1.29: Stereochemical model for pyrrolidine amide ODN mimics

As a result, POM hybridises with very high affinity to both complementary nucleic acids, while exhibiting unusual kinetic selectivity for RNA over DNA.[106] The introduction of a methyl group in the acetyl linker was found to suppress DNA affinity.[107] It was found

that mixed-sequences of these compounds showed thermal denaturation at high temperature (higher than non-modified PNAs), while cooling showed a transition at much lower temperature. This kinetic effect was attributed to the rigidity of the POM backbone, which prevents rearrangement necessary for the correct base-pairing.[108] Making POM backbone a little flexible by introducing methylene groups near either the amino- or the carboxy-group resulted in a lower duplex stability, but complete selectivity for RNA over DNA.[109]

Introduction of a methylene bridge between the 5- membered ring and the nucleobase led to another pyrrolidine- PNA[110] (Figure **1.30**).

(2S,4S)-aeg-pyrrolidine-PNA
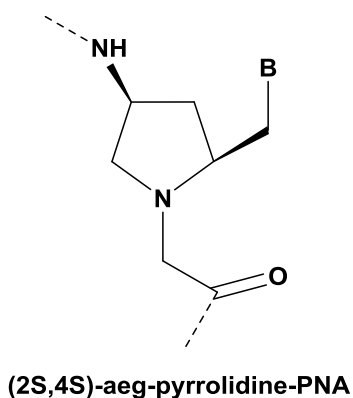
Figure 1.30: Cyclic PNA analogues containing five-membered rings

Diastereomeric monomers bearing T, A, C, G, nucleobases were introduced in PNA oligomers and the complexation with DNA and RNA sequences was studied. It was found that: (i) (2*R*,4*S*) homopyrimidine PNA stabilize PNA2-DNA triplexes.(ii) (2*S*,4*R*) stereoisomers in mixed sequences affects enhanced DNA duplex stability (iii) (2*S*,4*S*) and (2*R*,4*R*) remarkably enhance PNA:RNA duplex stability.

All the pyrrolidine modifications show preference for the antiparallel DNA binding. Thus the effect of stereochemistry is not clear-cut, and relative conformational freedom of the five-membered ring can account for this.

Another example is the highly selective RNA recognition achieved recently by a new pyrrolidine based PNA: backbone extended pyrrolidine (*bep*PNA)[111] (Figure **1.31**)

(2S,4S)-Bep-PNA
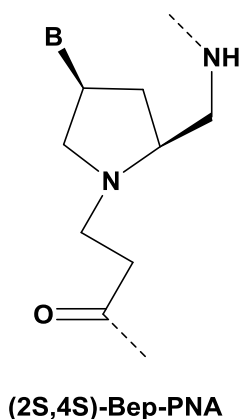
Figure 1.31: Cyclic PNA analogues containing five-membered rings

Binding of this to DNA is weak both for triplex of duplex structures. However, alternate monomers of aegPNA and *bep*PNA showed remarkably high stability with RNA. Therefore, it seems that RNA complexation has different stereochemical and conformational requirements than DNA binding.

Appella *et al.*[112] have designed PNA monomers using molecular models based on the appropriate β-torsion angle using derivatives of *trans*-1,2-cyclopentane units

trans-(1S,2S)-cyclopentyl-PNA
tcyp-PNA
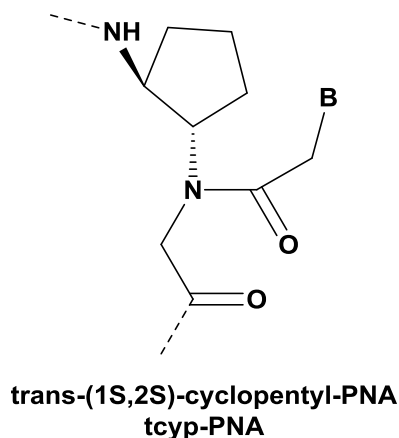
Figure 1.32: Cyclic PNA analogues containing five-membered rings

Thus *trans*-cyclopentane-modified PNA (*tcyp*PNA) structure (Figure **1.32**), which is equivalent to covalently closing the aminoethyl glycine PNA backbone, showed selectivity towards DNA with high levels of mismatch discrimination.[113] The same

authors reported increased stabilization of PNA-DNA duplex, triplexes and quadruplexes induced by the presence of *tcyp*PNA units.[114]

cis-(1R,2S)-cyclopentyl-PNA
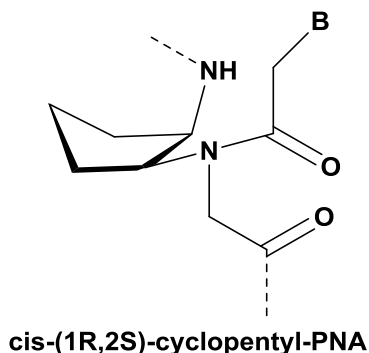
Fig 1.33: Cyclic PNA analogues containing five-membered rings

Cis-(1*R*,2*S*)-cyclopentyl PNAs analogues (Figure **1.33**), (the same as *tcyp*-PNA, except for stereochemistry) with β = ± 25° hybridize to DNA\RNA without discrimination because the ring puckering of the cyclopentane ring.[115]

The N-(pyrrolidinyl-2-methyl)glycine (pmg) PNA monomer (Figure **1.34**), R = H, n = 1], earlier reported by Slaitas *et al.*,[116] was incorporated in mixed purine/pyrimidine PNA sequences. It was found that pmg-PNA monomers considerably destabilize the duplex formed either with DNA or RNA (-14 ℃ to -16 ℃).

pmg-PNA:R=H,n=1
pet-PNA:R=H,NH$_2$,guanidine,n=2
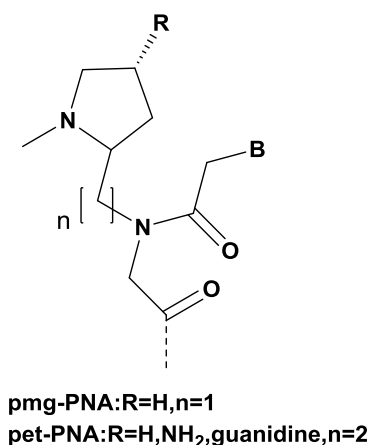
Figure 1.34: Cyclic PNA analogues containing five-membered rings

To reduce the destabilizing effect of pmg-PNA, the N-(pyrrolidinyl-2-ethyl)glycine (pet) PNA (Figure **1.34**), R = H, n= 2], which contains an extended backbone, was recently reported by Kumar *et al.*[117] It was found that incorporation of pet-PNA monomers in a

mixed sequence remarkably improves the PNA-DNA duplex stability (+3-9 ℃); but slightly destabilizes duplexes with RNA by 2-6 ℃. This suggests that the destabilizing effect due to the large constraint of the pyrrolidine ring in pmg-PNA could be compensated by the additional flexibility of an extended backbone.

Insertion of an amino/guanidino unit at the 4- position of the pyrrolidine ring of pet-PNA monomer (Figure **1.34**), R = amino/guanidino, n= 2], further improved the duplex stability. Thus, the combination of chirality, flexibility through extended backbone and electrostatic interactions might be useful in stabilizing pyrrolidine-based PNADNA/ RNA duplexes.

Incorporation of an ether linker between the 5-membered ring of pyrrolidine and the C-terminus of the monomer led to a new class of pyrrolidine-based PNAs named "Pyrrolidine Oxy-Peptide Nucleic Acids (POPNAs)" (Figure **1.35**).[117]

trans-L-pyrrolidine oxy-PNA   trans-L-pyrrolidine amino-PNA
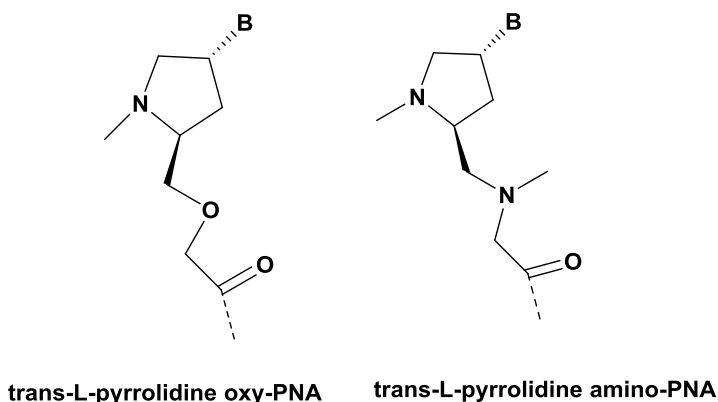
Figure 1.35: Cyclic PNA analogues containing five-membered rings

Although all the diastereoisomers have been shown to successfully hybridize DNA and RNA, it was found that the cis-L-POPNAs formed the most stable duplex. The wide adaptability of POPNAs to DNA and RNA, was attributed to their highly flexible backbone, which contains ether linkages.

Synthesis of pyrrolidine-based peptide nucleic acids, that contain a tertiary amine in the backbone (PAPNAs = Pyrrolidine- based Amino Peptide Nucleic Acids) (Figure **1.35**) was also reported.[118] A mixed sequence of trans-L PAPNA and POPNA monomers was

synthesized and was more efficiently delivered into CHO cells than the corresponding POPNA oligomer, despite no increase in duplex stability was observed.

Cyclic PNA analogues containing six-membered rings:

In contrast to the rigid locked chair conformation of a cyclohexane system, the cyclopentane ring is more flexible and can be easily conformationally adjusted. An example of the behaviour of two stereoisomers of a 6-membered ring PNA is the discrimination between the parallel versus antiparallel DNA reported for a single modified (2*S*, 5*R*) aminoethyl pipecolic PNA unit[119] (Figure **1.36**) inserted in the middle of the strand.

(2R,5S)-aepip-PNA   **(3R,6R)-piperidone-PNA**
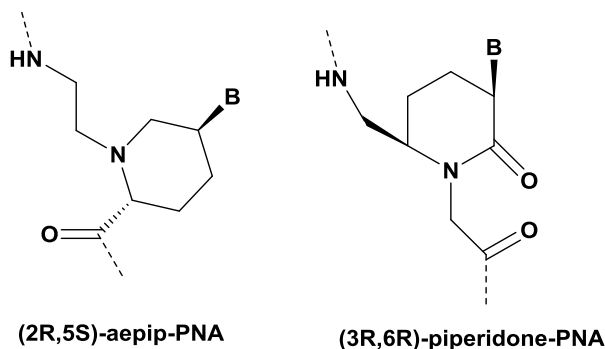
Figure 1.36: Cyclic PNA analogues containing six-membered rings

The effect is highly dependent on the position of the stereocenters, as it has been already seen for flexible chiral PNAs. PNAs derived from piperidinone[120] (Figure **1.36**) were also reported, though the rigidity of the ring and their particular geometry led to a decrease of PNA:DNA duplex stability; however, the best performing was the (3*R*,6*R*)-isomer, which is in line with proper group arrangement.

The substitution of the aminoethyl residue with *trans*- 1,2-diaminocyclohexane gave a PNA (Figure **1.37**) whose performances were found to be dependent on stereochemistry, the (*S*,*S*)-isomer being more effective.[121]

From proposed molecular model of a di-axial arrangement of the substituents, the 180° dihedral angle was not optimal for DNA binding, thus leading to a destabilizing effect. The *cis*-1,2 equatorial-axial (S,R/R,S)-cyclohexanyl PNAs (chPNAs) (Figure **1.37**) with

$\beta \pm 65°$ were designed on the basis of modelling. The chPNAs expressed remarkable differences in duplex stability with their DNA and RNA complexes, depending on number of modification and stereochemistry. There is a highly significant preference for these compounds to form a duplex with RNA as compared to DNA,[122] as also found in a modeling study.[123]
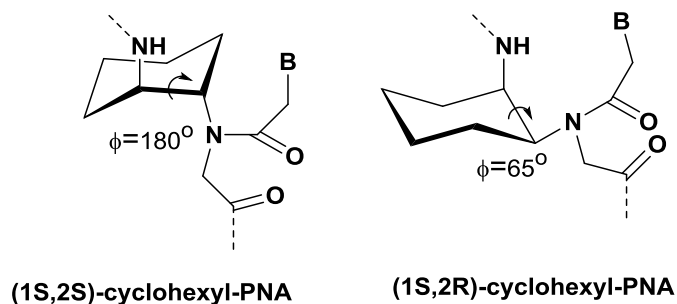

(1S,2S)-cyclohexyl-PNA   **(1S,2R)-cyclohexyl-PNA**

Figure 1.37: Cyclic PNA analogues containing six-membered rings

A fully modified decamer of pyrrolidinyl- PNA (Figure **1.38**)[124] in which a D-1-aminopyrrolidine-2- carboxylic acid spacer (with an hydrazine residue) was introduced in the N-terminal part of the monomer, showed a remarkable preferential affinity for complementary DNA over RNA.[125]

Vilaivan *et al*. have reported a composite structure of particular interest, prolyl- (ACPC)- PNA (Figure **1.38**), consisting of alternating α-amino acid proline as a nucleobase carrier and chiral 2- aminocyclopentane carboxylic acid (ACPC). This structure also showed selectivity for DNA over RNA and was tested in mixed sequences, showing sequence recognition and direction control.[126]

In an attempt to improve the solubility of PNAs in biological fluids, a number of structural modifications have been reported which have incorporated charged or hydrophilic functional groups along the backbone. Promising examples of this type include the oxy-PNAs (Figure **1.39**)[127] the phosphono-PNAs (Figure **1.39**)[128] backbone. In addition, a significant amount of effort has been devoted to developing analogs and conjugates with good cell membrane permeability.

pirrolidinyl-PNA   prolyl-(ACPC)-PNA
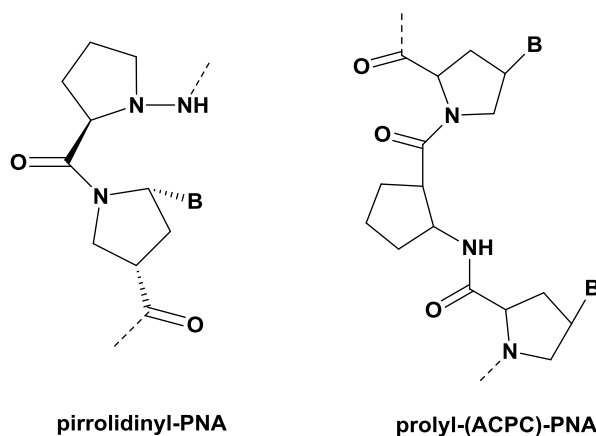
Figure 1.38: Cyclic PNA analogues containing five-membered rings

X=O,NH
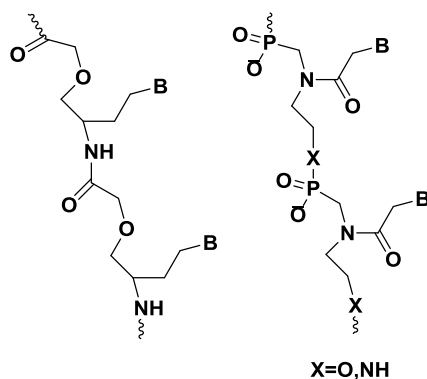
Figure 1.39: Hydrophilic backbone of PNA

Non-peptide backbone PNA: Several PNA analogues in which peptide bonds are replaced by other linkages, such as ester or phosphodiester bond have been reported. These include analogues that are based on N-(2aminoethyl) aminomethyl phosphonic acid (PPNA, PHONA, PGNA, PAGNA) and molecules with amine in the backbone.[129] Flexible backbones containing a secondary amine replacing the secondary amide (PANA) (Figure **1.40**) were introduced by Myers *et al.*[130] Analysis of the thermal stability on PANA/DNA duplexes revealed that incorporation of one PANA monomer does not destabilize the duplex.

Phoshpono PNAs (PPNA) (Figure **1.40**), were introduced to overcome the poor solubility issue of PNA in aqueous environment. They interact with DNA and RNA forming triplexes whose stability is reduced as compared to those formed by natural DNA. Also

PPNA/DNA hybrids showed destabilization due to the charge repulsion between phosphates on DNA and phosphate in PPNA.
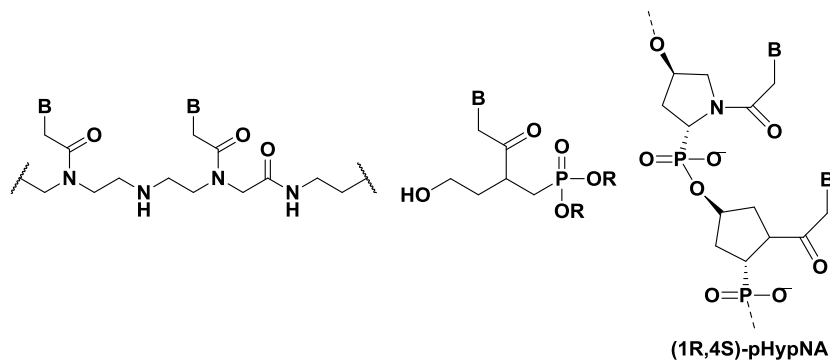
Figure 1.40: Non-peptide backbone in PNA

Conformationally constrained analogues with a trans- 4-hydroxy-*N*-acetylpyrrolidine-2-phosphonate (pHypNAs) backbone exhibit interesting binding properties, as they hybridise complementary DNA and RNA with high affinity and specificity.[131] Moreover, pHypNAs show good ability to penetrate cell membranes together with high antisense activity in a cell-free system, in living cells and in model organism.

Analogues with modification on the nucleobase: Substitution of natural bases for analogues can be used for interfering with the hybridization process, for example N^4-benzoyl cytosine[132] (Figure **1.41 (a)**) has been shown to cause inhibition of triplex formation. Whereas E-base[133] (Figure **1.41b**) rationally designed to recognize T-A base pair, stabilizes a triplex even if the target strand contains one or two pyrimidine residues. 2-Thiouracil[134] (Figure **1.41c**) along with 2,6-diaminopurine[134] (Figure **1.41d**) was used as a non-natural base pair in PNA-DNA recognition and was shown to lead to 'double duplex invasion'.
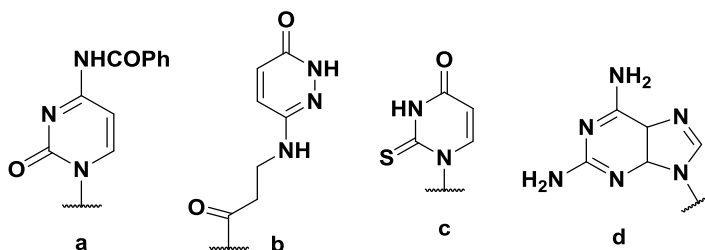
Figure 1.41: Modified nucleobases

Pyrimidines with extended aromatic moieties as a means of increasing the stacking energy and hence the stability of the hybridized complexes represent another class of modified nucleobases. Incorporation of tricyclic phenothiazine,[135] (Figure **1.42a**) a substitute to cytosine and bicyclic/tricyclic naphthyridinones,[135] (Figure **1.42b &1.42c**) substitute to thymine, showed a modest increase in affinity.
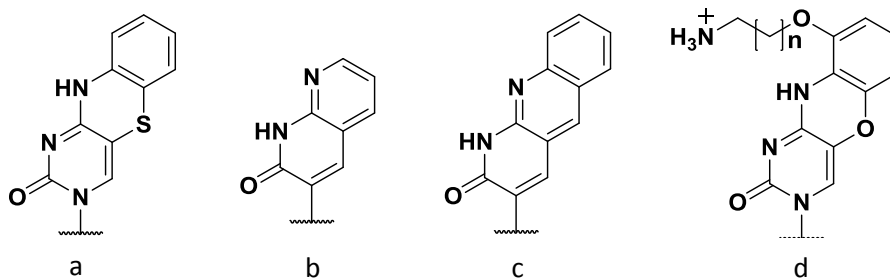
Figure 1.42: Modified nucleobases

Tricyclic cytosine[136] (Figure **1.42d**) analogues based on the phenoxazine gave the high increased affinity and sequence specificity towards target. This shows that along with molecular stacking overlap, electronic factors contribute to base pair stacking stabilization. Also 3-Nitropyrrole[137] (Figure **1.43a**) and 5-nitroindole[138] (Figure **1.43b**) have been incorporated into PNA as universal bases.
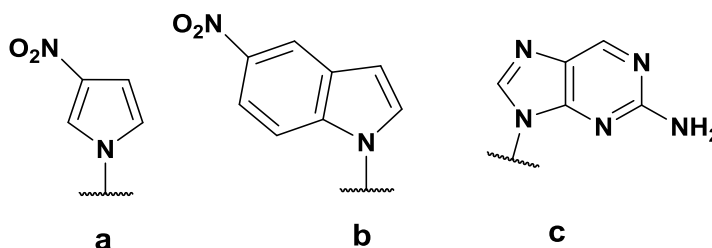
Figure 1.43: Modified nucleobases

Nucleobase modifications can also help to make PNA fluorescent. 2-Aminopurine[138] (Figure **1.43c**) being intrinsically fluorescent can be used to study PNA-DNA interaction dynamics.

Substitution of the natural nucleobases with ligands such as bipyridine and 8-hydroxyquinoline can be used to incorporate transition metal ion into PNA.[139] Intrahelix

base pairing properties of a nucleobase involve both hydrogen bonding and stacking properties.

1.8 Applications of PNA:

This section describes diverse PNA applications in gene therapeutics, molecular biology, functional genomics etc.

PNA in antisense and antigene therapy: Because of their strand invasion property and being chemically and biologically stable, PNAs can be used to design gene therapeutic drugs.[140] The primary requisite is the identification of targets and a suitable cellular delivery system for them. There are basically two strategies involved in using PNAs as therapeutic drugs, namely antigene and antisense methods.

PNAs as antigene agents: In antigene strategy the PNAs' interfere with the transcription of a particular gene. PNAs can do it because of their ability to form a stable triplex structure or a strand invasion or strand displacement complex with DNA. Such complexes by a structural hindrance block the stable functioning of RNA polymerase and thus work as antigene agents (Figure **1.44**).

PNA targeted against the promoter region can form a stable PNA/DNA complex that restricts the DNA access of the corresponding polymerase. Nielsen *et al.*[141] have demonstrated that even an 8-mer PNA (T_8) is capable of blocking phage T_3 polymerase activity.
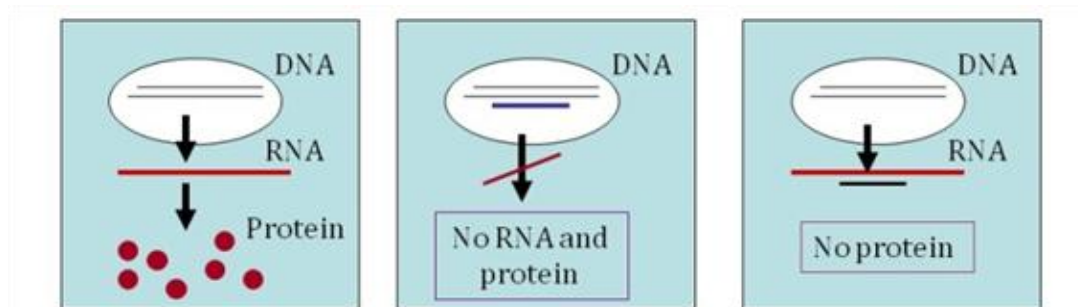
Figure 1.44: Antigene & antisense inhibition strategy[141]

PNAs as antisense agents: In the case of antisense strategy the nucleic acid analogues can be designed to recognize and hybridise to complementary sequences in mRNA and thereby inhibit its translation (Figure **1.44**). Normally, the PNA antisense effect is based on the steric blocking of either RNA processing, transport into cytoplasm, or translation. I*n vitro* translation experiments involving rabbit reticulocyte lysates concluded that both duplex-forming (mixed sequence) and triplex-forming (pyrimidine rich) PNAs are capable of inhibiting translation at targets overlapping the AUG start codon.[142] Recently PNAs and PNA-peptide conjugates have been used for redirecting RNA splicing in therapeutic applications such as Duchenne Muscular Dystrophy in cells as well as animal models.[143] In another example, PNA has also shown to inhibit microRNA, miR-155 which is expressed in haematopoietic systems in cultured B cells and in mice.[144]

Inhibition of replication: It is also possible for using PNA to inhibit the elongation of DNA primers by DNA polymerase. Further, the inhibition of DNA replication should be possible if the DNA duplex is subjected to strand invasion by PNA under physiological conditions or if the DNA is single stranded during the replication process. Efficient inhibition of extra chromosomal mitochondrial DNA, which is largely single stranded during replication, has been demonstrated by Taylor *et al.*[145]

Interaction of PNA with enzymes

RNase H enzyme

The activation of the intracellular enzyme RNase H by oligonucleotides to cleave RNA bound to deoxyribonucleic acid oligomers depends on the chemical structure of RNase H-stimulating oligonucleotides. The antisense oligonucleotide with an RNase H activity (e.g., phosphorothioate oligos) is considered a better antisense molecule (inhibitor) than one without the activity (methylphosphonates and hexitol nucleic acids).[146] Despite their remarkable nucleic acid binding properties, PNAs generally are not capable of stimulating RNase H activity on duplex formation with RNA. However, recent studies have shown that DNA/PNA chimerae are capable of stimulating RNase H activity. On formation of a chimeric RNA double strand, PNA/DNA can activate the RNA cleavage activity of RNase H (Figure **1.45**). Cleavage occurs at the ribonucleotide sites basepaired

to the DNA part of the chimera. Moreover, this cleavage is sequence specific in such a way that certain sequences of DNA/PNA chimeras are preferred over others.
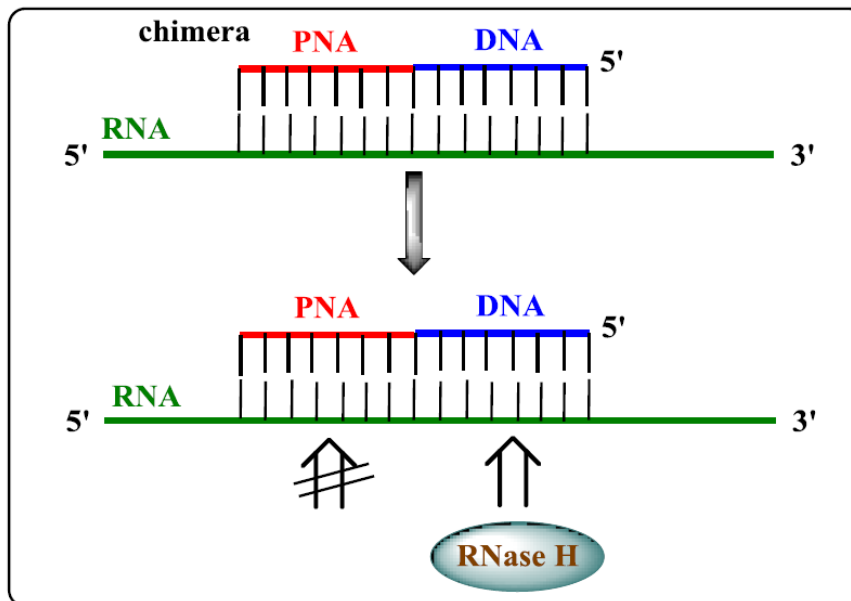

Figure 1.45: Schematic representation of RNase H-mediated cleavage activity after the binding of a PNA:DNA chimera to a RNA target

Polymerase and reverse transcription: In general, there is no direct interaction of PNA with either DNA polymerase or reverse transcriptase. However, it is reported that there is indirect involvement of PNA in inhibiting these enzyme functions (activity) under *in vitro* conditions.

Nielsen et al.[147] demonstrated that the primer extension catalyzed by *Taq*-polymerase can be terminated by incorporating a PNA oligomer (PNA-H(t)$_{10}$) into the system which binds to a (dA)$_{10}$ sequence in the template and thereby terminate the primer extension. The reverse transcription of *gag* gene of HIV I is also inhibited *in vitro* by PNAs, by using a bis-PNA construct, which is more efficient than the corresponding mono PNA construct.[148]

PNA as a molecular-biological tool:
PNA for artificial restriction system: There are many sequences which are not recognized by the restriction enzymes; in such cases, PNAs with sequences

complementary thereto the recognition sequences are designed. These PNAs hybridise to the complementary targets on dsDNA via a strand invasion mechanism and loop out the non-complementary DNA sequences.[149] The single-stranded looped-out fragments of DNA are then removed by S1 nuclease, which cleaves single stranded nucleic acids, releasing 59-phosphoryl mono oroligonucleotides. Therefore PNA can be used as a cutting tool in combination with S1 nuclease to make an 'artificial restriction enzyme' system. If two PNAs are used for this purpose and allowed to bind to two adjacent targets on either the same or opposite DNA strands, it will essentially open up the entire region, making the substrate accessible for the nuclease digestion and thereby increasing the cleavage efficiency.[150]

PNA for rare enzyme cutting: A problem of using restriction enzymes is that it cleaves the DNA at more than one place if there are a number of restriction sites on the DNA sequence. PNAs in combination with methylases and other restriction endonucleases can act as rare genome cutters and can be used to solve this problem. This method is called the PNA-assisted rare cleavage (PARC) technique and it uses the strong sequence-selective binding of PNAs, preferably bis-PNAs, to short homopyrimidine sites on large DNA molecules.[151] The DNA is efficiently protected from enzymatic digestion at all sites except for those bound to PNA. Thus short PNA sequences, particularly positively charged bis-PNAs, in combination with various methylation/restriction enzyme pairs can constitute an extraordinary new class of rare genome cutters.

Enhanced PCR amplification: The polymerase chain reaction (PCR) has been widely used for various molecular genetic applications including the amplification of variable number of tandem repeat (VNTR) loci for the purpose of genetic typing.[152] However, in some cases, preferential amplification of small allelic products relative to large allelic products presents a problem. This results in an incorrect typing in a heterozygous Sample. PNA has been used to achieve an enhanced amplification of VNTR locus D1S80(6) For PCR amplification, small PNA oligomers block the template that becomes unavailable for intra- and interstrand interaction during re-association step. Although re-association is blocked by PNA, primer extension can occur. This approach shows the

potential of PNA application for PCR amplification where fragments of different sizes are required to be more accurately and evenly amplified. Since the probability of differential amplification is less, the risk of misclassification is greatly reduced.

The high-affinity binding of PNA oligomers has led to the development of new applications of PNA, especially as a diagnostic probe for detecting genetic mutations: applications are possible for the detection of genetic mutation and mismatch analysis that can use its unique hybridization properties.

Single base pair mutation analysis using PNA directed PCR clamping: Amplification of the target nucleic acid by the PCR technique is considered an important step for detection of genetic diseases. This novel technique is based on high specific binding of PNA to DNA, higher stability of a PNA–DNA duplex compared to the corresponding DNA–DNA duplex, and its inefficiency to act as a primer for DNA polymerases. Single-base-pair mutation or single-nucleotide polymorphism (SNP) analysis is possible using the PCR technique if PNA is synthesized targeting the primer binding site (Figure **1.46**).[153]
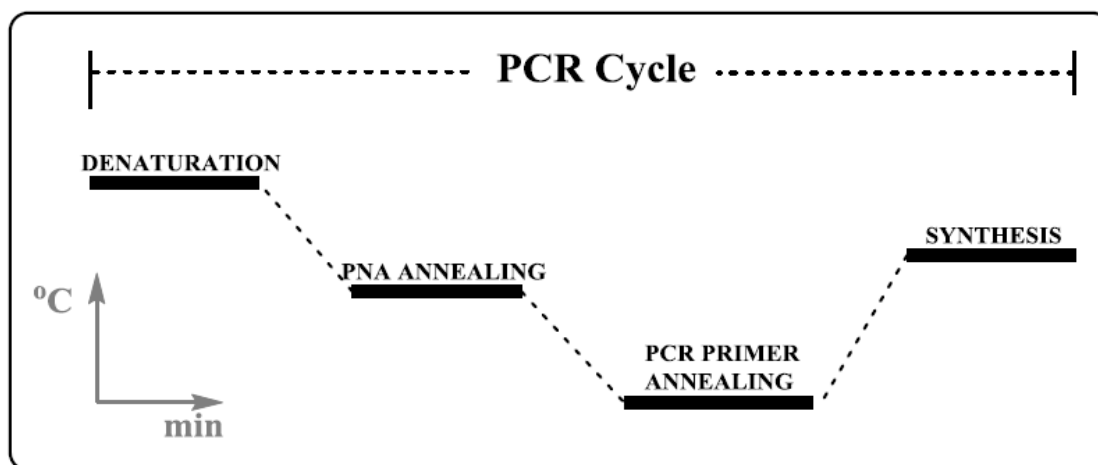
Figure 1.46: Schematic of PCR cycle profile used in PNA-directed clamping

Basically, in the PNA directed PCR clamping technique, at the annealing step the PNA is targeted against one of the PCR primer sites. The temperature set for this step is higher than that for normal PCR primer annealing, where the PNA is selectively bound to the

DNA molecule. The PNA, which binds to the primer binding site instead of the primer, effectively blocks the formation of a PCR product. PNA is able to discriminate between fully complementary and single mismatch targets (mutations) in a mixed target PCR. Hence the binding of primer will be favored to out-compete PNA annealing. Consequently, mutated sequences will be preferentially amplified. This PNA clamping is able to discriminate three different point mutations at a single position.

PNA as biosensor for nucleic acids

Surface-attached PNA molecular beacons: Molecular beacons are molecules with a fluorescent dye at one terminus and a quencher molecule at the other.[154]

When its conformation is such that the fluorophore and quencher lie next to each other, the molecule does not emit a signal, since the emission spectrum of the fluorophore and the absorption spectrum of the quencher overlap and the energy emitted by the fluorophore is absorbed by the quencher. On hybridization, the molecule stretches out, separating the quencher and the fluorophore and the fluorescent dye emits a signal, thus reporting the occurrence of hybridisation. Molecular beacons represent a versatile tool in DNA diagnostics. Although these molecules initially had a hairpin structure with a stem, it was later found, especially for PNA molecules, that a stem is not required for their functioning. In contrast to DNA molecular beacons, stemless PNA beacons (Figure 1.**47**) are less sensitive to ionic strength, and the quenched fluorescence of PNA is not affected by DNA-binding proteins. This enables the usage of PNA beacons under conditions that are not feasible for DNA beacons. Immobilisation on both flat surfaces and optical fibres has been reported for both DNA and PNA beacons.

PNA probe for microarray: Microarrays usually make use of DNA probes, which can be synthetic oligonucleotides or longer enzymatically generated DNA, specifically PCR products and isolated clone DNA. The probes are immobilised sensor molecules of known sequence. Although DNA probes work well, they have problems of selectivity, sensitivity and stability under various conditions. With DNA probes of longer length, such as PCR products, sensitivity is not a problem but selectivity is greatly reduced.

Oligomers normally used for DNA sequencing by hybridisation have a relatively low duplex stability. Another common problem of using DNA probes is that DNA sequences form stable duplexes only in the presence of a salt, which is needed to counteract the inter-strand repulsion. Such conditions, however, also stabilise secondary and tertiary structures within a target molecule. Sequences might therefore not be accessible and be prevented from hybridisation to the gridded DNA.
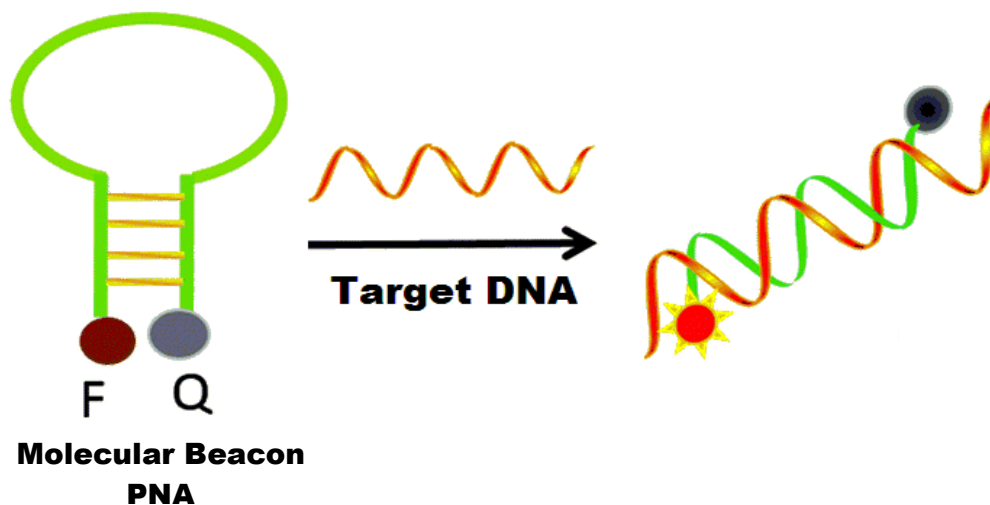

Figure 1.47: Schematic representation of molecular beacon

1.9 Scope of present work:

Peptide nucleic acids provide a novel class of compounds with wide biological potential. In view of the chemical and biological consequences of this hybrid structure, PNA has a unique position compared with many other nucleic acid derivatives and could make an impact particularly in the fields of antigene and antisense therapy and probe-based assays. The main advantage of PNA is the combination of many features that are very similar to those of natural DNA with additional characteristics that are rather different. The major drawbacks of PNA like poor water solubility, inefficient cellular uptake, self-aggregation and ambiguity in directional selectivity of binding restrict its applications in terms of designing PNA-based gene targeted drugs. Hence, various modifications of PNA to overcome these limitations have been employed by different research groups as described in previous section.

Chapter 2: Design and synthesis of *gem*-dialkyl substituted PNA monomers and their oligomerization.

In contrast to well-known strategies towards chiral, cyclic and conformationaly constrained PNAs, the approach in the present thesis is to achieve the desired selectivity towards nucleic acids by keeping PNAs achiral and acyclic. The chapter deals with the design, synthesis, characterization of novel γ and β-C-substituted PNA monomers (Figure **1.48**) and their incorporation of these modified PNA units at various positions in the mixed purine-pyrimidine sequence using solid phase peptide synthesis.
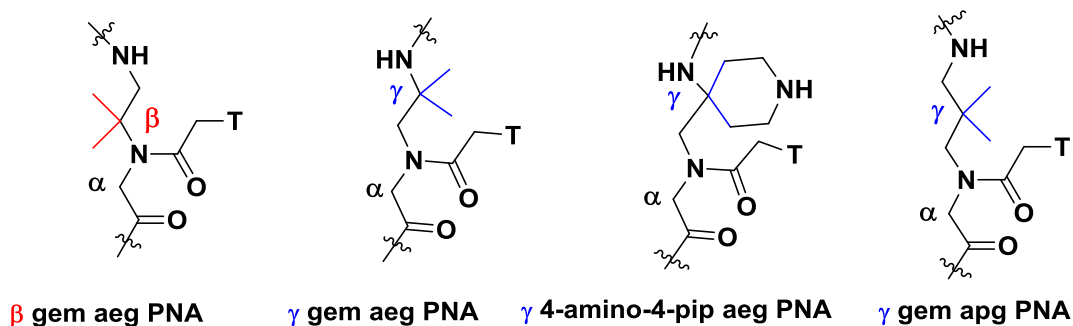
Figure 1.48: Chemical structures of modified PNA monomers

Chapter 3: This chapter deals with the biophysical evaluation of various modified PNA oligomers. Temperature dependent UV absorbance studies give the determination of thermal stabilities of PNA: DNA duplexes with complementary DNA. Mismatch basepair specificity is also determined from these studies. The effect of various substitutions at γ and β position on the conformation of PNA: DNA duplexes are investigated by Circular Dichroism (CD) studies.

Chapter 4, Section A: Self-assembly

Molecular self-assembly is the spontaneous organization of molecules under thermodynamically favoured conditions into structurally well-defined and stable arrangements through non-covalent interactions. i.e hydrogen bonding, electrostatic attraction, hydrophobic force and van der Waals interactions. Among the many self-assembly systems (DNA, protein/peptide, lipid and surfactant), peptides have drawn much attention in nanoscience and nanotechnology due to their desirable

chemical/physical properties and biological functionalities. The morphology of self-assembled peptide nanostructures depends on various factors like pH, temperature, solvent etc. PNAs comprising the peptide backbone and nucleobases of oligonucleotides, may exhibit different nanostructures. With this idea we thought of studying the ability of dialkyl substituted PNA's to form nanostructures in single strand and duplex form with complementary DNA using FESEM.

In this Chapter, self-assembling properties for single stranded PNAs and in duplex form with complementary DNA were investigated.

Chapter 4, Section B: Cell uptake studies of PNA analogues

This chapter deals with cell permeation studies of the fluorescently labeled modified PNA analogs into NIH 3T3 (normal fibroblast) and breast cancer causing MCF-7 cell lines. The differential cell permeation ability of various PNA oligomers is quantitatively studied by fluorescence activated cell sorter (FACS) analysis.

1.10 References:

1. Alberts, B.; Johnson, A.; Lewis, J.; Raff, M.; Roberts, K.; Wlater, P. Molecular *Biology of the Cell* (4th ed.). Garland Science. **2002**, pp. 120-121.
2. Watson, J. D.; Crick, F. H. C. Nature, **1953**, *171*, 737-738.
3. Hoogsteen, K. *Acta. Crystal*. **1963**, *16*, 907-916.
4. (a) Crick, F. H. C. Codon-Anticodon pairing. The Wobble Hypothesis. J. Mol. Biol. 1966, 19, 548-555. (b) Soll, D.; Cherayil, J. D.; Bock, R. M.; *J. Mol. Biol*. **1967**, *29*, 97-112.
5. Seeman, N. C.; Rosenberg, J. M.; Rich, A. *Proc. Natl. acad. Sci*. USA **1976**, *73*, 804.
6. (a) Brahms, J.; Mommaerts, W. F. H. M. *J. Mol. Biol*. **1964**, *10*, 73-85. (b) Fuller, W.; Wilkins, M. H. F.; Wilson, H. R.; Hamilton, L. *J. Mol. Biol*. **1965**, *12*, 60-80. (c) Dickerson, R. E. *Methods in Enzymol*. **1992**, *211*, 67-111. (d) Saenger, W. (Ed) Springer-Verlag, New York, **1984**. (e) Wang, A. H. J.; Quigley, G. J.; Kolpak, F. J.; Van der M. G.; Van Boom, J. H.; Rich, A. *Science*, **1981**, *211*, 171-176.
7. *Molecular Cell* 17:671–682
8. (a) Seeman, N. C. *Nature* **2003**, *421*:427-431. (b) Seeman, N. C. *Annu Rev Biochem* **2010**, *79*:65-87
9. (a) Seeman, N. C.; J. Theor. *Biol*. 99, 237, **1982** (b) Rothemund, P. W. *Nature*. **2006**, *440*:297-302.
10. Petrillo M. L, Newton C. J.; Cunningham R. P.; Ma RI, Kallenbach N. R.; Seeman N. C. *Biopolymers* **1998**, *27*:1337-1352
11. (a) Weile J and Knabbe C, **2009**. *Anal Bioanal Chem* **394**: 731-742 (b) Muldrew K L, **2009**. *Curr OpinPediatr 21*: 102-111.
12. Bennett, C.F. *Antisense Nucleic Acid Drug Dev* **2002**, *12*, 215-24.
13. Uherek C, Wels W, **2000,** *Adv Drug Deliv* Rev *44*:153–166
14. Johnston S A, Talaat A M, McGuire M G. **2002,** *Arch Med Res* 33:325–329
15. Santoro S W, Joyce G F. **1997**; *94*: 4262–6.
16. Santiago F S, Lowe H C, Kavurma M M, Chesterman C N, Baker A, Atkins D G, Khachigian L M. *Nat Med* **1999**; *5*: 1264–9.
17. Zhang L, Gasper W A, Stass SA *et al.* **2002**, *Cancer Res* 62:5463–5469
18. A. Fire, S. Xu, M. K. Montgomery, S. A. Kostas, S. E. Driver and C. C. Mello, *Nature*, **1998**, 391, 806.
19. http://www.landesbioscience.com/
20. E. Bernstein, A. A. Caudy, S. M. Hammond and G. J. Hannon, *Nature*, **2001**, 409, 363.
21. (a) T. A. Rand, K. Ginalski, N. V. Grishin and X. Wang, Proc. Natl. Acad. Sci. U. S. A., 2004, 101, 14385. (b) C. Matranga, Y. Tomari, C. Shin, D. P. Bartel and P. D. *Zamore, Cell*, **2005**, 123, 607.
22. http://www.alnylam.com
23. T. A. Rand, S. Petersen, F. Du and X. Wang, *Cell*, **2005**, 123, 621.

24. Y. Lee, M. Kim, J. Han, K. H. Yeom, S. Lee, S. H. Baek and V. N. Kim, *EMBO J.*, **2004**, *23*, 4051.

25. Han J, Lee Y, Yeom K-H *et. al.* **2004**, *Genes Dev* 18:3016–3027

26. E. Lund, S. G¨uttinger, A. Calado, J. E. Dahlberg and U. Kutay, *Science*, **2004**, 303, 95.

27. Bernstein E, Caudy AA, Hammond SM *et al* **2001**, *Nature* 409:363–366

28. L. He and G. J. Hannon, *Nat. Rev. Genet.*, **2004**, *5*, 522.

29. M. Kiehntopf, E. L. Esquivel, M. A. Brach and F. Herrmann, *Lancet*, **1995**, *345*, 1027

30. K. Kruger, P. J. Grabowski, A. J. Zaug, J. Sands, D. E. Gottschling and T. R. Cech, *Cell*, **1982**, *31*, 147

31. (a) R. Robinson, *PLoS Biol.*, **2004**, *2*, e28. (b) D. Mueller, U. Stahl and V. Meyer, *J. Microbiol. Methods*, **2006**, *65*, 585; (c) T. L. H. Jason, J. Koropatnick and R. W. Berg, *Toxicol. Appl. Pharmacol.*, **2004**, 201, 66.

32. (a) N. Usman and L. M. Blatt, J. Clin. *Invest*, **2000**, *106*, 1197. (b) A. Peracchi, *Rev. Med. Virol.*, **2004**, *14*, 47.

33. J. Morschh¨auser, K. S. Barker, T. T. Liu, J. BlaB-Warmuth, R. Homayouni and P. D. Rogers, *PLoS Pathog.*, **2007**, *3*, e164.

34. A. Bielinska, R. A. Shivdasani, L. Q. Zhang and G. J. Nabel, *Science*, **1990**, *250*, 997.

35. (a) S. Ohuchi, BioRes. *Open Access*, **2012**, *1*, 265. (b) H. P. Dwivedi, R. D. Smiley and L. A. Jaykus, *Appl. Microbiol. Biotechnol.*, **2013**, *97*, 3677. (c) N. Duan, S. Wu, X. Chen, Y. Huang, Y. Xia, X. Ma and Z. Wang, *J. Agric. Food Chem.*, **2013**, *61*, 3229. (d) M. Avci-Adali, N. Wilhelm, N. Perle, H. Stoll, C. Schlensak and H.P. Wendelk, *Nucleic Acid Ther.*, **2013**, *23*, 125. (e) K. Ninomiya, K. Kaneda, S. Kawashima, Y. Miyachi, C. Ogino and N. Shimizu, *Bioorg. Med. Chem. Lett.*, **2013**, *23*, 1797.

36. P. L. Iversen, T. K. Warren, J. B. Wells, N. L. Garza, D. V. Mourich, L. S. Welch, R. G. Panchal and S. Bavari, *Viruses*, **2012**, *4*, 2806

37. (a) Y. Kasahara, S. Kitadume, K. Morihiro, M. Kuwahara, H. Ozaki, H. Sawai, T. Imanishi and S. Obika, *Bioorg. Med. Chem. Lett.*, **2010**, *20*, 1626; (b) L. Beigelman, J. Matulic-Adamic, P. Haeberli, N. Usman, B. Dong, R. H. Silverman, S. Khamnei and P. F. Torrence, *Nucleic Acids Res.*, **1995**, *23*, 3989; (c) A. D. Keefe, S. Pai and A. Ellington, *Nat. Rev. Drug Discovery*, **2010**, *9*, 537.

38. (a) S. Hoffmann, J. Hoos, S. Klussmann and S. Vonhoff, *Current Protocols in Nucleic Acid Chemistry*, **2011**, chapter 4, unit 4.46.1–30; (b) A. Vater and S. Klussmann, *Curr. Opin. Drug Discovery Dev.*, **2003**, *6*, 253.

39. (a) J. M. Healy, S. D. Lewis, M. Kurz, R. M. Boomer, K. M. Thompson, C. Wilson and T. G. McCauley, *Pharm. Res.*, **2004**, *21*, 2234; (b) T. Kawaguchi, H. Asakawa, Y. Tashiro, K. Juni and T. Sueishi, *Biol. Pharm. Bull.*, **1995**, *18*, 474; (c) S. R.

Watson, Y. F. Chang, D. O'Connell, L. Weigand, S. Ringquist and D. H. Parma, *Antisense Nucleic Acid Drug Dev.*, **2000**, *10*, 63.

40. B. J. Hicke and A. W. Stephens, J. Clin. *Invest*., **2000**, *106*, 923.

41. E. W. Ng, D. T. Shima, P. Calias, E. T. Cunningham, Jr, D. R. Guyer and A. P. Adamis, *Nat. Rev. Drug Discovery*, **2006**, *5*, 123.

42. (a) Y. Kasahara, S. Kitadume, K. Morihiro, M. Kuwahara, H. Ozaki, H. Sawai, T. Imanishi and S. Obika, , *Bioorg. Med. Chem. Lett.*, **2010**, *20*, 1626–1629; (b) L. Beigelman, J. Matulic- Adamic, P. Haeberli, N. Usman, B. Dong, R. H. Silverman, S. Khamnei and P. F. Torrence, *Nucleic Acids Res*., **1995**, *23*, 3989–3994; (c) A. D. Keefe, S. Pai and A. Ellington, *Nat. Rev. Drug Discovery*, **2010**, *9*, 537–550.

43. P. C. Zamecnik and M. L. Stephenson, *Proc. Natl. Acad. Sci.* U. S. A., **1978**, 75, 280.

44. B. A. Armitage, *Nat. Chem. Biol.*, **2005**, *1*, 185.

45. (a) B. A. Armitage, *Nat. Chem. Biol*., **2005**, 1, 185. (b) H. A. Quigley, *Lancet*, **2011**, 377, 1367.

46. Bennett, C. F.; Swayze, E. E. *Annu. Rev. Pharmacol. Toxicol.* **2010**, *50*, 259-293.

47. (a) J. Mickelfield, *Curr. Med. Chem.*, **2001**, 8, 1157. (b) D. R. Corey, J. Clin. *Invest*., **2007**, *117*, 3615.(c) (i) T. P. Prakash, A. M. Kawasaki, E. V. Wancewicz, L. Shen, B. P. Monia, B. S. Ross, B. Bhat and M. Manoharan, *J. Med. Chem.*, **2008**, *51*, 2766; (ii) J. Wengel, *Acc. Chem. Res.*, **1999**, *32*, 301.

48. (i) C. F. Bennett and E. E. Swayze, *Annu. Rev. Pharmacol. Toxicol.*, **2010**, *50*, 259– 293 (ii) S. M. Rahman, T. Baba, T. Kodama, M. A. Islam and S. Obika, *Bioorg. Med. Chem.*, **2012**, *20*, 4098–4102; (iii) E. DeClerq, F. Eckstein and T. C. Merigan, Science, 1969, 165, 1137–1139.

49. (i)Brown, D. A.; Kang, S. H.; Gryaznov, S. M.; De Dionisio, L.; Heidenreich, O.; Sullivan, S.; Xu, X.; Neerenberg, M. I. *J. Biol. Chem.* **1994**, *43*, 26801-26805.(ii) Guvakova, M. A.; Yakubov, L. A.; Vlodavsky, I.; Tonkinson, J. L.; Stein, C. A. *J. Biol. Chem.* **1995**, *270*, 2620-2627. (iii) Rockwell, P., O'Connor, W.; King, K.; Goldstein, N. I.; Zhang, L. M.; Stein, C. A. *Proc. Natl Acad. Sci. USA,* **1998**, *94*, 6523-6528

50. (a) T. P. Prakash, *Chem. Biodiversity,* **2011**, *8*, 1616–1641; (b) T. P. Prakash and B. Bhat, *Curr. Top. Med. Chem.*, **2007**, *7*, 641–649.

51. (a) S. Obika, K. Morio, D. Nanbu, Y. Hari, H. Itoh and T. Imanishi, *Tetrahedron*, **2002**, *58*, 3039–3049; (b) S. Obika, D. Nanbu, Y. Hari, K. Morio, Y. In, T. Ishida and T. Imanishi, *Tetrahedron Lett.*, **1997**, *38*, 8735–8738; (c) A. A. Koshkin, J. Fensholdt, H. M. Pfundheller and C. J. Lomholt, *J. Org. Chem.*, **2001**, *66*, 8504– 8512; (d) J. K. Watts, *Chem. Commun.*, **2013**, *49*, 5618–5620; (e) S. Obika, J. Andoh, T. Sugimoto, K. Miyashita and T. Imanishi, *Tetrahedron Lett.*, **1999**, *40*, 6465–6468; (f) R. Steffens and C. J. Leumann, *J. Am. Chem. Soc.*, **1999**, *121*, 3249– 3255.

52. (a) B. De Bouvere, L. Kerreinans, C. Hendrix, H. De Winter, G. Schepers, *Nucleosides Nucleotides*, **1997**, *16*, 973–976; (b) M. T. Migawa, T. P. Prakash, G. Vasquez, P. P. Seth and E. E. Swayze, *Org. Lett.*, **2013**, *15*, 4316– 4319; (c) J. Wang, B. Verbeure, I. Luyten, M. Froeyen, C. Hendrix, H. Rosemeyer, F. Seela, A. Van Aerschot and P. Herdewijn, *Nucleosides, Nucleotides Nucleic Acids,* **2001**, *20*, 785–788; (d) D. Sabatino and M. J. Damha, *J. Am. Chem. Soc.*, **2007**, *129*, 8259– 8270.

53. (a) Y. Yoshimura, B. A. Otter, T. Ueda and A. Matsuda, *Chem. Pharm. Bull.*, **1992**, *40*, 1761–1769; (b) B. Ravindra Babu, L. Keinicke and J. Wengel, *Nucleosides, Nucleotides Nucleic Acids*, **2003**, *22*, 1313–1315; (c) M. J. Camarasa, M. J. P´erez-P´erez, A. San-F´elix, J. Balzarini and E. De Clercq, *J. Med. Chem.*, **1992**, *35*, 2721–2727; (d) L. A. Paquette, *Aust. J. Chem.*, **2004**, *57*, 7–17.

54. B. S. Sproat, A. I. Lamond, B. Beijer, P. Neuner and U. Ryder, *Nucleic Acids Res.*, **1989**, *17*, 3373.

55. M. P. McGowan, J. Tardif, R. Ceska, L. J. Burgess, H. Soran, I. Gouni-Berthold, G. Wagener and S. Chasan-Taber, *PLoS One*, **2012**, *7*, e49006.

56. W. Guschlbauer and K. Jankowski, *Nucleic Acids Res.*, **1980**, *8*, 1421–1433.

57. T. Aboul-Fadl, *Curr. Med. Chem.*, **2005**, *12*, 2193–2214.

58. (a) O. Seitz, *Chem., Int. Ed.*, **1999**, *38*, 3466–3469; (b) K. Y. Lin and M. D. Matteucci, *J. Am. Chem. Soc.*, **1998**, *120*, 8531–8532; (c) K. Y. Lin, R. J. Jones and M. Matteucci, *J. Am. Chem. Soc.*, **1995**, *117*, 3873–3874.

59. (i) P. Herdewijn, *Antisense Nucleic Acid Drug Dev.*, **2000**, *10*, 297–310. (ii) H. Peacock, A. Kannan, P. A. Beal and C. J. Burrows, *J. Org. Chem.*, **2011**, *76*, 7295–7300; (iii) S. Verma and F. Eckstein, *Annu. Rev. Biochem.*, 1998, 67, 99–134.

60. (i) Obka, S.; Nanbu, D.; Hari, Y.; Andoh, J. –I.; Mori, K. –I.; Doi, T.; Imanishi, T. *Tetrahedron Lett.* **1998**, *39*, 5401-5404. (ii) Petersen, M.; Wengel, J. *Trends Biotechnol.* **2003**, *21*, 74-81.

61. F. J. Schnell, S. L. Crumley, D. V. Mourich and P. L. Iversen, BioRes. *Open Access*, **2013**, *2*, 61.

62. (i) Sazani, P.; Gemignani, F.; Kang, S. H.; Maier, M. A.; Manoharan, M. et al. *Nature Biotechnol.* **2002**, *20*, 1228-1233. (ii) Alter, J.; Lou, F.; Rabinowitz, A.; Yin, H.; Rosenfeld, J. *et al. Nat. Med.* **2006**, *12*, 175-177.

63. Wang, J.; Verbeure, B.; Luyten, I.; Lescrinier, E.; Froeyen, M.; Hendrix, C.; Rosemeyer, H.; Seela, F.; van Aerschot, A.; Herdewijn, P. *J. Am. Chem. Soc.* **2000**, *122*, 8595-8602.

64. Verbeure, B.; Lescrinier, E.; Wang, J.; Herdewijn, P. *Nucleic Acids Res.* **2001**, *29, 4*941-4947.

65. Nielsen, P. E.; Egholm, M.; Berg, R. H.; Buchardt, O. Science 1991, 254, 1497-1501.

66. Egholm, M. *et al. Nature* 365, 566-568(1993)

67. (a) Brown, S. C.; Thomson, S. A.; Veal, J. M.; Davis, D. G. *Science*, **1994**, *265*, 777-780. (b) (i) Leijon, M.; Graeslund, A.; Nielsen, P. E.; Buchardt, O.; Norden, B.; Kristensen, S. M.; Eriksson, M. *Biochemistry*, **1994**, *22*, 9820-9825. (ii) Eriksson, M.; Nielsen, P. E. *Nat. Struct. Biol*. **1996**, *3*, 410-413. (c) Bets, L.; Josey, J. A.; Veal, J. M.; Jordan, S. R. *Science*, **1995**, *270*, 1838-1841. (d) Rasmussen, H.; Kastrup, J. S.; Nielsen, J. N.; Nielsen, J. M.; Nielsen, P. E. *Nat. Struct. Biol*. **1997**, *4*, 98-101.

68. Uhlmann, E.; Will, D. W.; Breipohl, G.; Langner, D.; Ryte, A. *Angew. Chem. Int. Ed. Engl.* **1996**, *35*, 2632- 2635.

69. Nielsen, P. E.; Egholm, M.; Berg, R. H.; Buchardt, O. *Science*, **1991**, *254*, 1497-1501.

70. (a) Nielsen, P. E.; Egholm, M.; Berg, R. H.; Buchardt, O. *Anti-Cancer Drug Design*. **1993**, *8*, 53 - 63. (b) J. C. Hanvey, N. J. Peffer, J. E. Bisi, S. A. Thomson, R. Cadilla, J. A. Josey, D. J. Ricca, C. F. Hassman, M. A. Bonham, K. G, Au, S. G. Carter, D. A. Bruckenstein, A. L. Boyd, S. A. Noble, L. E. Babiss, *Science*, **1992**, *258*, 1481-1485

71. Nielsen, P. E. *Acc. Chem. Res*. **1999**, *32*, 624-630.

72. Marsh, T. C.; Vesenka, J.; Henderson, E. *Biochemistry*, **1994**, *33*, 10718-10724.

73. Forman, S. L.; Fettinger, J. C.; Pieraccini, S.; Gottarelli, G.; Davis, J. T. *J. Am. Chem. Soc.* **2000**, *122*, 4060-4067.

74. West, R. T.; Garza, L. A.; Winchester, W. R.; Walmsley, J. A. *Nucleic Acids Res.* **1994**, *22*, 5128-5134.

75. Demidov, V. V.; Frank-Kamenetskii, M. D.; *Trends Biochem. Sci.* **2004**, *29,* 62-71.

76. Nielsen, P. E, *Pure Appl. Chem.* **1998**, *70*, 105-110.

77. (i) Nielsen, P. E, *Pure Appl. Chem.* **1998**, *70*, 105-110. (ii) Hyrup, B.; Nielsen, P. E. *Bioorg. Med. Chem.* **1996**, *4*, 5-23.

78. Koppelhus, U.; Nielsen, P. E. *Adv. Drug Delivery Rev*. **2003**, *55*, 267-280.

79. (i) DE KONING M, VAN DER MAREL GA, OVERHAND M: *Curr. Opin. Chem. Biol.* **2003**, *7* : 734 -740. (ii) ROMANELLI A, SAVIANO M, PEDONE C: *Recent Res. Devel. Organic. Chem.* **2004**, *8* : 237 -254.

80. Nielsen, P.E.; Haaima, G. *Chem. Soc. Rev.* **1997**, *26*, 73-78.

81. Corradini, R.; Sforza, S.; Tedeschi, T.; Marchelli R. *Seminars in OrganicSynthesis*. Società Chimica Italiana, **2003**; pp. 41-70.

82. Dueholm, K.L.; Petersen, K.H.; Jensen, D.K.; Egholm, M.; Nielsen, P.E.; Buchardt, O. *Bioorg. Med. Chem. Lett.* **1994**, *4*, 1077–1080.

83. (a) Dueholm, K.L.; Petersen K.H.; Jensen D.K.; Egholm, M. Nielsen, P.E.; Buchardt, O. *Bioorg. Med. Chem. Lett.* **1994**, *4*, 1077-1080. (b) Haaima, G.; Lohse, A.; Buchardt, O.; Nielsen, P.E. *Angew. Chem. Int. Ed. Engl.* **1996**, *35,* 1939-1942. (c) Sforza, S.; Haaima, G.; Marchelli, R.; Nielsen, P.E. Chiral *Eur. J. Org. Chem.* **1999**, 197-204.

84. Tedeschi, T.; Sforza, S.; Corradini, R., Dossena, A.; Marchelli R. *Chirality,* **2005**, *17,* S196-S204.

85. Zhou, P.; Dragulescu-Andrasi, A.; Bhattacharya,B.; O"Keefe, H.;Vatta, P.; Hyldig-Nielsen, J. J.; Ly, D. H. *Bioorg. Med. Chem. Lett*. **2006**, *16*, 4931-4935

86. Gourishankar, A.; Ganesh, K.N. *Artificial DNA PNA XNA* **2012**, *3*, 5–13.

87. (a) Myers, M.C.; Witschi, M.A.; Larionova, N.V.; Frank, J.M.; Haynes, R.D.; Hara, T.; Grajkowski, A.; Appella, D.H. *Org. Lett.* **2003**, *5*, 2695–2698. (b) Pokorski, J.K.; Witschi, M.A.; Purnell, B.L.; Appella, D.H. *J. Am. Chem. Soc.* **2004**, *126*, 15067–15073. (c) Pokorski, J.K.; Myers, M.C.; Appella, D.H. *Tetrahedron Lett*. **2005**, *46*, 915–917. (d) Govindaraju, T.; Kumar, V.A.; Ganesh, K.N. *Chem. Commun*. **2004**, 860–861. (e) Govindaraju, T.; Kumar, V.A.; Ganesh, K.N. *J. Am. Chem. Soc*. **2005**, *127*, 4144–4145. (f) Lagriffoule, P.; Wittung, P.; Ericksson, M.; Jensen, D.K.; Norden, B.; Buchardt, O.; Nielsen, *Chem. Eur. J.* **1997**, *3*, 912–919. (g) Bregant, S.; Burlina, F.; Vaissermann, J.; Chassaing, G. *Eur. J. Org. Chem.* **2001**, *2001*, 3285–3294. (h) Bregant, S.; Burlina, F.; Chassaing, G. *Bioorg. Med. Chem. Lett*. **2002**, *12*, 1047 1050.

88. Sugiyama, T.; Imamura, Y.; Demizu, Y.; Kurihara, M.; Takano, M.; Kittaka, *Bioorg. Med. Chem. Lett*. **2011**, *21*, 7317–7320.

89. Kosynkina, L.; Wang, W.; Liang, T.C. *Tetrahedron Lett.* **1994**, *35*, 5173–5176.

90. (a) Tedeschi, T.; Sforza, S.; Corradini, R.; Marchelli, R. *Tetrahedron Lett.* **2005**, *46*, 8395–8399. (b) Englund, E.A.; Appella, D.H. *Org. Lett.* **2005**, *7*, 3465–3467. (c) Dose, C.; Seitz, O. *Org. Lett.* **2005**, *7*, 4365–4368. (d) Ficht, S.; Dose, C.; Seitz, O. *ChemBioChem* **2005**, *6*, 2098–2103.

91. Englund, E. A.; Appella, D. H. *Angew. Chem. Int. Ed.* **2007**, *46*, 1414–1418.

92. (a) Dose, C.; Seitz, O. Convergent Synthesis of Peptide Nucleic Acids by Native Chemical Ligation. *Org. Lett.* **2005**, *7*, 4365–4368. (b) Ficht, S.; Dose, C.; Seitz, O. *ChemBioChem* **2005**, *6*, 2098–2103. (c) Stanfield, C.F.; Parker, J.E.; Kanellis, P. *J. Org. Chem.* **1981**, *46*, 4797–4798. (d) Rittle, K.E.; Homnick, C.F.; Ponticello, G.S.; Evans, B.E. *J. Org. Chem.* **1982**, *47*, 3016–3018. (e) Dragulescu-Andrasi, A.; Rapireddy, S.; Frezza, B.M.; Gayathri, C.; Gil, R.R.; Ly, D.H. *J. Am. Chem. Soc.* **2006**, *128*, 10258–10267. (f) De Koning, M.C.; Petersen, L.; Weterings, J.J.; Overhand, M.; van der Marel, G.A.; *Tetrahedron* **2006**, *62*, 3248–3258.

93. Avitabile, C.; Moggio, L.; Malgieri, G.; Capasso, D.; Gaetano, S.D.; Saviano, M.; Pedone, C.; Romanelli, A. *PLoS One* **2012**, *7*, e35774.

94. Crawford, M.J.; Rapireddy, S.; Bahal, R.; Sacui, I.; Ly, D.H. *J. Nucleic Acids* **2011**, doi:10.4061/2011/652702.

95. De Koning, M.C.; Petersen, L.; Weterings, J.J.; Overhand, M.; van der Marel, G.A.; Filippov, *Tetrahedron* **2006**, *62*, 3248–3258.

96. Manicardi, A.; Fabbri, E.; Tedeschi, T.; Sforza, S.; Bianchi, N.; Brognara, E.; Gambari, R.; Marcgelli, R.; Corradini, R. *ChemBioChem* 2012, 13, 1327-1337.

97. Mitra, R.; Ganesh, K.N. *Chem. Commun.* **2011**, *47*, 1198–1200. 84. Mitra, R.; Ganesh, K.N. *J. Org. Chem.* **2012**, *77*, 5696−5704.

98. Shriraishi, T.; Pankratova, S; Nielsen, P. E. *Chem. Biol.* **2005**, *12*, 923-929

99. Jain, D. R and Ganesh, K. N. *J. Org. Chem.* **2014**, *79*, 6708-6714

100. Govindaraju, T.; Madhuri, V.; Kumar, V. A.; Ganesh, K.N. *J. Org. Chem.* **2006**, *71*, 14-21.

101. Kumar V.A; Ganesh, K. N. *Acc. Chem. Res.,* **2005**, 38, 404-412.

102. (a) Gagamani, B.P.; Kumar, V. A.; Ganesh K. N. *Tetrahedron,* **1996**, *52*, 15017-15030. (b) Gagamani, B.P.; Kumar, V.A.; Ganesh K. N. *Tetrahedron,* **1999**, *55*, 177-192. (c) Jordan, S.; Schwemler, C.; Kosch, W.; Kretschmer, A.; Schwenner, E.; Milke B. *bioorg. Med. Chem. Lett.,* **1997**, *7*, 687-690. (d) D'Costa, M.; Kumar, V.; Ganesh, K.N. *Org. Lett.,* **2001**, *3*, 1281- 1284.

103. Püschl, A.; Tedeschi, T.; Nielsen, P.E. *Org. Lett.,* **2000**, *2*, 4161-4163.

104. Kumar V.; Pallan, P.S.; Meena; Ganesh K.N. *Org. Lett.,* **2001**, *3*, 1269-1272. Kumar V.; Meena. *Nucleos. Nucleot. Nucl. Acids,* **2003**, *22*, 1101-1104.

105. (i) Hickman, D. T.; King, P. M.; Cooper, M. A.; Slater, J. M.; Micklefield, *J. Chem. Comm.*, **2000**, 2251-2252. (ii) Hickman, D. T.; Tan, T.H.S.; Morral, J.; King, P. M.; Cooper, M. A.; Micklefield, *J. Org. Biomol. Chem.*, **2003**, *1*, 3277-3292. (3) Tan, T. H. S.; Hickman, D. T.; Morral, *J. Chem. Commun.* **2004**, 516-517.

106. (a) Hickman, D.T.; King, P.M.; Cooper, M. A.; Slater, J.M.; Micklefield, J. *Chem. Commun.,* **2000**, 2251-2252. (b) Hickman, D. T.; Tan, T.H.S.; Morral, J.; King, P.M.; Cooper, M.A.; Micklefield,J. *Org. Biomol. Chem.,* **2003**, *1*, 3277-3292; (c) Tan, T.H.S.; Hickman, D.T.; Morral, J.; Beadham, I.G.; Micklefield, J. *Chem. Commun.,* **2004**, 516-517.

107. Khan, A.I.; Tan, T.H.S.; Micklefield, J. *Chem. Commun.,* **2006**, 1436-1438.

108. Worthington, R.J.; O'Rourke, A.P.; Morral, J.; Tan, T.H.S.; Micklefield, J. *Org. Biomol. Chem.*, **2007**, *5*, 249-259.

109. Worthington, R.J.; Bell, N. M.; Wong, R.; Micklefield J. *Org. Biomol. Chem.,* **2008**, *6*, 92-103.

110. Kumar V.A; Ganesh, K. N. *Acc. Chem. Res.,* **2005**, *38*, 404-412.

111. Govindaraju, T.; Kumar, V.A. *Tetrahedron,* **2006**,*62*, 2321-2330.

112. Myers, M.C.; Witschi, M.A.; Larionova, N.V.; Franck, J.M.; Haynes, R.D.;Hara, T.; Grajkowski, A.; Appella, D.H. *Org. Lett.,* **2003**, *5,* 2695-2698.

113. Pokorski, J.K.; Nam, J.-M.; Vega, R.A.; Mirkin, C.A., Appella, D.H. *Chem. Commun.,* **2005**, 2101-2103.

114. Englund, E.A.; Xu, Q.; Witschi, M.A.; Appella, D.H. *J. Am. Chem. Soc.,* **2006**, *128*, 16456-16457.

115. Govindaraju, T.; Kumar, V.A.; Ganesh, K.N. *Chem. Commun.,* **2004**, 860-861.

116. Slaitas, A.; Yeheskiely, E. *Eur. J. Org. Chem.,* **2002**, 2391-2399.

117. Gokhale, S. S.; Kumar, V. *Org. Biomol. Chem.,* **2010**, *8*, 3742-3750.

118. Kitamatsu, M.; Shigeyasu, M.; Okada, T.; Sisido, M. *Chem. Commun.,* **2004**, 1208-1209.

119. Kitamatsu, M.; Kashiwagi, T; Matsuzaki, R.; Sisido, M. *Chem Lett.,* **2006**, *35*, 300-301.

120. Shirude, P.S.; Kumar, V.A.; Ganesh, K.N. *Tetrahedron,* **2004**, *60*, 9485-9491.

121. Lagriffoule, P.; Wittung, P.; Eriksson, M.; Jensen, K.; Nordèn, B.; Buchardt, O.; Nielsen, P.E. *Chem. Eur. J.,* **1997**, *3*, 912-919.

122. Govindaraju, T.; Madhuri, V.; Kumar, V.A.; Ganesh, K.N. *J. Org. Chem.,* **2006**, *71*, 14-21.

123. Sharma, S.; Sonavane, U. B.; Joshi, R. R. *J. Biomol. Struct. Dyn.,* **2010**, *27*, 663-676.

124. Vilaivan, T.; Suprarpprom, C.; Harnyyuttanakorn, P.; Lowe, G. *Tetrahedron Lett.,* **2001**, *42*, 5533-5536.

125. Vilaivan, T.; Lowe, G. A. *J. Am. Chem. Soc.,* **2002**, *124*, 9326-9327.

126. Vilaivan T. ; Srisuwannaket, C.. *Org. Lett.,* **2006**, *8*, 1897-1900.

127. (a) Kuwahara, M.; Arimitsu, M.; Shigeyasu, M.; Saeki, N.; Sisido, M. *J. Am. Chem. Soc*. **2001**, *123*, 4653–4658. (b) Kuwahara, M.; Arimitsu, M.; Sisido, M. *J. Am. Chem. Soc*. **1999**, *121*, 256–257.

128. (a) Peyman, A.; Uhlmann, E.; Wagner, K.; Augustin, S.; Weiser, C.; Will, D. W.; Breipohl, G. Angew. *Chem. Int. Ed.* **1997**, *36*, 2809–2812. (b) Efimov, V. A.; Choob, M. V.; Buryakova, A. A.; Kalinkina, A. L.; Chakhmakhcheva, O. G. *Nucleic Acids Res.* **1998**, *26*, 566–575.

129. (a) VAN DER LAAN AC, STRÖMBERG R, VAN BOOM JH *et al.*: *Tetrahedron Lett.* **1996**, *37* (43): 7857 -7860. (b) PEYMAN A, UHLMANN E, WAGNER K *et al.*: *Angew. Chem. Int. Ed. Eng.* **1996**, *35* (22): 2636 -2638. (c) PEYMAN A, UHLMANN E, WAGNER K *et al.*: *Angew. Chem.* **1997**, *36* (24): 2809 -2812. (d) PEYMAN A, UHLMANN E, WAGNER K *et al.*: *Nucleosides Nucleotides* **1998**, *17*:1997-2001 (e) EFIMOV VA, CHOOB MV, KALINKINA AL *et al.*: *Collect. Czech. Chem. Commun.* **1996**, *61*:S262-S264 (f) EFIMOV V A, CHOOB M V, BURYAKOVA A A, KALINKINA A L, CHAKHMAKHCHEVA O G: *Nucleic Acids Res.* **1998**, *26* (2): 566-575 (g) EFIMOV V A, CHOOB M V, BURYAKOVA A A, CHAKHMAKHCHEVA O G: *Nucleosides Nucleotides* **1998**, *17* : 1671 -1679.

130. MYERS M C, POKORSKI J K, APPELLA D H. *Org. Lett.* **2004**, *6* (25): 4699 -4702.

131. EFIMOV VA, BIRIKH KR, STAROVEROV DB *et al.*:. *Nucleic Acids Res.* **2006**, *34* (8): 2247 -2257.

132. CHRISTENSEN L, HANSEN H F, KOCH T, NIELSEN P E. *Nucleic Acids Res.* **1998**, *26* (11): 2735 -2739.

133. ELDRUP A B, DAHL O, NIELSEN P E *J. Am. Chem. Soc.* **1997**, *119* : 11116 -11117.

134. LOHSE J, DAHL O, NIELSEN P E: *Proc. Natl. Acad. Sci. USA* **1999**, *96* (21): 11804 -11808.

135. (i) ELDRUP A B, NIELSEN B B, HAAIMA G *et al. Eur. J. Organ. Chem.* **2001**, *9*: 1781 -1790. (ii) ELDRUP A B, CHRISTENSEN C, HAAIMA G, NIELSEN P E. *J. Am. Chem. Soc.* **2002**, *124* (13): 3254 -3262.

136. RAJEEV KG, MAIER MA, LESNIK EA, MANOHARAN M. *Organ. Lett.* **2002**, *4* (25): 4395 -4398.

137. (i) CHALLA H, STYERS ML, WOSKI SA: *Org. Lett.* **1999,** *1* (10): 1639 -1641. (ii) LOAKES D. *Nucleic Acids Res.* **2001**, *29*: 2437 -2447.

138. (a) GANGAMANI B P, KUMAR V A, GANESH K N. *Chem. Communol.* **1997**, 1913 -1914 (b) Vysabhattar, R.; Ganesh, K. N. *Tetrahedron Lett*. **2008**, *49*, 1314-1318.

139. (a) POPESCU DL, PAROLIN TJ, ACHIM C. *J. Am. Chem. Soc.* **2003**, *125* (21): 6354 -6355. (b) FRANZINI RM, WATSON RM, PATRA GK *et al.*: *Inorg. Chem.* **2006**, 45 (24): 9798 -9811 (c) WATSON RM, SKORIK YA, PATRA G K, ACHIM C. *J. Am. Chem. Soc.* **2005**, *127* (42): 14628 -14639.

140. (a) Demidov V V, *Drug Discov Today* **7**:153–155, **2002** (b) Nielsen P E, *Curr Opin Struct Biol* **9**:353–357, **1999** (c) Hanvey J C, Peffer N J and Bisi J E, *Science* **258**:1481–1485, **1992**.

141. Ray, A.; Norden, B. *FASEB J*. **2000**, *14*, 1041-1060.

142. Knudsen, H.; Nielsen, P. E. *Nucleic Acids Res.***1996** *24*, 494-500.

143. Ivanova, G.B; Arzumanov, A.; Yin, H.; Wood, M. J. A.; Lebleu, B.; Gait, M. J. *Nucleic Acids Res.* **2008**, 36, 6418-6428.

144. Fabani, M. M.; Goodger, C. A.; Williams, D.; Lyons, P. A.; Torres, A. G.; Smith, K. G. C.; Enright, A. J.; Gait, M. J.; Vigorito, E. *Nucleic Acids Res.* **2010**, 38, 4466-4475.

145. Taylor, R. W.; Chinnery, P. F.; Turnbull, D. M.; Lightowlers, R. N. *Nature Genet.* **1997**, *15*, 212-215.

146. Uhlmann, E.; Peyman, A.; Breipohl, G.; Will, D. W. *Angew. Chem. Int. Ed.* **1998**, *37*, 2796-2823.

147. Nielsen, P. E., Egholm, M. Berg, R. H: and Buchardt, O. **1993** *Anti-Cancer Drug Design 8* 53–63

148. Mologni, L., leCoutre, P., Nielsen, P. E., and Gambacorti- Passerini, C. **1998** *Nucleic Acids Res.* **26,** 1934–1938.

149. Demidov V V, *Expert Rev Mol Diagn* **1**:343–351, **2001**.

150. Demidov V, Frank-Kamenetskii M D, Egholm M, Buchardt O and Nielsen P E, *Nucleic Acids Res* **21**:2103–2107, **1993**.

151. Veselkov AG, Demidov V, Nielsen PE and Frank-Kamenetskii MD, *Nucleic Acids Res* **24**:2483–2487, **1996**.

152. Demers D B, Curry E T, Egholm M and Sozer A C, *Nucleic Acids Res* **23**:3050–3055, **1995**.

153. Orum, H.; Nielsen, P.E.; Egholm, M.; Berg, R. H.; Buchardt, O.; Stanley, C.*Nucleic Acids Res.* **1993**, *21*, 5332-5336.

154. (a) Tyagi S and Kramer F A, *Nat Biotechnol* **14**:303–308, **1996**. (b) Kuhn H, Demidov V V, Gildea B D, Fiandaca M J, Coull J M and Frank-Kamenetskii M D, *Antisense Nucleic Acid Drug Dev* **11**:265–270, **2001**.

CHAPTER 2

Design and synthesis of *gem*-dialkyl substituted PNA monomers and their oligomerization

PNA modifications by introducing dialkyl groups at γ and β-position in the backbone have been described in this chapter. Modifications have been designed to improve hybridization efficiency, and orientation selectivity is towards nucleic acids by keeping PNAs achiral and acyclic.

2.1 Introduction

The beginning of the investigations for developing oligonucleotides (ODNs) as potential therapeutic agents has triggered the search for nucleic acid mimics with improved properties[1.] Complete replacement of sugar-phosphate backbone by achiral, acyclic and uncharged scaffold in aminoethylglycyl peptide nucleic acids (PNA) is the most prominent example and has been extensively studied in the last two decades since its discovery in 1991 (Figure **2.1**).[2] In PNA nucleobases are attached to the polyamide backbone through conformationally rigid tertiary acetamide linker. The strong and sequence specific binding of PNA to both complementary DNA and RNA along with its unique strand invasion properties has proved to be extremely beneficial to both chemists and biologists working towards the development of ultimate antisense oligonucleotides.[3]
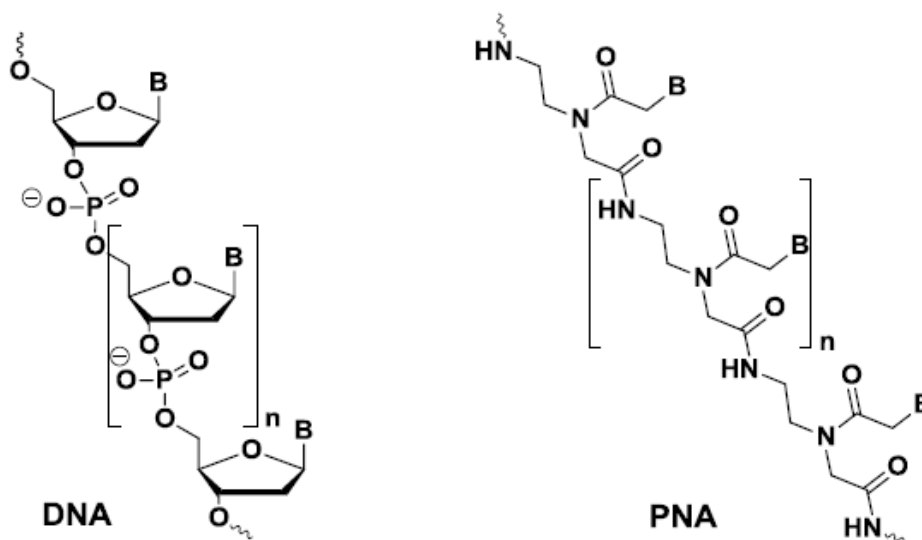
Figure 2.1 Structural comparison of DNA and PNA (B=nucleobase)

The optimal number of bonds between the nucleobases was found to be six which corresponds to that found in DNA thereby providing the correct inter-nucleobase spacing.[4] The stability of the PNA interaction with DNA is such that strand invasion of DNA by PNA is thermodynamically favored, and can take place via duplex, triplex or double duplex formation.

The unnatural polyamide linkage enables PNA to evade recognition and degradation by proteases and nucleases.[5] These properties make PNA an attractive reagent for numerous applications in biology and medicine.[6] Unfortunately, PNA falls short of some crucial properties like poor water solubility and low cellular uptake.[7] Also ambiguity in the orientation selectivity between parallel and antiparallel binding to complementary oligonucleotide hampers their applications. To overcome these limitations various modifications were attempted which have improved PNA properties to different extents. Modifications in the backbone to make chiral, acyclic PNA analogs having the stereocentre at α or γ carbon[8] and β-carbon[9] have led to improvements in PNA properties (Figure **2.2**). The functionalization at these positions of the monomer may also preorganize the PNA strand but importantly it has the effect of shifting the PNA preference towards a right handed or left handed conformation, depending on the configuration of the new stereogenic centres. This, in turn, affects the stability of the PNA:DNA duplex through the control of helix handedness.[10]
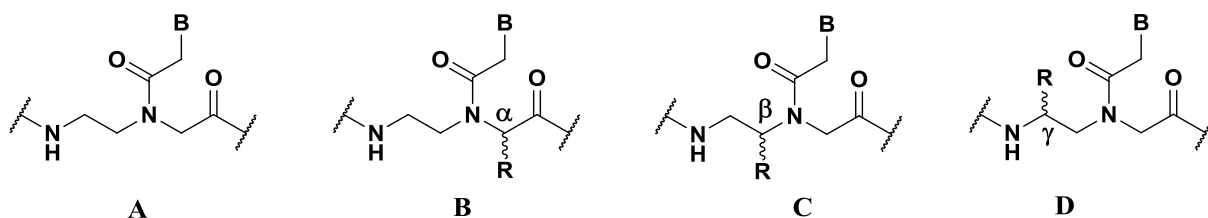
Figure 2.2 Structures of achiral aeg-PNA and chiral α, β- and γ-modified PNA (B-D) (R = amino acid side chain or other modifications, B = nucleobase)

Structure-activity relationships showed that the original design containing a 6- atom repeating unit and a 2-atom spacer between the backbone and the nucleobase was optimal for DNA recognition.[11] Introduction of different functional groups with different charges/polarity/flexibility have been described and are extensively reviewed.[12] These studies showed that a "constrained flexibility" was necessary to have good DNA binding, since too flexible or too rigid structures did not perform as unmodified PNAs. A highly flexible backbone would require a very high loss of entropy for efficient binding whereas a very rigid backbone would prevent DNA binding due to a difficult fit to adopt to target structure.[13]

The first approach to modify *aeg* PNA, was extension of the PNA backbone by one methylene group at ethylenediamine side, glycine side or attachment of nucleobase though ethylenecarbonyl instead of methylenecarbony linker (Figure **2.3**).[14] The extension of PNA backbone drastically decreased the stability of derived PNA:DNA duplexes compared to unmodified PNA:DNA duplex.

Another key structural feature of PNA monomers is the central amide linker between the base and the backbone. This tertiary amide functionality is conformationally labile and occurs in both the E and Z-rotameric forms in uncomplexed PNA.[15] (Figure **2.4**)
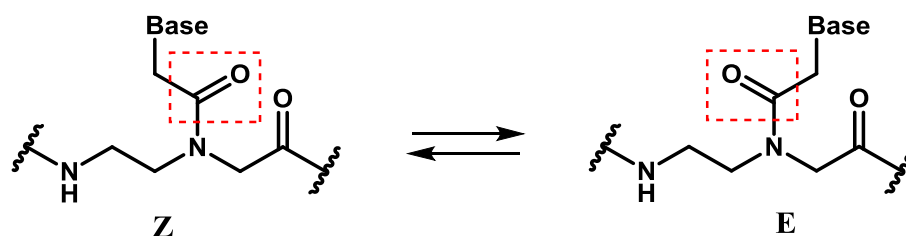
Figure 2.4 Chemical structure of the two rotameric forms of PNA

In PNA/PNA, PNA/DNA, and PNA/RNA duplexes the PNA bases carrying the amide bond are mostly in the Z conformation.[16] It was speculated that blocking the nucleobase-backbone bond in the right conformation would result in an improvement in the affinity and specificity of hybridization. Therefore, the amide bond was replaced by an isostructural carbon double bond, affording PNA analogues (olefinic PNA-OPA) with the nucleobase-backbone linker locked in the Z or E conformation.[17] (Figure **2.5**)
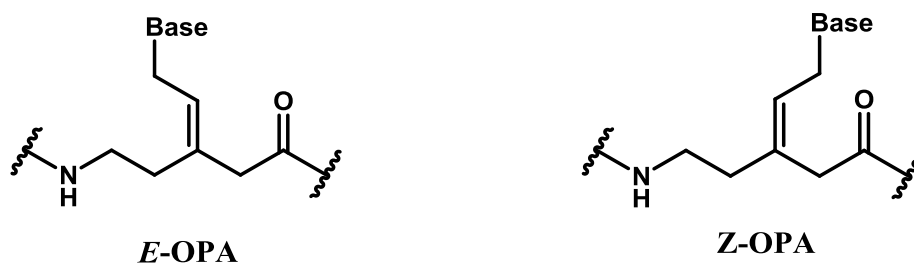
Figure 2.5 Structure of (*E*) - and (*Z*) - OPA

Compared to PNA, fully modified (*E*)-OPA oligoamides showed a drop in thermal stability and an inverted preference for parallel strand orientation in duplexes with complementary DNA.[18] In contrast to PNA, fully modified OPA-T sequences (*E* and *Z*) were not able to form triple helical structures. The OPA system thus revealed that the amide functionality in the base-linker unit in PNA significantly determines the affinity and preferred strand orientation in PNA/DNA duplexes. Furthermore, this amide linkage seems to be responsible for the propensity to form (PNA)$_2$ DNA triplexes.

The PNA literature suggested that several issues are to be considered while designing and decorating new PNA monomer such as length of the backbone and the linker, the chirality of the carbon atoms on the backbone, the steric hindrance, the orientation and the position of substituents within the backbone, the orientation of the nucleobase with respect to the backbone, in order to foster PNA's use in medicinal chemistry.

The next section deals with the preorganising the aeg-PNA backbone by restricting the free rotation of C2(γ)-C3(β) bond by installing bulkier dialkyl groups in order to improve its binding affinity and specificity towards DNA/RNA.

2.2 Rationale behind the work

Previous efforts from this laboratory[19] and that of others[20] to structurally alter the aeg-PNA backbone have resulted in a number of acyclic, cyclic and chiral backbone modifications to generate a variety of PNA analogs.

The aeg-PNA backbone composed of C-C and C-N bonds is highly flexible with a capacity to reorganize slowly into the preferred conformation for hybridization with cDNA or RNA. Pre-organizing the aeg-PNA backbone into "hybridization-competent conformation" is expected to impart entropic advantages for selective or preferential binding to DNA or RNA. Indeed, rational modifications of aeg-PNA backbone by introduction of cis-1,2-disubstituted cyclohexyl moiety to match the dihedral angle of the lone C-C bond in ethylenediamine segment to 60° found in PNA:RNA duplexes, resulted

in achieving significant discrimination in binding of complementary isosequential DNA and RNA with preference for binding to RNA.[21]

Similarly, the introduction of chirality into aeg-PNA backbone has shown more selectivity for parallel or antiparallel binding depending on the nature of modifications, while introduction of cationic side chains have improved solubility and enhanced cell uptake.[22]

Another simpler way to impart steric constrain without incorporating rigid and chiral cyclic moieties was successfully attempted by introducing gem-dialkyl substitution into the flexible aminoethylglycine backbone of PNA.[23] A number of *aib*-containing peptides occur naturally and the gem-dimethyl substitution on α carbon is well known to promote helices in polypeptides.[24] This feature, although not directly extendible to PNA (which is not a classical peptide), provided an initial rationale for synthesis of the gem-dimethyl substituted aedmg-PNA (Figure **2.6B**). To examine the correlated effects of steric constrain developed due to gem-dimethyl glycine on the backbone in the adjoining aminoethyl segment in backbone, PNA analogs having aminopropyl (apdmg) (Figure **2.6C**) moiety have been examined for comparative studies of the DNA/RNA complementation abilities.
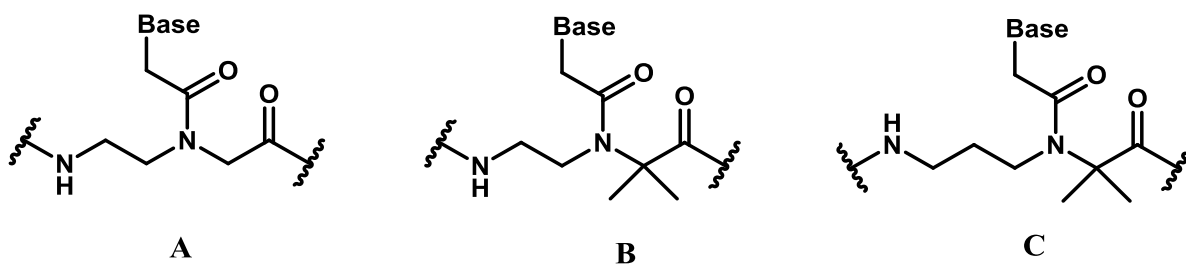
Figure 2.6 Structures of PNAs (**A**) aeg-PNA (**B**) aedmg-PNA (**C**) apdmg-PNA

Such acyclic, achiral backbone having gem-dialkyl function are not only be rigid, but the steric constraints imposed lead to favorable pre-organization, with the inherent binding to complimentary DNA enhanced due to entropic factors. This gem-dialkyl effect on glycine is transmitted to adjacent propylenediamine chain as well since apdmg-PNA stabilizes both DNA and RNA hybrids.

The incorporation of gem-dimethyl substituted aedmg-PNA monomer into the aeg-PNA backbone preferentially increased the Tm of the derived complexes with DNA as compared with RNA. This perhaps arises from a structural preorganization of the backbone due to steric constrains imposed by the gem-dimethyl unit leading to a better base stacking of base pairs in DNA/RNA complexes.

The earlier study from our group[25] has shown that restricting the rotation of Cγ-Cβ bond by incorporating cyclohexyl ring along the Cγ-Cβ bond to adjust the β-dihedral angle to ± 65° by PNAs show strong preference for RNA binding (Figure **2.7**).

(1S,2R)-cyclohexyl-PNA
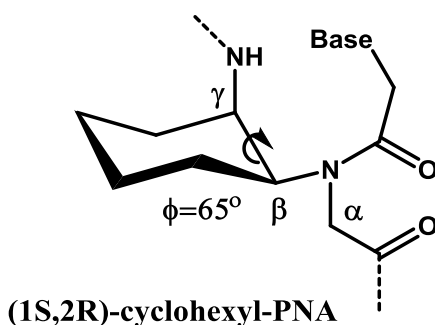
Figure 2.7 Cyclic six-membered PNA analogues

The above two examples showed that fine tuning of PNA backbone with appropriate rigidity either by non-chirality (gem-dialkyl group) or by chirality and constraining into a ring (cyclohexyl ring), may lead to "hybridization-competent conformation" to impart entropic advantages for selective or preferential binding to DNA or RNA. Based on this survey, it was aimed to combine both these fragments, and synthesize PNA monomers with rigidity confined to a single atom instead along a bond like cyclohexyl ring, with incorporation of gem-dimethyl group at Cγ and Cβ atom.

These monomers may result in tuning the PNA backbone to DNA/RNA binding by introduction of rigidity without any associated chirality. The present objective is to incorporate gem-dialkyl group at Cγ and Cβ atom. The gem dialkyl substitution can also

become part of a spiro ring that also carries an amino group to introduce cationic nature and improve the solubility (Figure **2.8**).

These modified PNA monomers have been synthesized and incorporated in to PNA oligomers to examine its hybridization properties. The rationale behind the design of each monomer is discussed further.

(a) γ gem aeg PNA   (b) γ 4-amino-4-pip aeg PNA   (c) β gem aeg PNA   (d) γ gem apg PNA
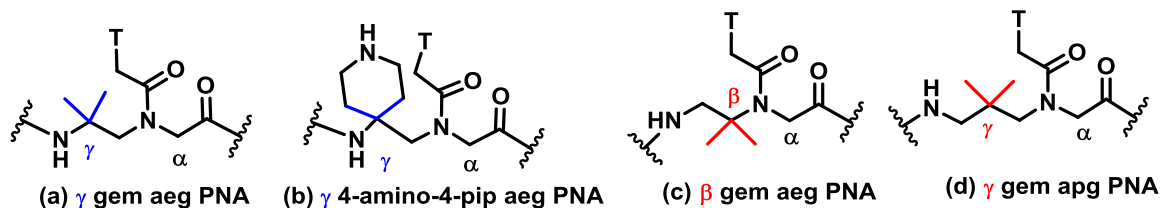
Figure 2.8 Target PNA analogues modified at γ and β-position

2.2.1 γ-gem-dimethyl aminoethylglycyl PNA (γ-gem aeg PNA) and γ-4-amino-4-piperidine aminoethylglycyl PNA (γ-pip aeg PNA)

Among the large number of structural modifications that have been made to the backbone of PNA, the most promising modification with respect to functional group diversification, and conformational preorganization is the installation of a chiral center at the γ-backbone.[26] Installation of the chiral center at the γ-position forces the PNA backbone to adopt either a right-handed or a left-handed helix, depending on the stereochemistry as a result of steric clash between substituent at the C-γ position and tertiary amide nitrogen N4'. The helix is stabilized by sequential base-stacking. The crystal structure of a PNA-DNA duplex with complete γ-backbone modification illustrates that γ-PNA possesses conformational flexibility while maintaining sufficient structural integrity to adopt the P-helical conformation on hybridization with DNA.[27]

It is noteworthy that γ-PNAs in the single-strand state (determined by NMR) and in the hybrid duplex state (determined by X-ray crystallography) adopt similar conformations. In contrast to α-PNA, which is sensitive to steric hindrance arising from side chains at the α-position, the γ-position could accommodate various hindered side chains without

inducing adverse effects on the hybridization properties of PNAs. Helical handedness can be induced with conformational preorganization and without chiral center.

These results inspired the design and synthesis of a γ-C- substituted PNA incorporating gem-dialkyl group in the aeg PNA backbone (Figure **2.8 a**) in order to investigate its potential as an effective modified oligonucleotide in order to improve its performances in terms of affinity and specificity towards complementary oligonucleotides.

Helical handedness can be induced with conformational preorganisation. The chair conformation of the six-membered rings determines the orientation of the ring substituents with respect to each other. These attributes can be combined together to arrive at a six membered PNA analogue (Figure **2.8 b**) that would be positively charged due to the presence of tertiary amine group and through its conformational restrain could lead to achieve maximum advantages for binding to target DNA/RNA sequences.

2.2.2 *β*-gemdimethyl aminoethylglycyl PNA (*β*-gem aeg PNA)

Although some cyclic PNA analogues contain a chiral center at the β-position, PNAs with a single substituent only at the β-position (β-PNAs) have not been explored until 2011, Sugiyama *et al.* reported the first β-PNA bearing a methyl group at the β-position.[28] In 2015, β, γ-bis-substituted PNA without involving cyclic structures has been reported.[29] The incorporation of a substituent at the β-position was expected to significantly affect the conformation and the DNA binding properties of PNA oligomers since the β-position of the PNA backbone corresponds to the C4' of the deoxyribose moiety of DNA and the C4' is a chiral carbon atom.

Here, the objective is to restrict the rotation of C2(γ)-C3(β) bond, in turn preorganizing aeg-PNA backbone by incorporating gem-dimethyl group (Figure **2.8 c**) at β-position, keeping PNA achiral and acyclic.

2.2.3 γ-gemdimethyl aminoprolylglycyl PNA (γ-gem apg PNA)

The first approach to modify *aeg* PNA, was extension of the PNA backbone by one methylene group at ethylenediamine side, glycine side or attachment of nucleobase though ethylenecarbonyl instead of methylenecarbony linker (Figure **2.9**).[30]
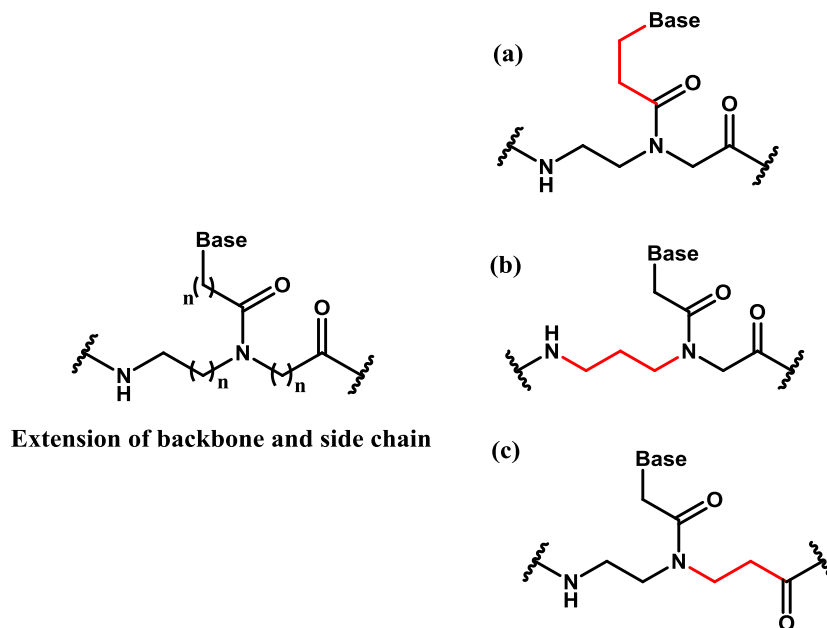
Figure 2.9 Extension of PNA backbone at (**a**) ethylenediamine side (**b**) glycine side chain (**c**) nucleobase attachment side

However, applying conformational constrain on glycine segment by introduction of gemdimethyl substitution lead to both better hybridization by pre-organizing the backbone for better stacking interaction of the base pairs. This gem-dialkyl effect on glycine is transmitted to adjacent propylenediamine chain since apdmg-PNA stabilizes both DNA and RNA hybrids (Figure **2.6 C**).

These results inspired the design and synthesis of γ-gemdimethyl aminoprolylglycyl PNA (γ-gem apg PNA) (Figure **2.8 d**).

2.3 Aim of the present work

The specific objectives of this section are:

➢ Synthesis of rationally designed γ dialkyl substituted PNA T-monomers
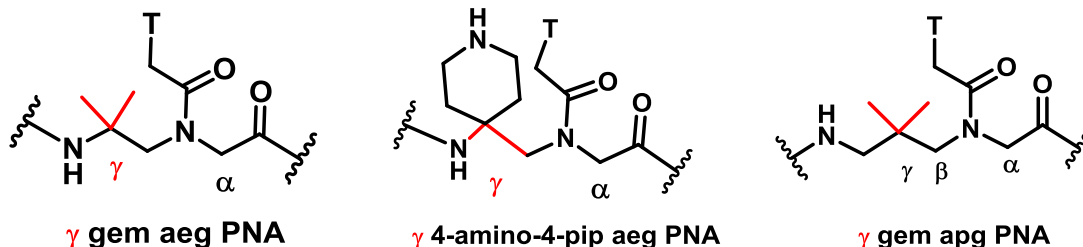
γ **gem aeg PNA**   γ **4-amino-4-pip aeg PNA**   γ **gem apg PNA**

➢ Synthesis of rationally designed β-gem dialkyl substituted PNA T-monomers

β **gem aeg PNA**
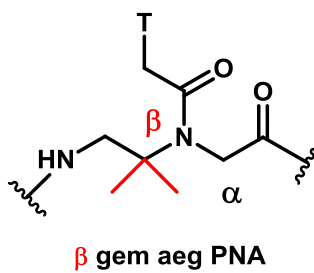
➢ Characterization of rationally synthesized PNA monomers and their intermediates by various spectroscopic techniques.

➢ Incorporation of *aeg* PNA monomers (A/T/G/C) and γ, β- dialkyl substituted PNA (T) monomers at various positions by solid phase synthesis.

➢ Cleavage of oligomers from the solid support, their purification by RP-HPLC and characterization by MALDI-TOF spectrometry.

2.3.1 Synthesis of modified PNA monomers

This section describes the synthesis of rationally designed γ and β- dialkyl substituted PNA T-monomers.

2.3.1a Synthesis of γ-gemdimethyl aminoethylglycyl (γ-gem aeg) PNA monomer

In an attempt towards the synthesis of target monomer, the commercially available 2-amino-2-methylpropan-1-ol **1** was heated with di-tert-butyl dicarbonate [(Boc)$_2$O] in aq. NaOH-dioxane to obtain Boc-protected 2-amino-2-methylpropan-1-ol **2.** This was

followed by the reaction of Boc-protected 2-amino-2-methylpropan-1-ol **2** in dry acetonitrile with diacetoxyiodo benzene (DAIB) and (2,2,6,6-tatramethyl-1-piperidinyloxy) TEMPO under cooling. This led to the formation of aldehyde tert-butyl (2-methyl-1-oxopropan-2-yl) carbamate **3** as the product. Aldehyde **3** was treated with glycine methyl ester hydrochloride in ethanol in the presence of DIPEA and sodium cynoborohydride to obtain Methyl (2-((tert-butoxycarbonyl) amino)-2 methylpropyl) glycinate **4** in quantitative yield. Compound **4** was converted to chloro derivative **5** using chloroacetyl chloride and triethyl amine. The condensation of the compound **5** with nucleobase thymine afforded γ-gemdimethyl aminoethylglycyl methyl ester **6** in quantitative amount. The appearance of peaks at δ **1.91** ppm and δ **7.1** ppm in ^{1}H NMR shows the presence of thymine in the desired product **6**. γ-gem aeg PNA ester was hydrolysed using aq. Lithium hydroxide solution to get γ-gem aeg PNA acid **7** (Scheme **2.1**), which was then used for incorporation into the desired PNA sequences by solid phase peptide synthesis.

SCHEME 2.1: Synthesis of (γ-gem aeg) PNA monomer
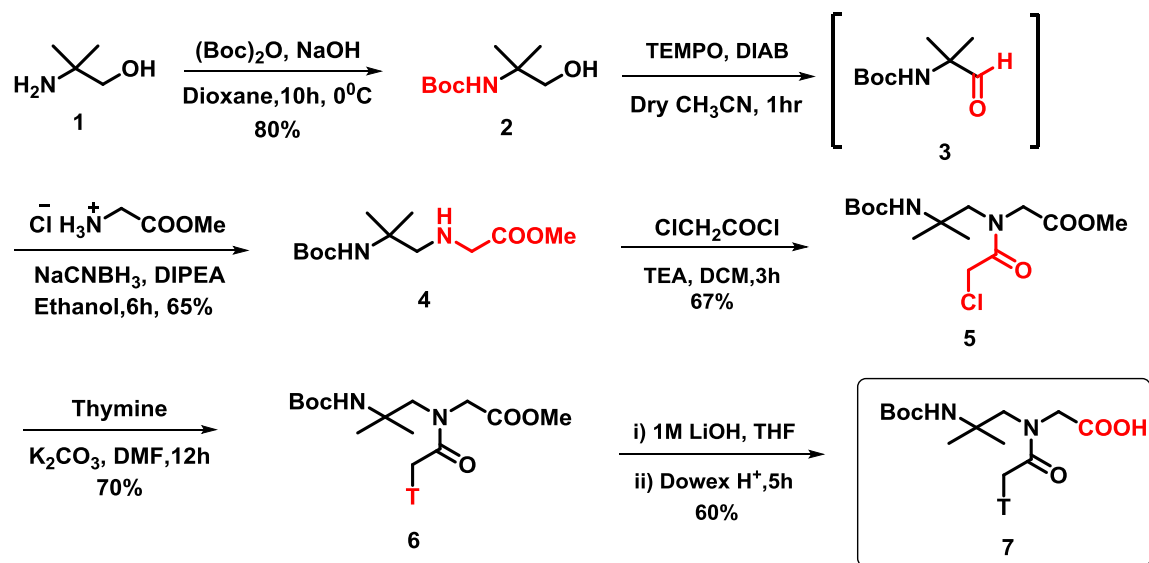
^{1}**H NMR for final Monomer 7:** (400MHz, DMSO-d^6) δ: 1.06 (ma.) (s, 3H) and 1.19(mi.) (s, 3H), 1.32 (s, 9H), 1.7(s, 3H), 3.46(ma.) (s, 1H) and 3.56(mi.) (s, 1H), 3.88(mi.) (s, 1H) and 4.11(ma.) (s, 1H), 4.44(ma.) (s, 1H) and 4.57(mi.) (s, 1H), 7.24(ma.) and 7.30(mi.) (s, 1H), 11.22 (ma.) and 11.24(mi.) (s, 1H).

All intermediates were purified by column chromatography and characterized by ^{1}H, ^{13}C NMR and mass spectral analysis (**Appendix I**).

2.3.1b Synthesis of γ-4-amino-4-piperidine aminoethylglycyl (γ-pip aeg) PNA monomer

As shown in scheme **2.2**, commercially available unnatural amino acid 4-amino-4-piperidine carboxylic acid **8** was converted to methyl ester derivative **9** using dimethyl sulfate and activated K_2CO_3 and the conversion was confirmed by the appearance of ^{1}H NMR peak at δ for $-CH_3$ group of methyl ester in the product. The methyl ester was reduced to give alcohol derivative **10** using sodium borohydride in absolute ethanol. This was followed by the reaction of alcohol **10** in dry acetonitrile with diacetoxyiodo benzene (DAIB) and (2, 2, 6, 6-tatramethyl-1-piperidinyloxy) TEMPO under cooling which led to the formation of aldehyde benzyl 4-((tert-butoxycarbonyl) amino)-4-formyl piperidine-1-carboxylate **11** as the product in 1.5h. Aldehyde **11** was trated with glycine methyl ester hydrochloride in ethanol in the presence of DIPEA and sodium cynoborohydride to obtain **benzyl** 4-((tert-butoxycarbonyl) amino)-4-(((2-methoxy-2-oxoethyl) amino) piperidine-1-carboxylate **12** in quantitative yield. The compound **12** was acylated using chloroacetyl chloride in presence of triethyl amine to get chloro derivative **13.** The chloro compound was reacted with nucleobase thymine in presence of activated K_2CO_3 to give γ-4-amino-4-piperidine aminoethylglycyl methyl ester **14** in quantitative amount. The presence of thymine was confirmed by the presence of peaks at δ **1.91** ppm and δ **7.1** ppm in ^{1}H NMR. γ-pip aeg PNA ester was hydrolysed using aq. LiOH to get γ-pip aeg PNA acid **15** (Scheme **2.2**). This was used for incorporation by solid phase peptide synthesis to obtain the desired PNA sequences.

^{1}H NMR for final Monomer 15: (400MHz, $CDCl_3$) δ: 1.39(ma.) and 1.50(mi.) (s, 9H), 1.86(s, 3H), 2.02(s, 2H), 4.20-4.81(m, 12H), 5.06(s, 2H), 7.02(mi.) and 7.07(ma.) (s, 1H), 7.32(s, 5H), 9.62-10.03(m, 1H)

All intermediates were purified by column chromatography and characterized by ^{1}H, ^{13}C NMR and mass spectral analysis (**Appendix I**).

SCHEME 2.2: Synthesis of (γ-pip aeg) PNA monomer
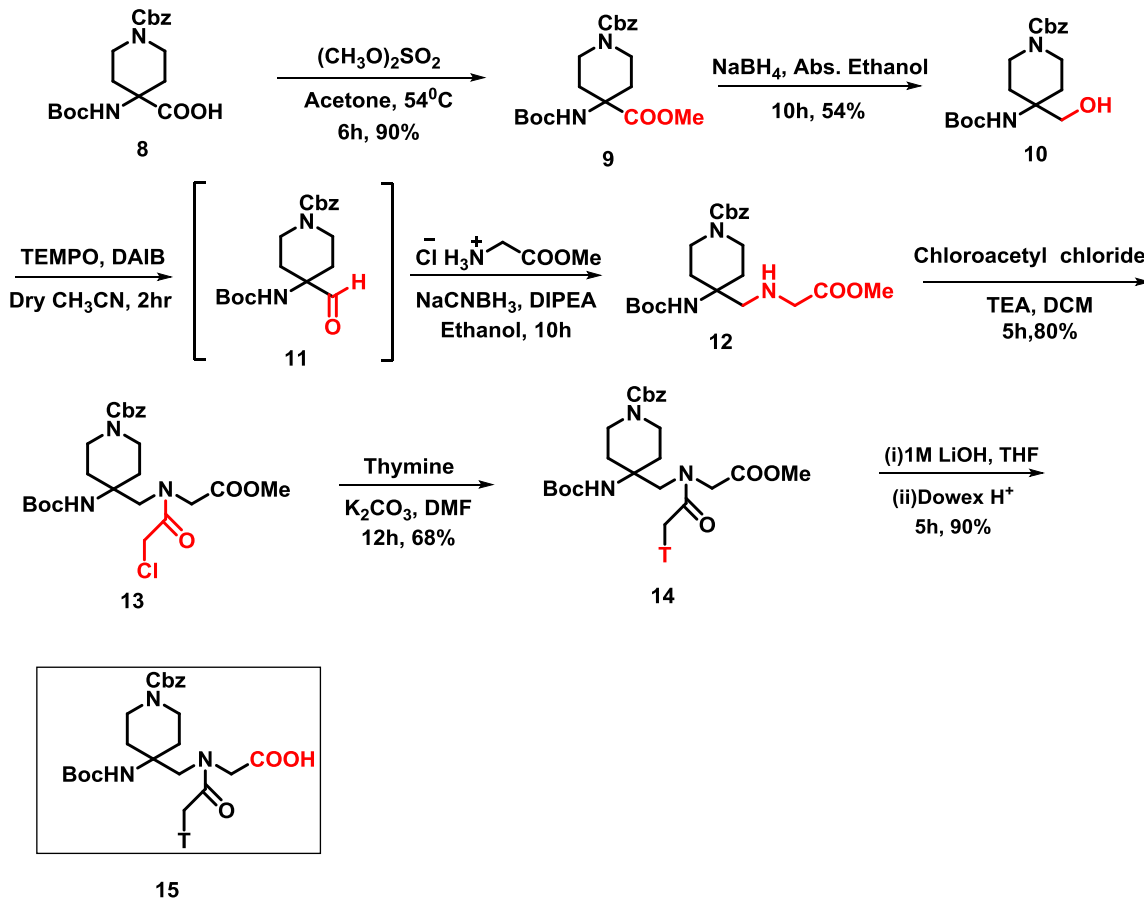
2.3.1c Synthesis of β-gemdimethyl aminoethylglycyl (β-gem aeg) PNA monomer

The commercially available 2-methylpropane-1, 2-diamine **16** was treated with di-tert-butyl dicarbonate, [(Boc)₂O] in THF to obtain Boc-protected diamine **17.** This was followed by the reaction of monoboc protected diamine **17** with ethylbromoacetate in acetonitrile in presence of triethyl amine to yield alkylated compound ethyl (1-((tert-butoxycarbonyl) amino)-2-methylpropan-2-yl)glycinate **18.** Compound **18** was treated with chloroacetyl chloride in DCM in presence of triethyl-amine to obtain acylated product **19.** To obtain the β-gem aeg PNA ester, chloro compound **19** was treated with nucleobase thymine in dry DMF in presence of K_2CO_3.The reaction yielded β-gem aeg PNA ester **21** in 20% along with the cyclic product **20** in 70%. The presence of thymine was confirmed by the presence of peaks at δ **1.91** ppm and δ **7.1** ppm in ^{1}H NMR spectrum. The β-gem aeg PNA ester **21** was hydrolysed using aq. LiOH solution to get

β-gem aeg PNA acid **22** (Scheme **2.3**) which was then used for incorporation by solid phase peptide synthesis to obtain the desired PNA sequences.

SCHEME 2.3: Synthesis of (β-gem aeg) PNA monomer
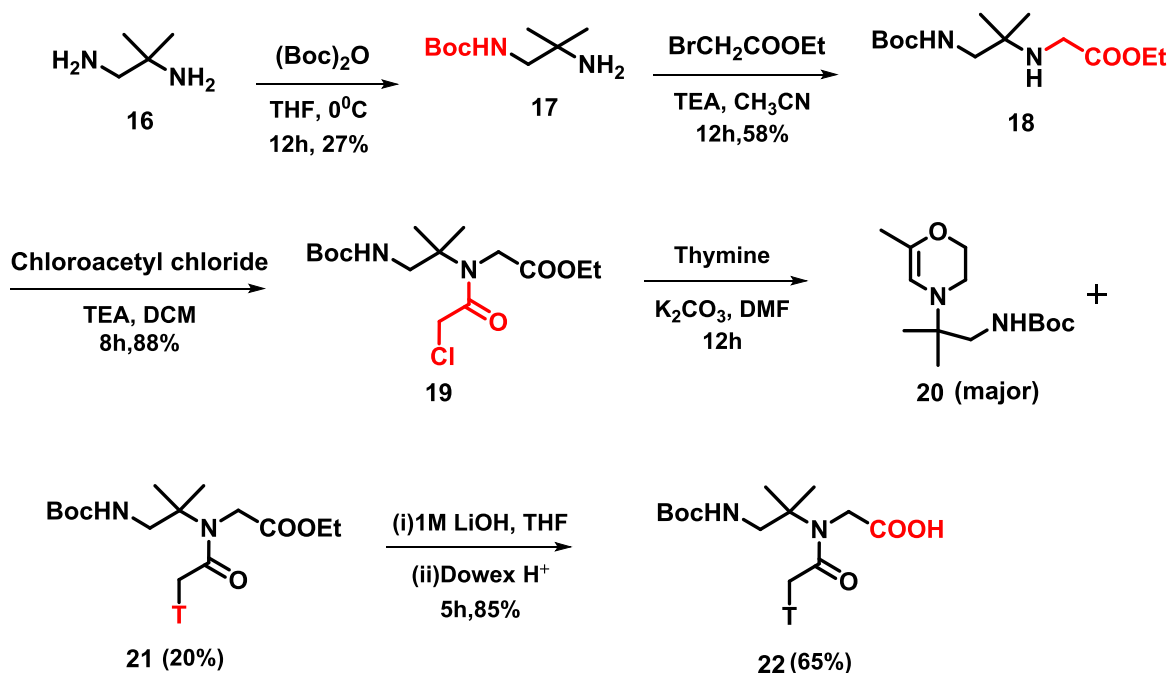
^{1}H NMR for final Monomer 22: (400MHz, DMSO-d$_6$) δ:1.20(s,6H), 1.34(s,9H), 3.34(bs,2H), 4.06(s,2H), 4.39(s,2H), 6.6(bs,1H), 7.21(s,1H), 11.2(s,1H)

All intermediates were purified by column chromatography and characterized by ^{1}H, ^{13}C NMR and mass spectral analysis (**Appendix I**).

2.3.1d Synthesis of γ-gemdimethyl aminoprolylglycyl (γ-gem apg) PNA monomer

A similar strategy was used for the synthesis of γ-gem apg PNA monomer **28** using commercially available 2,2-dimethylpropane-1,3-diamine **23** as starting material. As discussed above, diamine **23** was treated with di-tert-butyl dicarbonate, [(Boc)$_2$O] in THF to obtain mono Boc-protected diamine **24.** The compound **24** was alkylated to yield compound **25.** Acylation of compound **25** with chloroacetyl chloride in DCM in presence of triethylamine gave the chloro compound **26.** Alkylation of chloro compound **26** with

nucleobase thymine in presence of K_2CO_3 gave target γ-gem apg PNA ester monomer **27.** The presence of thymine was confirmed by the presence of peaks at δ in ^{1}H NMR. Ester monomer was then hydrolysed with aq. LiOH solution to get γ-gem apg PNA acid monomer **28** (Scheme **2.4**) which was then used for incorporation by solid phase peptide synthesis to obtain the target PNA sequences.

SCHEME 2.4: Synthesis of (γ-gem apg) PNA monomer
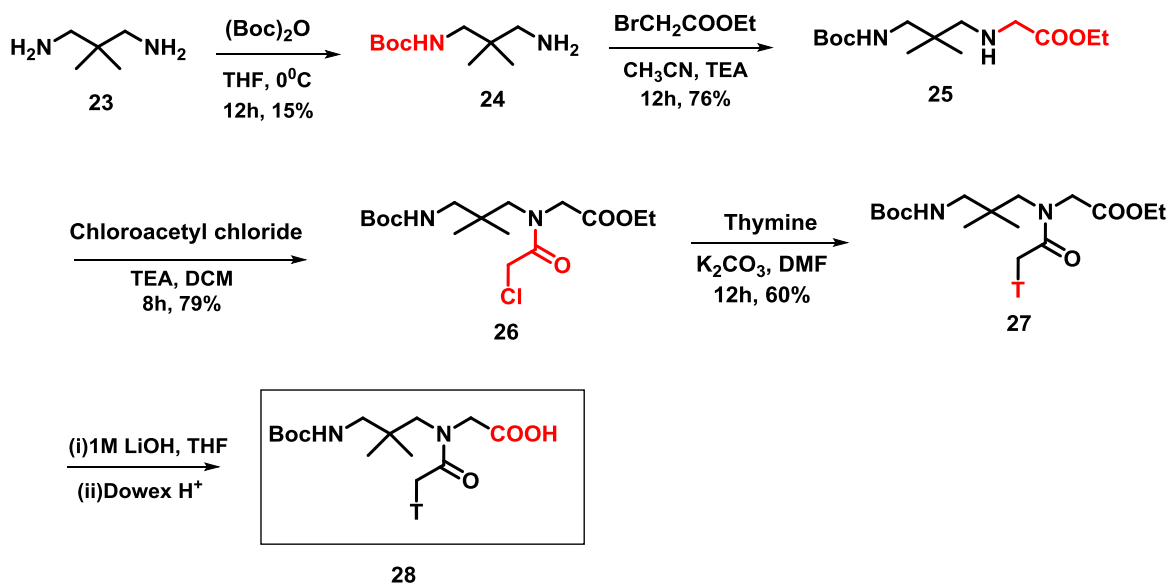
^{1}H NMR for final Monomer 28: (200MHz, D_2O) δ:1.20(s,6H), 1.34(s,9H), 3.34(bs,2H), 4.06(s,2H), 4.39(s,2H), 6.6(bs,1H), 7.21(s,1H), 11.2(s,1H)

All intermediates were purified by column chromatography and characterized by ^{1}H, ^{13}C NMR and mass spectral analysis (**Appendix I**).

2.4 Summary

To summarize, this section describes the synthesis and characterization of rationally designed PNA monomers by incorporating gem-dialkyl γ and β-position. All the intermediates have been characterized by ^{1}H & ^{13}C NMR spectroscopy, mass spectral analysis and other appropriate analytical data (Section **2.9B**). The next section deals with

the incorporation of these modified monomer units into oligomers at various desired positions using solid phase peptide synthesis.

2.5 Solid phase PNA synthesis

Peptides can be synthesized either by solution phase or by solid phase synthesis techniques.[31] The solution phase method of peptide synthesis can be used efficiently only for short chain peptides moreover, it requires a tedious separation and purification step after each coupling reaction. On the other hand, solid phase peptide synthesis can be efficiently used in the synthesis of several short and long chain peptides as well as in the synthesis of PNA oligomers.
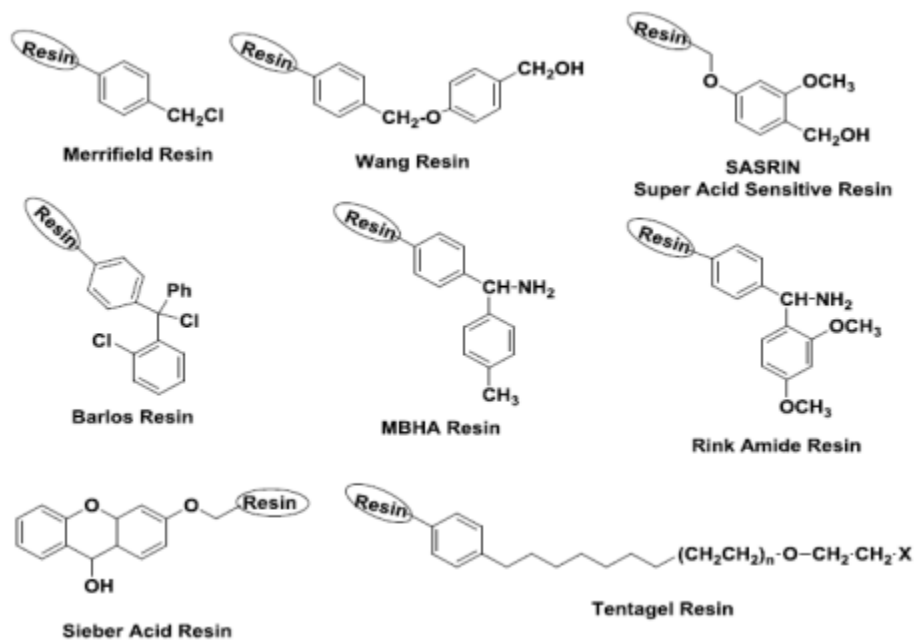
Figure 2.10: Representative structures of resin used in SPPS

The solid phase peptide synthesis first devised by Merrifield,[32] involves the combination of reagents with functional groups that are located on the surface and on the inside pores of beaded polymers.[33] Small solid beads are porous and insoluble in organic solvents. These beads are treated with functional units or linkers on which, peptide chains can be built. The beads are immersed in solvent containing the reagents which approach the solvated sites by diffusion. In contrast to solution phase, the solid phase method offers

several advantages. In solid phase synthesis, the *C*-terminal amino acid is linked to an insoluble support that also acts as a permanent protection for the carboxylic acid (Figure **2.10**). Then the next $N\alpha$-protected amino acid is coupled to the resin bound amino acid either by using an active pentafluorophenyl (pfp) or 3-hydroxy- 2,3-dihydro-4-oxo-benzotriazole (DHBt) ester, or by *in situ* activation with carbodiimide reagents. The excess amino acid is washed out and the deprotection and coupling reactions are repeated until the desired peptide sequence is achieved. The tedious purification step of intermediates after each coupling reaction is omitted. Finally, the resin bound peptide and the side chain protecting groups are cleaved in global deprotection step.

The advantages of solid phase synthesis are:

1) All the reactions are performed in a single vessel minimizing the loss due to transfer
2) Large excess of activated monomer carboxylic acid component can be used resulting in high coupling efficiency
3) Excess reagents can be removed by simple filtration and washing steps and
4) The method is amenable to automation and semi micro manipulation.

There are two routinely followed chemistries of solid phase peptide synthesis- **Fmoc** and **Boc** strategies, which use base labile and acid labile protecting groups respectively (Figure **2.11**). Solid-phase peptide synthesis proceeds in a C-terminal to N-terminal fashion. The N-terminus of amino acid monomers is protected by these two groups and added onto a deprotected amino acid chain. First protocol uses the *t*-butoxycarbony (*t*-Boc) group as $N\alpha$-protection that is removed by mild acidic conditions such as 50% TFA in DCM. The reactive side chains are protected with groups that are stable to mild acidic deprotection conditions and can be removed under strongly acidic conditions using HF in dimethylsufide or TFMSA in TFA. While in second protocol fluorenylmethyloxycarbonyl (Fmoc) group is used as $N\alpha$-protection which is stable to acidic conditions but can be cleaved efficiently with a base such as piperidine. The final peptide and side chain protecting groups can be cleaved with acid (50% TFA).
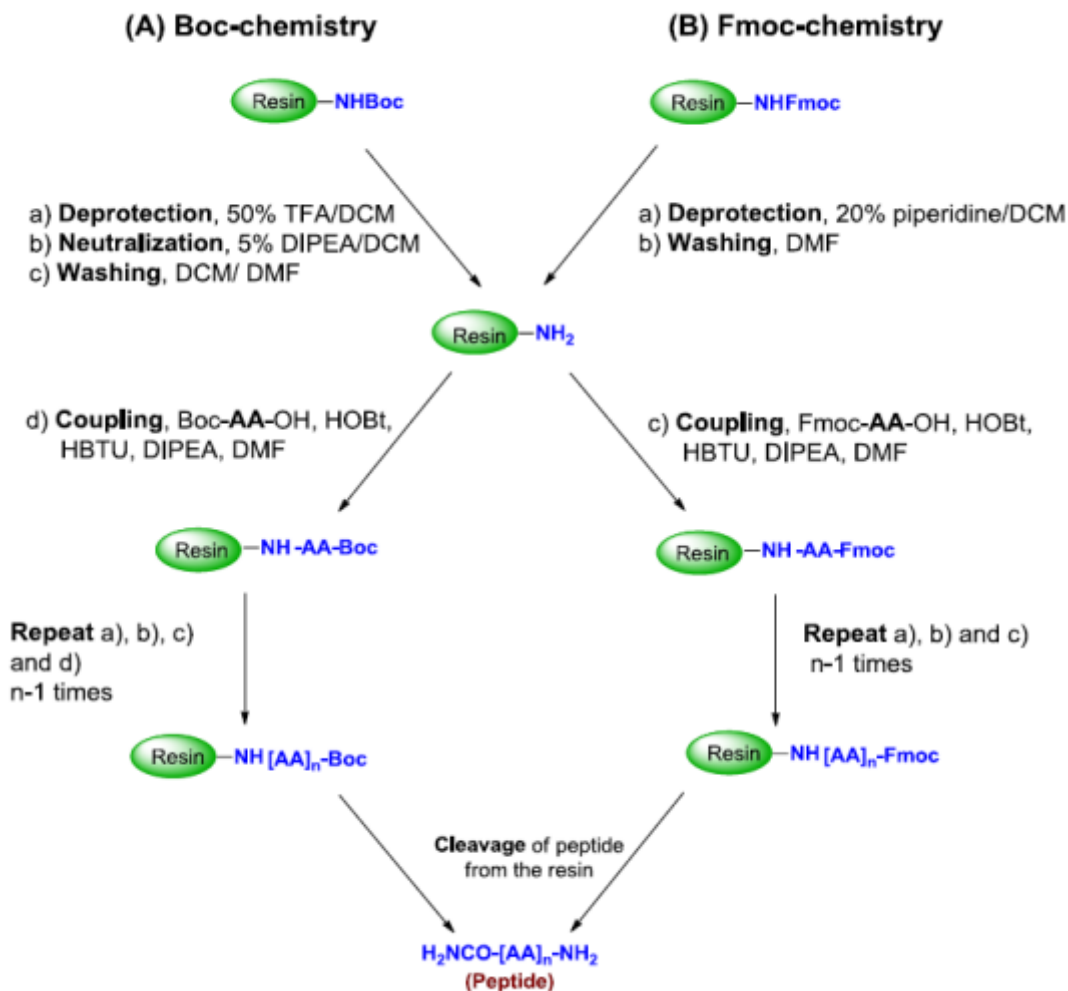
Figure 2.11 General protocols for SPPS (a) Boc-chemistry (b) Fmoc-chemistry

2.6 Results and Discussion

The synthesis, purification and characterization of PNA oligomers incorporating modified (γ dialkyl substituted/ β dimethyl) as well as unmodified *aeg* PNA monomers in the PNA sequence has been discussed in this section.

2.7 Synthesis of PNA oligomers

The PNA oligomers were synthesized by solid phase peptide synthesis protocol using *Boc* strategy. The modified PNA monomers were incorporated at desired positions in the unmodified *aeg* PNA sequence. PNA oligomerization was performed from C-terminus to

the N-terminus end using monomeric units with protected amino and carboxylic acid functions maintaining the orthogonality.
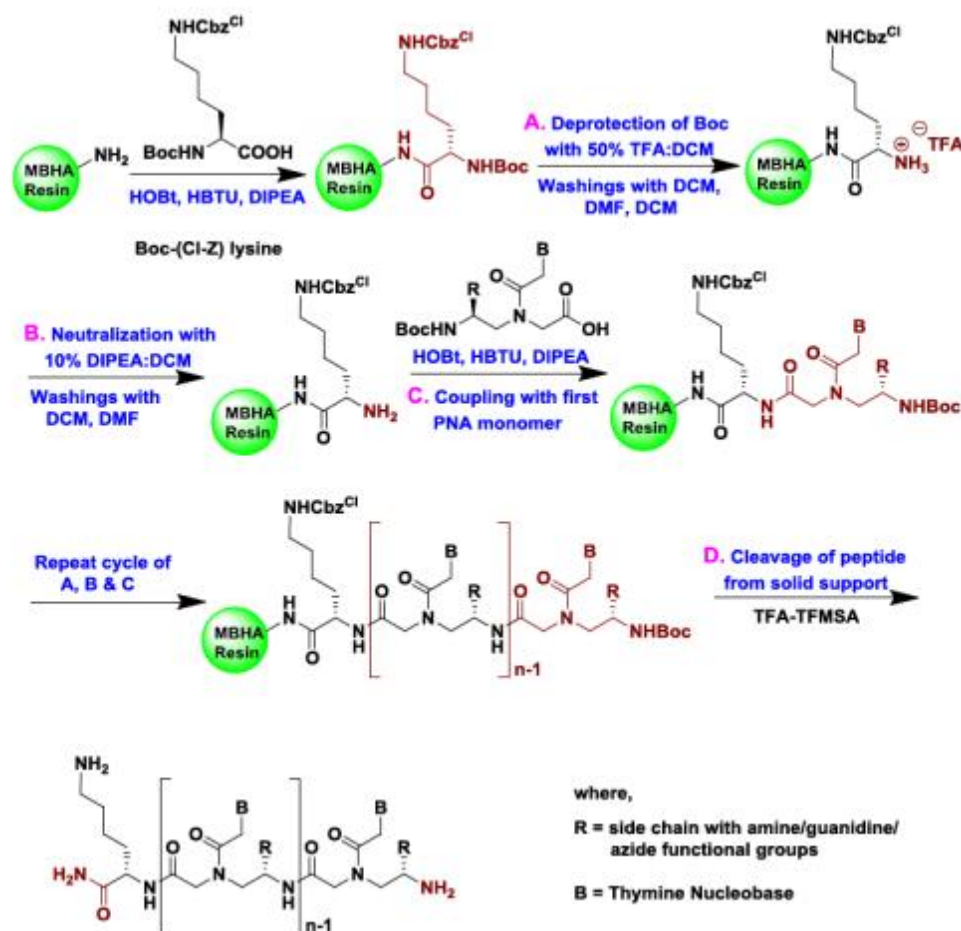
Figure 2.12 Solid phase PNA synthesis protocol by BOc strategy

MBHA resin (4-methyl–benzhydryl amine resin) was chosen as the solid support on which the oligomers were built and the monomers were coupled by *in situ* activation with PyBOP. In the synthesis of all oligomers, orthogonally protected (Boc/Cl-Cbz) L-lysine was selected as the *C*-terminal spacer-amino acid and it is linked to the resin through amide bond. The amine content on the resin was suitably lowered from 2 mmol/g to 0.35 mmol/g by partial acylation of amine content using calculated amount of acetic anhydride.[34] The free amine groups on the resin available for coupling was confirmed before starting synthesis by Kaiser's test.

The deprotection of the *N-t*-Boc protecting group and the completion of coupling reaction were monitored by Kaiser's test.[35] The *t*-Boc deprotection leads to a positive Kaiser's test, where the resin beads show blue color (Rheumann's purple). On the other hand, after completion of coupling reaction the resin beads were colorless which means a negative Kaiser's test. It is the most widely used qualitative test for the presence or absence of free amino group (deprotection/coupling).

Using the standard solid phase synthesis protocol (Figure **2.12**), the PNA oligomers of desired length incorporating modified as well as unmodified PNA monomers at desired positions were synthesized.

2.7.1 Synthesis of mixed purine-pyrimidine PNA oligomers

Mixed purine pyrimidine base sequences form duplexes of antiparallel or parallel orientations depending on their complementarity. By convention, in antiparallel orientation of PNA:DNA duplexes the *N*-terminus of the PNA faces the 3'-end of the DNA and *C*-terminal faces the 5'-end of DNA. While in parallel orientation, the *C*terminal of PNA faces the 3'-end of the DNA and the *N*-terminal faces the 5'-end of the DNA **(Figure 2.13).**

N ⟵——————— C   N ⟵——————— C

5' ⟵——————— 3'   3' ——————→ 5'

parallel mode   **antiparallel mode**
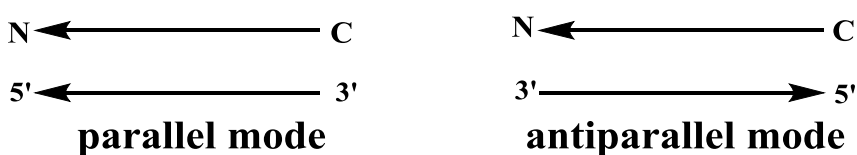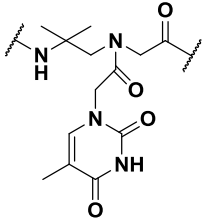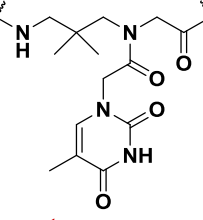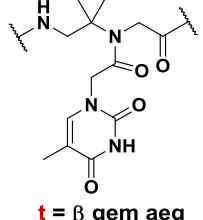
Figure 2.13: Antiparallel and parallel binding of PNA

In order to study the potential of duplex formation and the discrimination in DNA/RNA binding stability of the γ and β C-substituted multifunctional PNA oligomers, the mixed purine pyrimidine sequences were synthesized. The PNA sequences bearing modified (T) and unmodified (A/T/G/C) monomeric units were synthesized to improve the duplex stability and their cell permeation abilities. The decamer sequence H-GTAGATCACT-NH2 was used in all the current study, as its hybridization to DNA and RNA has been

thoroughly investigated.[36] This sequence contains three equally-spaced thymine residues as convenient points for substitution with modified monomers.

2.7.2 Table PNA oligomers with modified/unmodified monomers at various positions

Entry	Sequence Code	PNA sequences	Monomers used
1	*aeg* PNA **1**	H-G T A G A T C A C T-LysNH$_2$ 1 2 3 4 5 6 7 8 9 10	A/G/C/T=aeg PNA
2	γ gem-t^2 PNA **2**	H-G <u>t</u> A G A T C A C T-LysNH$_2$	
3	γ gem-t^6 PNA **3**	H-G T A G A <u>t</u> C A C T-LysNH$_2$	
4	γ gem-t^{2,6} PNA **4**	H-G <u>t</u> A G A <u>t</u> C A C T-LysNH$_2$	
5	γ gem-t^{2,6,10} PNA **5**	H-G <u>t</u> A G A <u>t</u> C A C <u>t</u>-LysNH$_2$	t = γ gem aeg
6	γ pip-t^2 PNA **6**	H-G <u>t</u> A G A T C A C T-LysNH$_2$	
7	γ pip-t^6 PNA **7**	H-G T A G A <u>t</u> C A C T-LysNH$_2$	
8	γ pip-t^{6,10} PNA **8***	H-G T A G A <u>t</u> C A C <u>t</u>-LysNH$_2$	t = γ pip aeg
9	γ gem apg-t^2 PNA **9**	H-G <u>t</u> A G A T C A C T-LysNH$_2$	
10	γ gem apg-t^6 PNA **10**	H-G T A G A <u>t</u> C A C T-LysNH$_2$	
11	γ gem apg-t^{2,6} PNA **11**	H-G <u>t</u> A G A <u>t</u> C A C T-LysNH$_2$	
12	γ gem apg-t^{2,6,10} PNA **12**	H-G <u>t</u> A G A <u>t</u> C A C <u>t</u>-LysNH$_2$	t= γ gem apg
13	β gem-t^2 PNA **13**	H-G <u>t</u> A G A T C A C T-ysNH$_2$	
14	β gem-t^6 PNA **14**	H-G T A G A <u>t</u> C A C T-LysNH$_2$	
15	β gem-t^{6,10} PNA **15**	H-G T A G A <u>t</u> C A C <u>t</u>-LysNH$_2$	
16	β gem-t^{2,6} PNA **16**	H-G <u>t</u> A G A <u>t</u> C A C T-LysNH$_2$	t = β gem aeg

γ gem = γ gemdimethyl, γ pip = γ piperidine, γ gem apg = γ gemdimethyl aminoprolylglycyl, β gem = β gemdimethyl.

** Further biophysical studies on **PNA 8** could not be carried out due to inadequate quantity*

2.7.3 Cleavage of the PNA oligomers from the solid support

The oligomers were cleaved from the solid support (L-lysine derivatized MBHA resin), using trifluoromethane sulphonic acid (TFMSA) in the presence of trifluoroacetic acid (TFA), which yielded PNA oligomers having L-lysine amide at their C-termini.[37] Side chain protecting groups of lysine as well as other nucleobase protections were also removed during this process. After cleavage reaction was over, the PNA oligomers obtained in solution were precipitated by addition of cold diethyl ether and the PNA oligomers were dissolved in de-ionized water.

2.7.4 Purification and characterization of the PNA oligomers

After cleavage from the solid support, PNA oligomers were purified by reverse phase high performance liquid chromatography (RP-HPLC). The purification of PNA oligomers was carried out on a semi-preparative C18 column using a gradient system of acetonitrile and water. The purity of PNA oligomers was checked by reinjecting the sample on the same C18 semi preparative column. All HPLC chromatograms are shown in Appendix I.

The integrity of these synthesized PNA oligomers was confirmed by MALDI-TOF mass spectrometry. In literature, various matrices like Sinampinic acid (3,5- dimethoxy-4 hydroxycinnamic acid), picolinic acid (PA), 2,5-dihydroxybenzoic acid (DHB), α-cyano-4-hydroxycinnamic acid (CHCA) etc. have been reported to record MALDI-TOF spectrum. Of these, DHB was used as matrix to record MALDI-TOF spectra for all synthesized PNAs.

The calculated and observed molecular weights for all PNAs with their molecular formulas and HPLC retention time in minutes are mentioned in Table **2.7.4**. The MALDI-TOF data for confirmation of mixed purinepyrimidine PNA oligomers are shown in **Appendix I.**

TABLE 2.7.4: MALDI-TOF spectral analysis of the synthesized PNA oligomers

Sr. No	PNA sequence code	Molecular Formula	Calculated Mass	Observed Mass	Retention Time (min)
1	aeg PNA **1**	$C_{114}H_{149}N_{60}O_{31}$	2854.1927	2854.6863	16.0
2	γ gem-t_2 PNA **2**	$C_{116}H_{153}N_{60}O_{31}$	2882.2240	2882.4302	17.6
3	γ gem-t_6 PNA **3**	$C_{116}H_{153}N_{60}O_{31}$	2882.2240	2882.2756	17.3
4	γ gem-$t_{2,6}$ PNA **4**	$C_{118}H_{157}N_{60}O_{31}$	2910.2553	2910.64	18
5	γ gem-$t_{2,6,10}$ PNA **5**	$C_{120}H_{161}N_{60}O_{31}$	2938.2866	2938.4849	19.2
6	γ pip-t_2 PNA **6**	$C_{118}H_{156}N_{61}O_{31}$	2923.2506	2923.2092 (2614.1152)	15.7
7	γ pip-t_6 PNA **7**	$C_{118}H_{156}N_{61}O_{31}$	2923.2506	2923.6196	15.2
8	β gem-t_2 PNA **8**	$C_{116}H_{153}N_{60}O_{31}$	2882.2240	2882.1616	17.3
9	β gem-t_6 PNA **9**	$C_{116}H_{153}N_{60}O_{31}$	2882.2240	2882.0698	16.8
10	β gem-$t_{6,10}$ PNA **10**	$C_{118}H_{157}N_{60}O_{31}$	2910.2553	2910.1594	18.2
11	β gem-$t_{2,6}$ PNA **11**	$C_{118}H_{157}N_{60}O_{31}$	2910.2553	2910.8999	18.4
12	γ gem apg-t_2 PNA **12**	$C_{117}H_{155}N_{60}O_{31}$	2896.2397	2896.5830	17.6
13	γ gem apg-t_6 PNA **13**	$C_{117}H_{155}N_{60}O_{31}$	2896.2397	2896.4778	17.2
14	γ gem apg-$t_{2,6}$ PNA **14**	$C_{120}H_{161}N_{60}O_{31}$	2938.2866	2938.7803	18.8
15	γ gem apg-$t_{2,6,10}$ PNA **15**	$C_{123}H_{167}N_{60}O_{31}$	2980.3336	2980.5967	19.5

Typical HPLC and MALDI-TOF of PNA **2**:
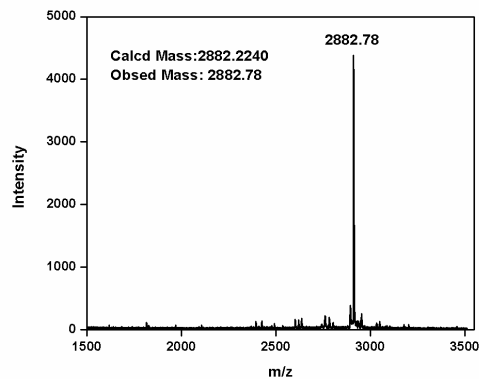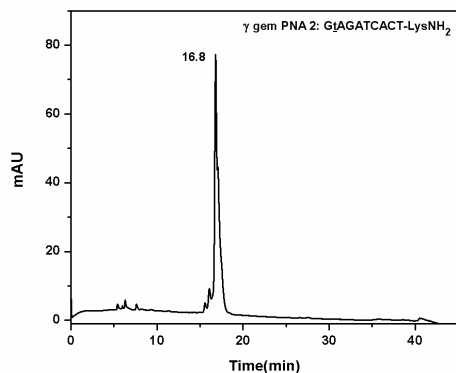
2.8 Summary

The rationally designed modified PNA monomers have been incorporated into 10-mer mixed purine-pyrimidine PNA sequence. These modified monomers were inserted into *aeg* PNA sequence at various positions using HOBt, HBTU and DIPEA as coupling reagent by solid phase peptide synthesis protocol. All the modified and unmodified PNA oligomers obtained by solid phase synthesis were cleaved from solid support using appropriate protocol. The PNA oligomers after cleavage were purified by RP-HPLC and characterized by MALDI-TOF spectrometry. Detailed experimental procedures and spectral data of all intermediates are discussed in section **2.9.** The third chapter deals with the investigation of biophysical properties of PNA oligomers.

2.9 Experimental

This section describes the detailed synthetic procedures and spectral characterization of the rationally designed PNA monomers.

2.9 A General

The chemicals used were of laboratory or analytical grade. All the solvents used were distilled or dried to carry out various reactions. Reactions were monitored using thin layer chromatography (TLC). Usual workup involved sequential washing of the organic extract with water and brine followed by drying the organic layer over anhydrous sodium sulphate and evaporation of solvent under vacuum. TLCs were carried out on pre-coated silica gel GF_{254} sheets (Merck 5554). TLCs were analysed under UV lamp, by Iodine spray and by spraying with Ninhydrin solution, followed by heating of the plate. Column chromatographic separations were performed using silica gel (60-120 or 100-200 mesh). ^{1}H and ^{13}C NMR spectra were recorded using Bruker AC-200 (200 MHz) or JEOL 400 MHz NMR spectrometers. The delta (δ) values for chemical shifts are reported in ppm and are referred to internal standard TMS or deuterated NMR solvents.

Mass spectra for reaction intermediates were obtained by Applied Biosystems 4800 Plus MALDI-TOF/TOF mass spectrometry using TiO_2 or 2,5- dihydroxybencoic acid (DHB) and the integrity of PNA oligomer was checked on the same instrument using DHB or CHCA as matrix. High resolution mass spectra for final PNA monomers were recorded on Synapt G2 High Definition Mass Spectrometry. PNA oligomers were purified on Agilent HPLC system using semi-preparative BEH130 C18 (10X250 mm) column.

2.9 B Procedures and spectral data

Tert-butyl (1-hydroxy-2-methylpropan-2-yl) carbamate 2

2
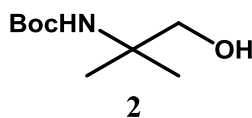
To a solution of 2-amino-2-methylpropan-1-ol **1** (5 g, 57 mmol) in 1:1 dioxane: water (60 ml) and 2N NaOH solution (13 ml), di-tert-butyl dicarbonate [(Boc)$_2$O] (13.15 g, 60 mmol) was added in portions in ice cold condition. The reaction mixture was further stirred at 0 ^{o}C for 12 h. After completion of reaction, dioxane was evaporated and product was extracted in ethyl acetate. The alcohol 2 was used further without purification. Yield (3 g, 30%) ^{1}H-NMR (200Hz, CDCl3) δ: 1.26(s, 6H), 1.43(s, 9H), 3.56(s, 2H), 4.85(bs, 1H) MS (MALDI-TOF) *m/z* calculated for CHNO [M+ Na]$^+$ 283.1637, observed: 283.1261.

Tert-butyl (2-methyl-1-oxopropan-2-yl) carbamate 3

3
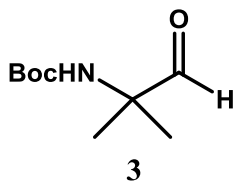
To a solution of compound **2** (2.5 g, 13.22 mmol) in dry acetonitrile, TEMPO (0.41 g, 0.26 mmol) and DIAB (4.26 g, 13.22 mmol) were added at ice cold condition and then

stirred at RT for 1hour. The reaction mixture was concentrated and the oxidized product aldehyde **3** was used for next reaction without further purification.

Methyl (2-((tert-butoxycarbonyl) amino)-2-methylpropyl)glycinate 4
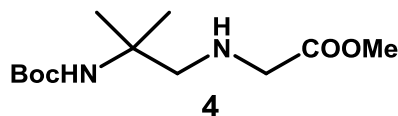
To the solution of aldehyde **3** (2.25 g, 11.9 mmol) and glycine methyl ester hydrochloride (6.6 g, 52.9 mmol) in ethanol, DIPEA (6.8 g, 52.9 mmol) was added in ice cold condition and stirred for 15min, and then sodium cynoborohydride (3.38 g, 52.9 mmol) was added in small portions at the same temperature and stirred at RT for 6 hours. After completion of reaction (monitored by TLC), ethanol was evaporated and product was extracted with ethylacetate. The organic layer was concentrated and subjected for column chromatography and the product **4** was eluted with 20% EtOAc in pet ether. Yield (2.3g, 67%); ^{1}H- NMR(400MHz, CDCl$_3$) δ: 1.26(s, 6H), 1.40(s, 9H), 2.18(bs, 1H), 2.63(s, 2H), 3.42(s, 2H), 3.70(s, 3H), 5.05(bs,1H); ^{13}C-NMR(100MHz, CDCl$_3$) δ: 25.2, 28.5, 51.2, 51.9, 52.3, 58.7, 78.8, 155.0, 173.0;

MS (MALDI-TOF) *m/z* calculated for C$_{12}$H$_{24}$N$_2$O$_4$ [M+ Na]$^+$ 283.1637, observed: 283.1261.

**Methyl N-(2-((tert-butoxycarbonyl) amino)-2-methylpropyl)-N-(2-chloroacetyl) glycinate 5**
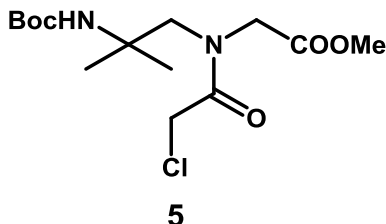
To the stirred solution of secondary amine **4** (0.150 g, 0.57 mmol) in DCM (1.5ml), triethylamine (0.175 g, 1.7 mmol) and chloroacetyl chloride (0.13 g, 1.15 mmol) were

added in ice cold condition and strirred for 3 hours at same temperature. After completion of reaction, DCM was added to reaction mixture and the product was extracted in DCM. The organic layer was concentrated and purified by column chromatography; the product **5** was eluted in 8% EtOAc in pet ether. Yield (67%); ^{1}H-NMR (400MHz, CDCl$_3$) δ: 1.26(ma.) (s, 4H) and 1.34(mi.)(s,2H), 1.42(mi.) (s, 3H) and 1.43(ma.)(s, 6H), 3.70(mi.)(s, 1H) and 3.74(ma.)(s, 1H), 3.76(bs, 1H) and 3.78(ma.) (s,2H), 4.03(ma.) (s, 1H) and 4.08(mi.)(s, 1H), 4.20(mi.)(s, 1H) and 4.23(ma.)(s, 1H), 4.48(ma.)(bs,1H) and 4.53(mi.)(bs, 1H).

HRMS (ESI/TOF) *m/z* calculated for C$_{14}$H$_{25}$ClN$_2$O$_5$ [M +Na] $^+$ 359.1342, observed: 359.1353.

Methyl N-(acetyl-2-t)-N-(2-((tert-butoxycarbonyl)amino)-2-methylpropyl)glycinate 6

6
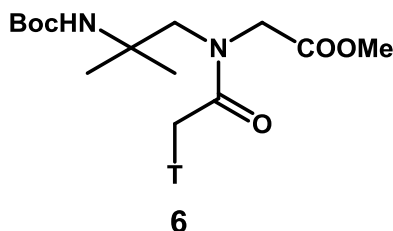
To the solution of chloro compound **5** (0.35 g, 1.0 mmol) in dry dimethylformamide (1.4 ml), thymine (0.157 g, 1.25 mmol) and K$_2$CO$_3$(0.1728 g, 1.25 mmol) were added at RT and stirred at same temperature for 12 h. After completion of reaction (monitored by TLC), DMF was rotaevaporated and water was added to reaction mixture, product was extracted in ethyl acetate. The organic layer was concentrated and subjected to column chromatography, **5** was eluted with 85% EtOAc in pet ether. Yield (70%); ^{1}H-NMR (400MHz, CDCl$_3$) δ: 1.22(ma.)(s, 3H), 1.38-1.42(m,9H), 1.89(mi.)(s,1H) and 1.91(ma.)(s, 2H), 3.71(mi.) (bs, 1H) and 3.72(ma.) (s, 1H), 3.76(mi.) (bs, 1H) and 3.79(ma.) (s, 2H), 4.08(mi.) (s, 1H) and 4.26(ma.) (s, 1H), 4.43(ma.) (s, 1H) and 4.62(mi.)(s, 1H), 4.51(ma.) and 4.69(mi.) (s, 1H). ^{13}C-NMR (100MHz, CDCl$_3$) δ: 12.3, 25.7, 25.9, 28.3, 29.6, 47.8, 47.9, 50.6, 52.1, 52.6, 53.7, 54.3, 110.6, 110.7, 141.0, 151.0, 151.1, 154.5, 1546, 164.1, 168.2, 168.5, 169.5, 170.3.

MS (MALDI/TOF) *m/z* calculated for $C_{19}H_{30}N_4O_7$ $[M+K]^+$ 465.1751, observed: 465.1560.

N-(acetyl-2-t)-N-(2-((tert-butoxycarbonyl) amino)-2-methylpropyl) glycine 7
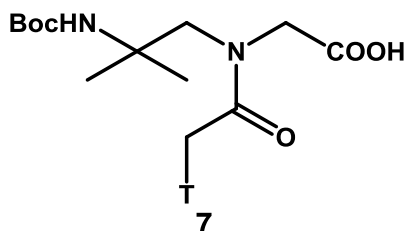

The ester compound **6** in THF was saponified with 10% LiOH at 0 ^{0}C for 5h. After completion of reaction, the reaction mixture was acidified with amberlite resin to pH 3. The reaction mixture was then concentrated to get acid monomer **7**. Yield (60%); ^{1}H-NMR (400MHz, DMSO-d^6) δ: 1.06 (ma.)(s, 3H) and 1.19(mi.) (s, 3H), 1.32 (s, 9H), 1.7(s, 3H), 3.46(ma.) (s, 1H) and 3.56(mi.) (s, 1H), 3.88(mi.) (s, 1H) and 4.11(ma.) (s, 1H), 4.44(ma.) (s, 1H) and 4.57(mi.) (s, 1H), 7.24(ma.) and 7.30(mi.) (s, 1H), 11.22 (ma.) and 11.24(mi.) (s, 1H). ^{13}C-NMR (100MHz, DMASO-d^6) δ: 12.4, 21.6, 25.6, 28.7, 48.5, 50.4, 53.7, 54.1, 78.2, 108.6, 142.6, 151.4, 154.9, 164.9, 169.4, 171.2, 191.4.

HRMS (ESI/MS) *m/z* calculated for $C_{18}H_{28}N_4O_7$ $[M+Na]^+$ 435.1855, observed: 435.1856.

1-benzyl 4-methyl 4-((tert-butoxycarbonyl) amino) piperidine-1, 4-dicarboxylate 9
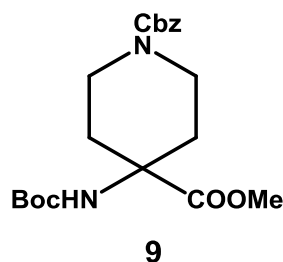
To a stirred solution of 4-(boc-amino)-1-Cbz-piperidine-4-carboxylic acid **8** (3.9 g, 10.3 mmol), K_2CO_3 (3.56 g, 25.7 mmol) in acetone (50 mL) was added dimethyl sulfate (1.68 g, 13.39 mmol) and reaction mixture was heated to 55 ◦C for 6 h under reflux condenser. Acetone was evaporated completely and water (30 mL) was added to the concentrate,

which was then extracted with ethyl acetate (3 x 40 mL). The combined ethyl acetate extracts were washed with brine, dried over an. Na_2SO_4, filtered and concentrated. The residue was purified on silica gel (60-120 mesh) using petroleum ether and ethyl acetate to give compound **9** as white solid (3.63 g, 90% yield). ^{1}H NMR (400 MHz, CDCl3); ^{13}C NMR (100 MHz, CDCl3) δ; 1.45(s, 9H), 1.98-2.05(m, 2H), 2.07-2.11(m, 2H), 3.25(t, 2H), 3.75(s, 3H), 3.90-3.93(d, 2H, J= 3Hz), 4.86(s, 1H), 7.37(s, 5H). [13]C(100MHz) δ: 28.2, 29.4, 32.7, 39.9, 52.7, 56.8, 61.6, 67.0, 126.8, 128.6, 137.3, 173.9.

HRMS (ESI/MS) *m/z* calcd for $C_{20}H_{28}N_2O_6$ [M+Na] [+] 415.1844 found 415.1841.

Benzyl 4-((tert-butoxycarbonyl) amino)-4-(hydroxymethyl) piperidine-1-carboxylate 10
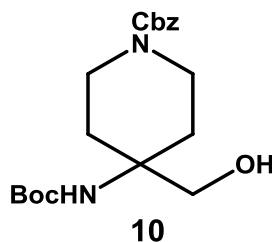
To a stirred solution of compound **9** (2 g, 5 mmol) in absolute ethanol (15 mL), sodium borohydride (0.96 g, 25.4 mmol) was added and reaction mixture was stirred for 10 h under nitrogen atmosphere at room temperature. Ethanol was evaporated completely and water (100 mL) was added to the concentrate which was extracted with ethyl acetate (3 x 75 mL). The combined organic layer was washed with brine, dried over an. Na_2SO_4, filtered and concentrated. The residue was then purified on silica gel (60-120 mesh) using petroleum ether and ethyl acetate to give compound **10** as white crystalline solid (1.0 g, 54% yield). ^{1}H NMR (400 MHz, CDCl3) δ; 1.42(S, 9H), 1.66-1.56(m, 2H), 1.88(d, J=11.6Hz, 2H), 3.22(t, J=10.8Hz, 2H), 3.67(S, 2H), 3.77(bs, 2H),5.11(S, 2H), 7.33(ma.) & 7.34(mi.) (s, 5H); ^{13}C NMR (100 MHz, CDCl3) δ ^{13}C NMR (100 MHz, CDCl3) δ: 156.03 (s), 155.32 (s), 136.74 (s), 128.60 (s), 128.07 (d, *J* = 14.2 Hz), 69.05 (s), 67.26 (s), 54.79 (s), 39.59 (s), 31.56 (s), 28.40 (s).

HRMS (ESI/MS) *m/z* calcd for $C_{19}H_{28}N_2O_5$ [M+Na][+] 387.1895, observed: 387.1894.

Benzyl 4-((tert-butoxycarbonyl) amino)-4-formyl piperidine-1-carboxylate 11

11
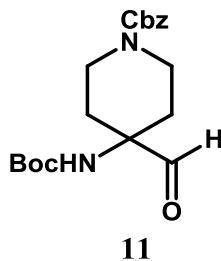
To a solution of compound **10** (2.02 g, 55.5 mmol) in dry acetonitrile, TEMPO (0.43 g, 0.27 mmol) and DIAB (1.78 g, 55.5 mmol) were added at RT and stirred for 1.5 h. The reaction mixture was concentrated and the oxidized product aldehyde **11** was used for next reaction without further purification.

Benzyl 4-(tert-butoxycarbonyl) amino-4-(((2-methoxy-2-oxoethyl) amino) piperidine-1-carboxylate 12

12
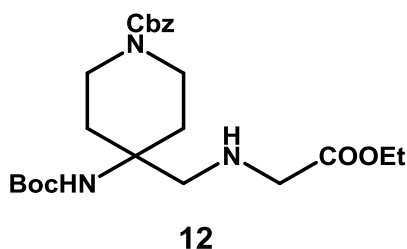
To the solution of aldehyde **10** (0.8 g, 21.9 mmol) and glycine ethyl ester hydrochloride (3.1 g, 22.2 mmol) in ethanol, DIPEA (2.8 g, 22.2 mmol) was added in ice cold condition and stirred for 15min, and then sodium cynoborohydride (1.42 g, 22.2 mmol) was added in small portions at the same temperature and stirred at RT for 10 h. After the completion of reaction (monitored by TLC), ethanol was evaporated and product was extracted with ethylacetate. The organic layer was concentrated and subjected for column chromatography and the product **12** was eluted with 30% EtOAc in pet ether. Yield (1.11 g, 90%); 1H- NMR(400MHz, CDCl$_3$) δ: 1.26(t, J=7.08Hz, 3H), 1.42(s, 9H), 1.46-1.54(m, 2H), 2.08(d, 2H), 2.81(s, 2H), 3.17(t, 2H), 3.39(s,2H), 3.82(bs, 2H), 4.17(q, 2H), 4.50(s, 1H),5.11(s,2H), 7.33(maj) & 7.34(min) (s,5H) ; ^{13}C-NMR(100MHz, CDCl$_3$)

δ:14.2, 28.3, 29.6, 32.4, 39.5, 51.5, 53.7, 55.3, 60.7, 67.0, 79.4, 127.8, 128.4, 136.8, 155.2, 172.3;

MS (MALDI-TOF) *m/z* calculated for $C_{23}H_{35}N3O6$ [M+ Na]$^+$, 472.2424 observed: 472.2306.

Benzyl 4-((2-chloro-N-(2-methoxy-2-oxoethyl) acetamido) methyl) piperidine-1-carboxylate 13
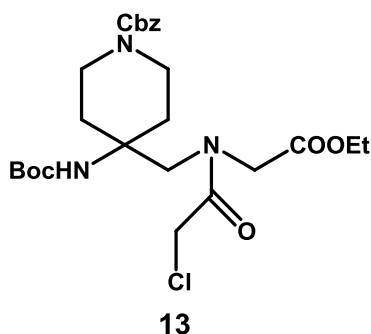
To the stirred solution of secondary amine **12** (2.49 g, 0.55 mmol) in DCM (40 ml), triethylamine (1.67 g, 16.6 mmol) and chloroacetyl chloride (1.25 g, 11 mmol) were added in ice cold condition and stirred for 5 hours at same temperature. After completion of reaction, DCM was added to reaction mixture and the product was extracted in DCM. The organic layer was concentrated and purified by column chromatography; the product **13** was eluted in 25% EtOAc in pet ether. Yield (80%); ^{1}H-NMR (400MHz, CDCl$_3$) δ: 1.31(t, J=7.32Hz, 3H), 1.41(min) & 1.43(maj) (s, 9H), 1.61-1.68 (m, 2H), 3.05(t, J=11.4Hz, 2H), 3.7(s, 2H), 3.9(d, J=11.2Hz, 2H), 3.99(s, 2H), 4.1-4.2(m, 4H), 5.1(maj) & 5.12(min)(s,2H), 7.34(maj) & 7.35(min) (s, 5H), ^{13}C-NMR(CDCl$_3$) δ: 14.2, 28.3, 32.4, 39.5, 51.5, 53.7, 55.3, 60.7, 67.0, 79.4, 127.8, 128.4, 136.8, 155.2, 172.3;

HRMS *m/z* calculated for $C_{25}H_{36}ClN_3O_7$ [M+H]+ 526.232, observed: 526.2318.

Benzyl 4-((tert-butoxycarbonyl) amino)-4-((N-(2-methoxy-2-oxoethyl) acetamido-2-t) methyl) piperidine-1-carboxylate 14

To the solution of chloro compound **12** (3.5 g, 68.5 mmol) in dry dimethylformamide (15 ml), thymine (1.03 g, 82.2 mmol) and K$_2$CO$_3$ (1.13 g, 82.2 mmol) were added at RT and

stirred at same temperature for 12 h. After completion of reaction (monitored by TLC), DMF was rota-evaporated and water was added to reaction mixture, product was extracted in ethyl acetate.

14
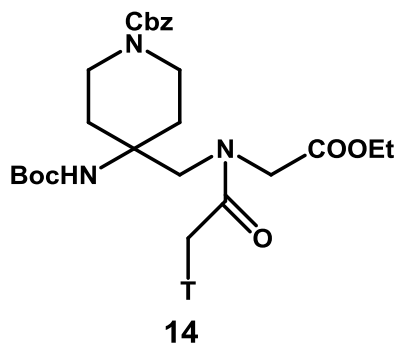
The organic layer was concentrated and subjected to column chromatography, compound **13** was eluted with 60% EtOAc in pet ether. Yield (68%); ^{1}H-NMR (400MHz, CDCl$_3$) δ: 1.34(t, 2H), 1.43(mi.) and 1.45(ma.) (s, 9H), 1.60(t, 2H), 1.81(s, 2H), 1.92(mi.) and 1.93(ma.) (s, 3H), 3.05(t, 2H), 3.78(ma.) and 3.89(mi.) (s, 2H), 3.91(bs, 2H), 4.26(ma.) and 4.28(mi.) (s, 3H), 4.38(bs, 2H), 4.57(s, 1H), 5.11(ma.) and 5.15(mi.) (s, 2H), 7.35(ma.) and 7.37(mi.) (s, 5H), 9.04(mi.) and 9.13(ma.) (s, 1H). ^{13}C NMR (100MHz, CDCl$_3$) δ: 12.1, 12.4, 13.9, 14.3, 28.3, 28.5, 47.8, 48.2, 53.1, 54.7, 54.9, 61.9, 62.0, 66.4, 66.9, 110.7, 110.8, 127.47, 12.6, 136.7, 140.8, 141.2, 150.7, 150.9, 154.8, 155.3, 164.3, 168.7, 169.8.

HRMS (ESI/MS) calculated for $C_{30}H_{41}N_5O_9$ [M+Na]$^+$ 638.2801, observed 638.2803.

N-(acetyl-2-t)-N-((1-((benzyloxy)carbonyl)-4-((tert-butoxycarbonyl)amino) piperidin-4-yl)methyl)glycine 15

15
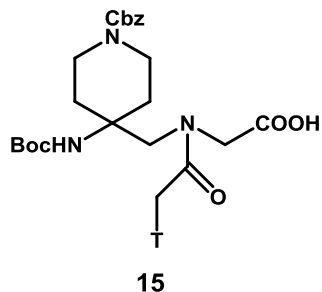
The ester compound **13** in THF was saponified with 10% LiOH at 0^{0}C for 5h. After completion of reaction, the reaction mixture was acidified with amberlite resin to pH 3. The reaction mixture was then concentrated to get acid monomer **14**. Yield (90%); [1]H-

NMR (400MHz, CDCl$_3$) δ: 1.39(ma.) and 1.50(mi.) (s, 9H), 1.86(s, 3H), 2.02(s, 2H), 4.20-4.81(m, 12H), 5.06(s, 2H), 7.02(mi.) and 7.07(ma.) (s, 1H), 7.32(s, 5H), 9.62-10.03(m, 1H). ^{13}C(100MHz) δ: 12.2, 15.3, 20.8, 28.1, 32.3, 39.6, 47.8, 65.8, 67.4, 110.2, 127.5, 128.8, 136.1, 141.3, 155.2, 165.3, 169.2, 175.8.

HRMS (ESI/MS) calculated for C$_{27}$H$_{36}$N$_5$O$_7$ [M+Na]$^+$ 610.2488, observed 610.2488

Tert-butyl (2-amino-2-methylpropyl) carbamate 17

17
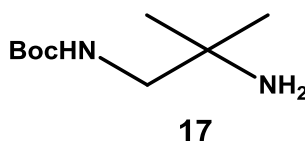
To the stirred solution of 2-methylpropane-1, 2-diamine (10 g, 114.0 mmol) in THF (500 ml), di-tert-butyl dicarbonate [(Boc)$_2$O] (6.19 g, 6.5 ml, 28.4 mmol) was added in portions in ice cold condition. The reaction mixture was further stirred at 0 °C for 12 h. After completion of reaction THF was removed completely. Product **15** was extracted in EtOAc and the organic layer was concentrated to give white solid compound **15** which was used without further purification (5.7 g, 27%).

Ethyl (1-((tert-butoxycarbonyl) amino)-2-methylpropan-2-yl)glycinate 18

18
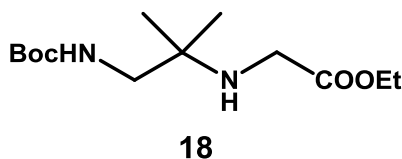
The amine compound (3 g, 15.9 mmol) was treated with ethylbromo acetate (1.9 mL, 17.5 mmol) in acetonitrile (90 mL) using triethyl amine (2.6 mL, 19.1 mmol) in ice cold condition and the reaction mixture was stirred at room temperature for 12 h. Acetonitrile was evaporated completely under vacuum and water was added to the concentrate. The aqueous layer was extracted with ethyl acetate and the combined organic layer was washed with sat. NaHCO$_3$, brine, dried over an. Na$_2$SO$_4$. The organic extract was concentrated on rota evaporator. The residue obtained was purified on silica gel (100-200

mesh) using petroleum ether and ethyl acetate to give compound **16** as yellowish oil (58%). ^{1}H NMR (400 MHz, CDCl$_3$) δ 1.06(s, 6H), 1.28(t, J=8Hz, 3H), 1.44(s, 9H), 3.01(d, 2H), 3.36(s, 2H), 4.14-4.24(q, J=8Hz, 2H), 5.14(bs, 1H); ^{13}C NMR (100 MHz, CDCl$_3$) δ;

HRMS (ESI/MS) calculated for C$_{13}$H$_{26}$N$_2$O$_4$ [M + H] $_+$ 275.1971, observed: 275.1977.

Ethyl N-(1-((tert-butoxycarbonyl) amino)-2-methylpropan-2-yl)-N-(2-chloroacetyl) glycinate 19

19
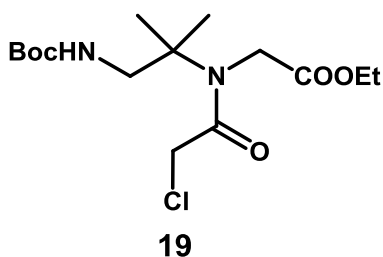
To an ice-cold solution of compound **16** (2.4 g, 88.9 mmol) and triethyl amine (2.69 g; 3.7 mL, 26.6 mmol) in dry DCM (50 mL) was added chloroacetyl chloride (2 g; 1.4 mL, 17.7 mmol) and reaction mixture was stirred for 8 h. To the reaction mixture DCM (20 mL) was added and washed with water (60 mL) and brine (60 mL). The organic layer was dried over an. Na$_2$SO$_4$, filtered and concentrated. The residue was then purified on silica gel (100-200 mesh) using petroleum ether and ethyl acetate to give compound **17** as colorless sticky oil (88%). ^{1}H NMR (400 MHz, CDCl$_3$) δ 1.31(t, J=7.1Hz, 3H), 1.35(s, 6H), 1.42(s, 9H), 3.60-3.61 (d, J=6.6Hz, 2H), 3.9 (s, 2H), 4.1 (s, 2H), 4.23-4.28 (q, J=7.12Hz, 2H), 5.12(bs, 1H); ^{13}C NMR (100 MHz, CDCl$_3$) 14.13, 25.0, 28.3, 43.7, 47.3, 47.5, 62.1, 62.2, 79.0, 156.4, 167.7, 170.3 ;

MS (MALDI-TOF) *m/z* calcd for C$_{15}$H$_{27}$ClN$_2$O$_5$ [M +K]$^+$ 389.1246, observed: 389.0901

Tert-butyl 4-(2-ethoxy-2-oxoethyl)-3, 3-dimethyl-5-oxopiperazine-1-carboxylate 20

To a solution of chloro compound **17** (1.4 g, 4.09 mmol) in dry DMF (8ml), thymine (0.59 g, 4.7 mmol) and K$_2$CO$_3$ (0.59 g, 4.3 mmol) were added at RT and stirred at same temperature for 12 h. After completion of reaction (monitored by TLC), DMF was

rotaevaporated and water was added to reaction mixture, product was extracted in ethyl acetate.

20
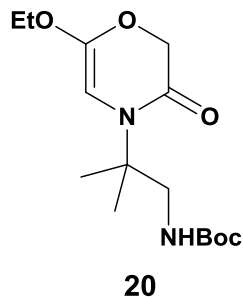
The organic layer was concentrated and subjected to column chromatography, compound **18** was eluted with 25% EtOAc in pet ether. Yield (70%); ^{1}H-NMR (400MHz, CDCl$_3$) δ: 1.15-1.17(d, J=6.8Hz, 6H), 1.23(t, J=7Hz, 3H), 1.35(s, 9H), ^{13}C-NMR(100MHz, CDCl$_3$) δ: 13.96, 23.2, 23.4, 28.3, 40.2, 48.4, 49.3, 58.2, 61.7, 79.0, 156.3, 166.0, 171.8. HRMS (ESI/MS) calculated for C$_{15}$H$_{26}$N$_5$O$_5$ [M+Na]$^+$ 337.1739, observed: 337.1741.

Ethyl N-(acetyl-2-t)-N-(1-((tert-butoxycarbonyl) amino)-2-methylpropan-2-yl) glycinate 21
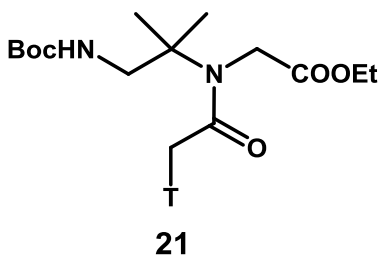
21

To a solution of chloro compound **17** (1.4 g, 4.09 mmol) in dry DMF (8 ml), thymine (0.59 g, 4.7 mmol) and K$_2$CO$_3$ (0.59 g, 4.3 mmol) were added at RT and stirred at same temperature for 12 h. After completion of reaction (monitored by TLC), DMF was rotaevaporated and water was added to reaction mixture, product was extracted in EtOAc. The organic layer was concentrated and subjected to column chromatography, compound **18** was eluted with 25% EtOAc in pet ether. Yield (80%); ^{1}H-NMR (400MHz, CDCl$_3$) δ: 1.35(s, 9H), 1.42(s, 9H), 1.9(s, 3H), 3.57-3.58(d, J=5.6Hz, 2H), 4.17(s, 2H), 4.24-4.30(m, 2H). 4.4(bs, 2H), 5.2(bs, 1H), 7.0(s, 1H), 9.2(bs, 1H); ^{13}C-NMR(100MHz, CDCl$_3$)δ:

12.35, 14.12, 25.06, 28.4, 46.7, 47.3, 49.7, 62.2, 79.1, 110.7, 141.1, 156.4, 167.9, 170.5. ; HRMS (ESI/MS) calculated for $C_{20}H_{32}N_4O_7$ [M+ Na]$^+$ 463.2168, observed: 463.2182.

.

N-(acetyl-2-t)-N-(1-((tert-butoxycarbonyl) amino)-2-methylpropan-2-yl) glycine 22

22
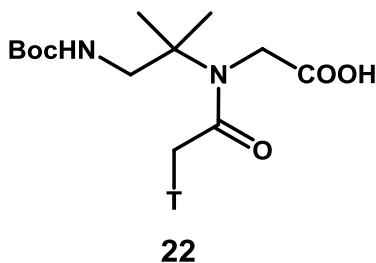
The ester compound **19** in THF was saponified with 10% LiOH at 0 ^{o}C for 5h. After completion of reaction, the reaction mixture was acidified with amberlite resin to pH 3. The reaction mixture was then concentrated to get acid monomer **20**. Yield (85%); ^{1}H-NMR (400MHz, DMSO-d$_6$) δ:1.20(s, 6H), 1.34(s, 9H), 3.34(bs, 2H), 4.06(s, 2H), 4.39(s, 2H), 6.6(bs, 1H), 7.21(s, 1H), 11.2(s, 1H); ^{13}C (100MHz, DMSO-d$_6$) δ: 12.5, 21.0, 24.7, 28.7, 46.5, 46.9, 49.8, 78.1, 108.4, 142.7, 151.5, 156.5, 164.9, 168.3, 172.5. HRMS (ESI/MS) calculated for $C_{18}H_{28}N_4O_7$ [M+Na]$^+$ 435.1855, observed: 435.1864.

Tert-butyl (3-amino-2, 2-dimethylpropyl) carbamate 24

24
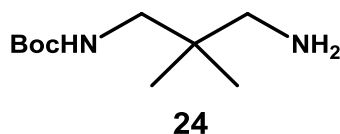
To a stirred solution of 2, 2-dimethylpropane-1,3-diamine (10 g, 98 mmol) in THF (500 ml), di-tert-butyl dicarbonate [(Boc)$_2$O] (2.13 g, 9.8 mmol) was added in portions in ice cold condition. The reaction mixture was further stirred at 0 ^{o}C for 12 h. After completion of reaction THF was removed completely. Product **21** was extracted in EtOAc. Organic layer was concentrated to give white solid compound **21** which was used without further purification (3 g, 15%)

Ethyl (3-((tert-butoxycarbonyl) amino)-2, 2-dimethylpropyl)glycinate 25

25
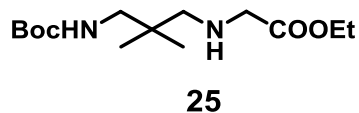
The amine compound **21** (3g, 14.8 mmol) was treated with ethylbromo acetate (2.7g, 16.3 mmol) in acetonitrile (60 mL) using triethyl amine (4.8g, 47.8 mmol) in ice cold condition and the reaction mixture was stirred at room temperature for 12 h. Acetonitrile was evaporated completely under vacuum and water was added to the concentrate. The aqueous layer was extracted with ethyl acetate. The combined organic layer was washed with sat. $NaHCO_3$, brine, dried over Na_2SO_4, filtered and concentrated on rota evaporator. The residue obtained was purified on silica gel (100-200 mesh) using petroleum ether and ethyl acetate to give compound 16 as yellowish oil (3.3 g,76%). ^{1}H NMR (400 MHz, $CDCl_3$) δ 0.83(s, 6H), 1.22(t, J=8Hz, 3H), 1.38(s, 9H), 2.33(s, 2H), 2.97-2.98 (d, J=6.4Hz, 2H), 3.31(s, 2H), 4.15-4.10 (q, J=8Hz, 2H), 5.42(bs, 1H); ^{13}C NMR(100 MHz, $CDCl_3$) δ; 14.2, 23.8, 28.4, 35.1, 49.3, 60.7, 78.7, 156.6, 172.7. HRMS *m/z* calcd for $C_{14}H_{28}N_2O_4$ [M + H] $_+$ 289.2127, observed: 289.2133.

Ethyl N-(3-((tert-butoxycarbonyl) amino)-2, 2-dimethylpropyl)-N-(2-chloroacetyl) glycinate 26

26
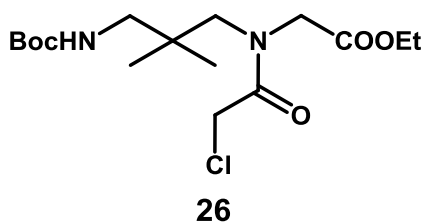
To an ice-cold solution of compound **22** (3 g, 10.4 mmol) and triethyl amine (3.1 g; 4.3 mL, 31.0 mmol) in dry DCM (30 mL) was added chloroacetyl chloride (2.35 g; 1.65 mL, 20.8 mmol) and the reaction mixture was stirred for 8 h. To the reaction mixture DCM (20 mL) was added and washed with water and brine. The organic layer was dried over Na_2SO_4, filtered and concentrated. The residue was then purified on silica gel (100-200 mesh) using petroleum ether and ethyl acetate to give compound 23 as colorless sticky oil

(79%). ^{1}H NMR (200 MHz, CDCl$_3$) δ: 0.86(s, 6H), 1.26(t, J=8Hz, 3H), 1.38(s, 9H), 2.81-2.82(d, J=6Hz, 2H), 3.14(s, 2H), 3.98(s, 2H), 4.14(s, 2H) 4.17-4.23(q, J=8Hz, 2H), 5.83(bs, 1H); ^{13}C-NMR(100MHz) δ: 14.0, 24.1, 28.1, 37.5, 41.5, 46.8, 52.3, 55.5, 62.3, 78.8, 156.6, 168.9, 169.4.

HRMS *m/z* calculated for C$_{16}$H$_{29}$ClN$_2$O$_5$ [M+Na] 387.1662, observed: 387.1666

Ethyl N-(acetyl-2-t)-N-(3-((tert-butoxycarbonyl) amino)-2, 2-dimethylpropyl) glycinate 27

27
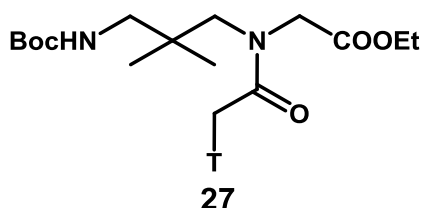
To the solution of chloro compound **23** (1.6 g, 4.5 mmol) in dry dimethylformamide (7 ml), thymine (0.68 g, 5.4 mmol) and K$_2$CO$_3$ (0.75 g, 5.4 mmol) were added at RT and stirred at same temperature for 12 h. After completion of reaction (monitored by TLC), DMF was rotaevaporated and water was added to reaction mixture, product was extracted in ethyl acetate. The organic layer was concentrated and subjected to column chromatography, compound **24** was eluted with 80% EtOAc in pet ether. Yield (60%); ^{1}H-NMR (200MHz, CDCl$_3$) δ: 0.9(s, 6H), 1.33(t, J=6Hz, 3H), 1.43(s, 9H), 1.94(maj) & 1.92(min) (s, 3H), 2.86-2.83(d, J=6Hz, 2H), 3.19(s, 2H), 4.20-4.32(m, 4H), 4.41(s, 2H), MS(EI) *m/z* calcd for C$_{20}$H$_{32}$N$_4$O$_7$ [M + K]$^+$ 478.2171, observed: 477.2370

N-(acetyl-2-t)-N-(3-((tert-butoxycarbonyl) amino)-2, 2-dimethylpropyl) glycine 28

28
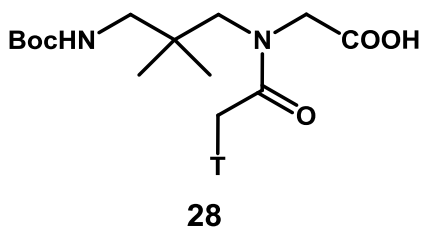
The ester compound **25** in THF was saponified with 10% LiOH at 0^0C for 5h. After completion of reaction, the reaction mixture was acidified with amberlite resin to pH 3. The reaction mixture was then concentrated to get acid monomer 25. Yield (75%); ^{1}H-NMR (200MHz, D_2O) δ:1.20(s, 6H), 1.34(s, 9H), 3.34(bs, 2H), 4.06(s, 2H), 4.39(s, 2H), 6.6(bs, 1H), 7.21(s, 1H), 11.2(s, 1H); [13]C (100MHz, DMSO-d_6)δ: ;

HRMS *m/z* calculated for $C_{19}H_{30}N_4O_7$ [M+H]+ 427.2192, observed: 427.2198.

2.9 C Synthesis of PNA oligomers by solid phase PNA synthesis

The modified and unmodified PNA monomers were incorporated into 10-mer PNA oligomer sequence using standard solid phase protocol on L-lysine derivatized MBHA resin having 0.35 mmol/g loading value. The PNA monomers were coupled sequentially to assemble PNA sequence using PyBOP and DIPEA in DMF/NMP as coupling reagents. The PNA oligomers were synthesized using repetitive cycles, each comprising the following steps:

Deprotection of the *N-t-*Boc group using 50% TFA in DCM (3 x 15 min)

- ➢ Washing of beads with DCM, DMF and again DCM (thrice each)
- ➢ Neutralization of the TFA salt of amine using 10% DIPEA in DCM to liberate free amine (3 x 10 min)
- ➢ Washing of beads with DCM and DMF (thrice each)
- ➢ Coupling of the free amine with the free carboxylic acid group of the incoming monomer (3 equivalents). The coupling reaction was carried out in DMF/NMP with PyBOP as coupling reagent in the presence of DIPEA.
- ➢ Capping (when needed) of the unreacted amino groups using acetic anhydride in pyridine:DCM

After each coupling and deprotection steps Kaiser's test was carried out for confirmation of PNA chain elongation which involved following reagents:

A. Ninhydrine (5.0 g) dissolved in ethanol (100 mL)
B. Phenol (80.0 mg) dissolved in ethanol (20 mL)

C. Potassium cyanide (2 mL, 0.001 M aq. Solution) added to 98 mL pyridine

Few resin beads were taken in a test tube, washed with ethanol and 3-4 drops from each of the above mentioned solutions were added. The test tube was heated for 1-2 min and the emergence of color was noted.

2.9 D Cleavage of the PNA oligomers from solid support

The MBHA resin (10 mg) with oligomers attached to it was stirred with thioanisole (20 µL) and 1, 2-ethanedithiol (8 µL) in an ice bath for 10 min. TFA (200µL) was added to it in cooled condition and kept in ice bath. TFMSA (16 µL) was added slowly with stirring to dissipate the heat generated. The reaction mixture was stirred for 1.5 to 2 h at room temperature. The resin was removed by filtration under reduced pressure and washed twice with TFA. The filtrate was combined evaporated on rotaevaporator at ambient temperature. The remaining amount of TFA was transferred to eppendorf tube and the peptide was precipitated with cold dry ether. The peptide was isolated by centrifugation and the precipitate was dissolved in de-ionized water.

2.9 E Purification of the PNA oligomers by RP-HPLC

PNA purification was carried out on Agilent HPLC system. For the purification of peptides, semi-preparative BEH130 C18 (10x250 mm) column was used. Purification of PNA oligomers was performed using water and CAN with gradient elution method: A to 100% B in 45 min; A= 0.1% TFA in $CH_3CN:H_2O$ (5:95); B= 0.1% TFA in $CH_3CN:H_2O$ (1:1) with flow rate of 3 mL/min. All the HPLC profiles were monitored at 254 nm wavelength. Fluorescent PNA oligomers were monitored using 254 nm wavelength.

2.10 References:

1. Uhlmann, E.; Peyman, A. *Chem. Rev*. **1990**, *90*, 543-584.

2. (a) Nielsen, P. E.; Egholm, M.; Berg, R. H.; Buchardt, O. *Science*, **1991**, *254*, 1497-1500. (b) Hyrup, B.; Nielsen, P. E. *Bioorg. Med. Chem. Lett*. **1996**, *1* ,165-177.

3. (a) Nielsen, P. E.; Haaima, G. *Chem. Soc. Rev*. **1997**, 73-78 (b) Nielsen, P. E.; Egholm, M.;Berg, R. H.; Buchardt, O. *Science*, **1991**, *254*, 1497-1500.

4. Egholm, M.; Buchardt, O.; Nielsen, P. E.; Berg, R. H. *J. Am. Chem. Soc*. **1992**, *114*, 1895-1897.

5. Demidov, V. V.; Potaman, V N.; Frank-Kamenetskii, M. D.; Egholm, M.; Buchardt, O.; Sonnichsen, S.H.; Nielsen, P.E. *Biochern. Phormucol*. **1994**, *48,* 1310-1313.

6. Nielsen, P. E. *Mol. Biotechnol.* **2004**, *26*, 233-248

7. (a) Uhlmann, E.; Peyman, A.; Breipohl, G.; Will, D. W. *Angew. Chem., Int. Ed*. **1998,** *37*, 2797-2823. (b) Koppelhus, U.; Nielsen, P. E. *Adv. Drug Delivery Rev.* **2003**, *55,* 267-280.

8. (a) Haaima, G.; Lohse, A.; Buchardt, O.; Nielsen, P. E. *Angew. Chem., Int. Ed.* **1996**, *35*, 1939-1942. (b) Puschl, A.; Sforza, S.; Haaima, G.; Dahl, O.; Nielsen, P. E. *Tetrahedron Lett*. **1998**, *39*, 4707-4710. (c) Sforza, S.; Galaverna, G.; Dossena, A.; Corradini, R.; Marchelli, R. *Chirality* **2002**, *14*, 7,591-598.

9. Sugiyama, T.; Imamura, Y.; Demizu, Y.; Kurihara, M.; Takano, M.; Kittaka, A. *Bioorg. Med. Chem. Lett*. **2011**, *21*, 7317-7320

10. Tedeschi, T.; Sforza, S.; Corradini, R.; Marchelli, R. *Tetrahedron Lett.* **2005**, *46*, 8395-8399.

11. Nielsen, P.E.; Haaima, G. *Chem. Soc. Rev.,* **1997**, *26*, 73-78.

12. Corradini, R.; Sforza, S.; Tedeschi, T.; Marchelli R. *Seminars in Organic Synthesis.* Società Chimica Italiana, **2003**; pp. 41- 70.

13. Ganesh, K. N.; Nielsen, P. E. *Curr. Org. Chem.* **2000**, *4*, 931-943.

14. (a) Uhlmann, E.; Peyman, A.; Breipohl, G.; Will, D. W. *Angew. Chem. Int. Ed*. **1998**, *37*, 2796-2823. (b) Hyrup, B.; Egholm, M.; Rolland, M.; Nielsen, P. E.; Berg, R. H.; Buchardt, O. *J. Chem. Soc. Chem. Commun*. **1993**, 519.

15. S. C. Brown, S. A. Thomson, J. M. Veal, D. G. Davis, *Science* **1994**, *265*, 777 - 780.

16. (a) S. C. Brown, S. A. Thomson, J. M. Veal, D. G. Davis, *Science* **1994**, *265*, 777 ± 780. (b) M. Leijon, A. Gräslund, P. E. Nielsen, O. Buchardt, B. NordeÂn, S. M. Kristensen, M. Eriksson, *Biochemistry*, **1994**, *33*, 9820 ± 9825. (c) L. Betts, J. A. Josey, J. M. Veal, S. R. Jordan, *Science,* **1995**, *270*, 1838 ± 1841. (d) H. Rasmussen, J. S. Kastrup, J. N. Nielsen, J. M. Nielsen, P. E. Nielsen, *Nat. Struct. Biol*. **1997**, *4*, 98 ± 101.

17. Schutz R, Cantin M, Roberts C *et* al .: Angew. *Chem. Int. Ed. Engl.* **2000**, *39(7)*:1250-1253.

18. Schu¨ tz, R.; Cantin, M.; Roberts, C.; Greiner, B.; Uhlmann, E.; Leumann, C. J. *Angew. Chem., Int. Ed.* **2000**, *39*, 1250-1253.

19. (a) Kumar V A, Ganesh K N. *Acc Chem Res*. **2005**; *38*:404-12; PMID:15895978; http://dx.doi.org/10.1021/ar030277e (b) Kumar V A, Ganesh K N. *Curr Top Med Chem*. **2007**; *7*:715-26; PMID:17430211; http://dx.doi.org/10.2174/156802607780487722 (c) Devi G, Ganesh K N. *Artif DNA PNA XNA,* **2010**; *1*:68-75; PMID:21686241; http://dx.doi.org/10.4161/ adna.1.2.13185 (d) Mitra R, Ganesh K N. *Chem Commun (Camb)*, **2011**; *47*:1198-200; http://dx.doi.org/10.1039/c0cc03988h

20. (a) Uhlmann E, Peyman A, Breipohl G, Will DW. PNA: *Angew Chem Int Ed*, **1998**; *37*:2796-823; http://dx.doi.org/10.1002/(SICI)1521-3773(19981102) 37:20,2796::AID-ANIE2796.3.0.CO;2-K (b) Nielsen PE. *Curr Opin Struct Biol*. **1999**; *9*:353-7; PMID:10361091; http://dx.doi.org/10.1016/S0959-440X(99)80047-5

21. (a) Govindaraju T, Kumar V A, Ganesh K N. *J Am Chem Soc*. **2005**; *127*:4144-5; PMID:15783176; http://dx.doi.org/10. 1021/ja044142v (b) Govindaraju T, Kumar V A, Ganesh K N. *J Org Chem*. **2004**; *69*:1858-65; PMID:15058930; http:// dx.doi.org/10.1021/jo035747x (c) Govindaraju T, Madhuri V, Kumar V A, Ganesh K N. *J Org Chem*. **2006**; *71*:14-21; PMID:16388612; http:// dx.doi.org/10.1021/jo051227l

22. (a) Haaima G, Lohse A, Buchardt O, Nielsen PE. *Angew Chem Int Ed Engl*. **1996**; 35:1939-42; http://dx.doi.org/10.1002/anie.199619391 (b) Menchise V, De Simone G, Tedeschi T, Corradini R, Sforza S, Marchelli R, *et al. Proc Natl Acad Sci USA* **2003**; *100*:12021-6; PMID:14512516; http://dx.doi.org/10.1073/pnas.2034746100 (c) Dragulescu-Andrasi A, Rapireddy S, Frezza BM, Gayathri C, Gil RR, Ly DH. *J Am Chem Soc,* **2006**; *128*:10258-67; PMID:16881656; http://dx.doi.org/10.1021/ja0625576

23. Gourishankar, A.; Ganesh, K.N. *Artificial DNA PNA XNA* **2012**, *3*, 5–13.

24. Karle I L, Balaram P. *Biochemistry* **1990**; *29*:6747-56; PMID:2204420; http://dx.doi.org/10.1021/bi00481a001

25. (a) Govindaraju T, Kumar V A, Ganesh K N. *J Am Chem Soc* **2005**; *127*:4144-5; PMID:15783176; http://dx.doi.org/10. 1021/ja044142v (b) Govindaraju T, Kumar V A, Ganesh K N. *J Org Chem*. **2004**; *69*:1858-65; PMID:15058930; http://dx.doi.org/10.1021/jo035747x (c) Govindaraju T, Madhuri V, Kumar V A, Ganesh K N. *J Org Chem*. **2006**; *71*:14-21; PMID:16388612; http:// dx.doi.org/10.1021/jo051227l

26. (a) Kosynkina, L.; Wang, W.; Liang, T. C. *Tetrahedron Lett*. **1994**, *35*, 5173. (b) Wu, Y.; Xu, J. C. *Tetrahedron* **2001**, *57*, 8107. (c) Falkiewicz, B.; Kolodziejczyk, A. S.; Liberek, B.; Wisniewski, K. *Tetrahedron* **2001**, *57*, 7909. (d) Englund, E. A.; Appella, D. H. *Org. Lett*. **2005**, *7*, 3465. (e) Tedeschi, T.; Sforza, S.; Corradini, R.; Marchelli, R. *Tetrahedron Lett*. **2005**, *46*, 8395. (f) Dose, C.; Seitz, O. *Org. Lett*. **2005**, *7*, 4365. (g) Huang, H.; Joe, G. H.; Choi, S. R.; Kim, S. N.; Kim, Y. T.; Pak, H. S.; Kim, S. K.; Hong, J. H.; Han, H.-K.; Kang, J. S.; Lee, W. *Arch. Pharm. Res.*

2012, *35*, 517. (h) Avitabile, C.; Moggio, L.; Malgieri, G.; Capasso, D.; Di. Gaetano, S.; Saviano, M.; Pedone, C.; Romanelli, A. *PLoS ONE* **2012**, *7*, 1. (i) De Costa, N. T. S.; Heemstra, J. M. *PLoS ONE* **2013**, *8*, 1. (j) Niu, Y.; Wu, H.; Li, Y.; Hu, Y.; Padhee, S.; Li, Q.; Cao, C.; Cai, J. *Org. Biomol. Chem.* **2013**, *11*, 4283. (k) Dezhenkov, A. V.; Tankevich, M. V.; Nikolskaya, E. D.; Smirnov, I. P.; Pozmogova, G. E.; Shvets, V. I.; Kirillova, Y. G. *Medeleev Commun.* **2015**, *25*, 47.

27. Yeh, J.I.; Boris Shivachev, B.; Rapireddy, S.; Crawford, M.J.; Gil, R.R.; Du, S.; Madrid, M.; Ly, D.H. *J. Am. Chem. Soc.* **2010**, *132*, 10717–10727.

28. Sugiyama, T.; Imamura, Y.; Demizu, Y.; Kurihara, M.; Takano, M.; Kittaka, A. *Bioorg. Med. Chem. Lett*. **2011**, *21*, 7317–7320.

29. Chem. Commun., 2015, 51, 7693-7696

30. (a) Uhlmann, E.; Peyman, A.; Breipohl, G.; Will, D. W. *Angew. Chem. Int. Ed.* **1998**, *37*, 2796-2823. (b) Hyrup, B.; Egholm, M.; Rolland, M.; Nielsen, P. E.; Berg, R. H.; Buchardt, O. *J. Chem. Soc. Chem. Commun.* **1993**, *519*.

31. (a) Bodansky, M.; Bodansky, A. *The Practice of Peptide Synthesis*, Springer-Verlog, Berlin, **1984**. (b) Stewart, J. M.; Young, J. D. *Solid Phase Peptide Synthesis*, W. H. Freeman & Co, New York, **1969**.

32. Merrifield, R. B. *J. Am. Chem. Soc.***1963**, *85*, 2149-2154.

33. Christensen, L.; Fitzpatrick, R.; Gildea, B.; Petersen, K.; Hansen, H. F.; Koch, C.; Egholm, M.; Buchardt, O.; Nielsen, P. E.; Coull, J.; Berg, R. H. *J. Peptide Sci.* **1995**, *3*, 175-183.

34. (a) Erickson, B. W.; Merrifield, R. B. *Solid Phase Peptide Synthesis. In the Proteins,* Vol. II, 3rd ed.; Neurath, H.; Hill, R. L. eds.; Academic Press, New York, **1976**, 255. (b) Merrifield, R. B.; Stewart, J. M.; Jernberg, N. *Anal. Chem.* **1966**, *38*, 1905-1914

35. (a) Kaiser, E.; Colescott, R. L.; Bossinger, C. D.; Cook, P. I. Anal. *Biochem.* **1970**, *34*, 595-598 (b) Kaiser, E.; Bossinger, C. D.; Cplescott, R. L.; Olsen, D. B. *Anal. Chim. Acta.* **1980**, *118*, 149-151 (c) Sarin, V. K.; Kent, S. B. H.; Tam, J. P.; Merrifield, R. B. *Anal. Biochem.* **1981**, *117*, 147.

36. Egholm, M.; Buchardt, O.; Christensen, L.; Behrens, C.; Freier, S. M.; Driver, D. A.; Berg, R. H.; Kim, S. K.; Norden, B.; Nielsen, P. E. *Nature.* **1993**, *365,* 566-568.

37. Christensen, L.; Fitzpatrick, R.; Gildea, B.; Petersen, K. H.; Hansen, H. F.; Koch, T.;Egholm, M.; Buchardt, O.; Nielsen, P. E.; Coull, J.; Berg, R. H. *J. Peptide Sci*. **1995**, *3*, 175-183.

2.11 Appendix I: Characterization data of synthesized compounds / PNA

^{1}H NMR of Compound 2:

GEMALCOHOLWED2AV2=29.ESP

LCMS of Compound 2:

D:\PRADNYA\NMR\GEMALK~1.ESP

¹H NMR of Compound 4:

¹³C NMR of compound 4:

¹H NMR of Compound 5:

PROTON GAMMA GEM CHLORO.ESP
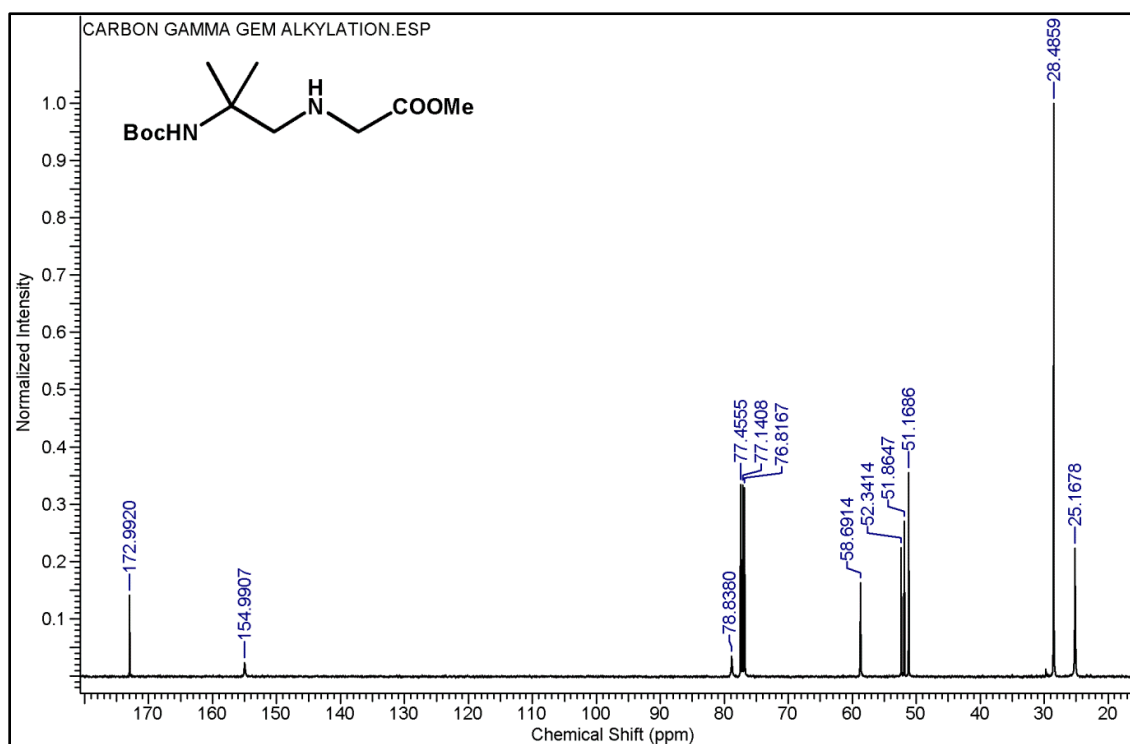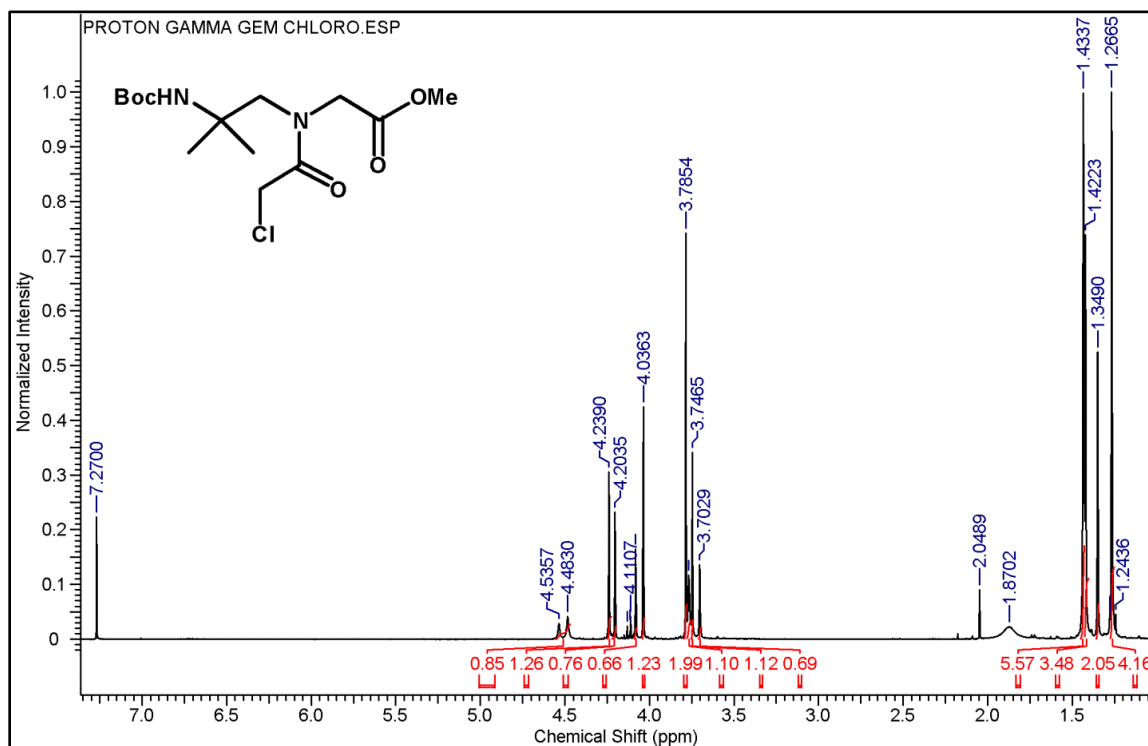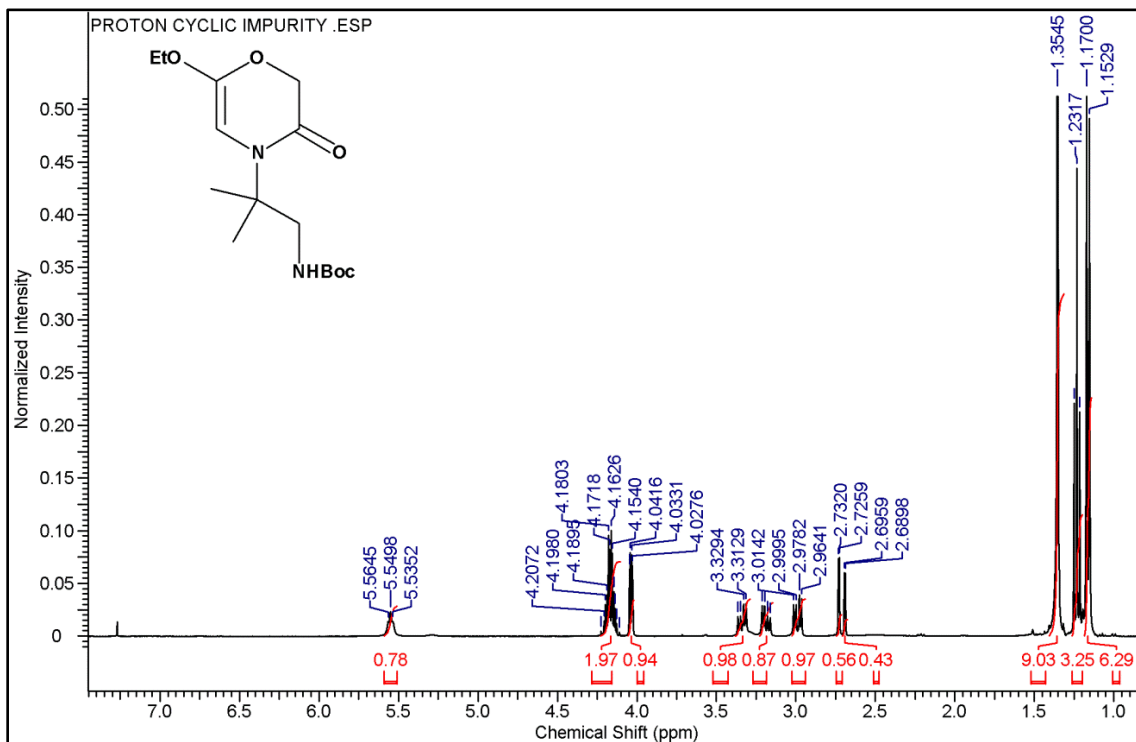
¹³C NMR of Compound 5:

C13.ESP
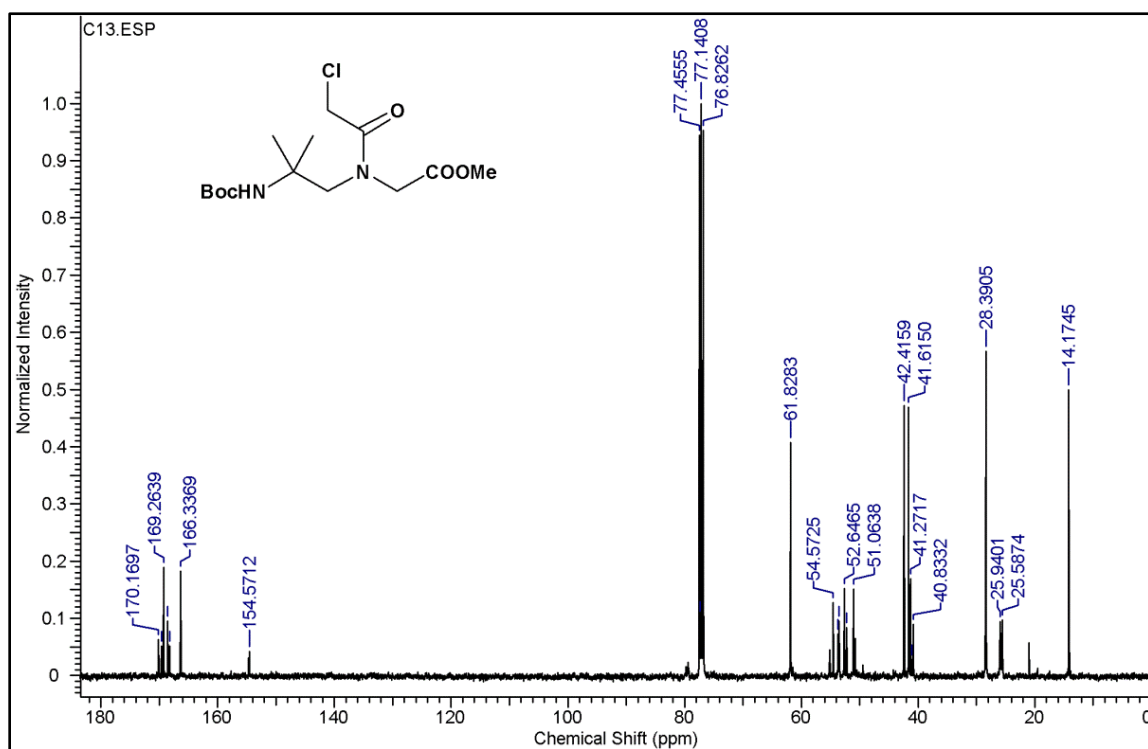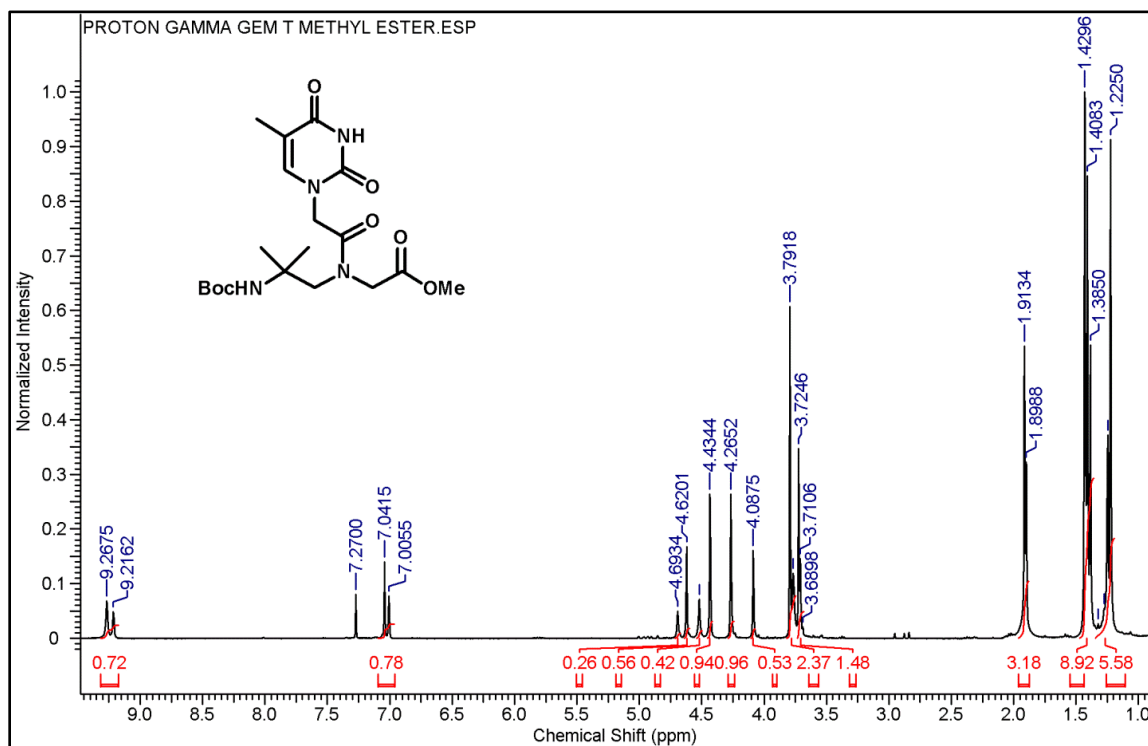
^{1}H NMR of Compound 6:

^{13}C NMR of Compound 6:
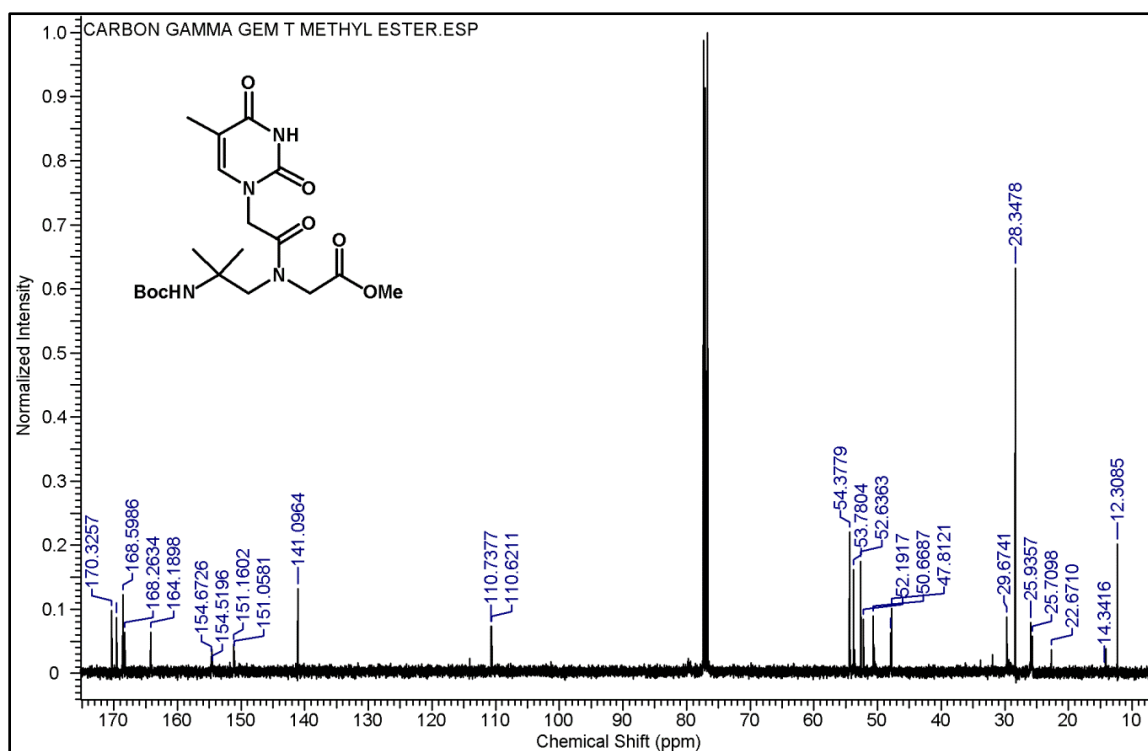
^{1}H NMR of Compound 7:
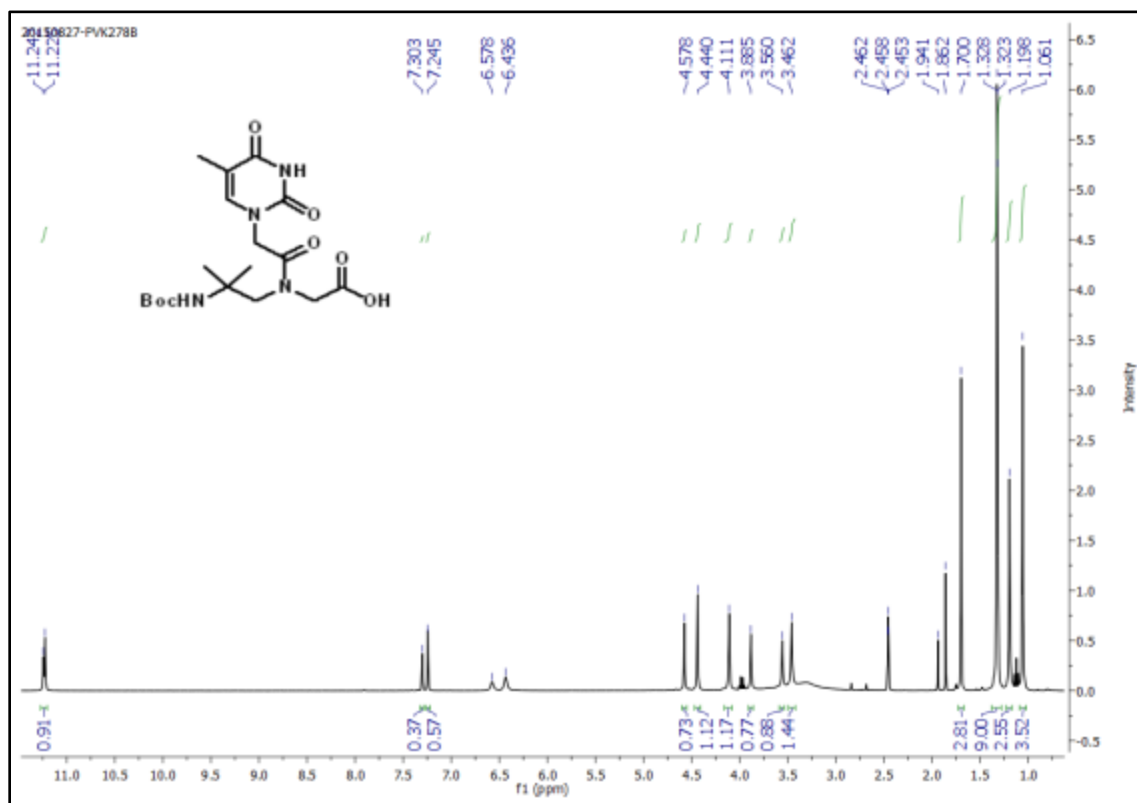
^{13}C NMR of Compound 7:
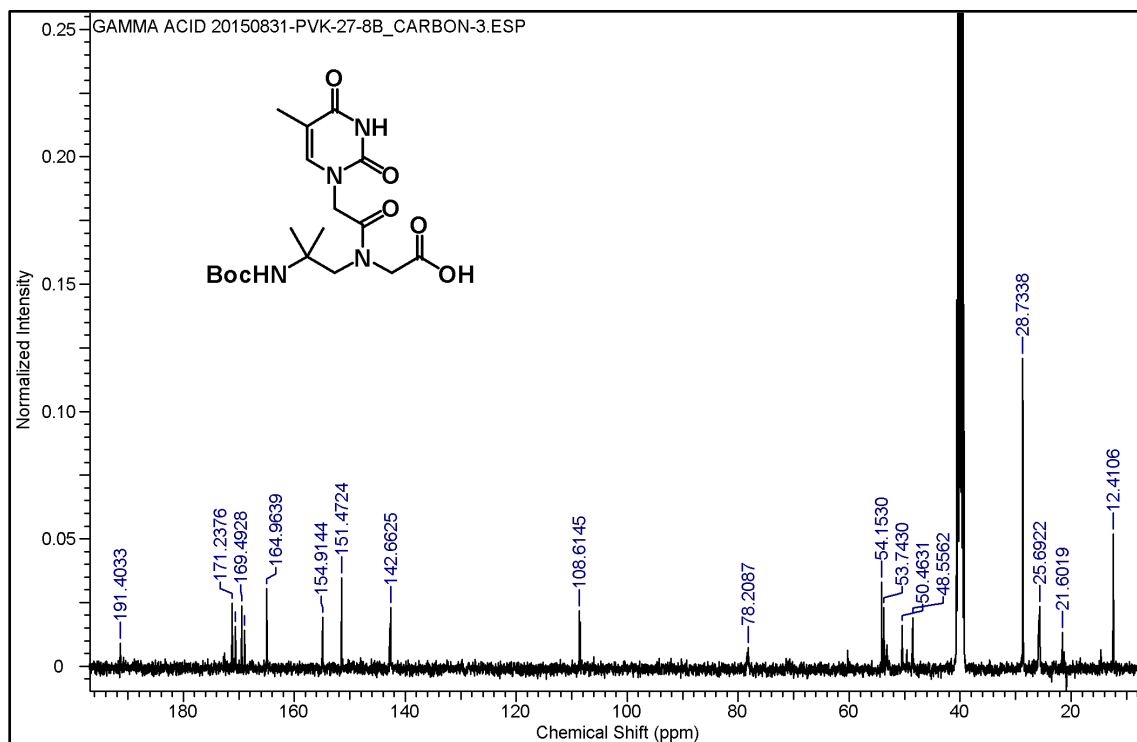
¹H NMR of Compound 9:
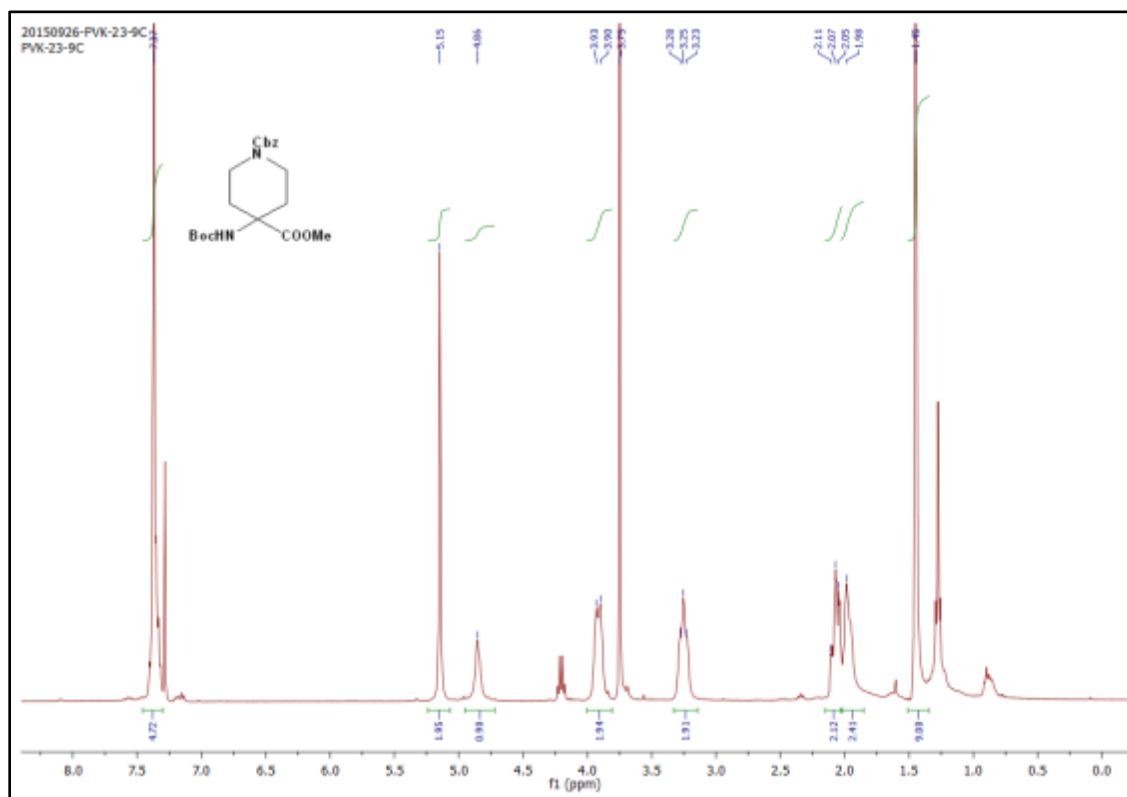
¹³C NMR of Compound 9:
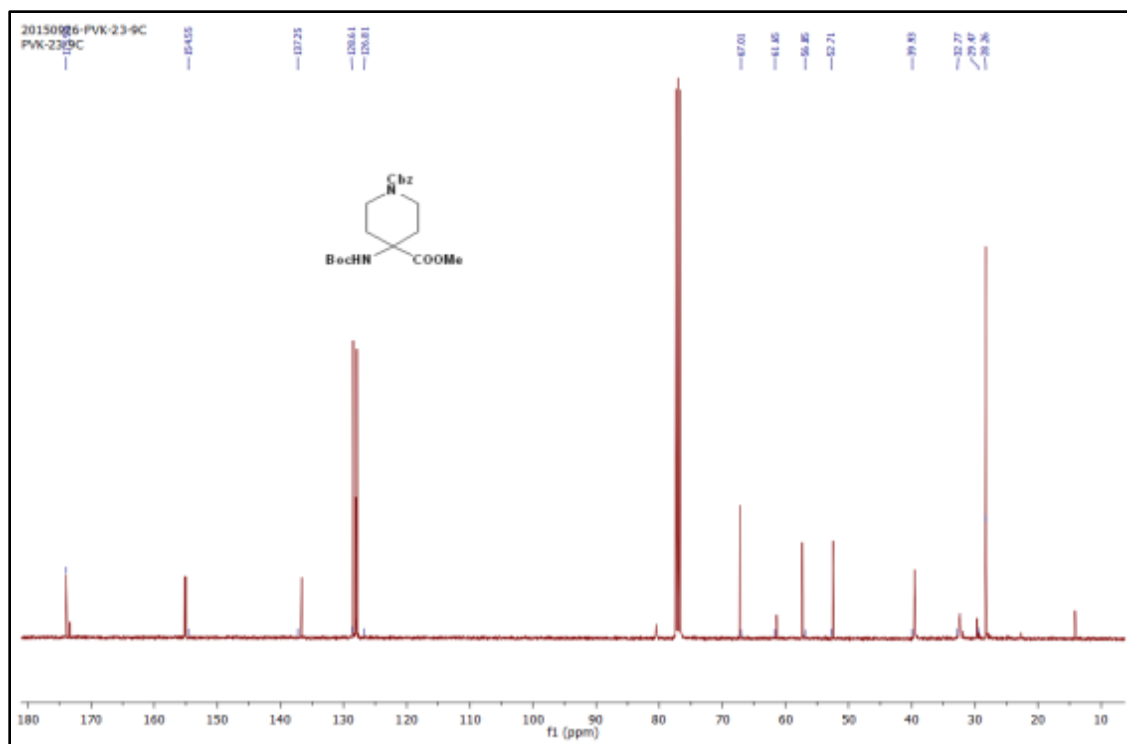
¹H NMR of Compound 10:
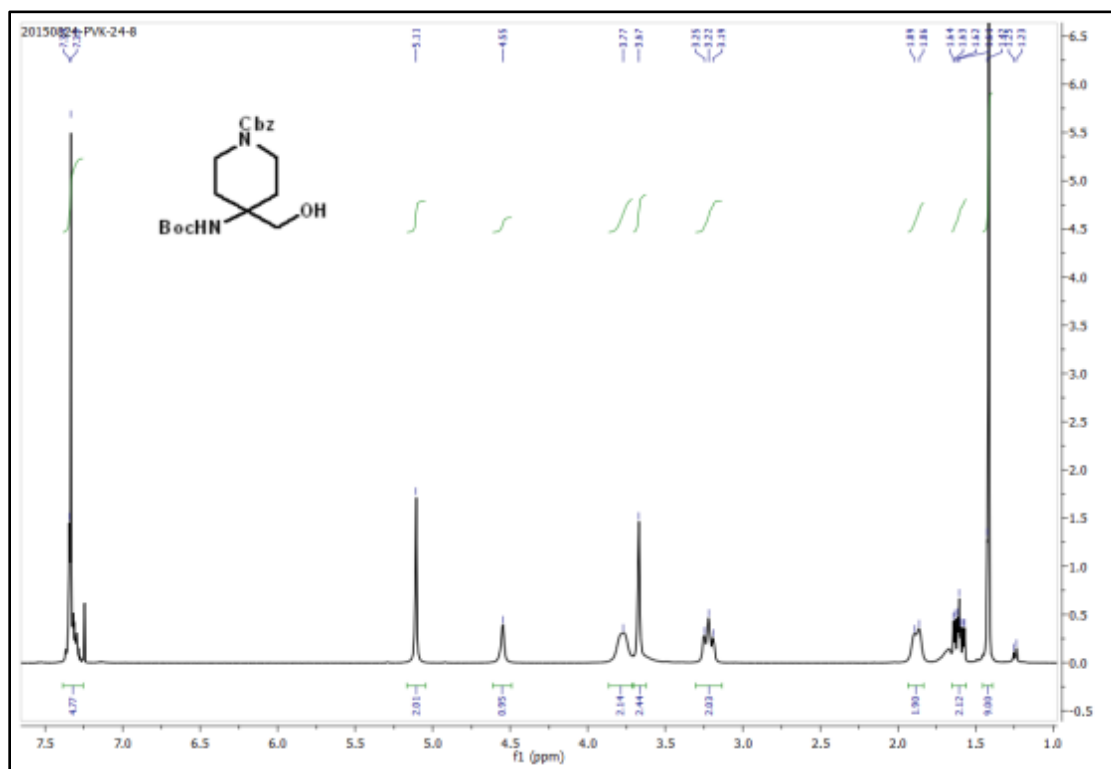
¹³C NMR of Compound 10:
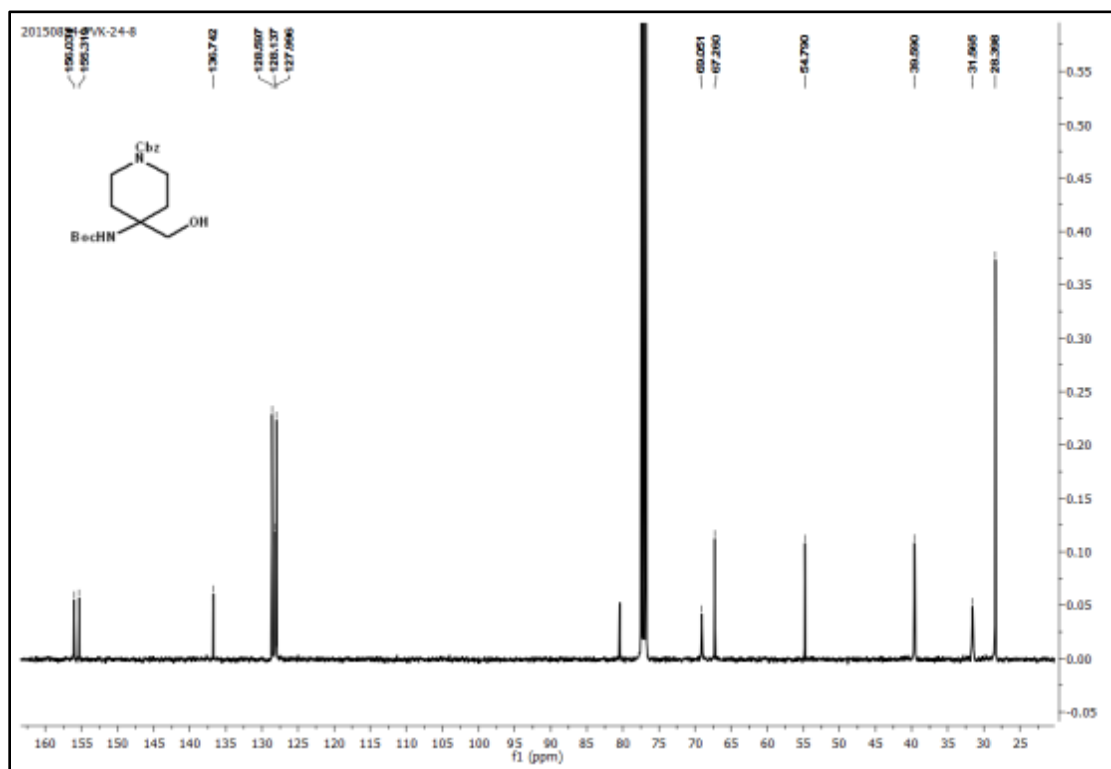
¹H NMR of Compound 12:
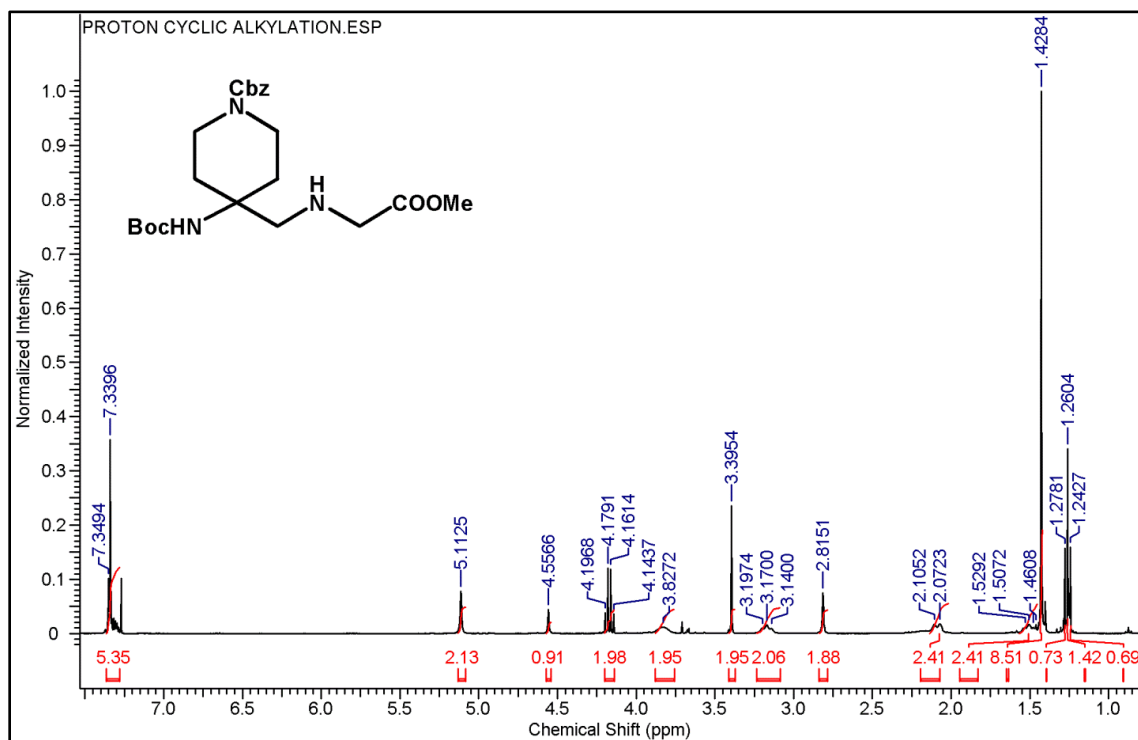
¹³C NMR of Compound 12:
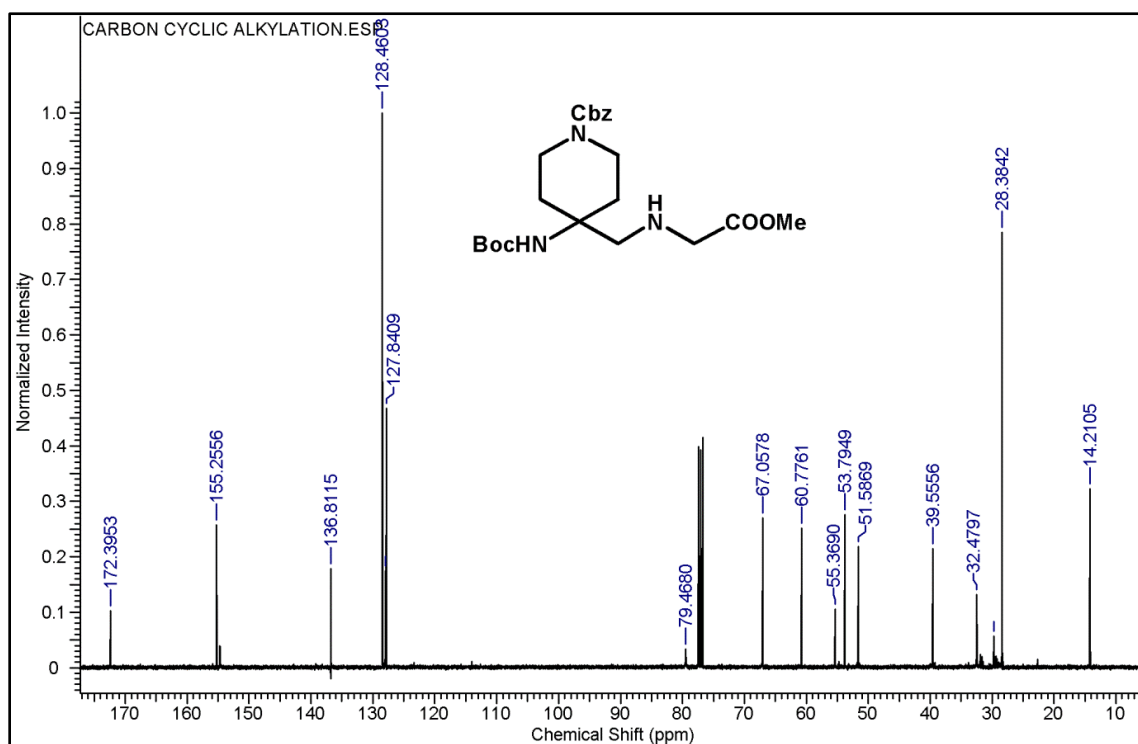
¹H NMR of Compound 13:
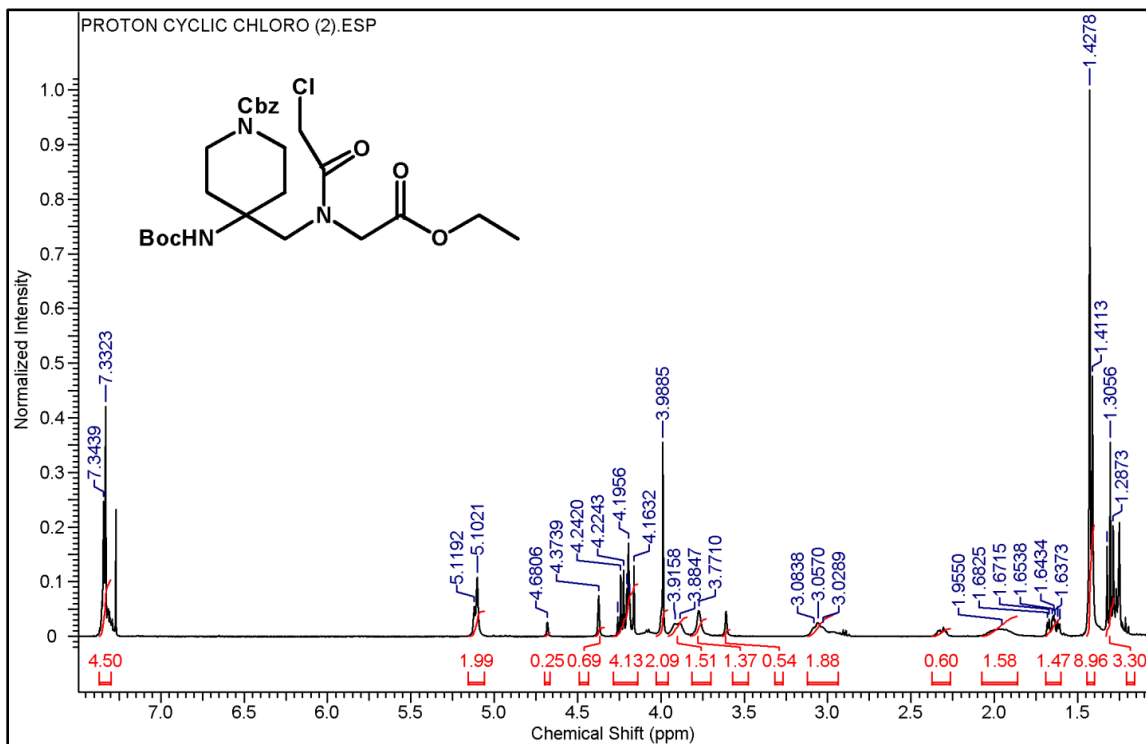
¹³C NMR of Compound 13:
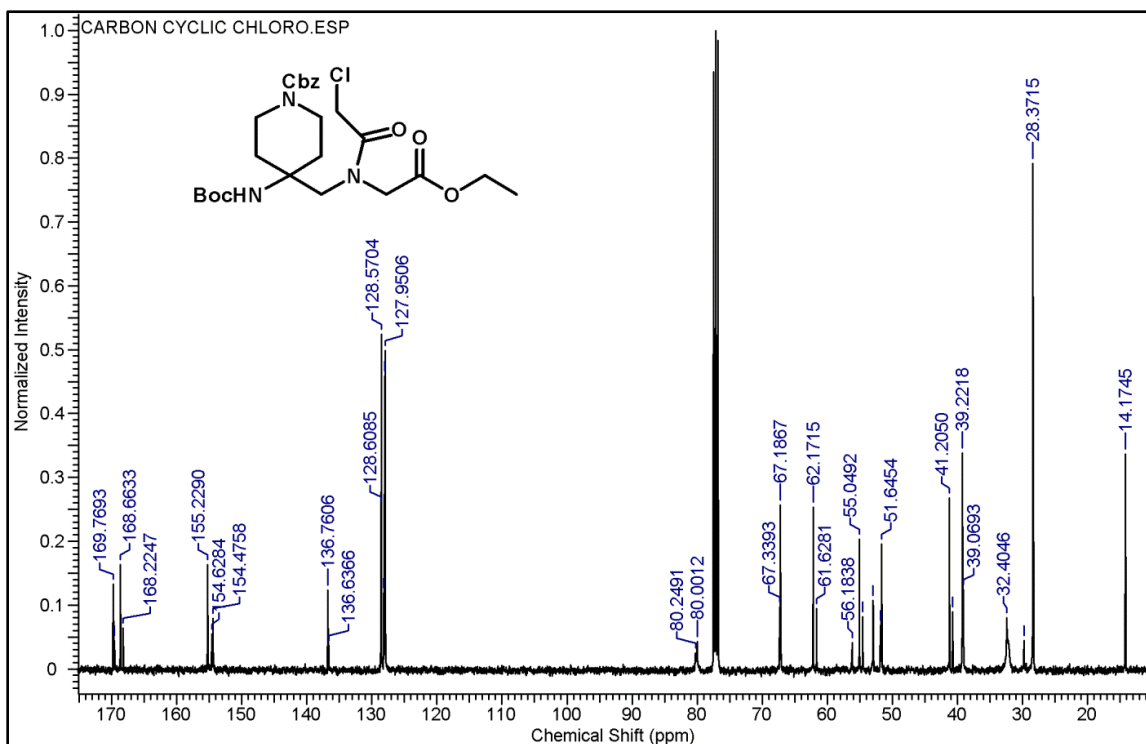
^{1}H NMR of Compound 14 (cyclic ester):
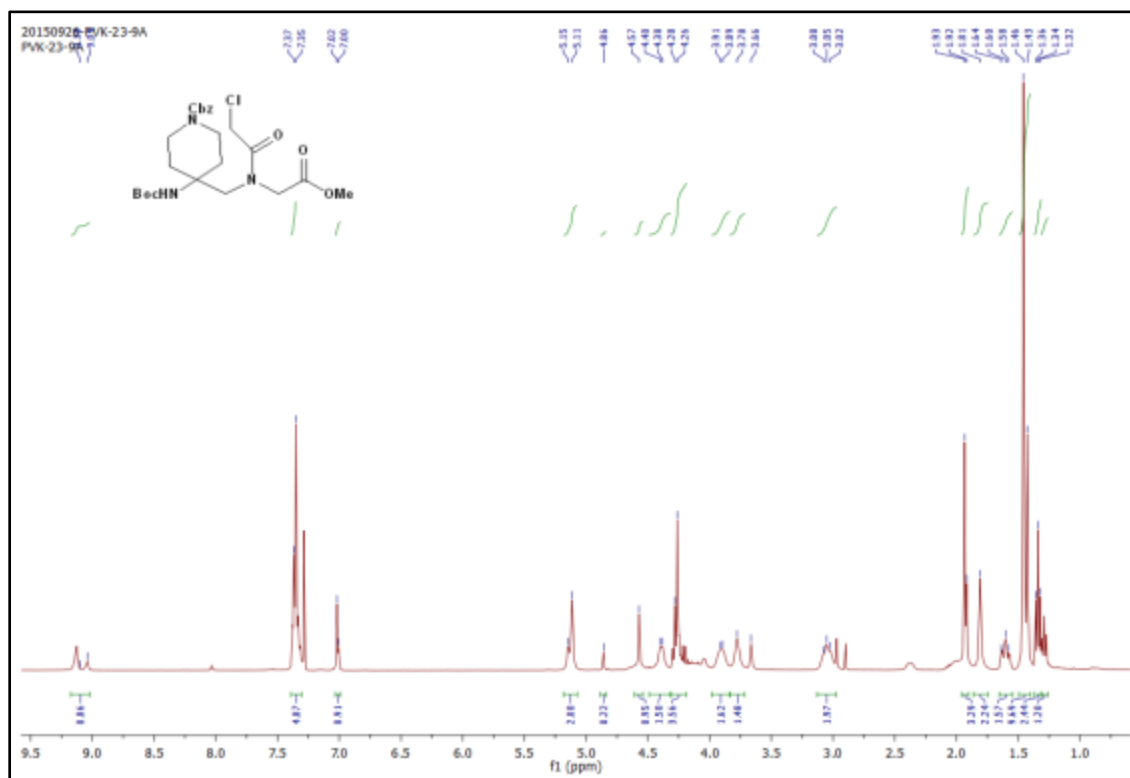
^{13}C NMR of Compound 14:
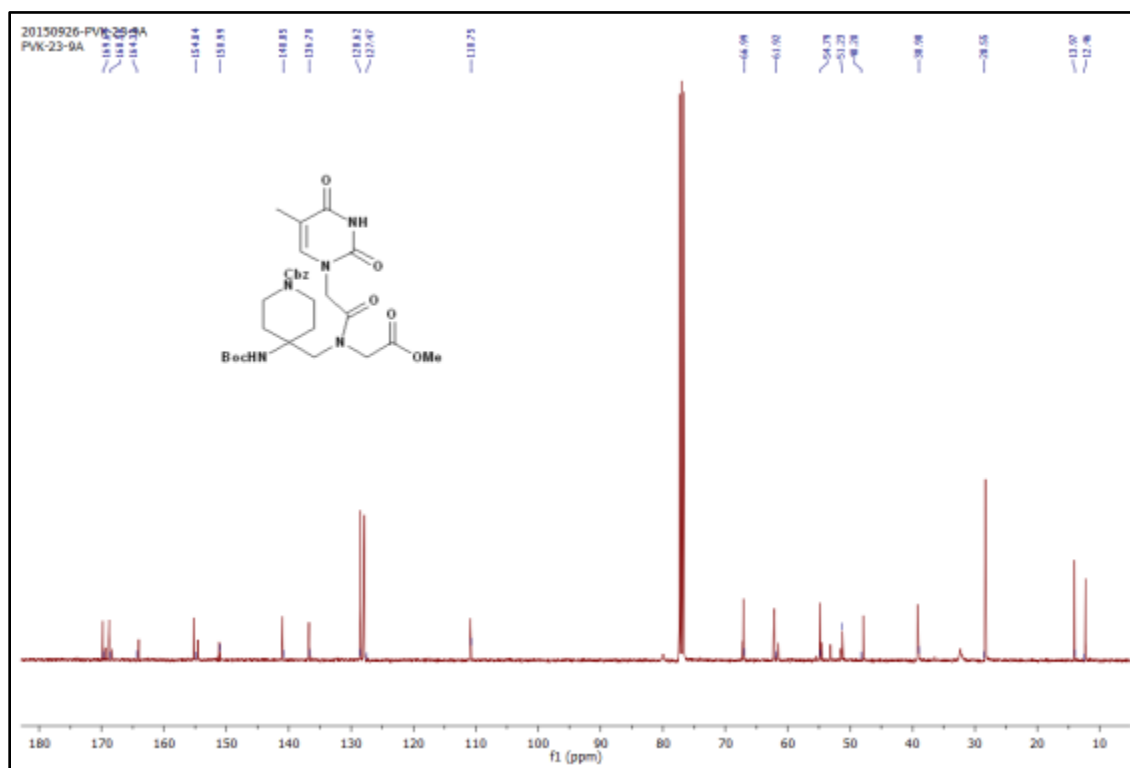
¹H NMR of Compound 15 (cyclic acid):
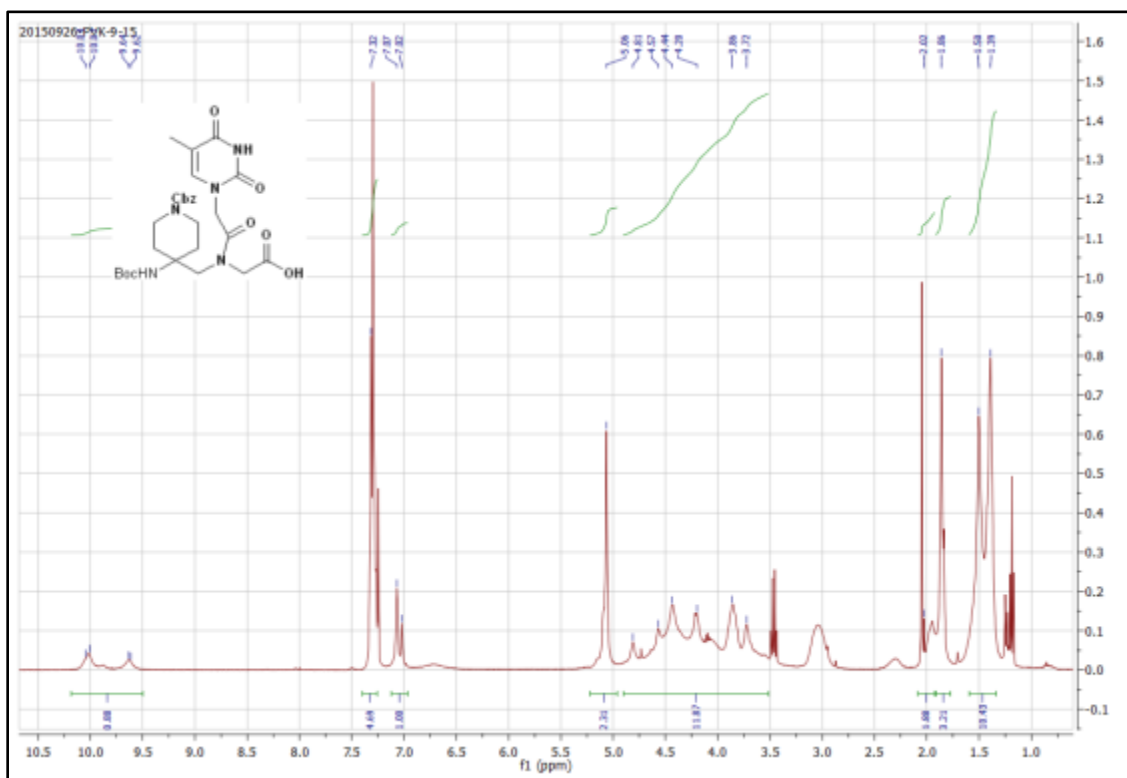
¹³C NMR of Compound 15(cyclic acid):
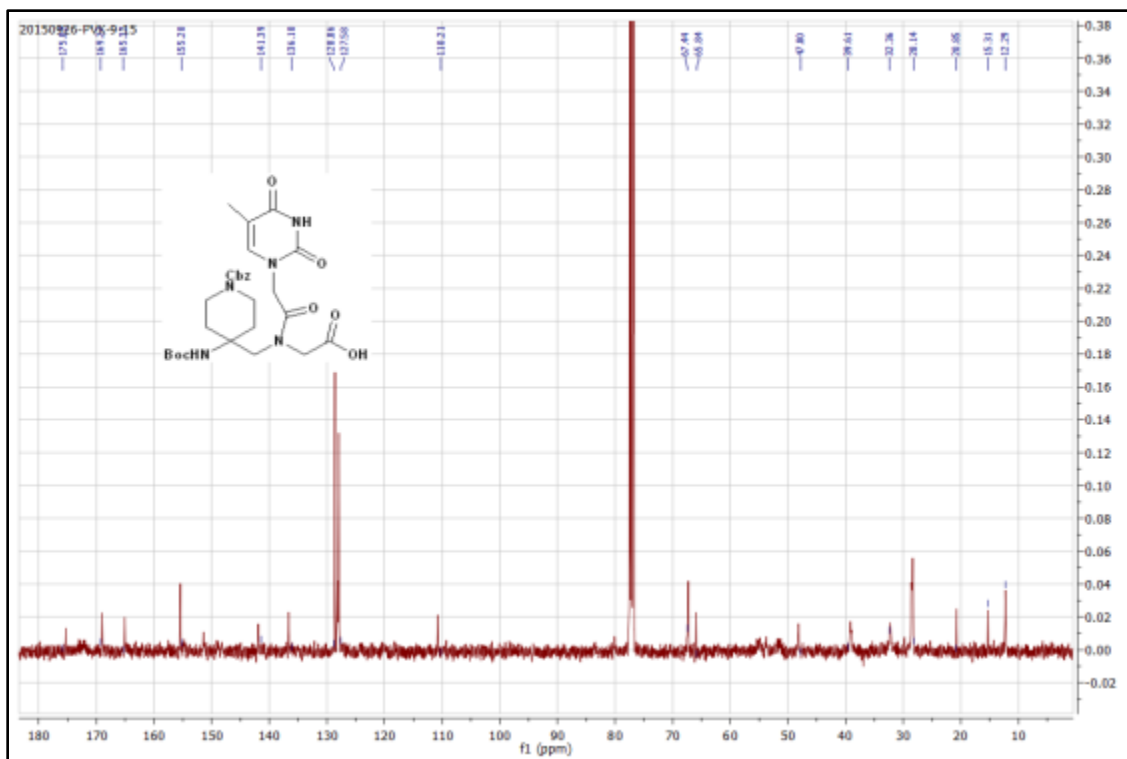
¹H NMR of Compound 18 (beta alk):
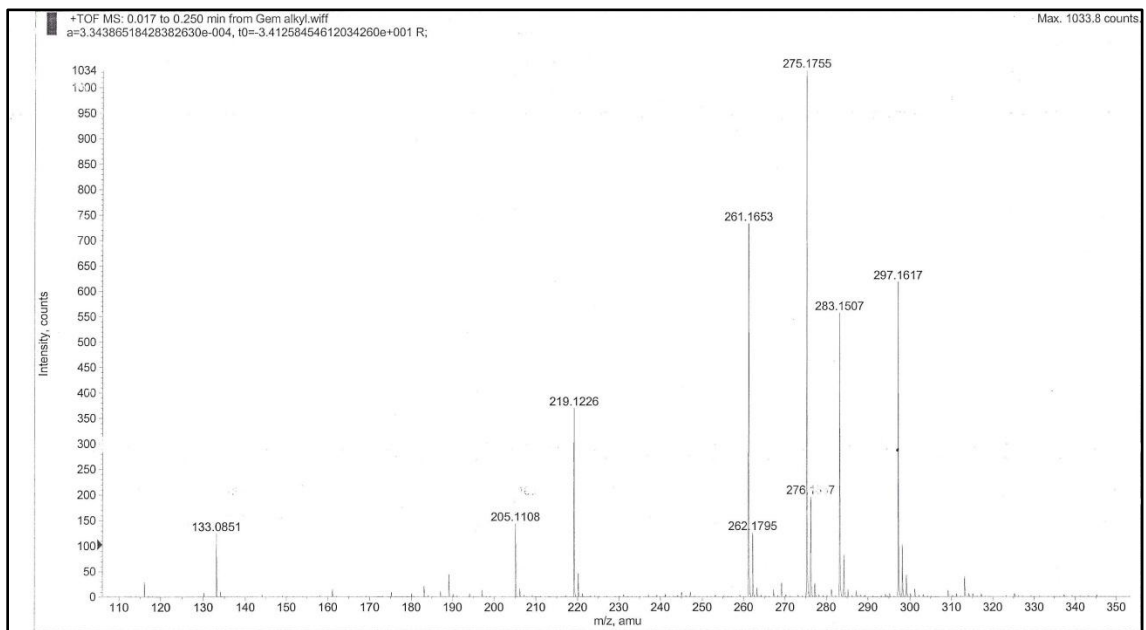
^{1}H NMR of Compound 19 (beta cl):
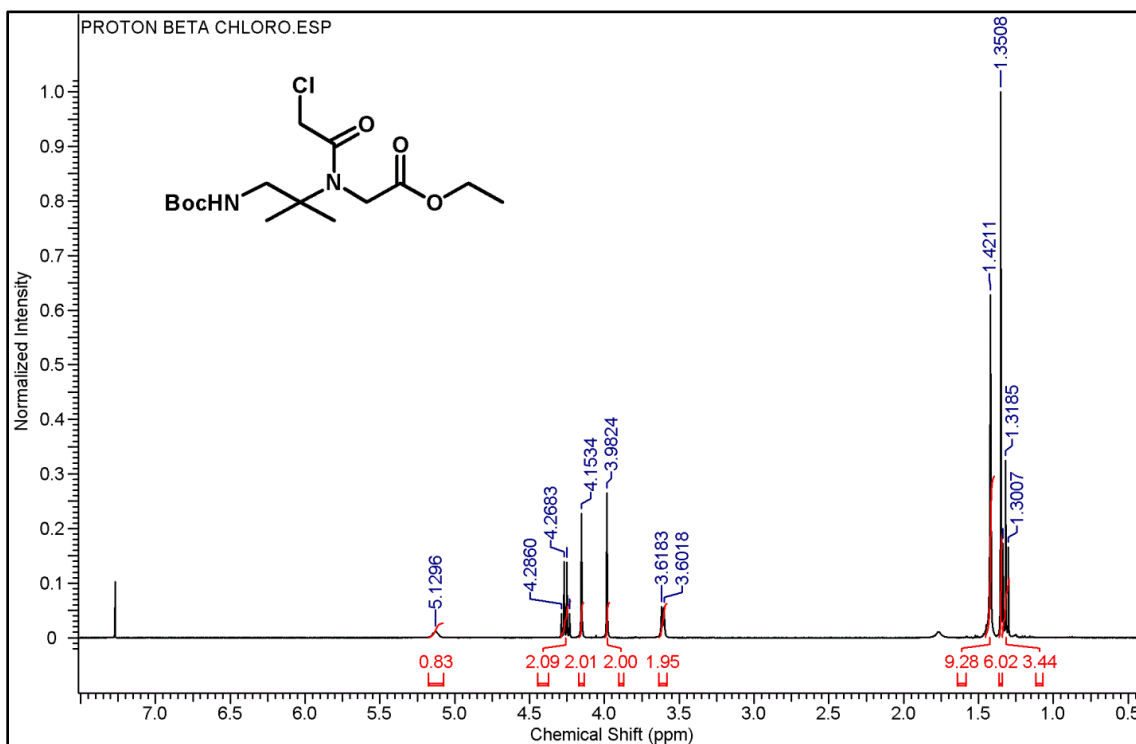
^{13}C NMR of Compound 19 (beta cl):
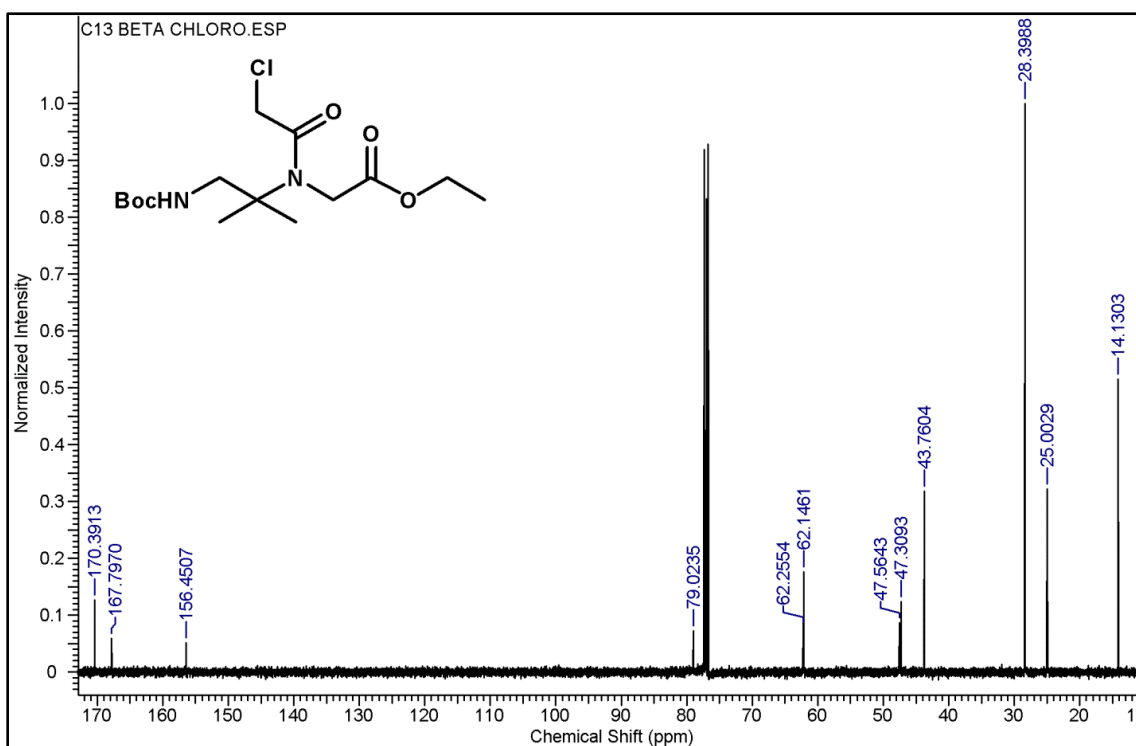
¹H NMR of Compound 20 (beta cyclic):

¹³C NMR of Compound 20 (cyclic):
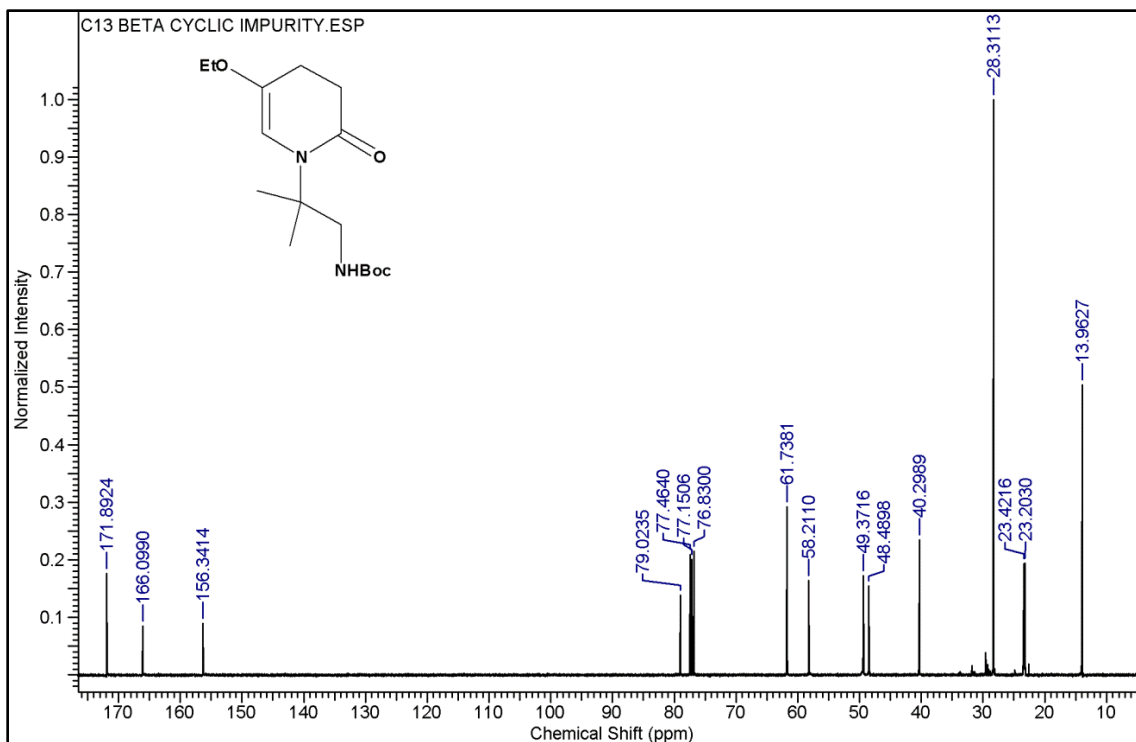
^{1}H NMR of Compound 21 (beta ester):
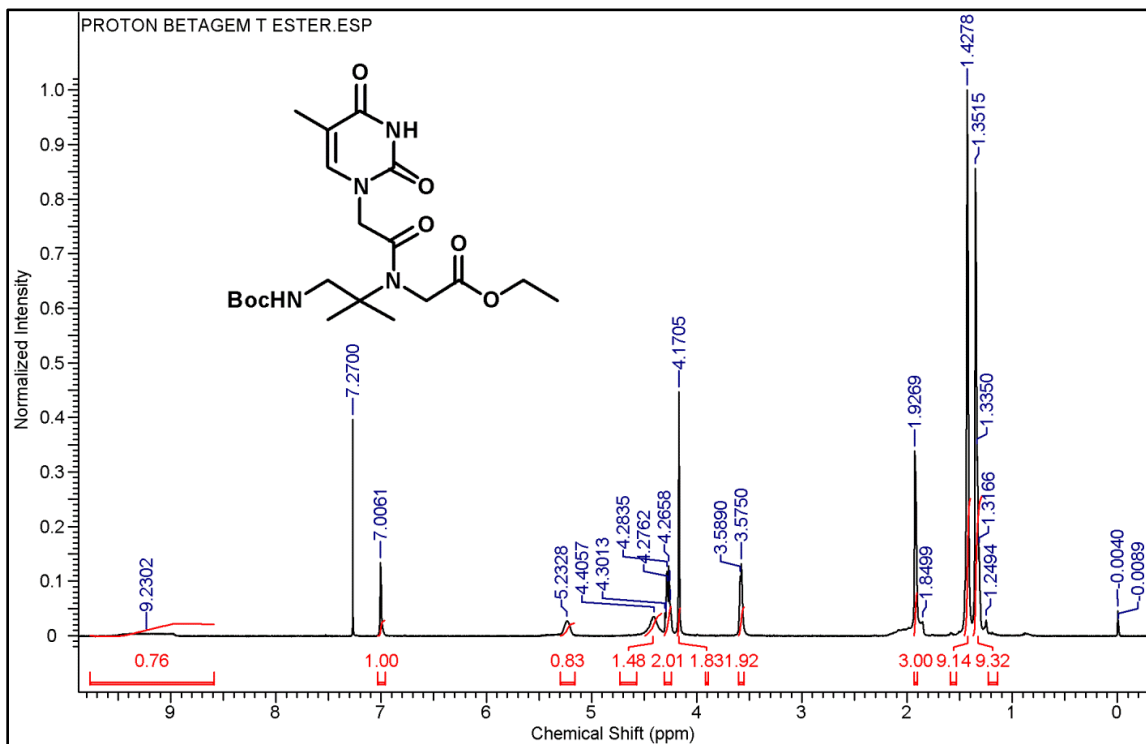
^{13}C NMR of Compound 21:
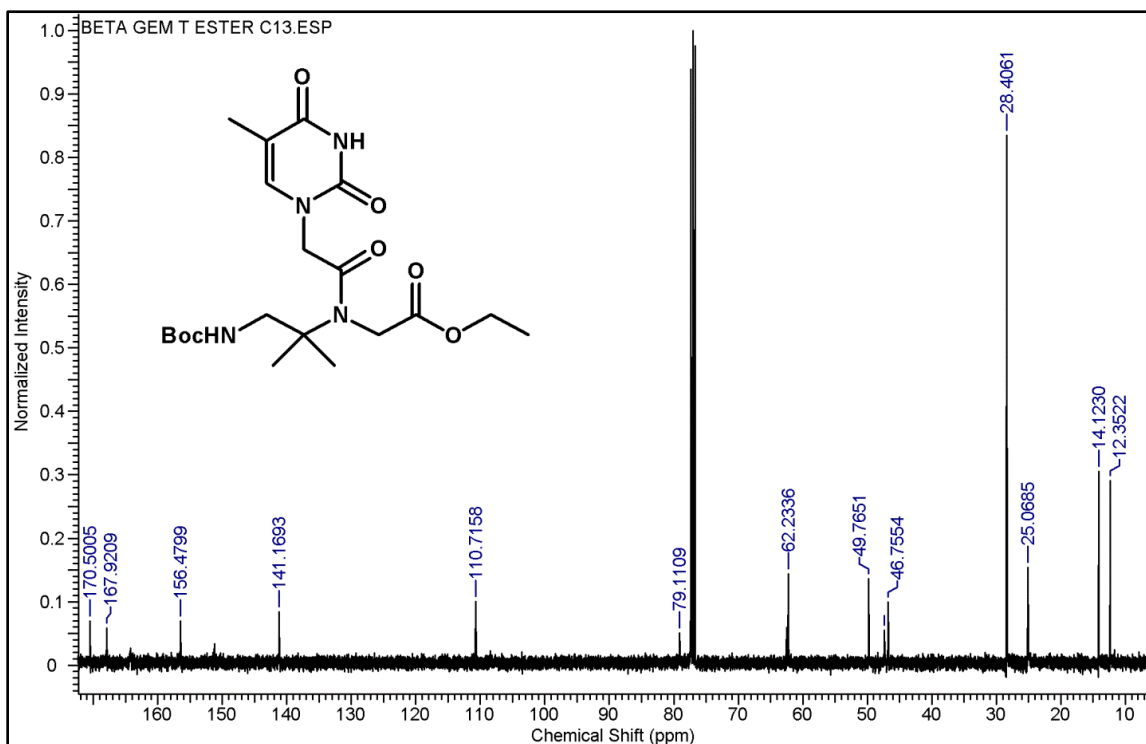
^{1}H NMR of Compound 22 (beta acid):
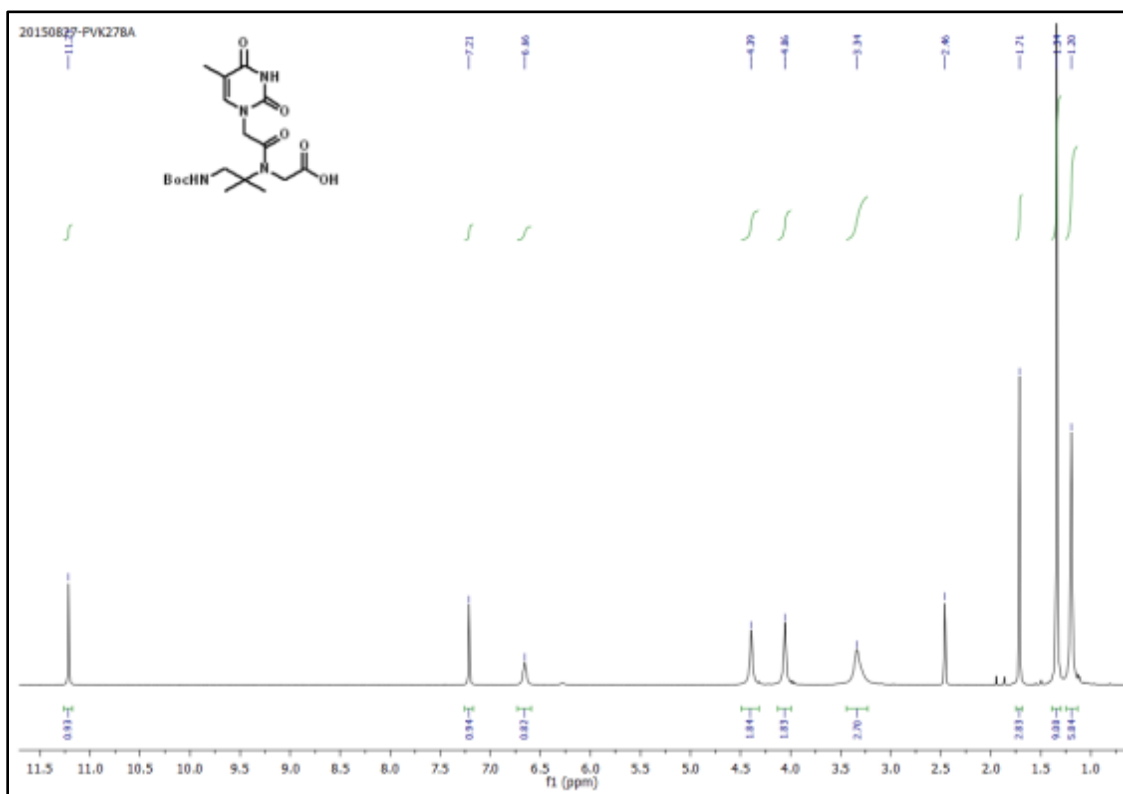
^{13}C NMR of Compound 22:
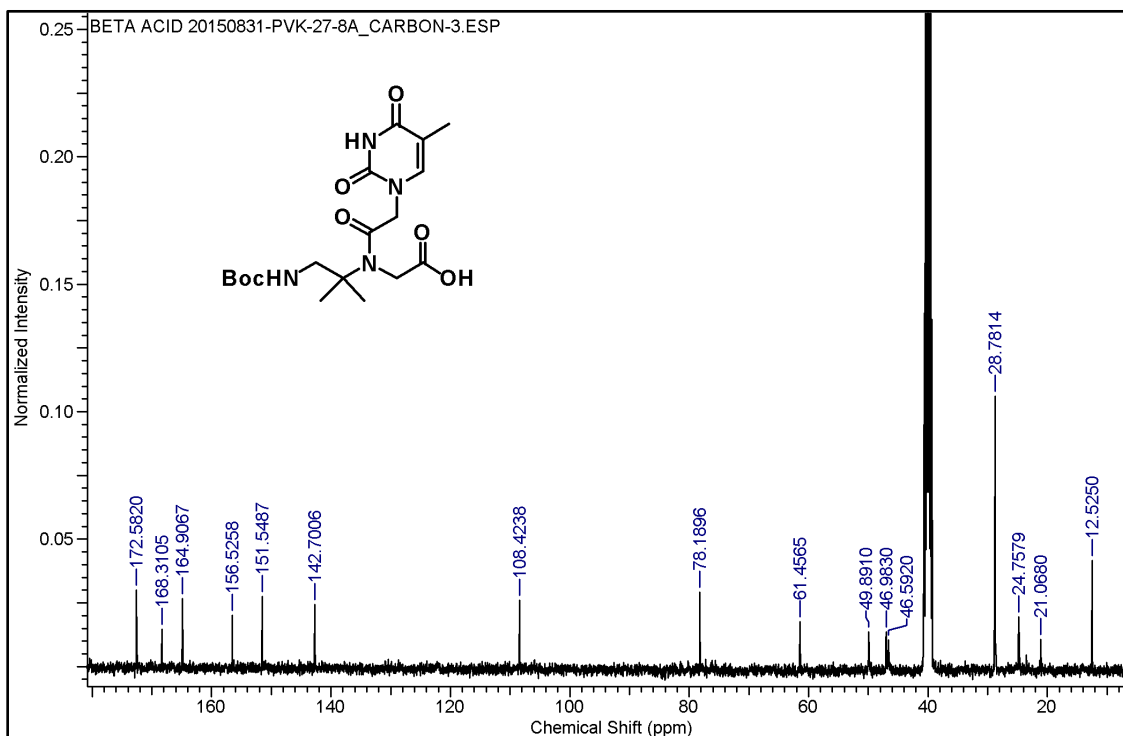
^{1}H NMR of Compound 25 (gem apg alk):
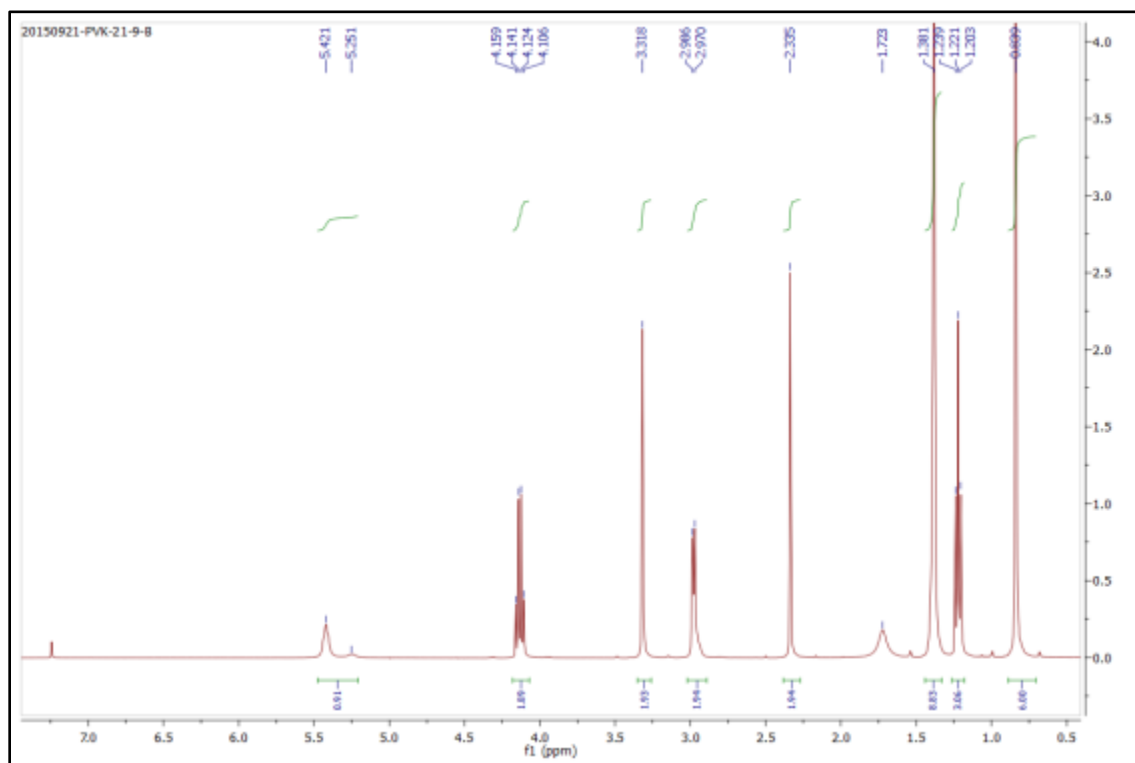
^{13}C NMR of Compound 25:
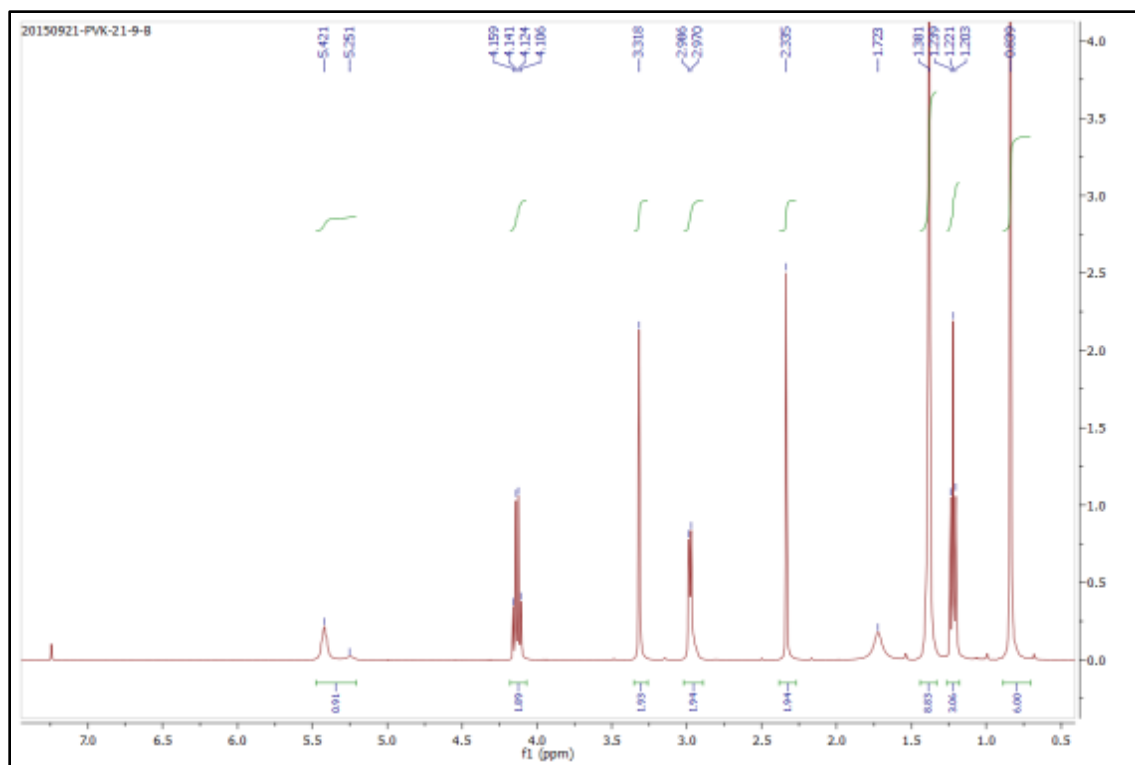
^{1}H NMR of Compound 26 (gem apg chloro):
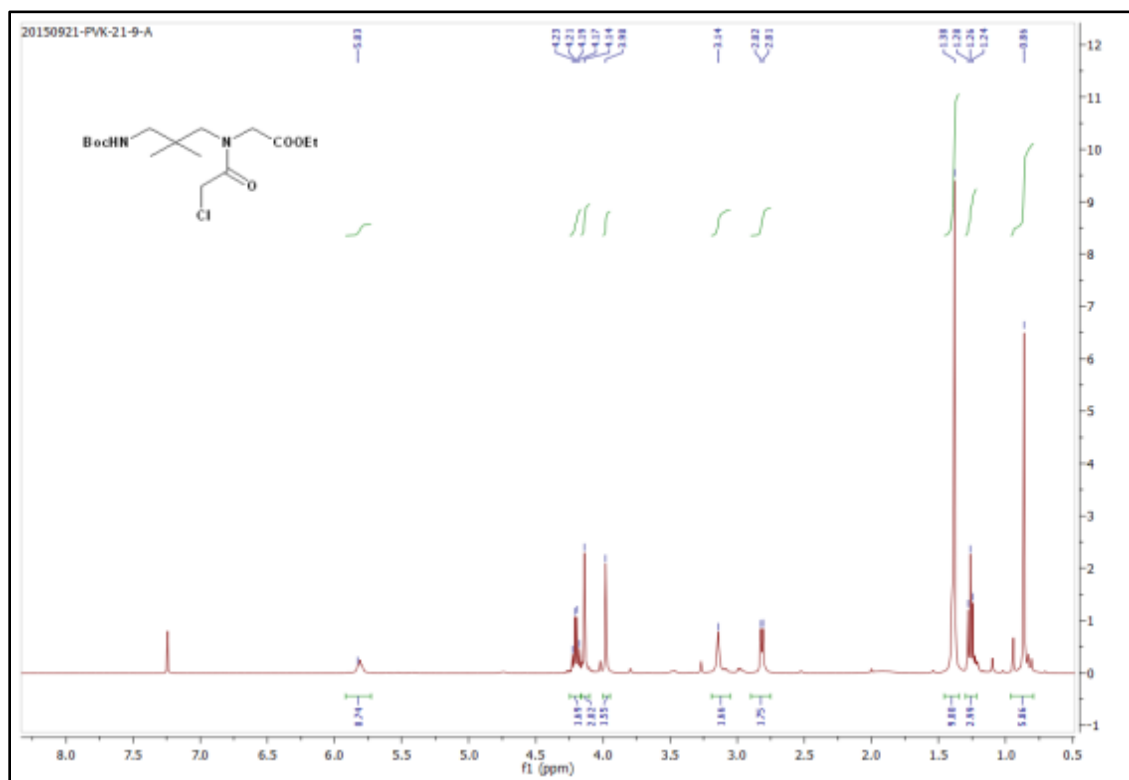
^{13}C NMR of Compound 26:
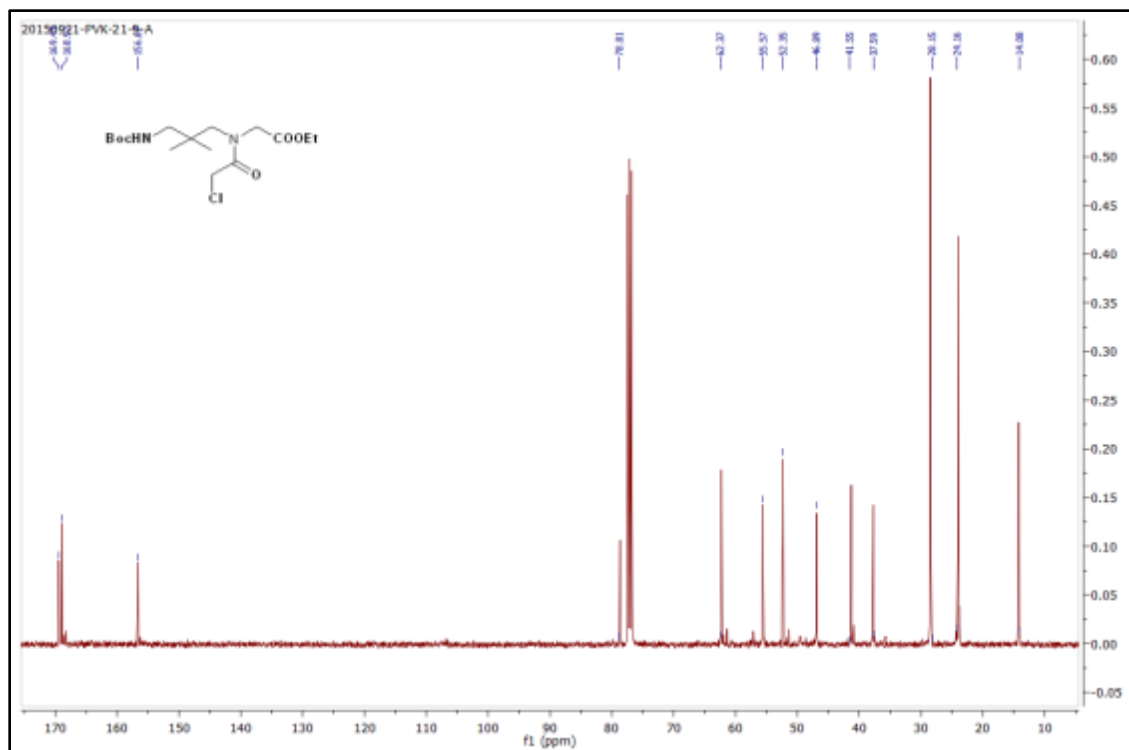
^{1}H NMR of Compound 27 (gem apg ester):
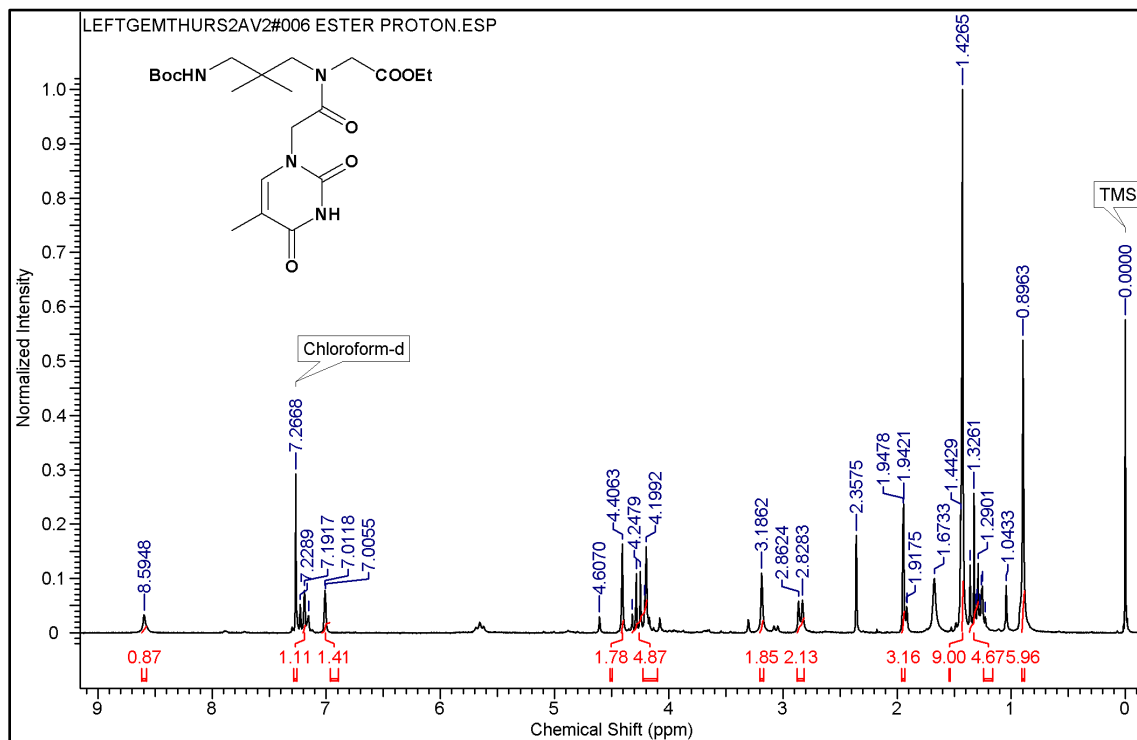
^{1}H NMR of Compound 28 (gem apg acid):
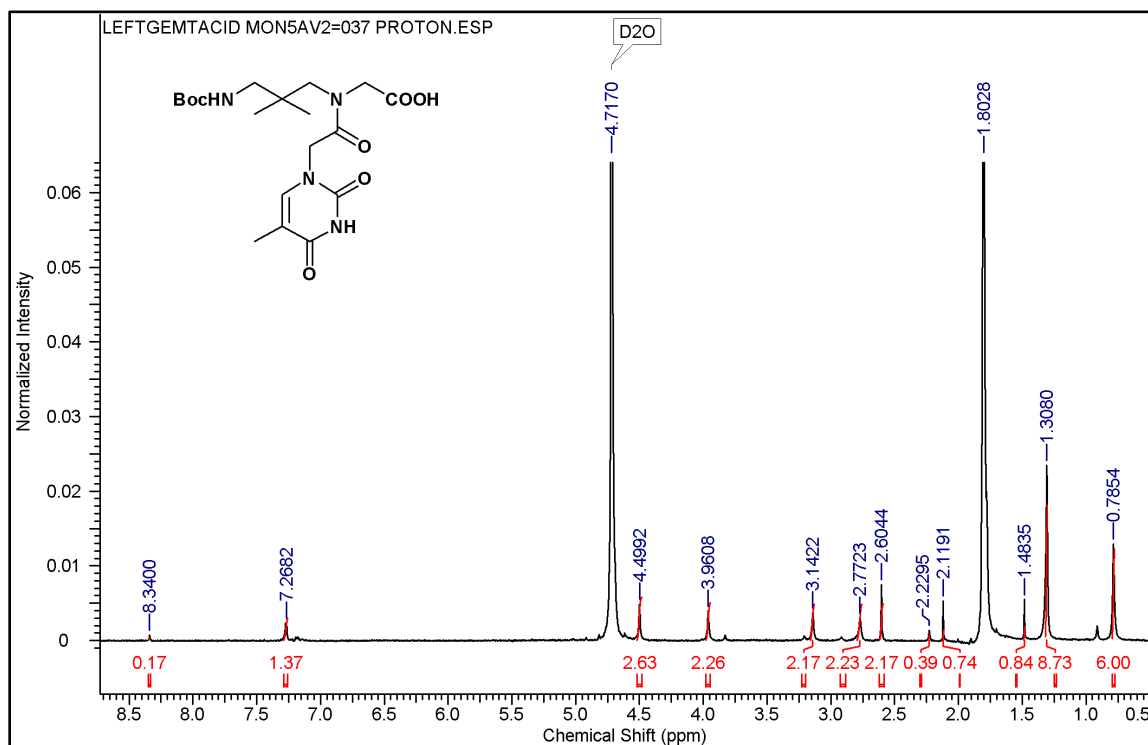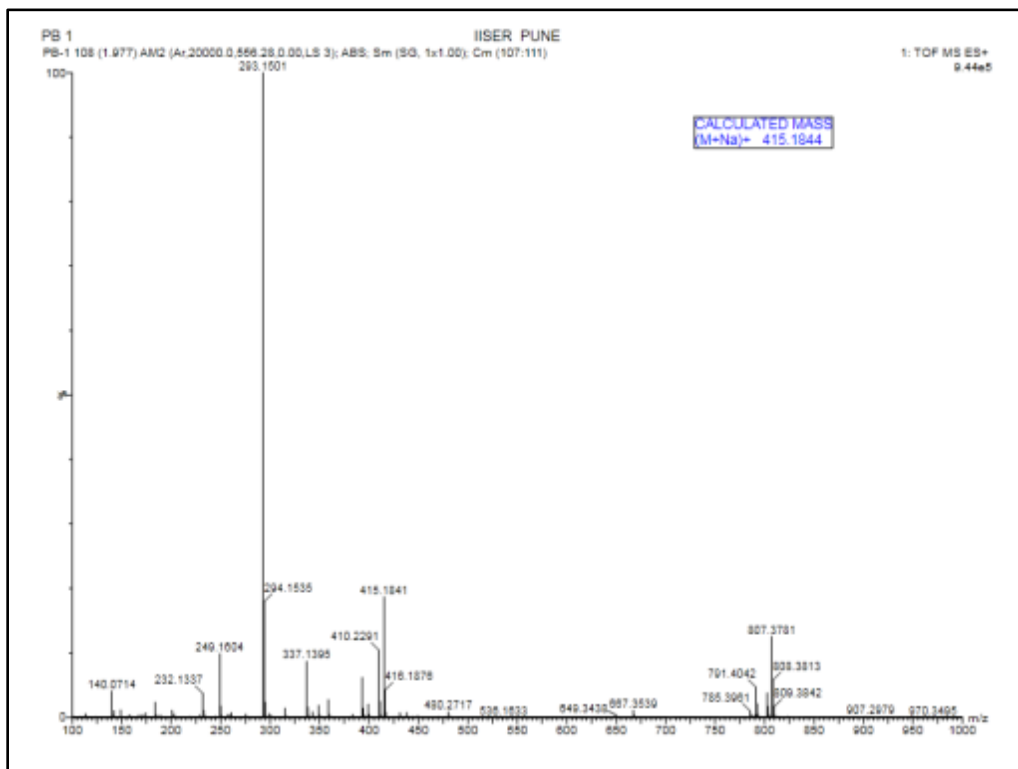
MALDI-TOF of Compound 4:
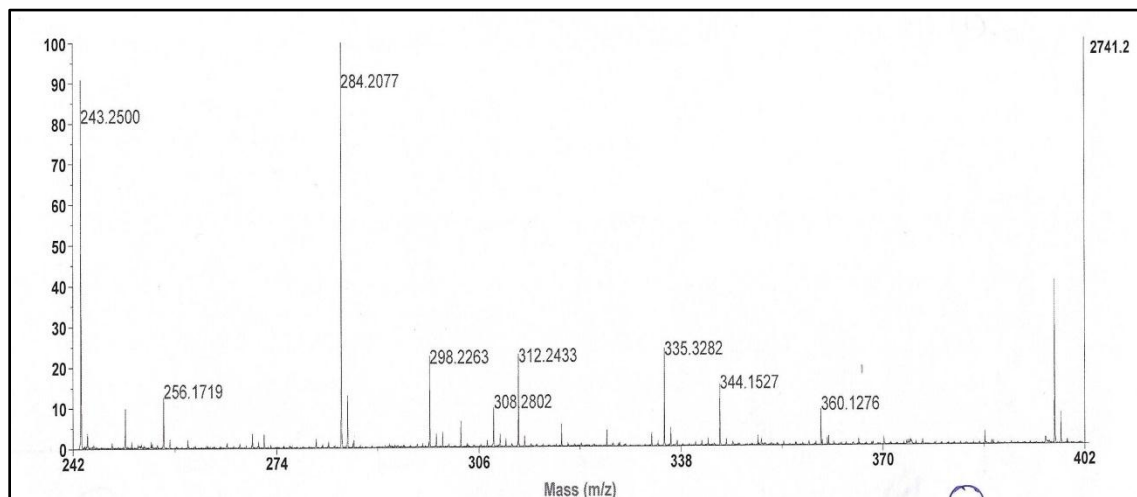
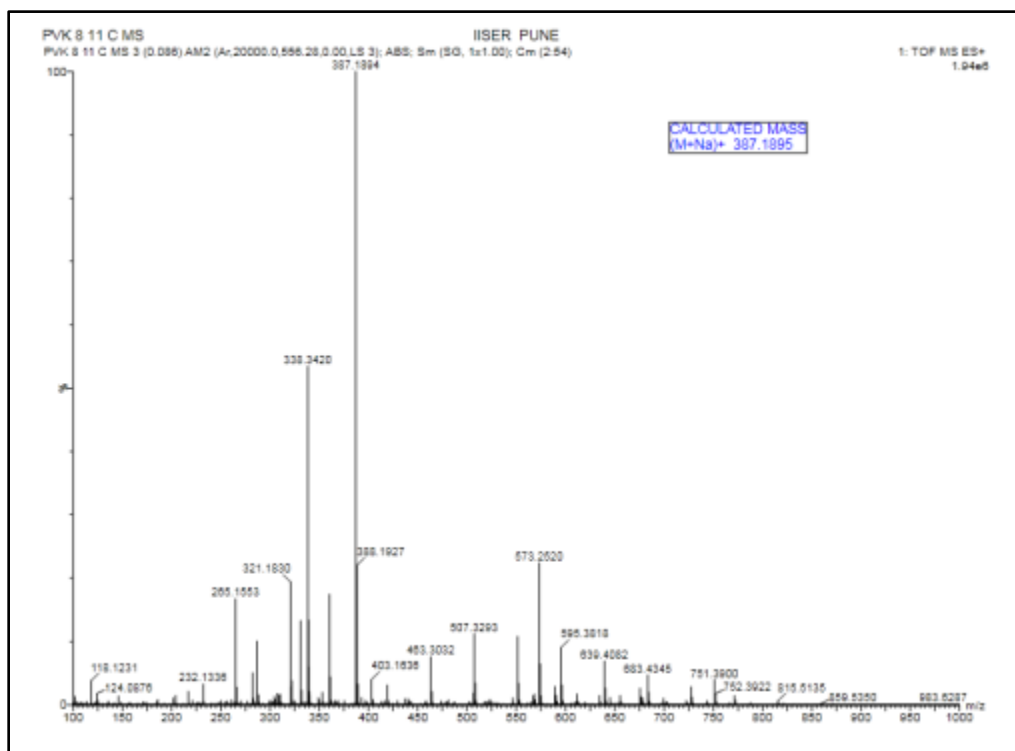**HRMS of Compound 5:**
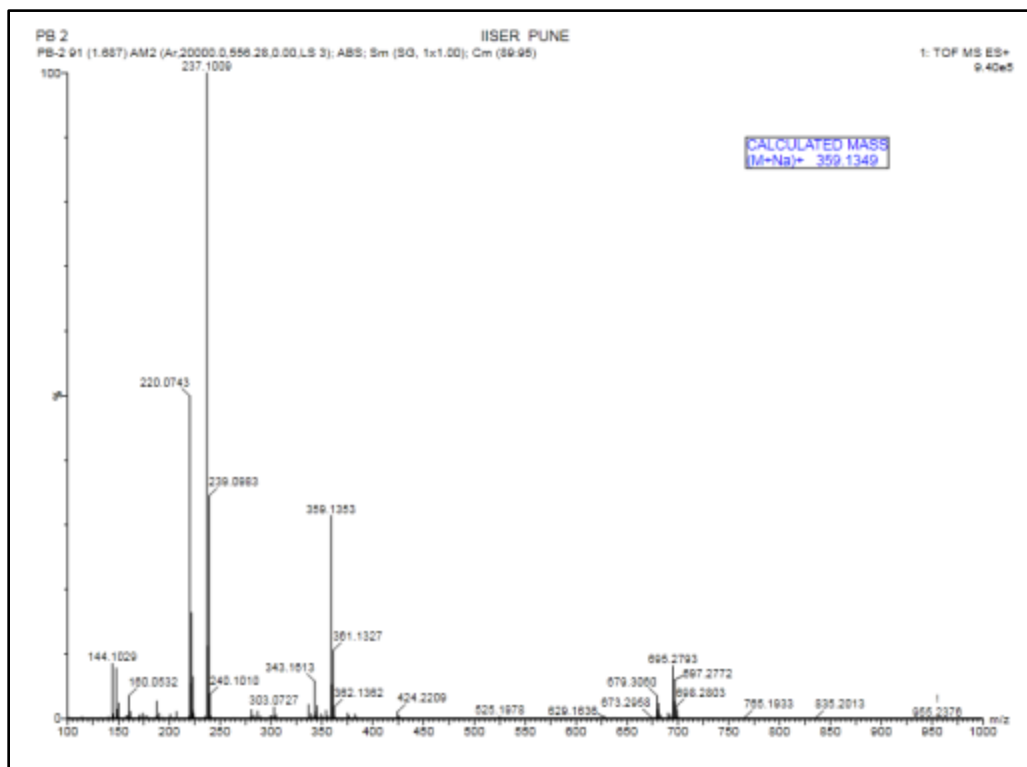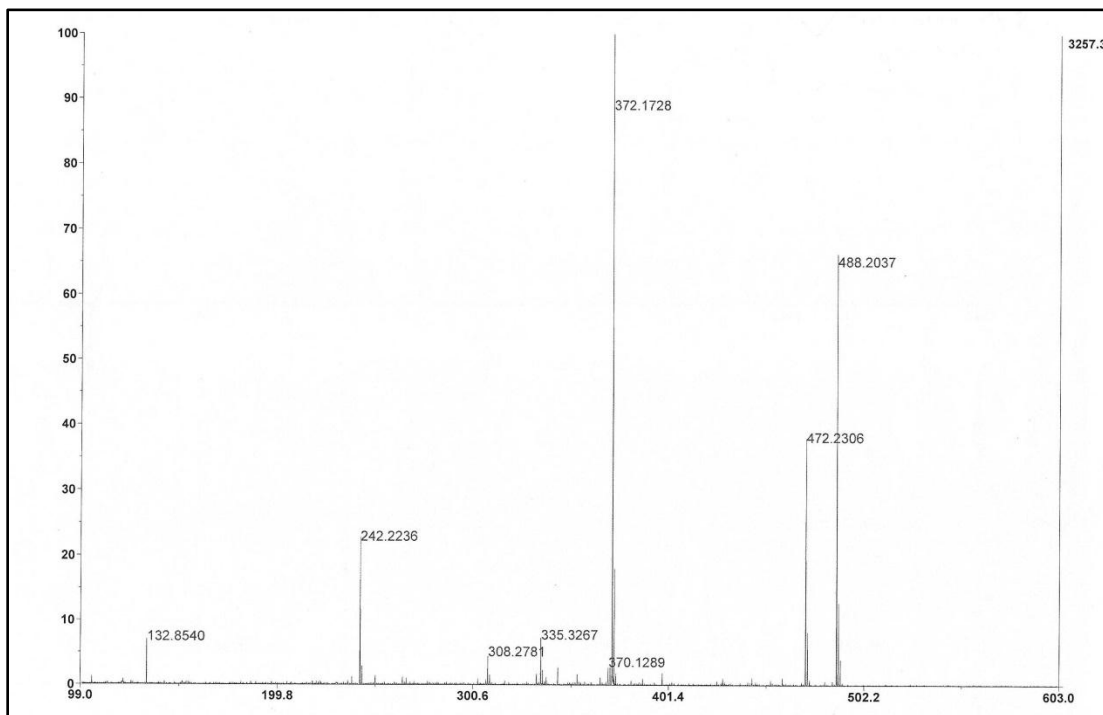
MALDI-TOF of Compound 6:
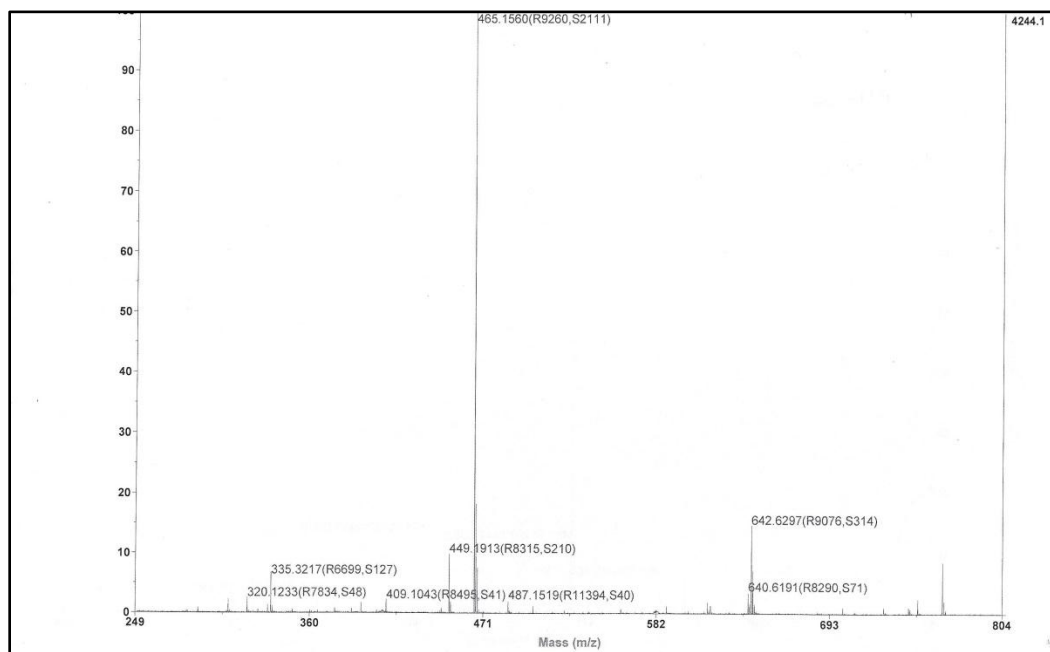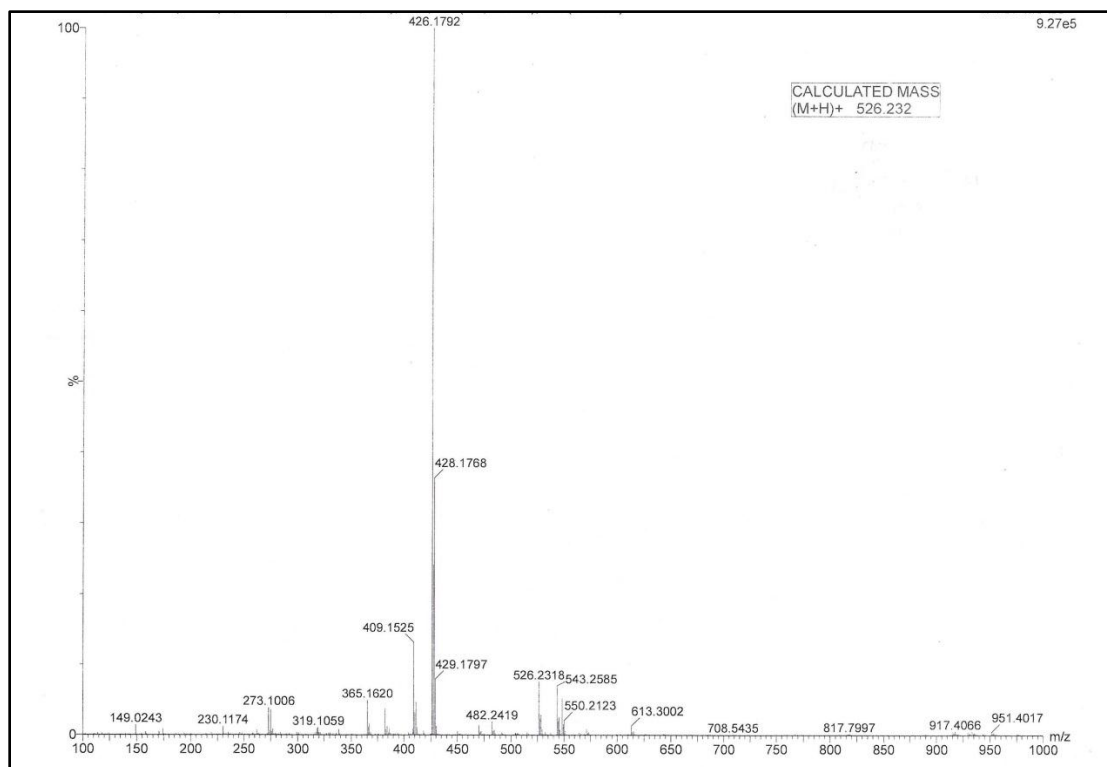

HRMS of Compound 7:
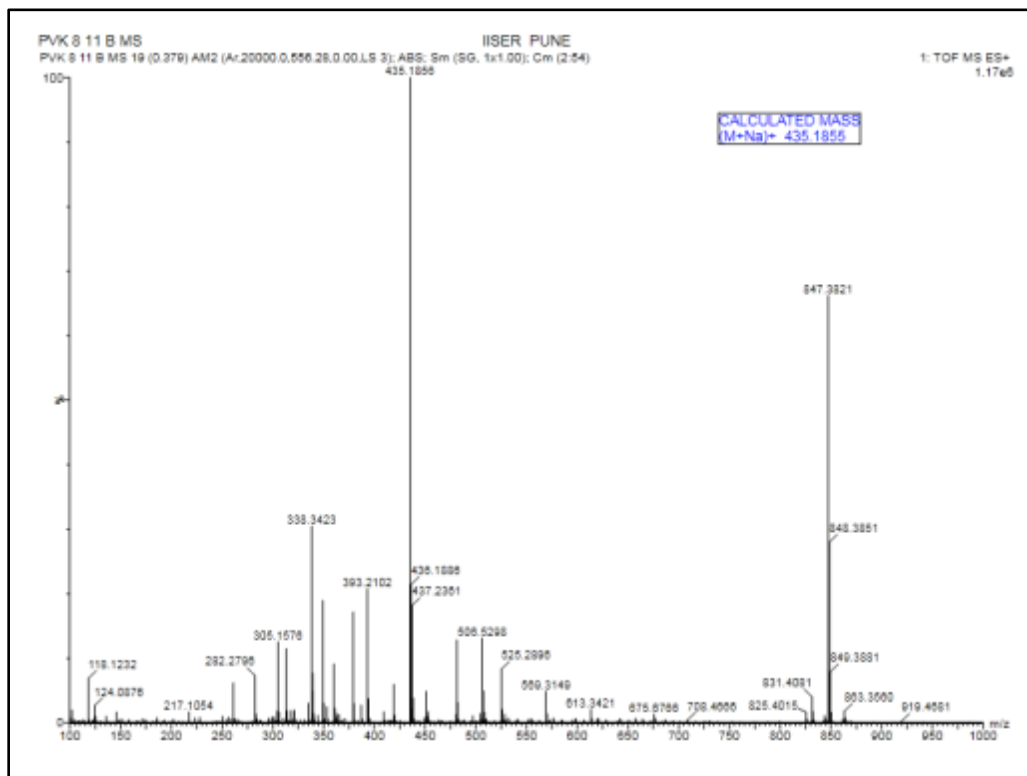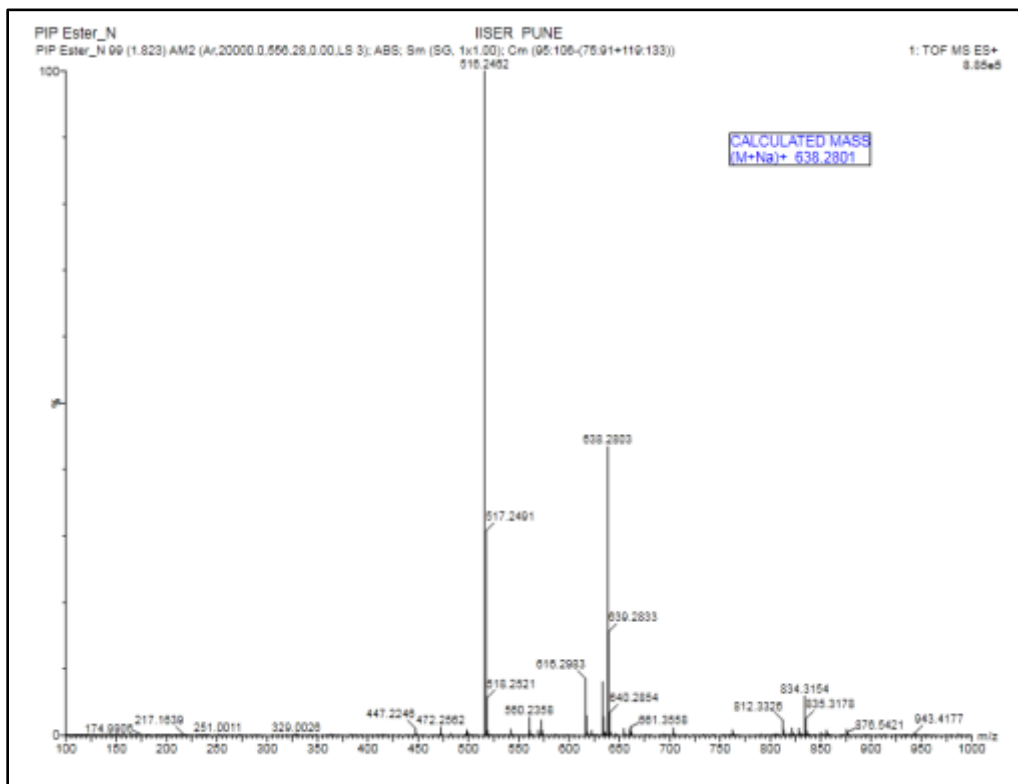
HRMS of Compound 9:
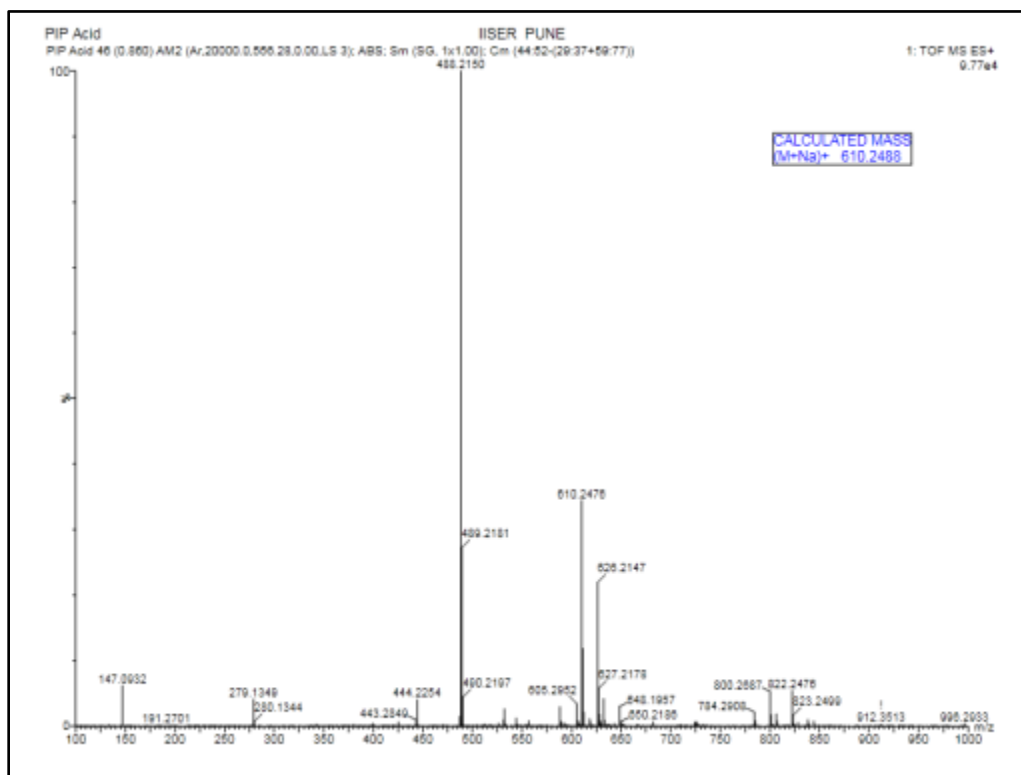

HRMS of Compound 10:

MALDI-TOF of Compound 12:
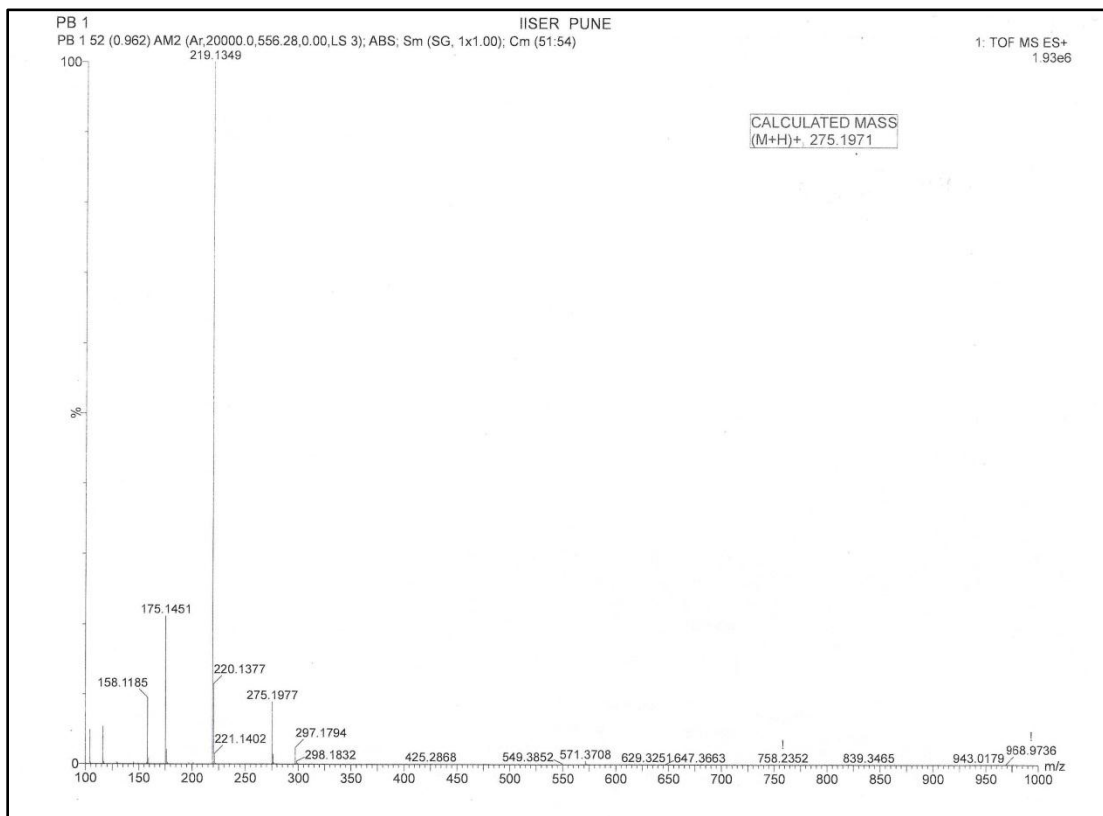

HRMS of Compound 13:

HRMS of Compound 14:

HRMS of Compound 15:

HRMS of Compound 18:

MALDI-TOF of Compound 19:
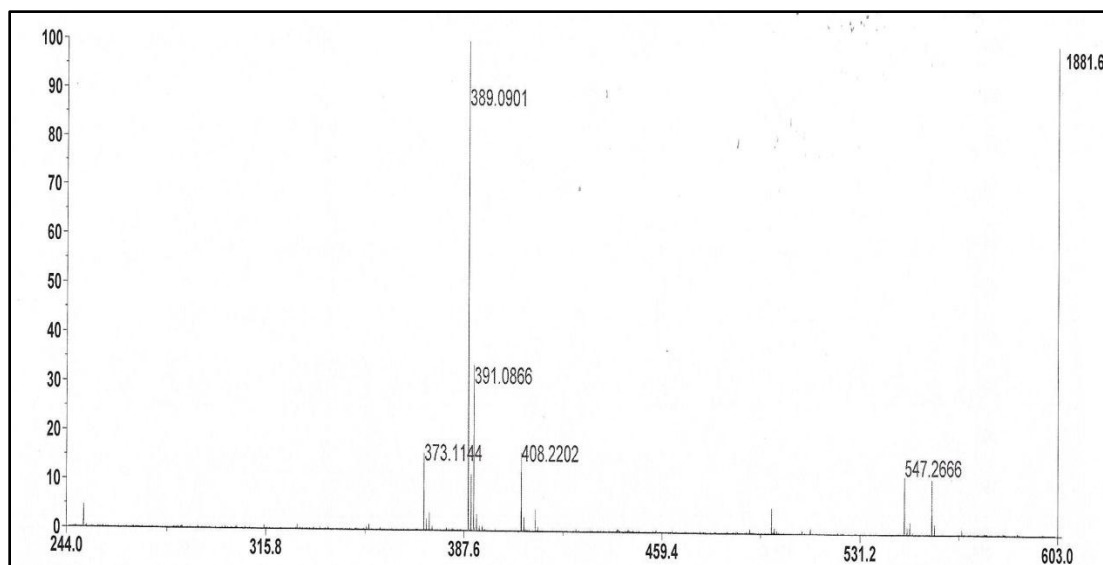
HRMS of Compound 20:
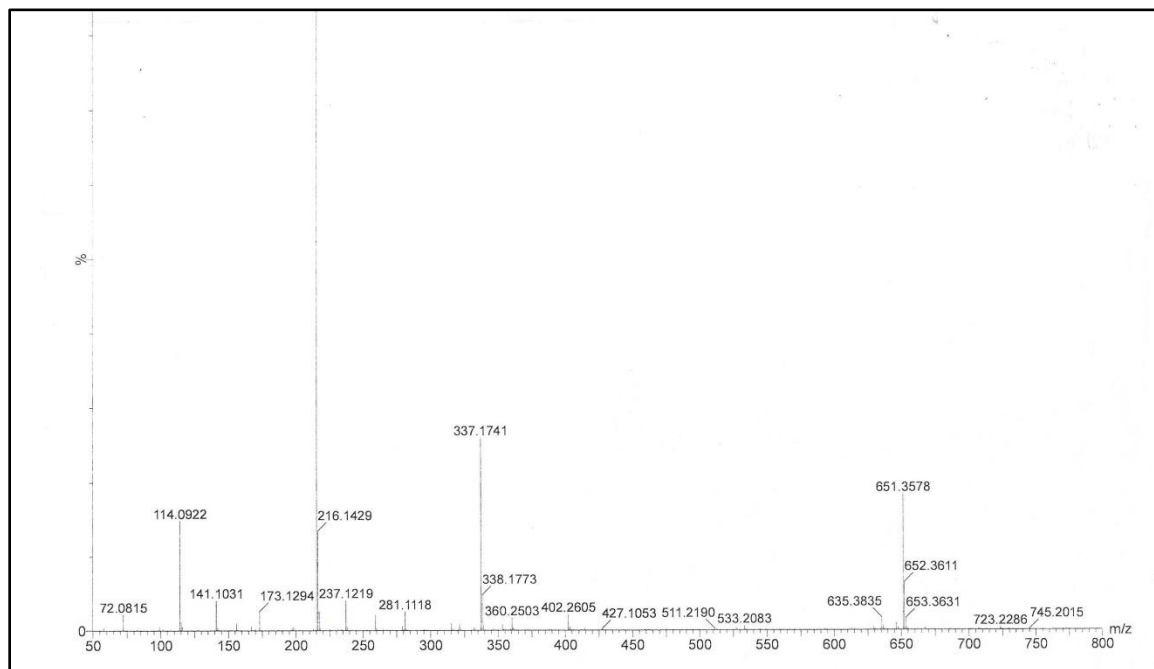
HRMS of Compound 21:
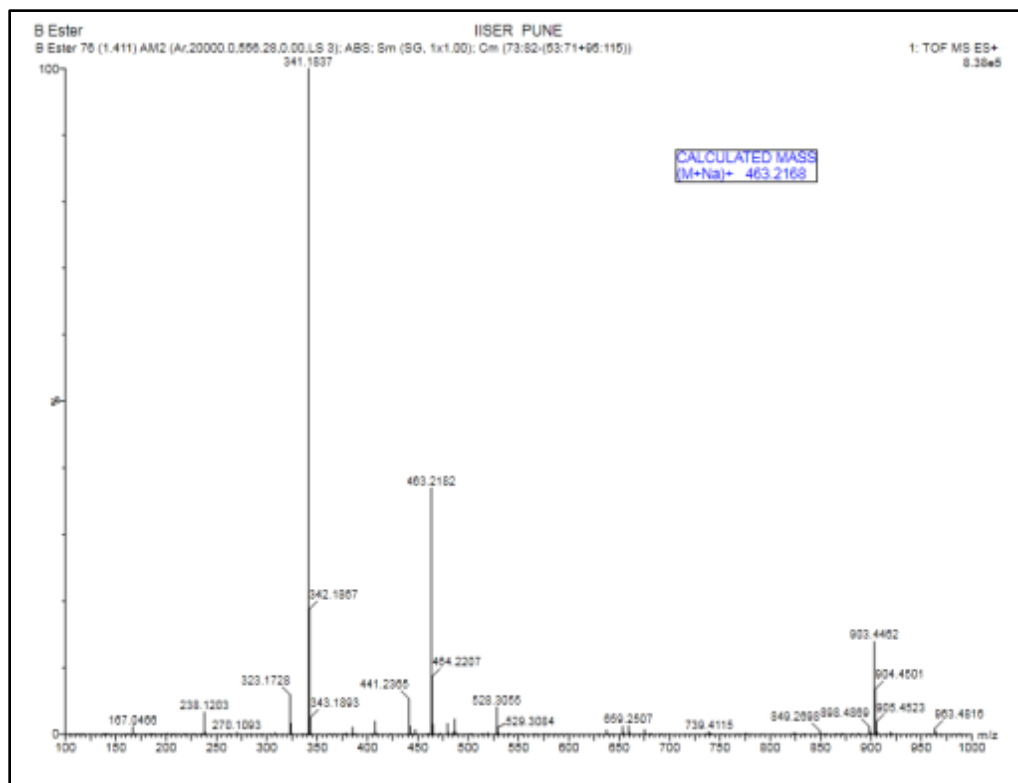
HRMS of Compound 22:
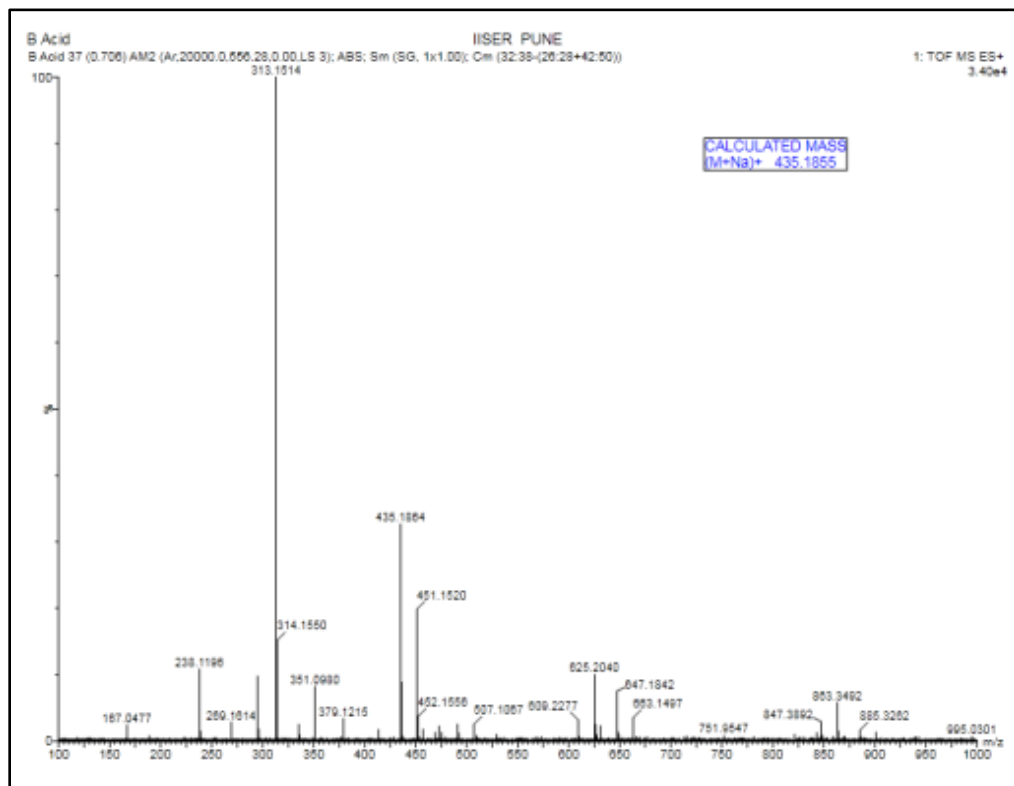
HRMS of Compound 25:
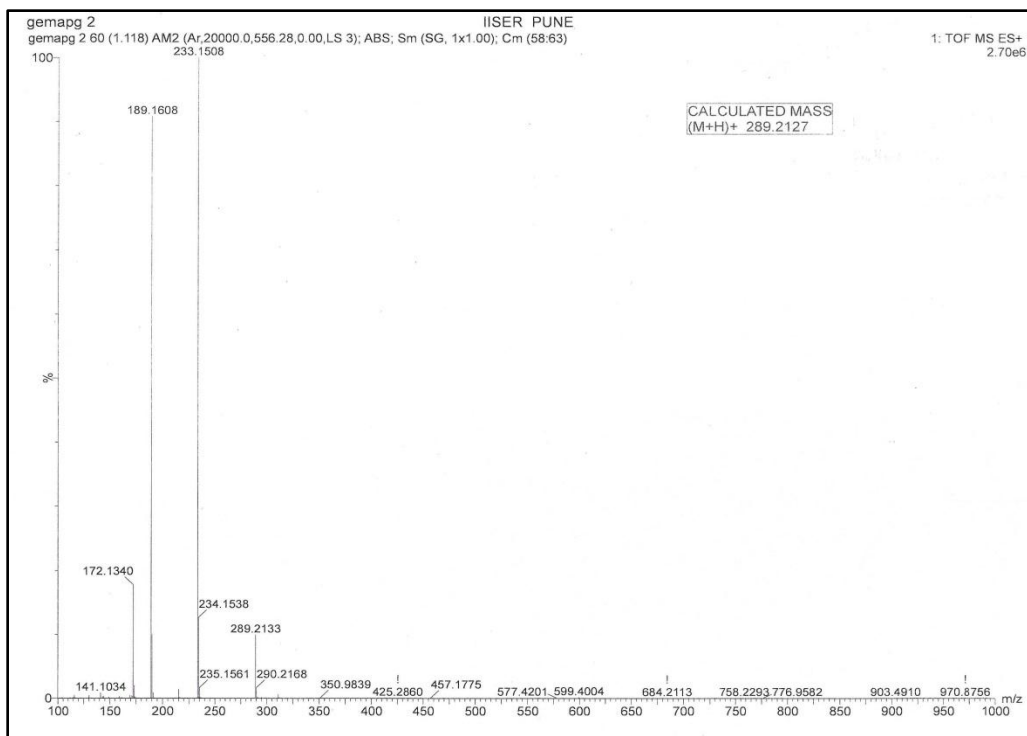
HRMS of Compound 26:
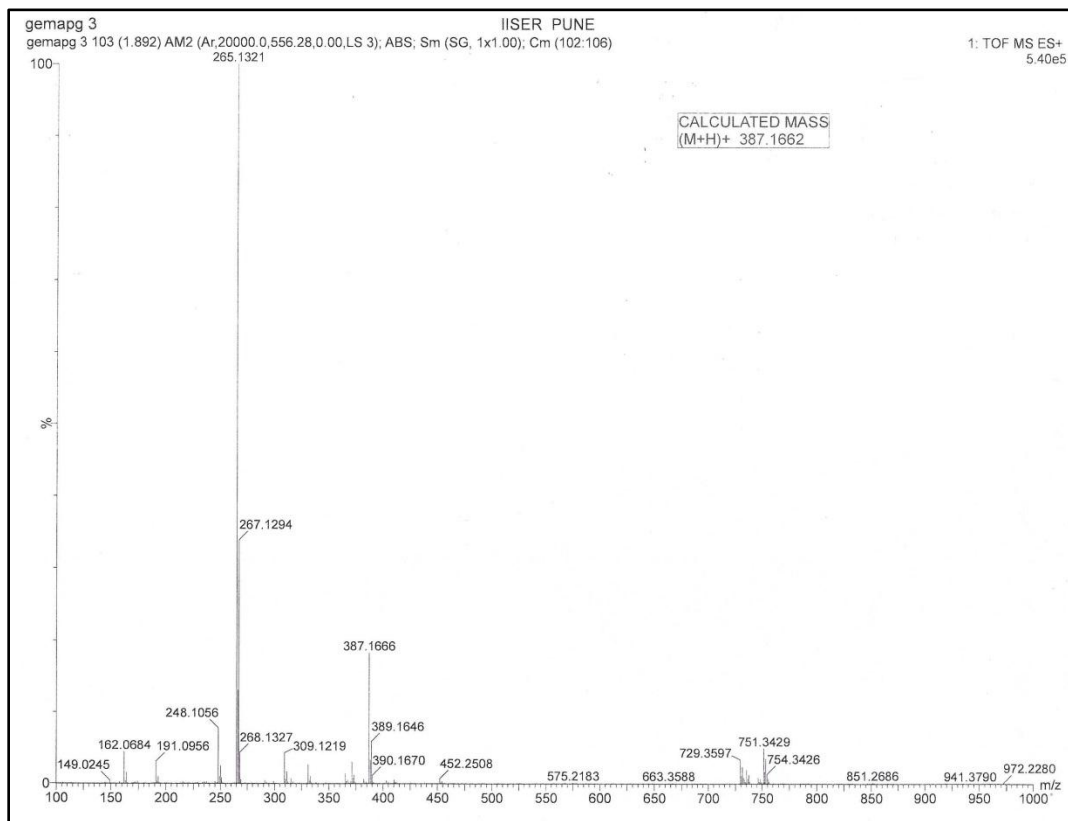
LCMS of Compound 27:
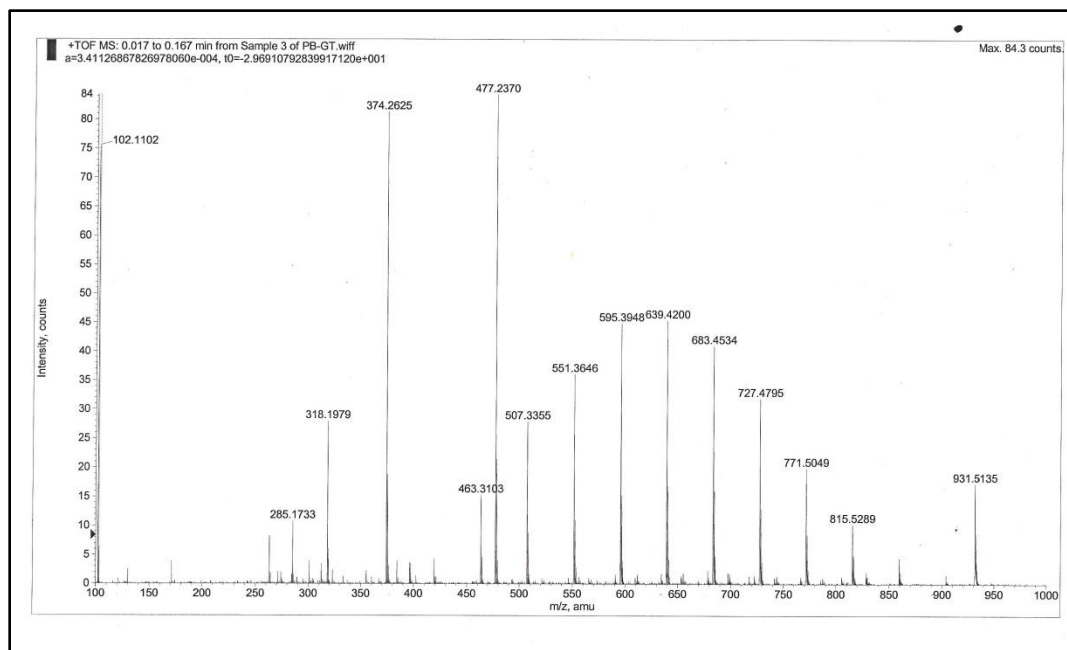
HRMS of Compound 28:
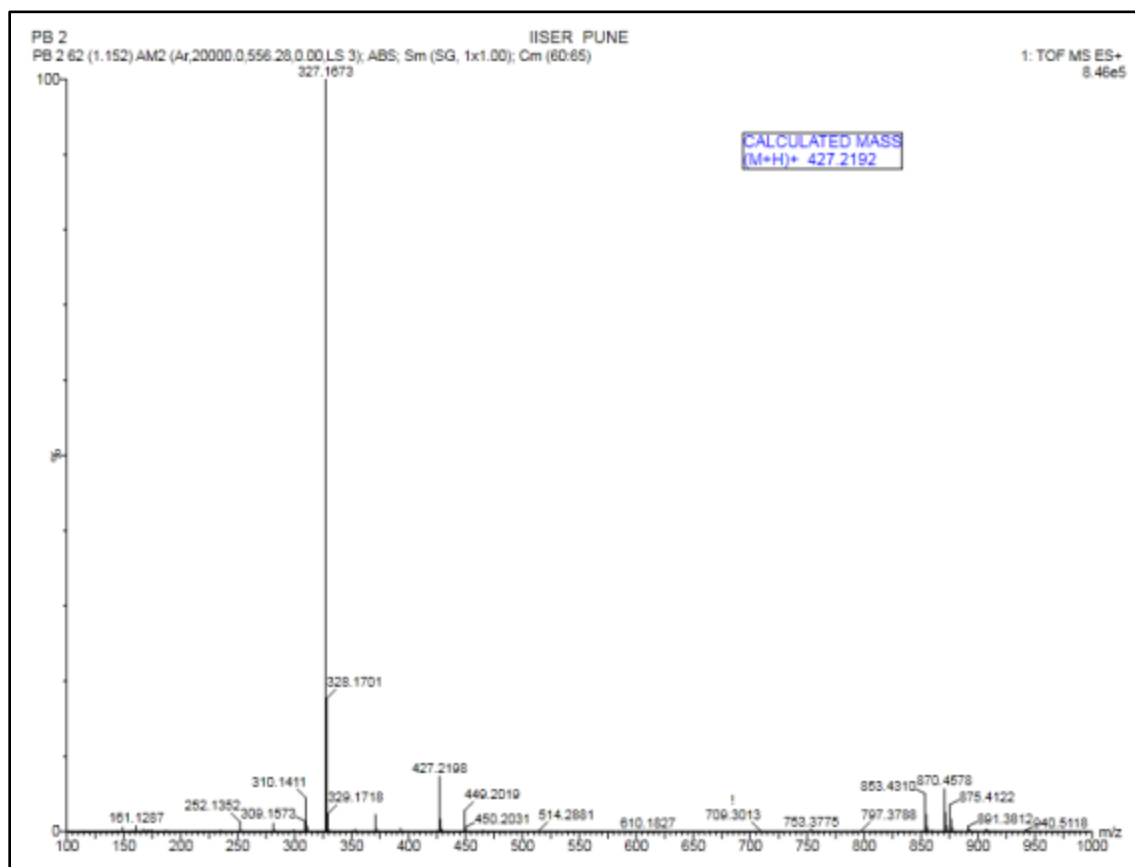
HPLC Trace of PNA 1:
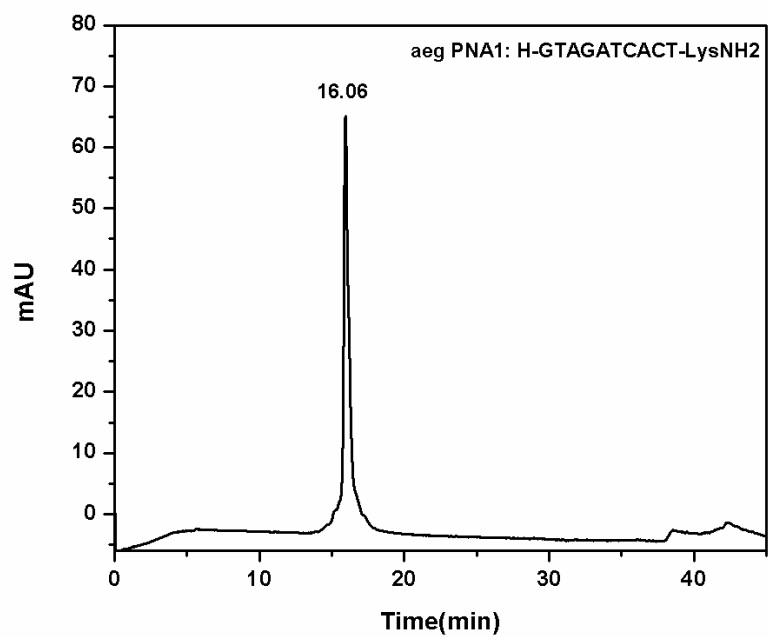
HPLC Trace of PNA 2:

HPLC Trace of PNA 3:

γ gem PNA3: HGTAGAtCACT-LysNH2

HPLC Trace of PNA 4:

γ gem PNA4: HGtAGAtCACT-LysNH2
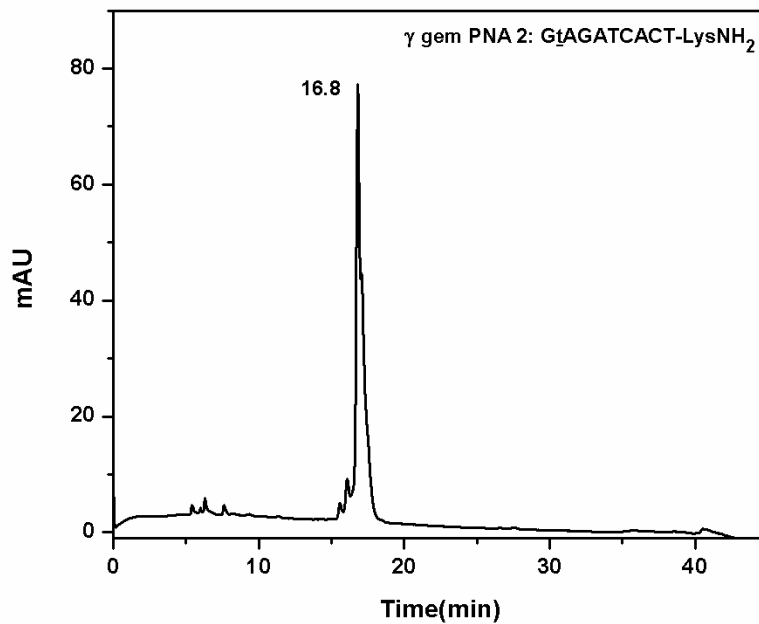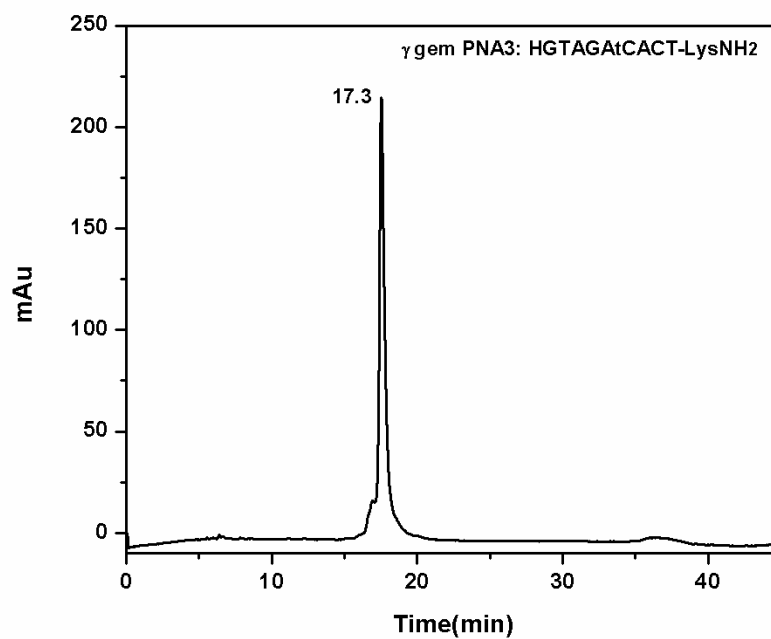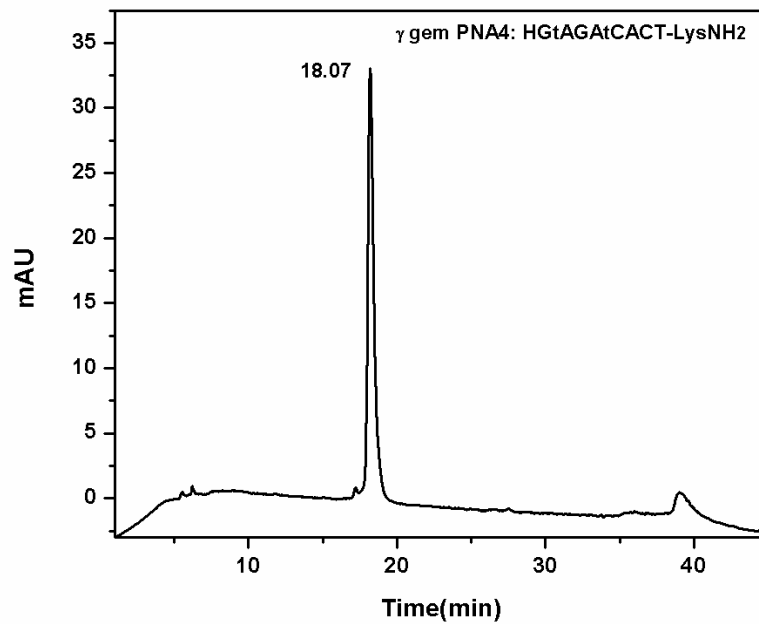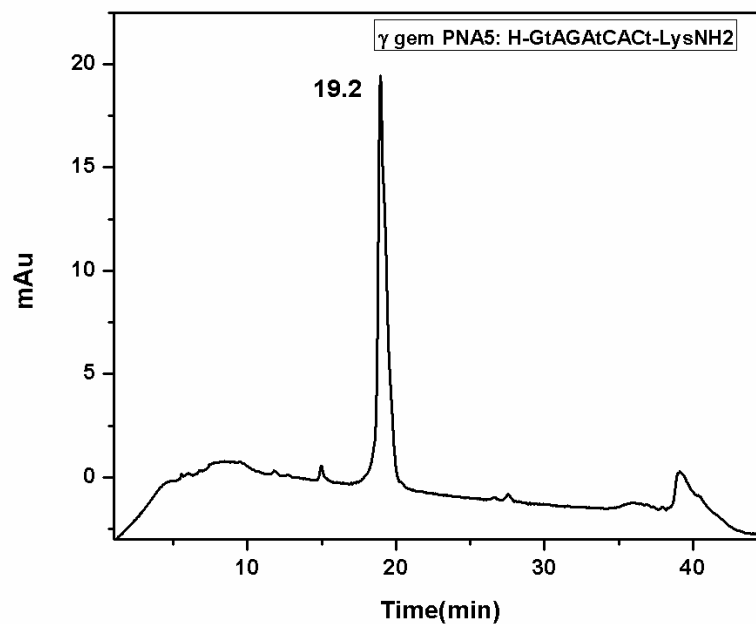
HPLC Trace of PNA 5:

HPLC Trace of PNA 6:

HPLC Trace of PNA 7:

γ pip PNA7: H-GTAGAtCACT-LysNH2
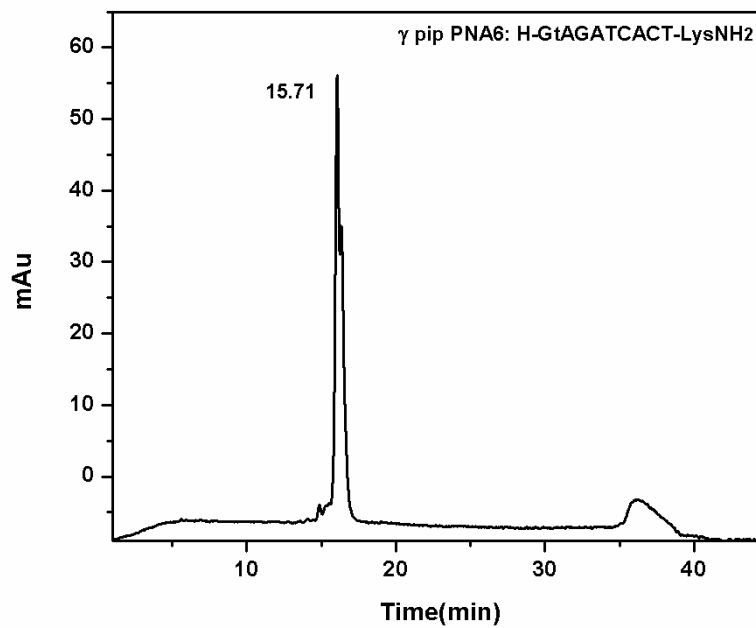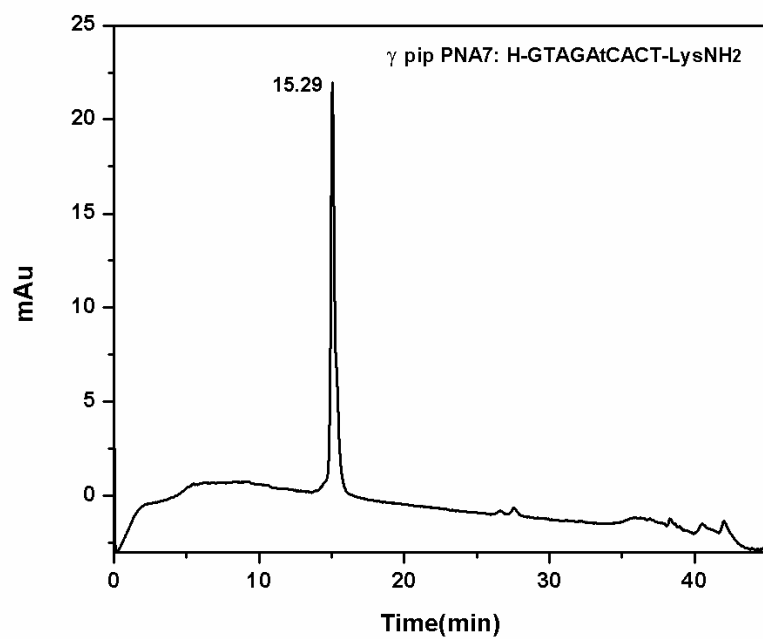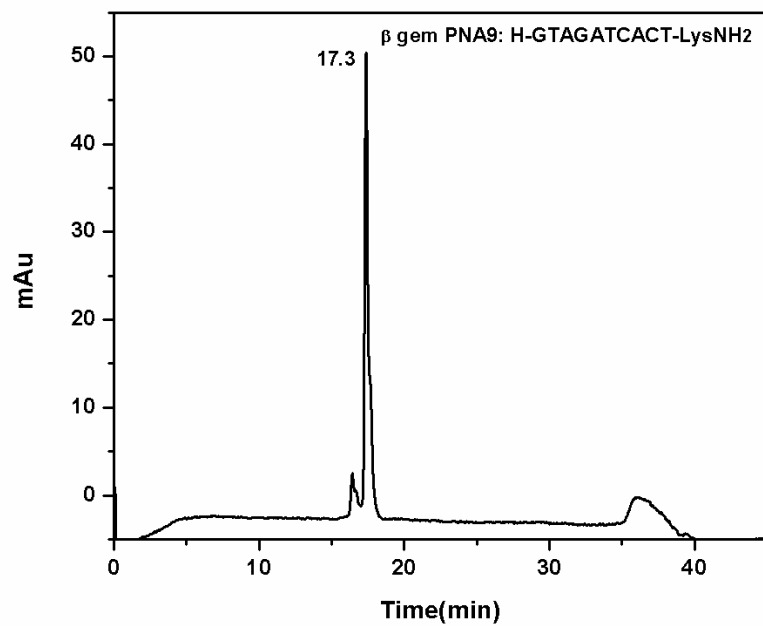
HPLC Trace of PNA 9:

HPLC Trace of PNA10:
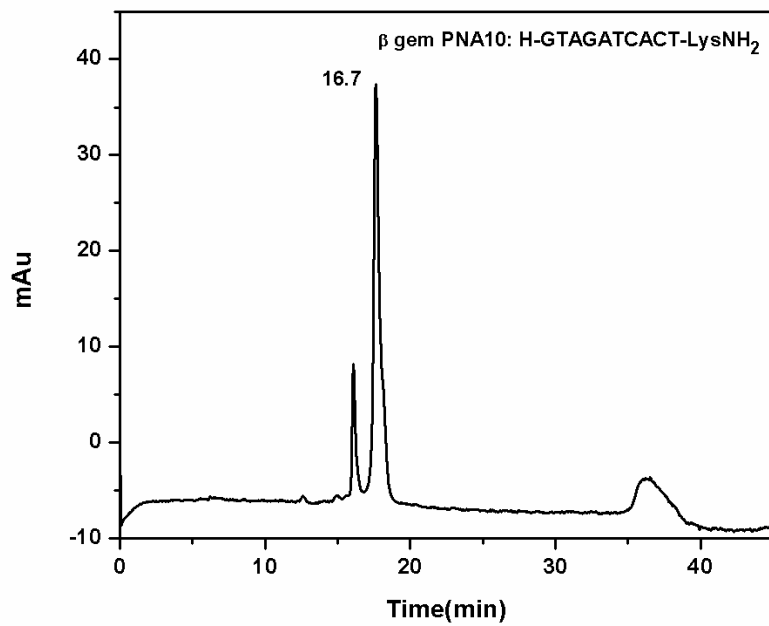
HPLC Trace of PNA 11:
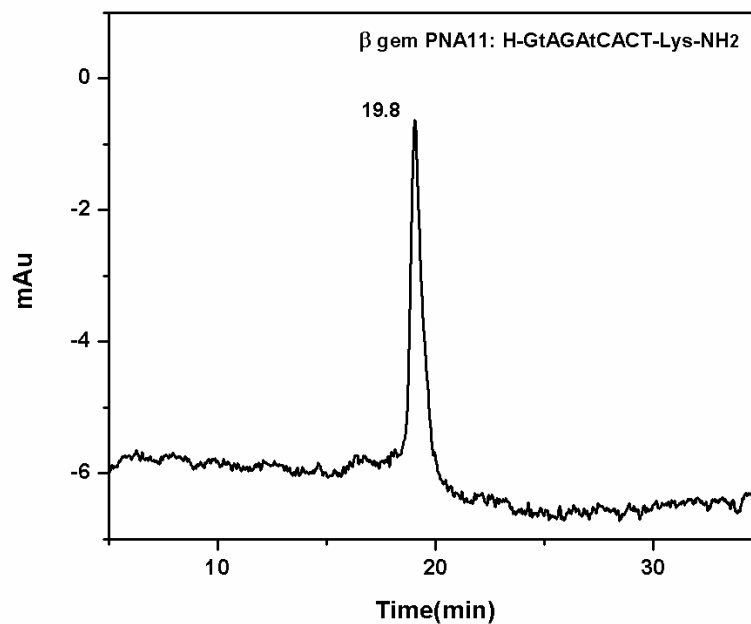
HPLC Trace of PNA 12:
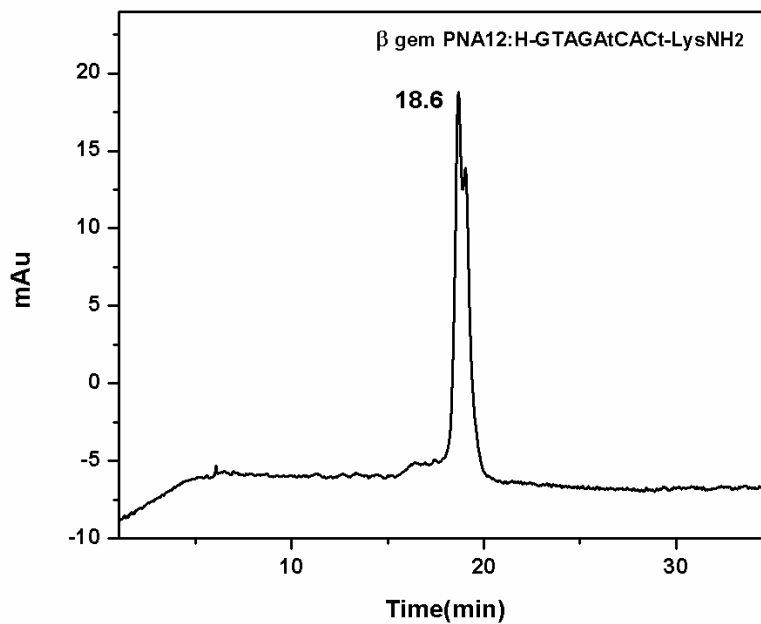
HPLC Trace of PNA 13:
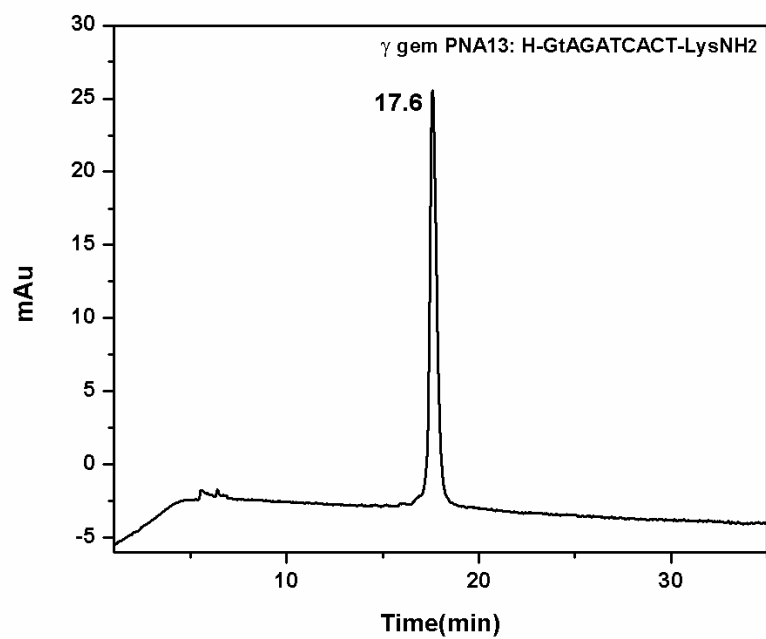
HPLC Trace of PNA 14:
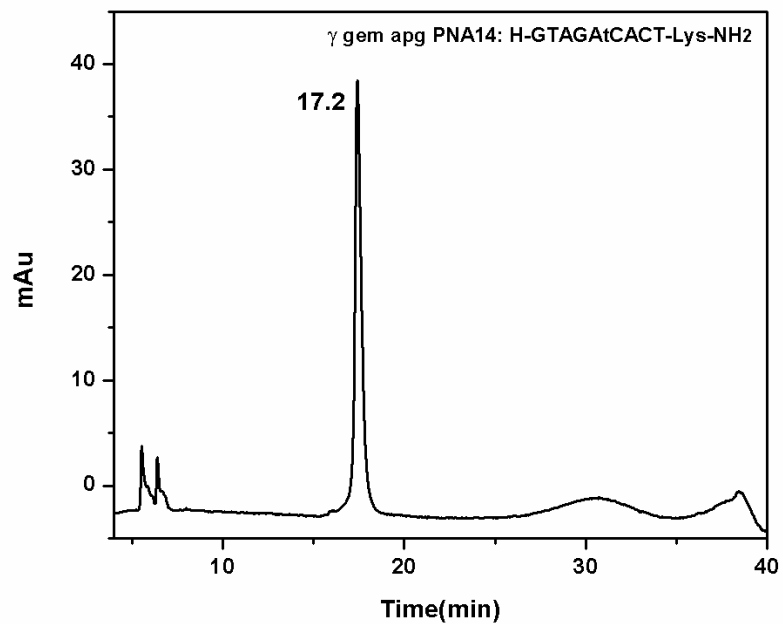
HPLC Trace of PNA 15:
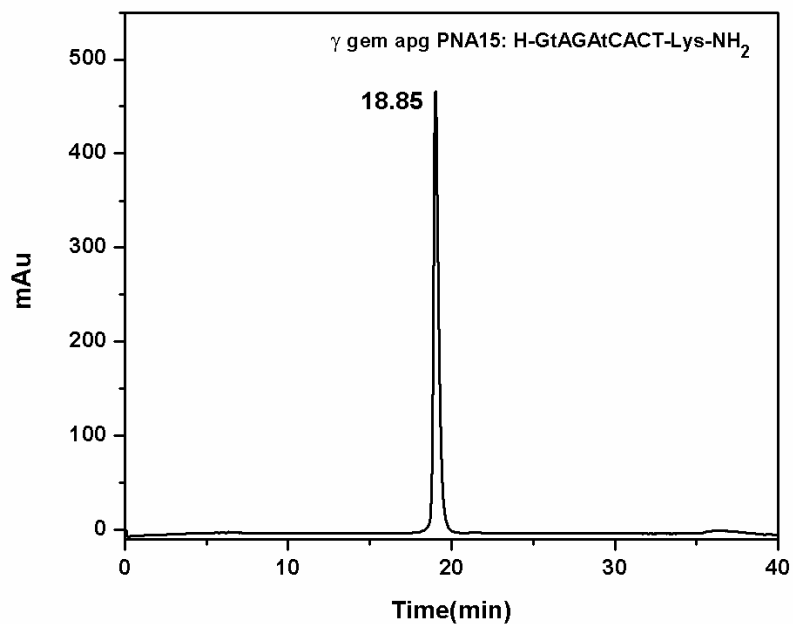
HPLC Trace of PNA 16:
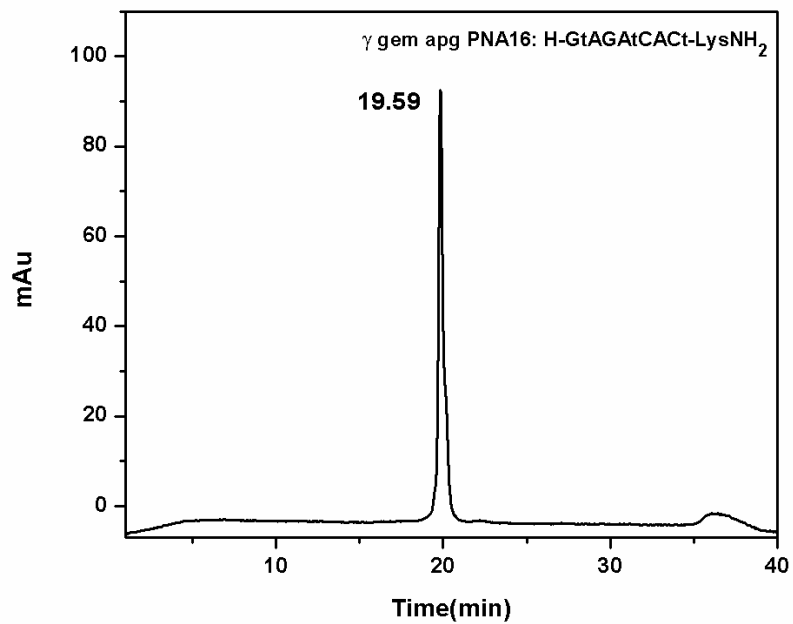
MALDI-TOF Mass of PNA 1:
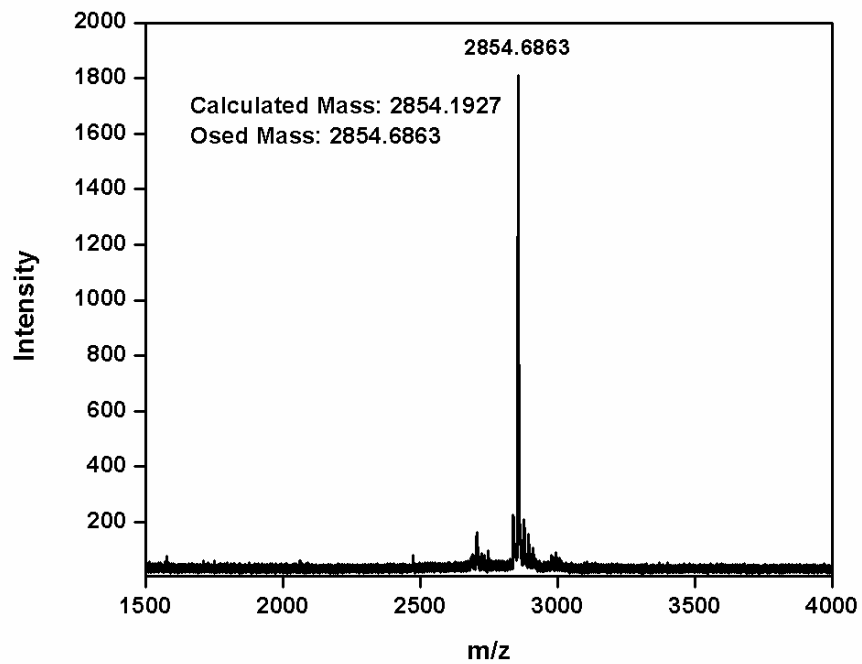
MALDI-TOF Mass of PNA 2:
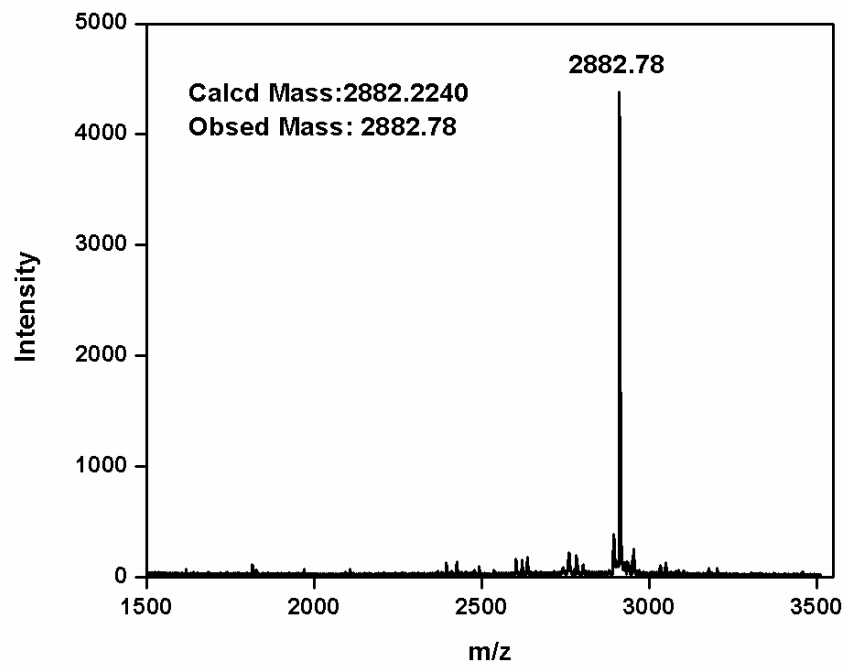
MALDI-TOF Mass of PNA 3:
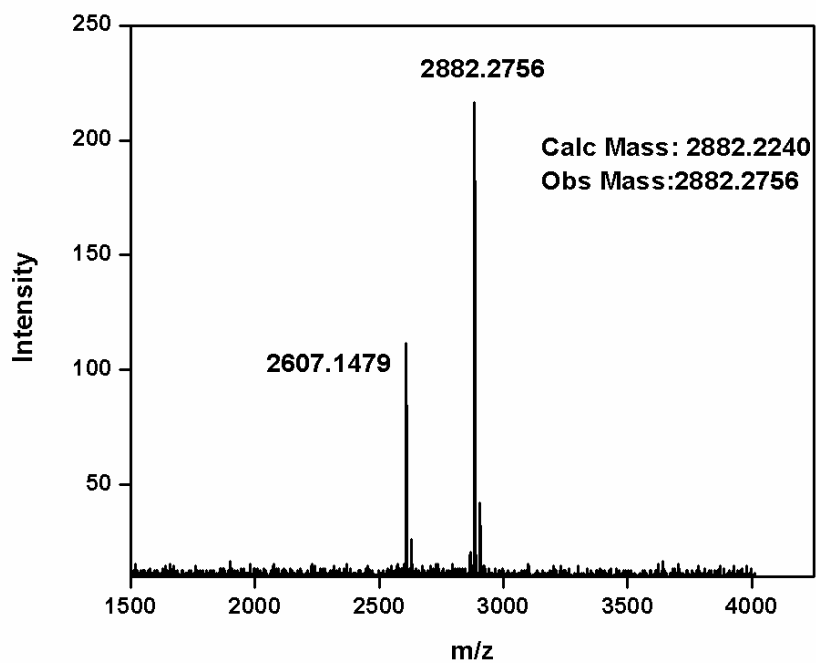
MALDI-TOF Mass of PNA 4:
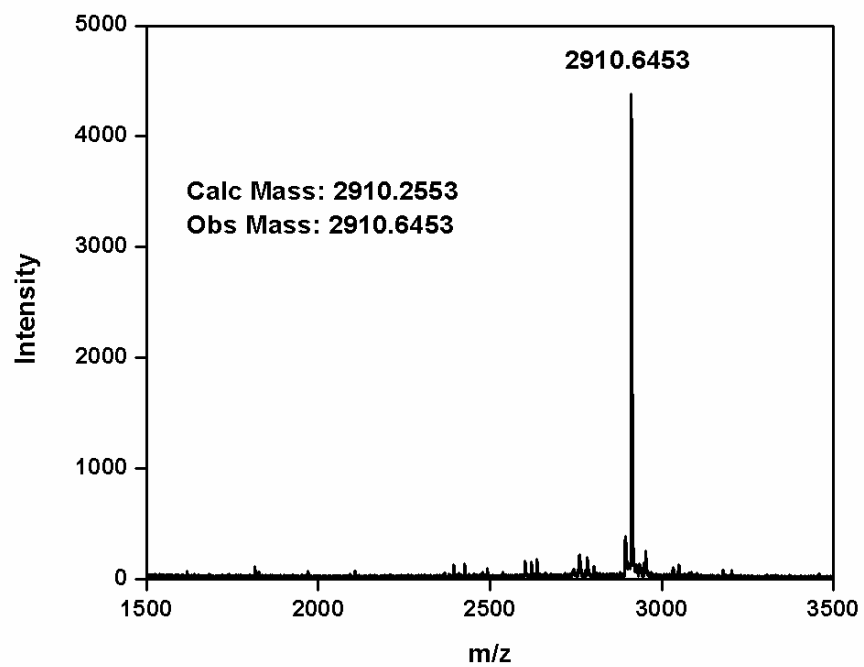
MALDI-TOF Mass of PNA 5:
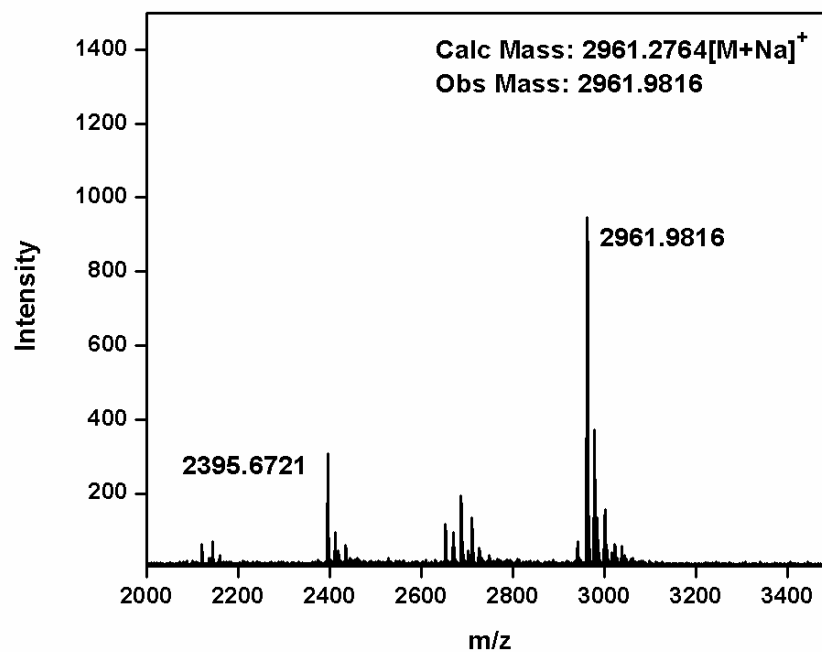
MALDI-TOF Mass of PNA 6:
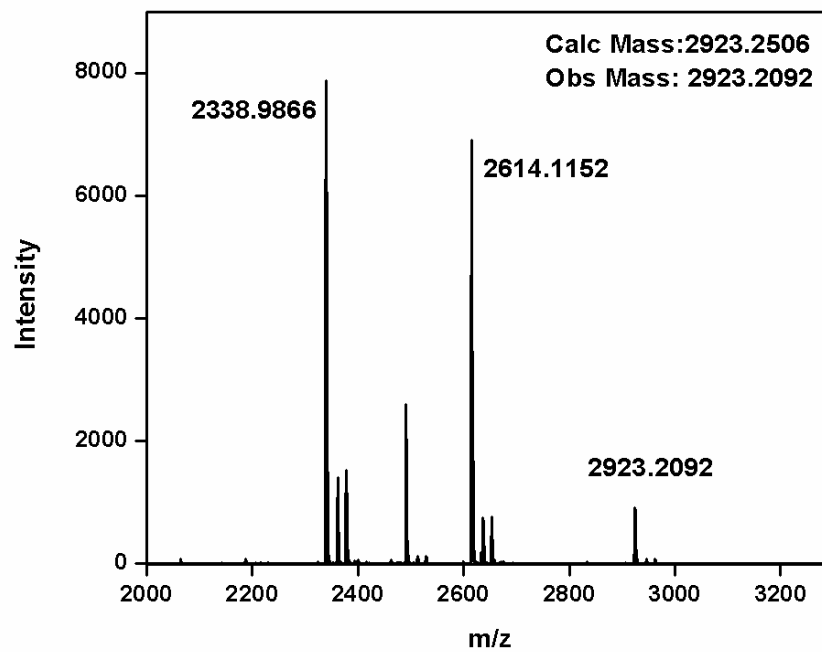
MALDI-TOF Mass of PNA 7:
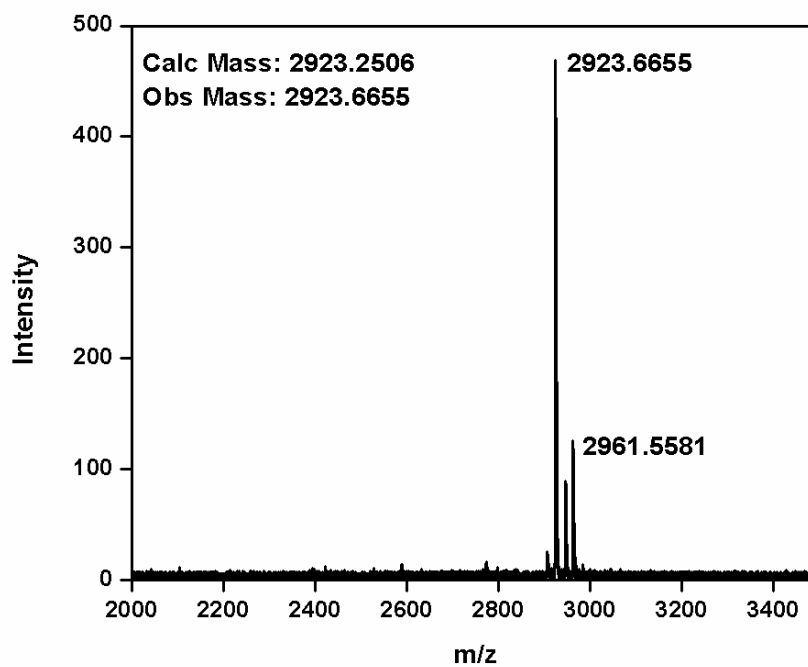
MALDI-TOF Mass of PNA 9:
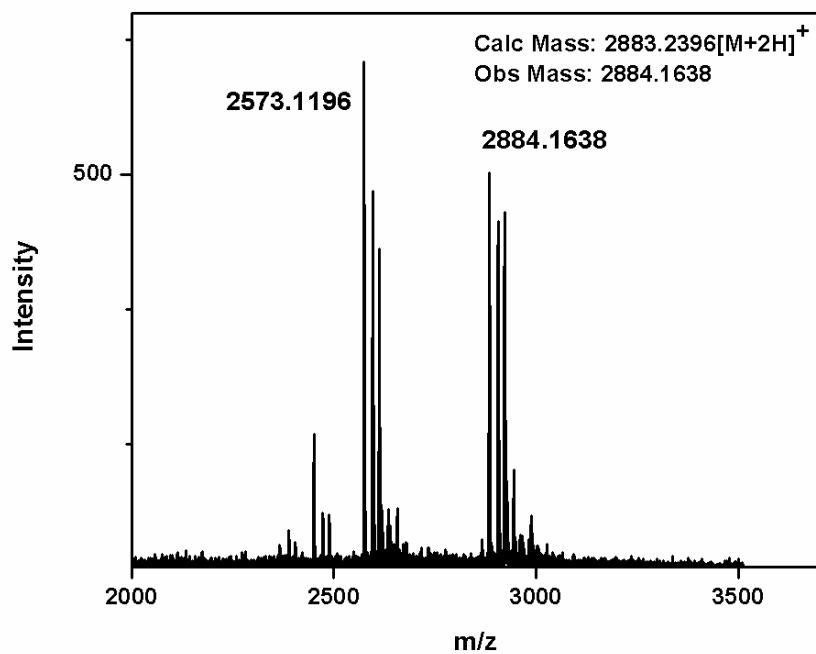
MALDI-TOF Mass of PNA 10:
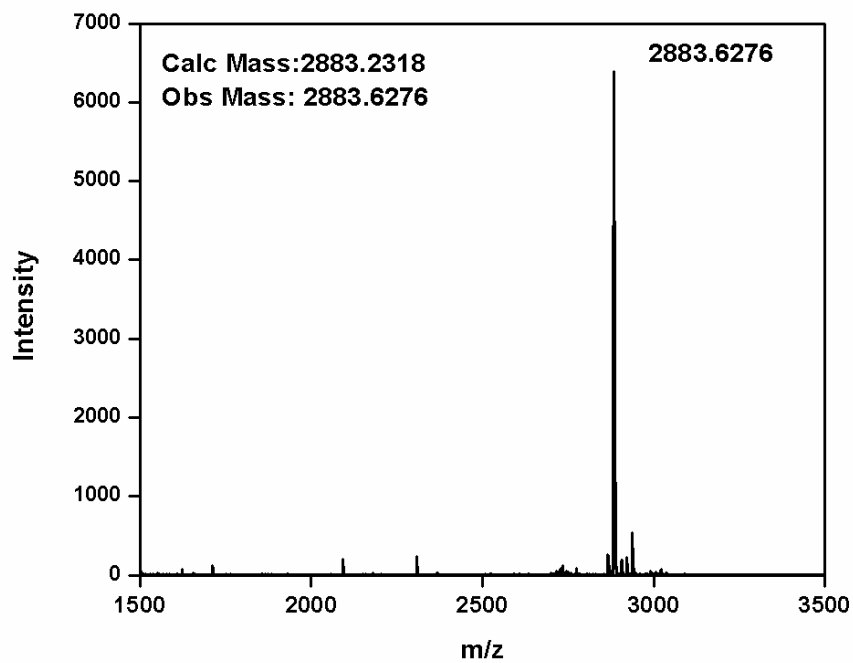
MALDI-TOF Mass of PNA 11:
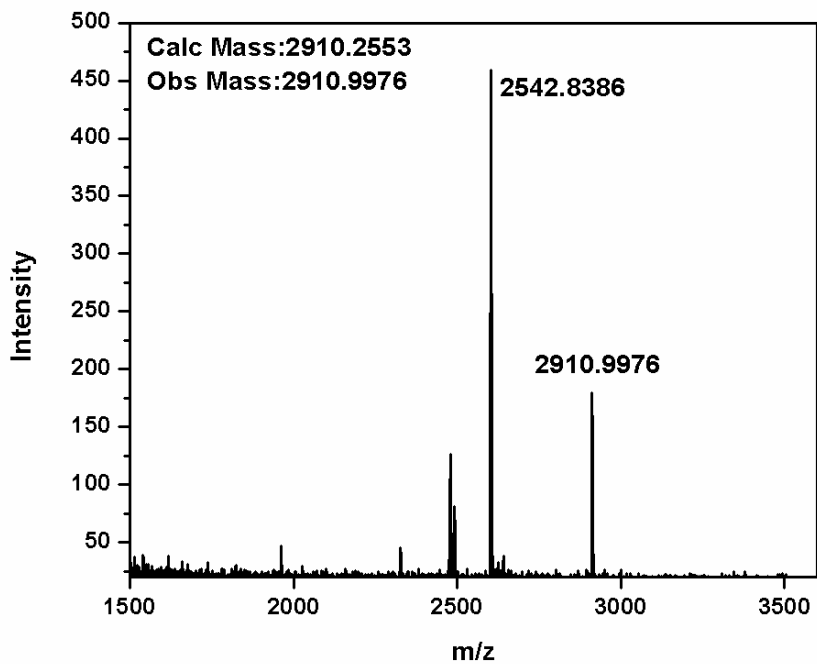
MALDI-TOF Mass of PNA 12:

MALDI-TOF Mass of PNA 13:

Calc Mass:2897.2475
Obs Mass:2897.5446

2897.5446

MALDI-TOF Mass of PNA 14:

Calc Mass: 2896.2397
Obs Mass:2897.5446

2897.5446
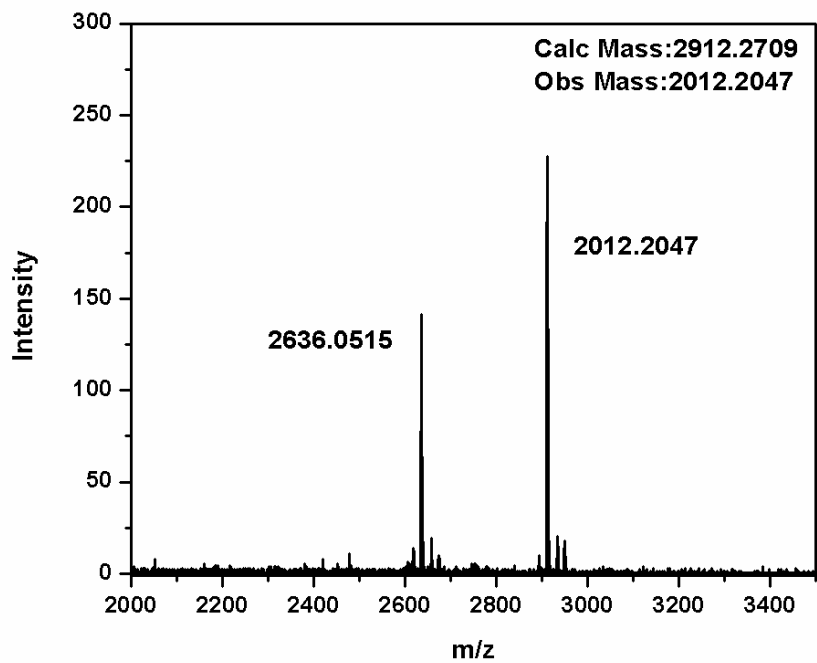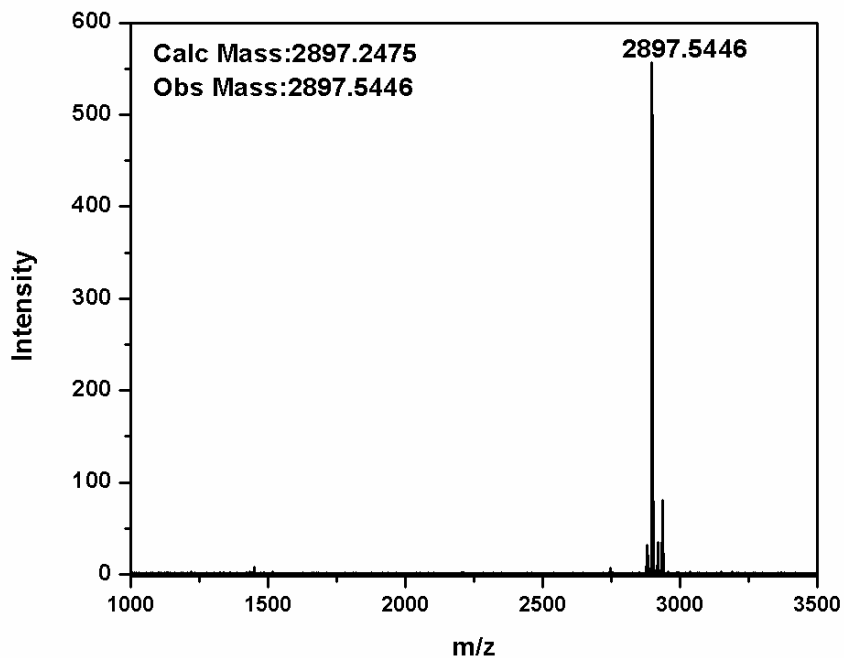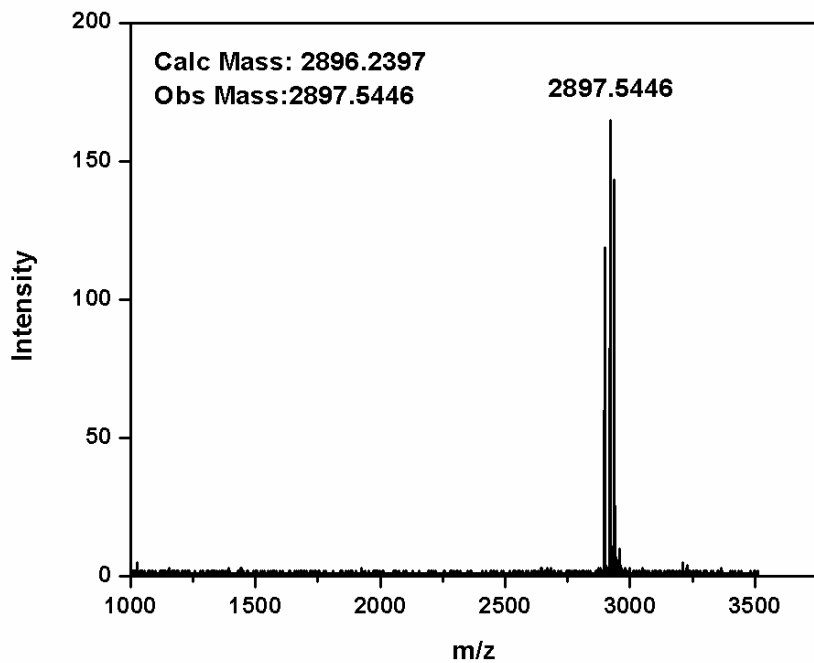
MALDI-TOF Mass of PNA 15:
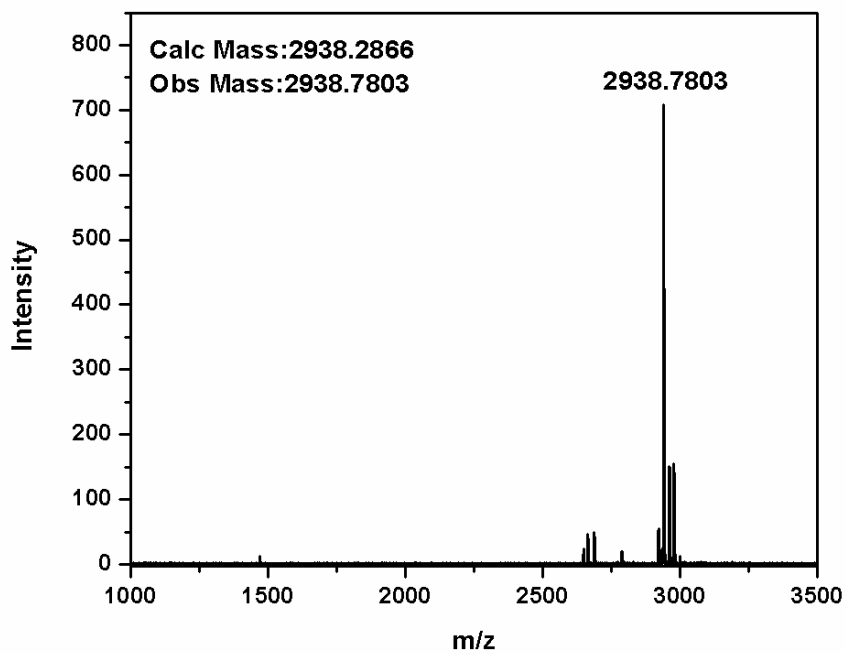
MALDI-TOF Mass of PNA 16:
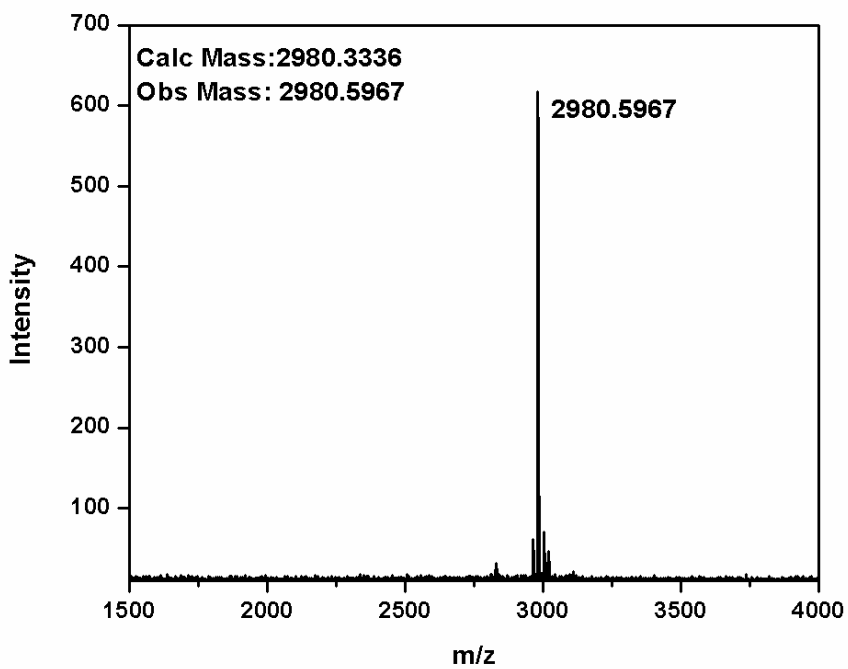
CHAPTER 3

Biophysical Studies of PNA Oligomers (UV-Tm and CD)

The effect of achiral, cationic and neutral functionalities on the affinity of PNA towards the complementary DNA and their thermal stabilities has been studied using various biophysical techniques. The comparative binding studies of various modified PNAs have been discussed.

3.1 Introduction:

Biophysics is an interdisciplinary science which uses the techniques from the physical sciences in order to understand the biological structure and their functions. These techniques are useful in studying the structure and properties of nucleic acids, proteins, peptides and their analogs.[1] The ability of antisense/antigene oligonucleotides to bind *in vitro* to the target DNA/RNA can be investigated by using various biophysical techniques like thermal UV-melting (UV-T_m), Circular Dichroism (CD), Fluorescence Spectroscopy and Gel Electrophoresis.

The preceding chapter discusses about the synthesis of rationally designed γ-C-substituted multifunctional PNA analogs. The modified PNA monomers were introduced into achiral *aeg* PNA at various positions by solid phase synthesis in order to study the effect of chirality and side chain functional groups in influencing the binding properties to target nucleic acids.

3.2 Rationale of the present work:

This chapter addresses the biophysical studies of various modified PNAs and their hybrids with complementary/mismatch nucleic acids using temperature dependent UV spectroscopy and CD spectroscopy. The biophysical studies have been carried out on the designed PNA analogs in order to investigate the effect of incorporated functional groups on the binding affinity to target nucleic acids. These studies give information about the binding selectivity, binding specificity, structural organization and the duplex stability which are important parameters to evaluate the antisense / antigene agents.

3.3 Biophysical techniques used to study the hybridization properties

This section describes the applications of various biophysical techniques used to study the properties of single stranded PNAs and PNA: DNA duplexes.

3.3.1 UV-melting

The two strands of complementary nucleic acids are held together by hydrogen bonding and the stacking interactions between the adjacent nucleobases. The stability of duplexes depends on the conditions like temperature, pH and the ionic strength under conditions that disrupt hydrogen bonding and stacking interactions. The two strands are no longer held together and the double helix is denatured. The duplex is said to melt when temperature is used as denaturing agent. Monitoring the UV absorption at 260nm as a function of temperature has been extensively used to study the thermal stability of various nucleic acid complexes including PNA-DNA/RNA hybrids[2]. The heteroaromatic bases interact via their π electron clouds when stacked together in the duplex in water. Because the UV absorbance of the bases is a consequence of π electron transitions, the magnitude of these transitions is affected when bases are stacked.

The increase in temperature results in diminished stacking interaction between adjacent bases and disruption of hydrogen bonds between base pairs leading to a complete loss of secondary structure. This results in an increase in absorbance at 260nm termed "hyperchromicity". The process is co-operative and the plot of absorbance at 260 nm vs temperature is sigmoidal (Figure **3.1A**). The midpoint of the sigmoidal transition is termed as the melting temperature, T_m.

| A | B |
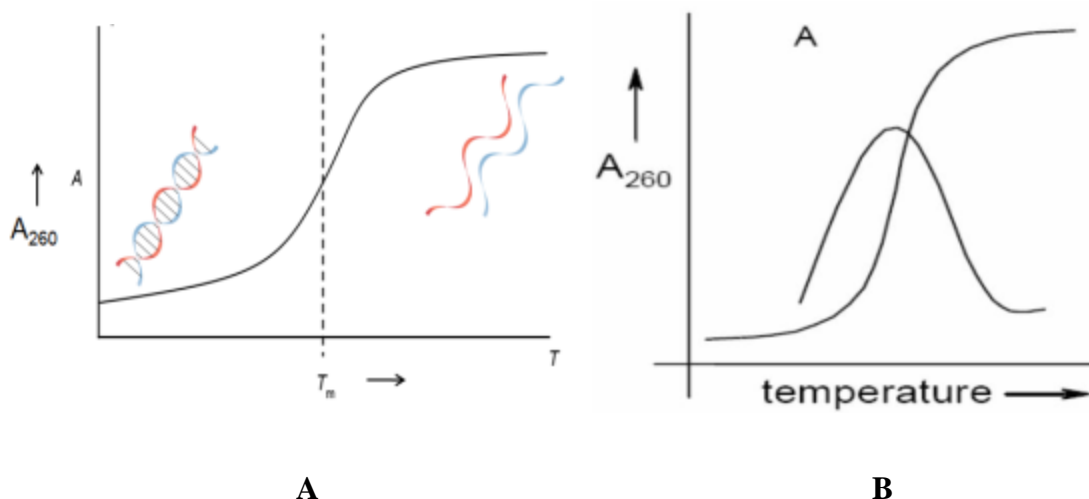
Figure 3.1: (**A**) Sigmoidal graph of UV-T_m; (**B**) Derivative plot of PNA: DNA duplex

The sigmoidal nature of transition suggests that at any temperature, nucleic acids exist in two states, duplexes or as single strands and at varying temperatures, the relative

proportions of two states change. A non-sigmoidal (e.g. sloping linear) transition with low hyperchromicity is a consequence of non-complementation. In many cases, the transitions are broad and the exact T_m values are obtained from the peak in first derivative plots (Figure **3.1B**). This technique has provided valuable information regarding the strength of base-dependent complementary interactions in nucleic acid hybrids involving DNA, RNA and PNA.

The binding stoichiometry of nucleic acids can be determined from the UV titration and the CD-mixing using Job's plot. The combination of UV absorption and the CD spectra provides the correct determination of complex formation and the strand stoichiometry. In literature, it has been shown that polypyrimidine PNA binds to complementary DNA in a 2:1 ratio forming PNA_2:DNA triplex[3] whereas the mixed purine-pyrimidine PNA binds in 1:1 ratio forming PNA:DNA duplex.[4] In this study, all PNAs are composed of mixed purine-pyrimidine bases so the PNA and DNA are mixed in 1:1 ratio.

3.3.2 Circular dichroism

Circular dichroism (CD) is a well-stablished tool used to study the conformational aspects of nucleic acids.[5] A CD curve is a plot of the molecular ellipticity $[\theta]$ versus the wavelength λ. The CD effect results from the fact that the right circularly ray is absorbed differently from left circularly polarized beam of light. However, CD does not give detailed molecular structural data as obtained from X-ray crystallography or NMR, but it can be used as a complementary tool to UV spectroscopy to evaluate the overall base-stacking patterns.

CD spectra are particularly valuable in determining the following aspects:
- ➢ Whether the individual strands themselves are self-coiled
- ➢ Whether the individual strands change their conformation upon binding to complementary oligonucleotide strand
- ➢ How the conformations of hybrid PNA:DNA complexes are related with hybrid DNA:DNA complexes
- ➢ Nature of helices: α, π (proteins); A, B (DNA)

CD spectra provide a reliable estimation of the overall conformational state of biopolymers and structural changes induced by modification as compared with the reference compound. In case of nucleic acids, the sugar units of the backbone possess chirality and the bases attached to sugars are the chromophores. CD spectroscopy monitors the structural changes of nucleic acids in solution and helps to diagnose whether new or unusual structures are formed by particular polynucleotide sequences.

3.4 Objectives of the present work:

This section presents biophysical studies of the modified PNAs in terms of the following aspects:

- ➢ Thermal stability, binding selectivity, specificity and discrimination of modified PNA towards complementary DNA using temperature-dependent UV spectroscopy
- ➢ Characterization of the PNA:DNA duplex structures by CD spectroscopy
- ➢ Analysis and comparison of the results of various biophysical studies

The structures of the modified PNA units incorporated in the *aeg* PNA sequence have been shown in the Figure **3.2**

(a) γ gem aeg PNA   (b) γ 4-amino-4-pip aeg PNA   (c) β gem aeg PNA   (d) γ gem apg PNA
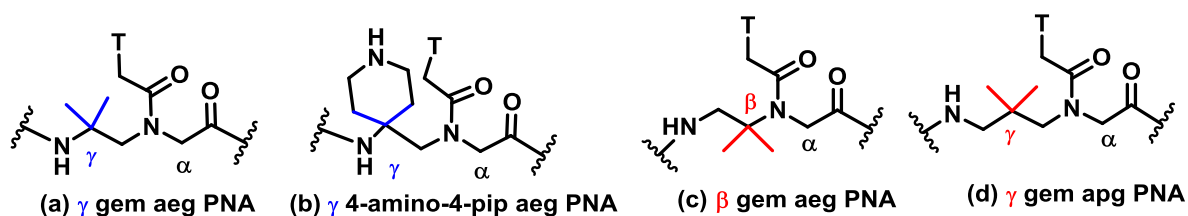
Figure 3.2: Modified PNA units

3.5 Results

The site-specific effects of introduction of modified PNA units at various positions in a 10 mer *aeg* PNA sequence on their duplex formation are studied by UV and CD

techniques. Thermal stabilities of PNA: DNA hybrids can be examined by temperature dependent UV absorption at 260 nm.

PNA:DNA can conform duplexes either in parallel or antiparallel orientation. When sequences of PNA are complimentary to DNA with N-terminus facing 5', it is assigned as parallel and with 3', it is assigned as antiparallel (Figure **3.3A**). Since it is easier to obtain synthetic DNA, both possibilities have been examined.

N ⟵——————— C   N ⟵——————— C
5' ⟵——————— 3'   3' ———————⟶ 5'
parallel mode   **antiparallel mode**

(A)

N   C
H-GTAGATCACT-LysNH$_2$ PNA
3'-CATCTAGTGA 5'   DNA 1
5 -CATCTAGTGA 3'   DNA 2
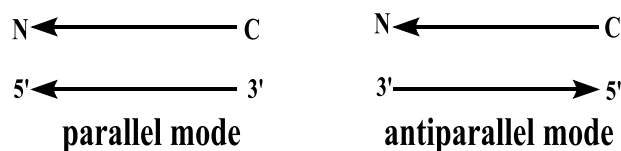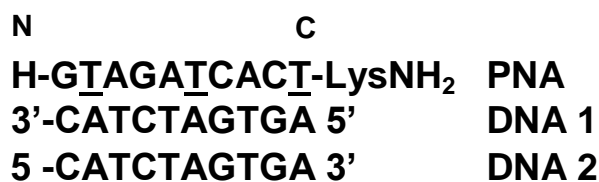
(B)

Figure 3.3: **(A)** Antiparallel and parallel binding of PNA; (B)

3.5.1 UV melting studies of PNA: DNA hybrids

The hybridization studies of modified PNA oligomers with their complementary antiparallel **DNA 1,** parallel **DNA 2** were carried out by temperature dependent changes in UV-absorbance. The thermal stabilities of duplexes of modified PNA(**a-d**) (Figure **3.2**) with complementary DNA**1** (antiparallel) and DNA**2** (parallel) were determined from UV-temperature plots. The T_m values were obtained from mid-points of the sigmoidal thermal stability curves of duplexes from various modified PNAs.

3.5.1a Thermal stability of *aeg* PNA and γ-gemdimethyl [γ-*gem*] *aeg* PNA: DNA duplexes:
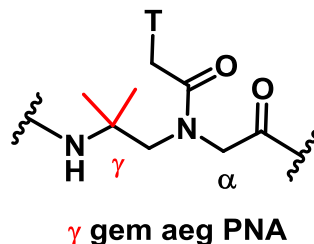
γ gem aeg PNA

In order to investigate the effect of modified PNA monomers on their corresponding duplexes, PNAs (**PNA 1** – **PNA 5**) were hybridized with complementary **DNA 1** (antiparallel) and **DNA 2** (parallel) as shown in (Figure **3.4**).

Figure 3.4: T_m curves of antiparallel and parallel γ-*gem* aeg PNA: DNA duplexes. Buffer: 10mM sodium phosphate, pH 7.2, NaCl 10mM

<u>**Antiparallel Duplexes:**</u>

The PNA: DNA duplexes derived from unmodified *aeg* **PNA 1** showed a T_m of 49.1 °C with **DNA 1** (Table **3.1**, entry **1**)**,** while the T_m of γ-*gem* modified PNA: DNA duplex showed variation as a function of the number and site of modification.

Single modification: The middle modified **PNA 2** destabilized the derived PNA: DNA**1** duplex by 1.8 °C (Table **3.1**, entry **2**), whereas **PNA 3** with N-terminus modification slightly destabilizes the PNA: DNA**1** duplex by 7.3 °C (Table **3.1**, entry **3**).

Double modification: **PNA 4** with two modified γ-*gem* aeg PNA monomers shows drastic destabilization of PNA: DNA**1** duplex by 8.7 ^{o}C (Table **3.1**, entry **4**).

Triple modification: Introduction of three modified units of γ-*gem* aeg PNA as in **PNA 5** remarkably decreased the thermal stability of PNA: DNA**1** duplex by 10.9 ^{o}C (Table **3.1**, entry **5**).

Table 3.1: UV-T_m of antiparallel PNA: DNA**1** duplexes with γ-*gem* aeg PNA units

Entry	PNA Code	PNA Sequence	DNA 1: 3' CATCTAGTGA5'	
			UV-T_m (^{o}C)	ΔT_m
1	aeg PNA **1**	H-GTAGATCACT-Lys NH$_2$	**49.1**	**-**
2	γ gem-t$_2$ PNA **2**	H-G**t**AGATCACT-LysNH$_2$	**47.3**	**-1.8**
3	γ gem-t$_6$ PNA **3**	H-GTAGA**t**CACT-LysNH$_2$	**41.8**	**-7.3**
4	γ gem-t$_{2,6}$ PNA **4**	H-G**t**AGA**t**CACT-LysNH$_2$	**40.4**	**-8.7**
5	gem-t$_{2,6,10}$ PNA **5**	H-G**t**AGA**t**CAC**t**-LysNH$_2$	**38.2**	**-10.9**

ΔT_m indicates the difference in T_m with control *aeg* PNA; ΔT_m values are accurate to ±0.5 ^{o}C

Parallel Duplexes:

The PNA: DNA duplexes derived from unmodified *aeg* **PNA 1** showed a T_m of 41.1 °C with **DNA 2** (parallel *p*) (Table **3.2**, entry **1**), while the T_m of γ-*gem* modified PNA: DNA duplex showed variation as a function of the number and site of modification.

Single modification: In case of Parallel DNA: PNA duplex, the middle modified **PNA 2** stabilized the PNA: DNA2 duplex by 1.9 ^{o}C (Table **3.2**, entry **2**) and the **PNA 3** with N-terminus modification stabilized the PNA: DNA2 duplex by 4.2^{o}C (Table **3.2**, entry **3**).

Double modification: In case of **PNA 4** with two modified γ-*gem* aeg PNA monomers, PNA: DNA**2** duplex was stabilized by 5 ^{o}C (Table **3.2**, entry **4**).

Triple modification: PNA **5**: DNA**2** duplex was stabilized by 7.2 ^{o}C due to incorporation of three γ-gem aeg PNA monomers. (Table **3.2**, entry **5**)

Table 3.2: UV-T_m of parallel PNA: DNA**2** duplexes with γ-*gem* aeg PNA units

Entry	PNA Code	PNA Sequence	DNA 2: 5' CATCTAGTGA3'	
			UV-T_m (^{o}C)	ΔT_m
1	aeg PNA **1**	H-GTAGATCACT-Lys NH$_2$	41.1	-
2	γ gem-t$_2$ PNA **2**	H-G**t**AGATCACT-LysNH$_2$	43	+1.9
3	γ gem-t$_6$ PNA **3**	H-GTAGA**t**CACT-LysNH$_2$	45.3	+4.2
4	γ gem-t$_{2,6}$ PNA **4**	H-G**t**AGA**t**CACT-LysNH$_2$	46.1	+5.0
5	gem-t$_{2,6,10}$ PNA **5**	H-G**t**AGA**t**CAC**t**-LysNH$_2$	48.3	+7.2

ΔT_m indicates the difference in T_m with control *aeg* PNA; ΔT_m values are accurate to ±0.5 ^{o}C.

3.5.1b Thermal stability of *aeg* PNA and γ-4-amino-4-piperidine (*γ-pip*) aeg PNA : DNA duplexes
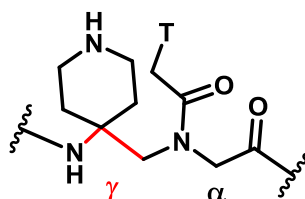
γ **4-amino-4-pip aeg PNA**

Thermal stability results of γ-4-amino-4-piperidine (*γ-pip*) modified aeg PNAs (**PNA 6-8**) with complementary antiparallel **DNA 1** and parallel **DNA 2** are shown in (Figure **3.5**).
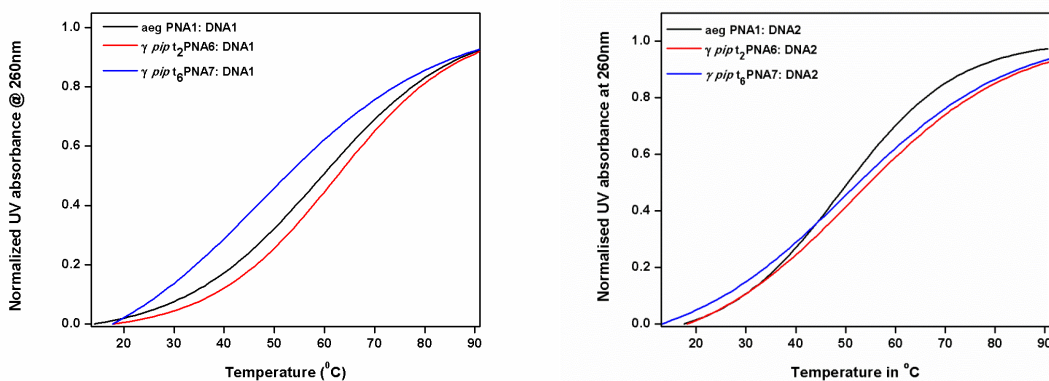
Figure 3.5: T_m curves of antiparallel and parallel γ *pip* aeg PNA: DNA duplexes. Buffer: 10mM sodium phosphate, pH 7.2, NaCl 10mM

Antiparallel Duplexes:

Single modification: Incorporation of *γ-pip* aeg PNA unit at N-terminus (PNA **6**) did not affect stability of the PNA**6**: DNA**1** duplex ($\Delta T_m = 0.5\,^{\circ}$C) (Table **3.3**, entry **2**), whereas incorporation of single unit of *γ-pip* aeg PNA into aeg PNA, at middle position destabilizes the PNA **7**: DNA **1** duplex by $9.3\,^{\circ}$C (Table **3.3**, entry **3**).

Table 3.3: UV-T$_m$ values of complementary PNA: antiparallel DNA1 duplexes with *γ-pip* aeg PNA units

Entry	PNA Code	PNA Sequence	DNA 1: 3' CATCTAGTGA5'	
			UV-T_m ($^{\circ}$C)	ΔT_m
1	aeg PNA **1**	H-GTAGATCACT-Lys NH$_2$	49.1	-
2	γ pip-t$_2$ PNA **6**	H-G**t**AGATCACT-LysNH$_2$	48.6	-0.5
3	γ pip-t$_6$ PNA **7**	H-GTAGA**t**CACT-LysNH$_2$	39.8	-9.3

ΔT_m indicates the difference in T_m with control *aeg* PNA, ΔT_m values are accurate to $\pm 0.5\,^{\circ}$C

Parallel Duplexes:

Single modification: The **PNA 6**:DNA**2** duplex was stabilized by $2.2\,^{\circ}$C (Table **3.4**, entry **2**) and **PNA 7**: DNA **2** duplex was stabilized by $1.5\,^{\circ}$C (Table **3.4**, entry **3**).

Table 3.4: UV-T$_m$ values of complementary PNA: Parallel DNA2 duplexes with *γ-pip* aeg PNA units

Entry	PNA Code	PNA Sequence	DNA 2: 5' CATCTAGTGA3'	
			UV-T_m ($^{\circ}$C)	ΔT_m
1	aeg PNA **1**	H-GTAGATCACT-Lys NH$_2$	41.1	-
2	γ pip-t$_2$ PNA **6**	H-G**t**AGATCACT-LysNH$_2$	43.3	+2.2
3	γ pip-t$_6$ PNA **7**	H-GTAGA**t**CACT-LysNH$_2$	42.6	+1.5

ΔT_m indicates the difference in T_m with control *aeg* PNA; ΔT_m values are accurate to $\pm 0.5\,^{\circ}$C

3.5.1c Thermal stability of *aeg* PNA and *β*-gemdimethyl [*β-gem*] *aeg* PNA: DNA duplexes.
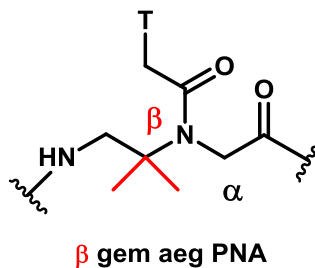
β gem aeg PNA

Gem dimethyl group was incorporated at β-position to investigate the modification site effect of introduced achiral rigidity on derived PNA: DNA hybrids (Figure **3.8**).
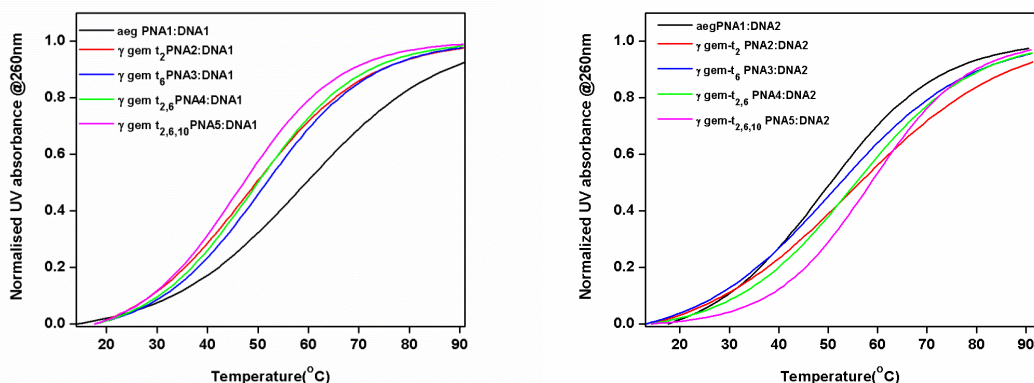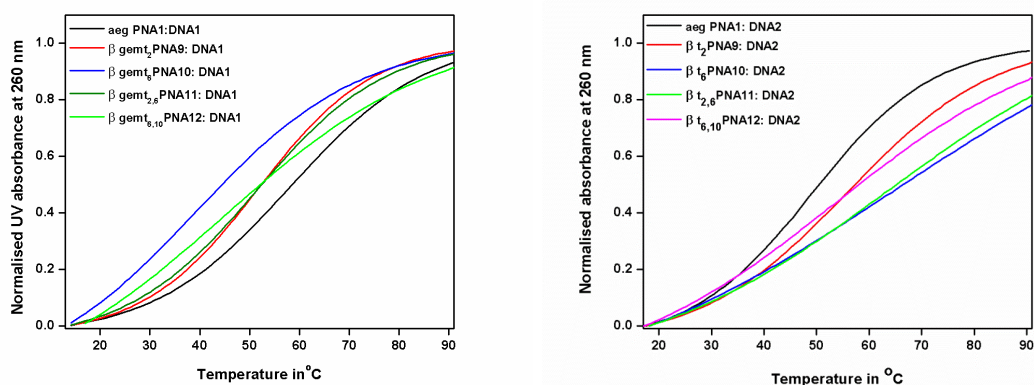

Figure 3.6: T_m curves of antiparallel and parallel *β gem* aeg PNA: DNA duplexes. Buffer: 10mM sodium phosphate, pH 7.2, NaCl 10mM

Antiparallel Duplexes:

Single modification: Single modification at N terminus and at middle position of aeg PNA destabilized the PNA: DNA**1** duples by 1.5 ^{o}C (Table **3.5**, entry **2**) and 12.5 ^{o}C (Table **3.5**, entry **3**) respectively.

Double modification: Incorporation of two modified units in PNA sequence destabilizes the derived PNA: DNA1 duplex. **PNA 11** with two modifications at middle and N-terminus destabilizes the PNA:DNA**1** duplex by 3.6 ^{o}C (Table **3.5,** entry **4**). **PNA 12** with two modifications at C-terminus and middle position destabilizes the duplex by 10.5^{o}C (Table **3.5**, entry **5**).

Table 3.5: UV-T_m values of complementary PNA: antiparallel DNA1 duplexes with β-gem aeg PNA units

Entry	PNA Code	PNA Sequence	DNA 1: 3' CATCTAGTGA5'	
			UV-T_m (^{o}C)	ΔT_m
1	aeg PNA **1**	H-GTAGATCACT-Lys NH$_2$	**49.1**	**-**
2	β gem t$_2$ PNA **9**	H-G**t**AGATCACT-LysNH$_2$	**47.6**	**-1.5**
3	β gem t$_6$ PNA **10**	H-GTAGA**t**CACT-LysNH$_2$	**36.6**	**-12.5**
4	β gem t$_{2,6}$PNA **11**	H-G**t**AGA**t**CACT-LysNH$_2$	**45.5**	**-3.6**
5	β gem t$_{6,10}$ PNA **12**	H-GTAGA**t**CAC**t**-LysNH$_2$	**38.6**	**-10.5**

ΔT_m indicates the difference in T_m with control *aeg* PNA; ΔT_m values are accurate to ±0.5 ^{o}C

Parallel Duplexes:

Single modification: Parallel DNA**2**: PNA duplex was stabilized by incorporation of single β gem aeg unit in PNA seq. Middle modified **PNA 9**: DNA**2** duplex was stabilized by 5.1^{o}C (Table **3.6,** entry **2**), while N-terminal modified **PNA 10**:DNA**2** duplex was stabilized by 11.7^{o}C (Table **3.6**, entry **3**)

Double modification: Incorporation of 2 β gem aeg units at N terminus and middle position stabilizes the **PNA 11**: DNA**2** duplex by 10.8^{o}C (Table **3.6**, entry **4**), whereas **PNA 12**:DNA**2** duplex was stabilized by 2.8 ^{o}C (Table **3.6**, entry **5**)

Table 3.6: UV-T_m values of complementary PNA: parallel DNA2 duplexes with β-gem aeg PNA units

Entry	PNA Code	PNA Sequence	DNA 2:5' CATCTAGTGA3'	
			UV-T_m (^{o}C)	ΔT_m
1	aeg PNA **1**	H-GTAGATCACT-Lys NH$_2$	**41.1**	**-**
2	β gem-t$_2$ PNA **9**	H-G**t**AGATCACT-LysNH$_2$	**46.2**	**+5.1**
3	β gem-t$_6$ PNA **10**	H-GTAGA**t**CACT-LysNH$_2$	**52.8**	**+11.7**
4	β gem-t$_{2,6}$ PNA **11**	H-G**t**AGA**t**CACT-LysNH$_2$	**51.9**	**+10.8**
5	β gem-t$_{6,10}$ PNA **12**	H-GTAGA**t**CAC**t**-LysNH$_2$	**43.9**	**+2.8**

ΔT_m indicates the difference in T_m with control *aeg* PNA; ΔT_m values are accurate to ±0.5 ^{o}C

3.5.1d Thermal stability of *aeg* PNA and γ-gemdimethyl (γ-gem apg) PNA: DNA duplexes.
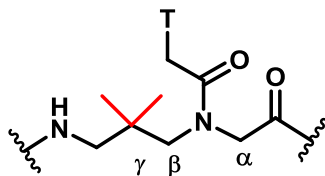
γ gem apg PNA

In order to investigate the effect of modified PNA monomers on their corresponding duplexes, PNAs (**PNA 13 – PNA 16**) were hybridized with complementary **DNA 1** (antiparallel) and **DNA 2** (parallel) as shown in (Figure **3.7**).

Figure 3.7: T_m curves of antiparallel and parallel γ-*gem* apg PNA: DNA duplexes. Buffer: 10mM sodium phosphate, pH 7.2, NaCl 10mM

Antiparallel Duplexes:

Single modification: Incorporation of gem dimethyl group at γ-position of aminoprolyl PNA backbone showed destabilization of duplex compared to unmodified aeg PNA. N-terminal (**PNA 13**) and middle modification (**PNA 14**) destabilized the PNA: DNA**1** duplex by 1.3 °C and 13.2 °C respectively (Table **3.7**, entry **2** & **3**).

Double modification: Incorporation of two units of γ-gem apg PNA destabilized the duplex considerably. Middle and N-terminal bimodified **PNA 15**:DNA**1** duplex was destabilsed by 19.7 °C (Table **3.7**, entry **4**).

Tri-modification: The duplex **PNA 16**:DNA**1** was destabilized enormously by 21.7 ^{o}C (Table **3.7**, entry **5**).

Table 3.7: UV-T_m values of complementary PNA: antiparallel DNA1 duplexes with γ-*gem* apg PNA units

Entry	PNA Code	PNA Sequence	DNA1: 3' CATCTAGTGA5'	
			UV-T_m (^{o}C)	ΔT_m
1	aeg PNA **1**	H-GTAGATCACT-Lys NH$_2$	49.1	-
2	γ gem-t$_2$ PNA **13**	H-G**t**AGATCACT-LysNH$_2$	47.8	-1.3
3	γ gem-t$_6$ PNA **14**	H-GTAGA**t**CACT-LysNH$_2$	35.9	-13.2
4	γ gem-t$_{2,6}$ PNA **15**	H-G**t**AGA**t**CACT-LysNH$_2$	29.4	-19.7
5	γ gem-t$_{2,6,10}$ PNA **16**	H-G**t**AGA**t**CAC**t**-LysNH$_2$	27.4	-21.7

ΔT_m indicates the difference in T_m with control *aeg* PNA; ΔT_m values are accurate to ±0.5 ^{o}C

Parallel Duplexes:

Single modification: Duplexes derived from parallel DNA2 were stabilized to some extent (Figure **3.10**). N-terminus modified **PNA 13**:DNA**2** duplex was stabilized by 11.3 ^{o}C and middle modified **PNA 14**:DNA**2** duplex was stabilized by 4.7 ^{o}C (Table **3.8**, entry **2** & **3**).

Double modification: Incorporation of two units of γ-gem apg PNA destabilized the duplex considerably. Middle and N-terminal bimodified **PNA 15**:DNA**2** duplex was destabilsed by 2.3 ^{o}C (Table **3.8**, entry **4**).

Tri-modification: The duplex **PNA 16**:DNA**2** destabilsed by 10.6 ^{o}C (Table **3.8**, entry **5**).

Table 3.8: UV-T_m values of complementary PNA:parallel DNA2 duplexes with γ-*gem* apg PNA units

Entry	PNA Code	PNA Sequence	DNA2: 5' CATCTAGTGA3'	
			UV-T_m (^{o}C)	ΔT_m
1	aeg PNA **1**	H-GTAGATCACT-Lys NH$_2$	41.1	-
2	γ gem-t$_2$ PNA **13**	H-G**t**AGATCACT-LysNH$_2$	52.4	+11.3
3	γ gem-t$_6$ PNA **14**	H-GTAGA**t**CACT-LysNH$_2$	45.8	+4.7
4	γ gem-t$_{2,6}$ PNA **15**	H-G**t**AGA**t**CACT-LysNH$_2$	38.8	-2.3
5	γ gem-t$_{2,6,10}$ PNA **16**	H-G**t**AGA**t**CAC**t**-LysNH$_2$	30.5	-10.6

ΔT_m indicates the difference in T_m with control *aeg* PNA; ΔT_m values are accurate to $\pm 0.5\,^o$C

3.5.2 UV-Tm studies of modified PNAs with complementary RNA

This section describes the hybridization properties of the modified PNAs with complementary parallel RNA**1** (5'GAUGUAGUGA3') and antiparallel RNA**2** (5'AGUGAUGUAG3')

3.5.2a UV-*Tm* studies with aeg PNA: RNA and γ-*gem aeg* PNA: RNA duplexes:

The thermal stability of the γ-*gem* substituted aeg PNAs (**PNA 2** – **PNA 5**) with complementary antiparallel RNA**1** and parallel RNA**2** was evaluated from temperature dependent UV absorbance (Figure **3.8**).
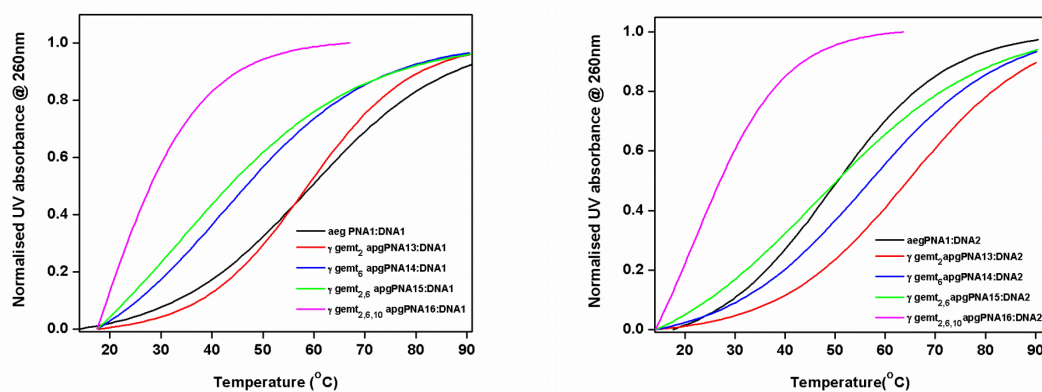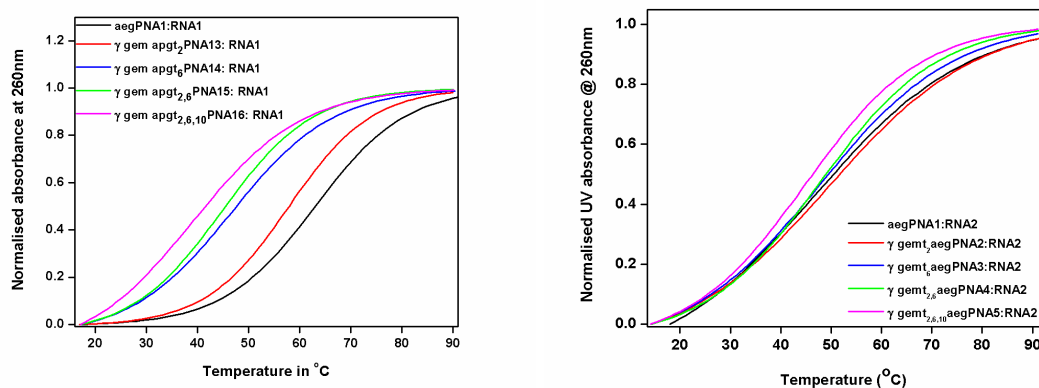

Figure 3.8: T_m curves of antiparallel and parallel γ-*gem* aeg PNA: RNA duplexes. Buffer: 10mM sodium phosphate, pH 7.2, NaCl 10mM)

Antiparallel Duplexes:

Single modification: The duplex of **PNA 2**:RNA**1** (with single modification at N-terminus) has almost T_m same as that of aeg **PNA 1**:RNA**1** duplex ($\Delta T_{m=}$ 0.2 ^{o}C) (Table **3.9**, entry **2**), While **PNA 3**: RNA**1** duplex with middle modification was destabilized by 3.6 ^{o}C (Table **3.9**, entry **3**).

Double modification: **PNA 4**:RNA**1** duplex destabilized by 5.7 ^{o}C (Table **3.9**, entry **4**)

Triple modification: **PNA 5**:RNA**1** duplex was destabilized by 8°C (Table **3.9**, entry **5**).

Table 3.9: UV-T_m values of complementary PNA: antiparallel RNA**1** duplexes with γ-*gem* aeg PNA units

Entry	PNA Code	PNA Sequence	RNA1: 3' CAUCUAGUGA5'	
			UV-T_m (^{o}C)	ΔT_m
1	aeg PNA **1**	H-GTAGATCACT-Lys NH$_2$	**51.3**	**-**
2	γ gem-t$_2$ PNA **2**	H-G**t**AGATCACT-LysNH$_2$	**51.5**	**+0.2**
3	γ gem-t$_6$ PNA **3**	H-GTAGA**t**CACT-LysNH$_2$	**47.7**	**-3.6**
4	γ gem-t$_{2,6}$ PNA **4**	H-G**t**AGA**t**CACT-LysNH$_2$	**45.6**	**-5.7**
5	γ gem-t$_{2,6,10}$ PNA **5**	H-G**t**AGA**t**CAC**t**-LysNH$_2$	**43.4**	**-8**

ΔT_m indicates the difference in T_m with control *aeg* PNA; ΔT_m values are accurate to ±0.5 ^{o}C

Parallel Duplexes:

Single modification: The duplex of **PNA 2**:RNA**2** and **PNA 3**:RNA**2** were slightly stabilized by 2°C and 1.1 ^{o}C respectively (Table **3.10**, entry **2** & **3**).

Double modification: **T**he duplex with complementary parallel RNA has *Tm* nearly same as the aeg **PNA 4**:RNA**2** duplex (Table **3.10**, entry **4**).

Triple modification: The duplex **PNA 5**:RNA**2** showed *Tm* slightly more that aeg PNA:RNA**2** duplex (Table **3.10**, entry **5**).

Table 3.10: UV-T_m values of complementary PNA: parallel RNA **2** duplexes with γ-*gem* aeg PNA units

Entry	PNA Code	PNA Sequence	RNA2: 5' CATCTAGTGA3'	
			UV-T_m (^{o}C)	ΔT_m
1	aeg PNA **1**	H-GTAGATCACT-Lys NH$_2$	**39.4**	
2	γ gem-t$_2$ PNA **2**	H-G**t**AGATCACT-LysNH$_2$	**41.4**	**+2**
3	γ gem-t$_6$ PNA **3**	H-GTAGA**t**CACT-LysNH$_2$	**40.5**	**+1.1**
4	γ gem-t$_{2,6}$ PNA **4**	H-G**t**AGA**t**CACT-LysNH$_2$	**40.0**	**+0.6**
5	γ gem-t$_{2,6,10}$ PNA **5**	H-G**t**AGA**t**CAC**t**-LysNH$_2$	**38.2**	**+1.2**

ΔT_m indicates the difference in T_m with control *aeg* PNA; ΔT_m values are accurate to ±0.5 ^{o}C

3.5.2b UV-*Tm* studies with *aeg* PNA, *γ pip* PNA with RNA duplexes:

The thermal stability of the *γ pip* substituted aeg PNAs (**PNA 6** & **7**) with complementary RNA**1** (antiparallel) and RNA**2** (parallel) was evaluated from temperature dependent UV absorbance (Figure **3.9**).

Figure 3.9: T_m curves of antiparallel and parallel *γ pip* PNA: RNA 2 duplexes
Buffer: 10mM sodium phosphate, pH 7.2, NaCl 10mM)

Antiparallel Duplexes:

Single modification: Single modified PNA, both at N-terminus of the aeg PNA sequence, destabilizes the derived PNA:RNA**1** duplex by 0.2 ^{o}C, whereas middle modified **PNA 7**:RNA**1** duplex was destabilized by 8.2 ^{o}C (Table **3.11**, entry **2** & **3** respectively).

Table 3.11: UV-T_m values of complementary PNA: antiparallel RNA1 duplexes with *γ pip* PNA units

Entry	PNA Code	PNA Sequence	RNA1: 5' CATCTAGTGA3'	
			UV-T_m (^{o}C)	ΔT_m
1	aeg PNA **1**	H-GTAGATCACT-Lys NH$_2$	**51.3**	
2	γ pip-t$_2$ PNA **6**	H-G**t**AGATCACT-LysNH$_2$	**51.5**	**+0.2**
3	γ pip-t$_6$ PNA **7**	H-GTAGA**t**CACT-LysNH$_2$	**43.1**	**-8.2**

ΔT_m indicates the difference in T_m with control *aeg* PNA; ΔT_m values are accurate to ±0.5 ^{o}C

Parallel Duplexes:

Single modification: Single modified PNA, both at N-terminus of the aeg PNA sequence, destabilizes the derived **PNA 7**:RNA**2** by 5.7 ^{o}C & 4.8 ^{o}C resp (Table **3.12**, entry **2** & **3**).

Table 3.12: UV-T_m values of complementary PNA: antiparallel RNA2 duplexes with *γ pip* PNA units

Entry	PNA Code	PNA Sequence	RNA2: 5' CATCTAGTGA3'	
			UV-T_m (^{o}C)	ΔT_m
1	aeg PNA **1**	H-GTAGATCACT-Lys NH$_2$	**39.4**	
2	γ gem-t$_2$ PNA **6**	H-G**t**AGATCACT-LysNH$_2$	**33.7**	**-5.7**
3	γ gem-t$_6$ PNA **7**	H-GTAGA**t**CACT-LysNH$_2$	**34.6**	**-4.8**

ΔT_m indicates the difference in T_m with control *aeg* PNA; ΔT_m values are accurate to ±0.5 ^{o}C

3.5.2c UV-Tm studies of *aeg* PNA and β-*gem aeg* PNA: RNA duplexes

The thermal stability of the β-*gem aeg* PNAs (**PNA 9 – 12)** with RNA**1** (antiparallel) and RNA**2** (parallel) was evaluated from temperature dependent UV absorbance (Figure **3.10**).
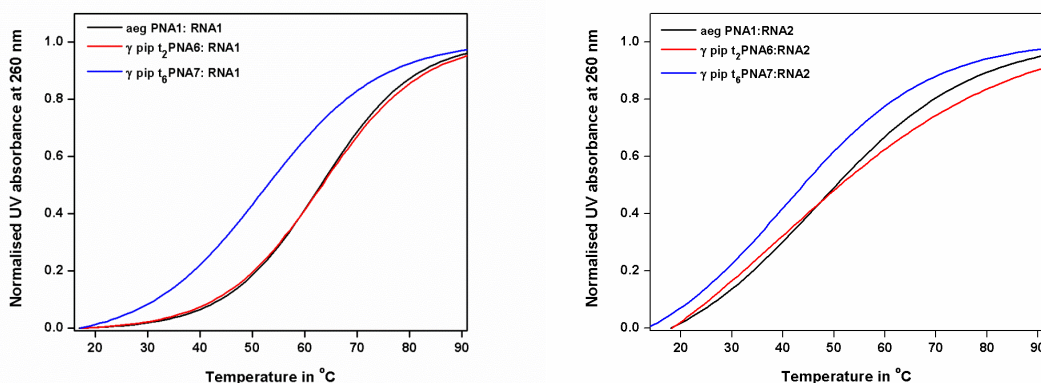
Figure 3.10: T_m curves of antiparallel and parallel β-*gem aeg* PNA:RNA duplexes. Buffer: 10mM sodium phosphate, pH 7.2, NaCl 10mM)

Antiparallel Duplexes:

*Single Modification***:** N-terminal modified **PNA 9**:RNA**1** duplex was destabilized by 2.2 °C, whereas middle modified **PNA 10**:RNA**1** duplex was destabilized by 17.8 °C (Table **3.13**, entry **2** & **3** respectively).

Double modification: **PNA 11** with two modifications at middle and N-terminus destabilizes the PNA:RNA**1** duplex by 18.6 °C (Table **3.13,** entry **4**). **PNA 12** with two modifications at C-terminus and middle position destabilizes the duplex by 11.2 °C (Table **3.13**, entry **5**).

Table 3.13: UV-T_m values of complementary PNA: antiparallel RNA1 duplexes with β-*gem aeg* PNA units

Entry	PNA Code	PNA Sequence	DNA2: 5' CATCTAGTGA3'	
			UV-T_m (°C)	ΔT_m
1	aeg PNA **1**	H-GTAGATCACT-Lys NH$_2$	**51.3**	**-**
2	β gem-t$_2$ PNA **9**	H-G**t**AGATCACT-LysNH$_2$	**49.1**	**-2.2**
3	β gem-t$_6$ PNA **10**	H-GTAGA**t**CACT-LysNH$_2$	**33.5**	**-17.8**
4	β gem-t$_{2,6}$ PNA **11**	H-G**t**AGA**t**CACT-LysNH$_2$	**32.7**	**-18.6**
5	β gem-t$_{6,10}$ PNA **12**	H-GTAGA**t**CAC**t**-LysNH$_2$	**40.1**	**-11.2**

ΔT_m indicates the difference in T_m with control *aeg* PNA; ΔT_m values are accurate to ±0.5 °C

Parallel Duplexes:

*Single Modification***:** Duplexes derived with complementary parallel RNA**2**, were also destabilized by 0.8 ^{o}C and 9.7 ^{o}C resp (Table **3.14**, entry **2** & **3**).

Double modification: The duplexes derived from PNA and complementary parallel RNA**2**, get stabilized by incorporation of β gem aeg units in PNA sequences. Incorporation of 2 β gem aeg units at N terminus and middle position stabilizes the **PNA 11**: RNA**2** duplex by 1.1 ^{o}C (Table **3.14**, entry **4**), whereas **PNA 12**:RNA**2** duplex was destabilized by 5.5 ^{o}C (Table **3.14**, entry **5**).

Table 3.14: UV-T_m values of complementary PNA: antiparallel RNA2 duplexes with β-*gem aeg* PNA units

Entry	PNA Code	PNA Sequence	RNA2: 5' CATCTAGTGA3'	
			UV-T_m (^{o}C)	ΔT_m
1	aeg PNA **1**	H-GTAGATCACT-Lys NH$_2$	**39.4**	**-**
2	β gem-t$_2$ PNA **9**	H-G**t**AGATCACT-LysNH$_2$	**38.6**	**-0.8**
3	β gem-t$_6$ PNA **10**	H-GTAGA**t**CACT-LysNH$_2$	**29.7**	**-9.7**
4	β gem-t$_{2,6}$ PNA **11**	H-G**t**AGA**t**CACT-LysNH$_2$	**40.5**	**+1.1**
5	β gem-t$_{6,10}$ PNA **12**	H-GTAGA**t**CAC**t**-LysNH$_2$	**33.5**	**-5.5**

ΔT_m indicates the difference in T_m with control *aeg* PNA; ΔT_m values are accurate to ±0.5 ^{o}C

3.5.2d UV-Tm studies of *aeg* PNA and γ-gem apg PNA: RNA duplexes:

The thermal stability of the γ-gem apg PNAs (**PNA 13 – 16**) with RNA**1** (antiparallel) and RNA**2** (parallel) was evaluated from temperature dependent UV absorbance (Figure **3.11**).
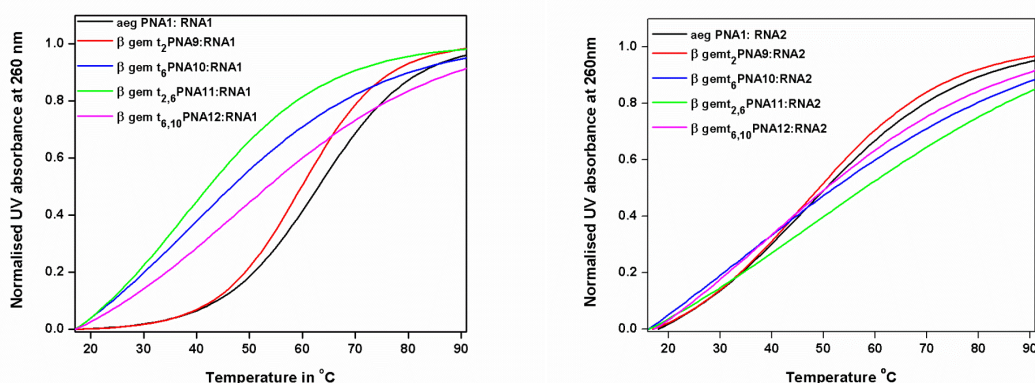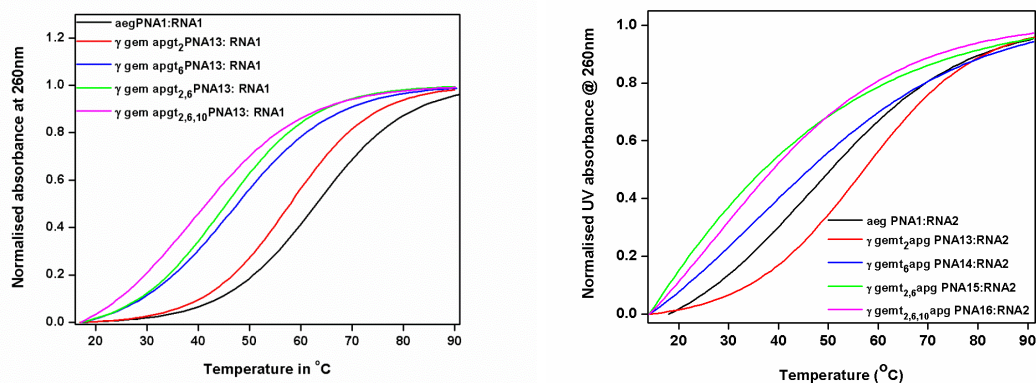
Figure 3.11: T_m curves of antiparallel and parallel γ-gem apg PNA:RNA duplexes. Buffer: 10mM sodium phosphate, pH 7.2, NaCl 10mM)

<u>Antiparallel Duplexes:</u>

Single modification: N-terminal (**PNA 13**) and middle modification (**PNA 14**) destabilized the PNA: RNA**1** duplex by 4.1 °C and 3 °C respectively (Table **3.15**, entry **2** & **3**).

Double modification: Middle and N-terminal bimodified **PNA 15**:RNA**1** duplex was destabilized by 13.6 °C (Table **3.15**, entry **4**).

Tri-modification: The duplex **PNA 16**:RNA**1** destabilized by 18 °C (Table **3.15**, entry **5**).

Table 3.15: UV-T_m values of complementary PNA: antiparallel RNA1 duplexes with γ-gem apg PNA units

Entry	PNA Code	PNA Sequence	RNA1: 5'CATCTAGTGA3'	
			UV-T_m (°C)	ΔT_m
1	aeg PNA **1**	H-GTAGATCACT-Lys NH$_2$	51.3	-
2	γ gem-t$_2$ PNA **13**	H-G**t**AGATCACT-LysNH$_2$	47.2	-4.1
3	γ gem-t$_6$ PNA **14**	H-GTAGA**t**CACT-LysNH$_2$	48.3	-3.0
4	γ gem-t$_{2,6}$ PNA **15**	H-G**t**AGA**t**CACT-LysNH$_2$	37.7	-13.6
5	γ gem-t$_{2,6,10}$ PNA **16**	H-G**t**AGA**t**CAC**t**-LysNH$_2$	33.3	-18

ΔT_m indicates the difference in T_m with control *aeg* PNA; ΔT_m values are accurate to ±0.5 °C

Parallel Duplexes:

Single modification: Duplexes derived from parallel RNA2 were stabilized to some extent N-terminus modified **PNA 13**:RNA**2** duplex was stabilized by 7.5 ^{o}C and middle modified **PNA 14**:RNA**2** duplex was destabilized by 9.1 ^{o}C (Table **3.16**, entry **2** & **3**).

Double modification: **A** well-defined sigmoidal curve was not observed for **PNA 15**:RNA**2** duplex (Table **3.16**, entry **4**).

Tri-modification: **PNA 16**:RNA**2** destabilized by 15.3 ^{o}C (Table **3.16**, entry **5**).

Table 3.16: UV-T_m values of complementary PNA: antiparallel RNA2 duplexes with γ-gem apg PNA units

Entry	PNA Code	PNA Sequence	RNA2:5' CATCTAGTGA3'	
			UV-T_m (^{o}C)	ΔT_m
1	aeg PNA **1**	H-GTAGATCACT-Lys NH$_2$	39.4	-
2	γ gem-t$_2$ PNA **13**	H-G**t**AGATCACT-LysNH$_2$	46.9	+7.5
3	γ gem-t$_6$ PNA **14**	H-GTAGA**t**CACT-LysNH$_2$	30.3	-9.1
4	γ gem-t$_{2,6}$ PNA **15**	H-G**t**AGA**t**CACT-LysNH$_2$	nd	nd
5	γ gem-t$_{2,6,10}$ PNA **16**	H-G**t**AGA**t**CAC**t**-LysNH$_2$	24.1	-15.3

ΔT_m indicates the difference in T_m with control *aeg* PNA; ΔT_m values are accurate to ±0.5 ^{o}C

3.5.3 CD spectroscopic studies of *ss* PNAs and PNA: DNA duplexes:

The effect of gem dialkyl substitution on the conformation of PNA: DNA duplexes were studied by CD spectroscopy. The single stranded PNA being achiral does not show any significant CD signatures. However, being a polyamide, it can form either left or right handed coil structures with equal facility. Even though *ss*PNA shows low profile CD signals, PNA: DNA complexes exhibit characteristic CD signatures because of the helicity induced by the chiral DNA in PNA: DNA complex.

The CD profile of PNA- antiparallel DNA **1** hybrid duplex is very similar to that of **PNA** – DNA **2** hybrid, with a positive band at 266 nm & 220 nm and a low-intensity negative

band at 242 nm & 210 nm. However, in parallel duplex, positive band at 266 nm and 220 nm and negative band at 240 nm has been observed. Except for variations in intensity, no significant changes seen for the band positions.

The CD spectra for mixed purine pyrimidine single stranded aeg **PNA 1**, PNA oligomers containing γ gem aeg **PNA 2 – PNA 5** and their complexes formed with complementary antiparallel DNA **1** and parallel DNA **2** are shown in Figure **3.12** & **3.13**.
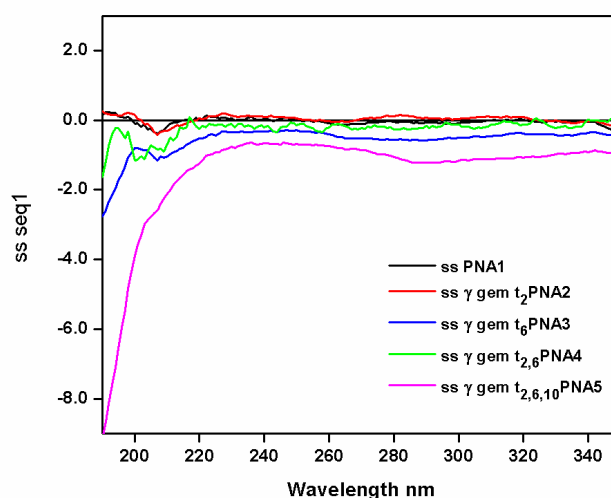

Figure 3.12: CD spectra of *ss aeg* PNA **1**, *ss γ-gem aeg* PNA **2-5**

Figure 3.13: (**A**) Duplexes of PNA **1-5** with complementary antiparallel DNA **1**

(**B**) Duplexes of PNA **1-5** with complementary parallel DNA **2**

The CD spectra for single stranded *aeg* **PNA 1**, γ-*pip* PNA oligomers **PNA 6-7** and their complexes formed with complementary antiparallel DNA**1** and parallel DNA**2** are shown in Figure **3.14** & **3.15.**

Figure 3.14: CD spectra of *ss aeg* PNA **1**, *ss* γ-*pip aeg* PNA **6-7**

Figure 3.15: (A) Duplexes of PNA **6-7** with complementary antiparallel DNA **1**

(B) Duplexes of PNA **6-7** with complementary parallel DNA **2**

The CD spectra for single stranded *aeg* **PNA 1**, β PNA oligomers **PNA 9-12** and their complexes formed with complementary antiparallel DNA**1** and parallel DNA**2** are shown in Figure **3.16 & 3.17**.

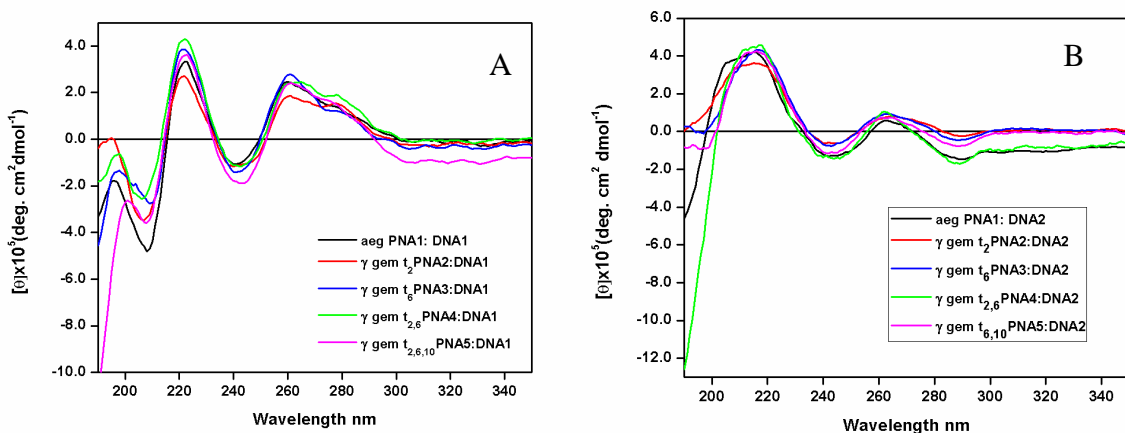**Figure 3.16:** CD spectra of *ss aeg* PNA **1,** *ss* β-gem *aeg* PNA **9-12**

Figure 3.17: (A) Duplexes of PNA **9-12** with complementary antiparallel DNA **1**
(B) Duplexes of PNA **9-12** with complementary parallel DNA **2**

The CD spectra for single stranded aeg PNA1, γ gem apg PNA oligomers PNA13-16 and their complexes formed with complementary antiparallel DNA1 and parallel DNA2 are shown in Figure **3.18 & 3.19**.

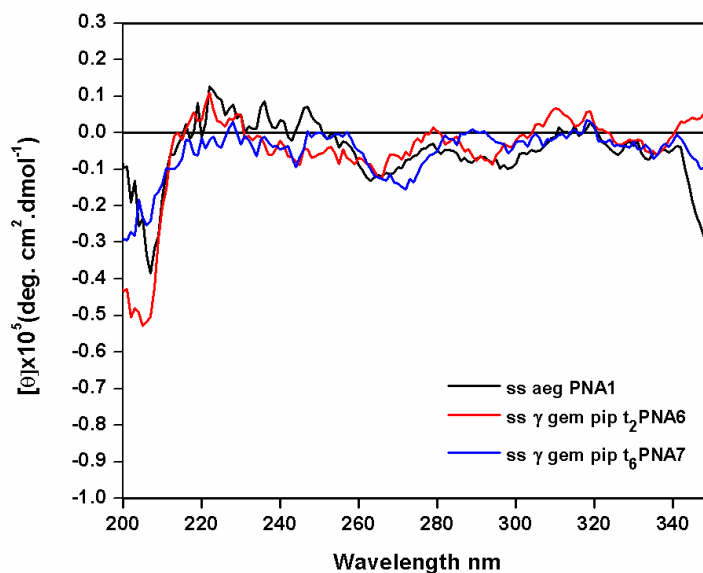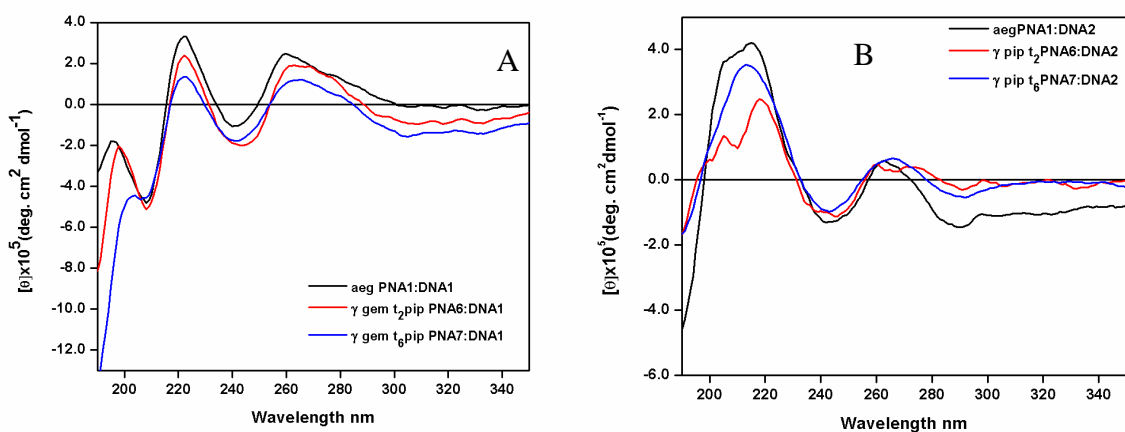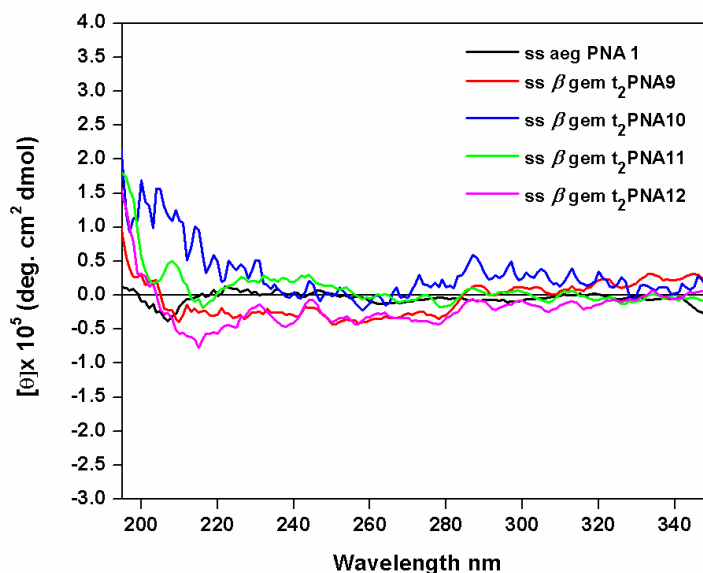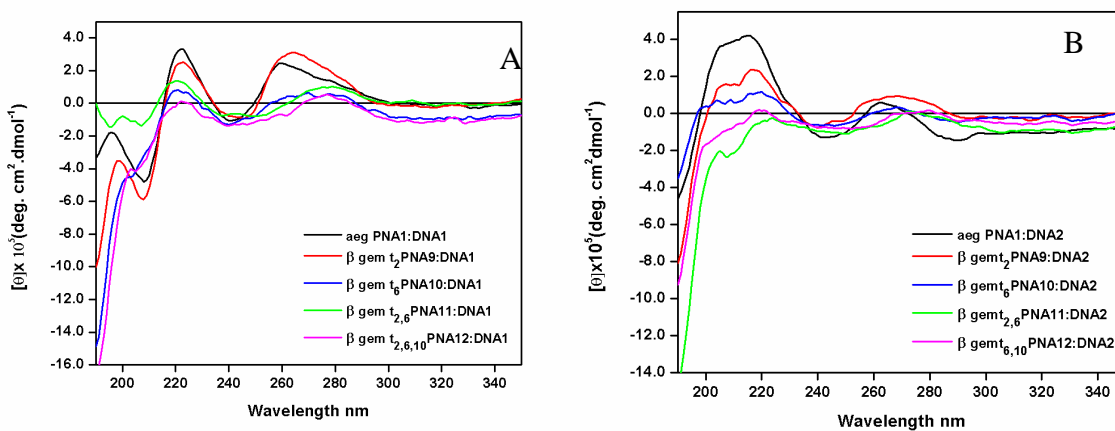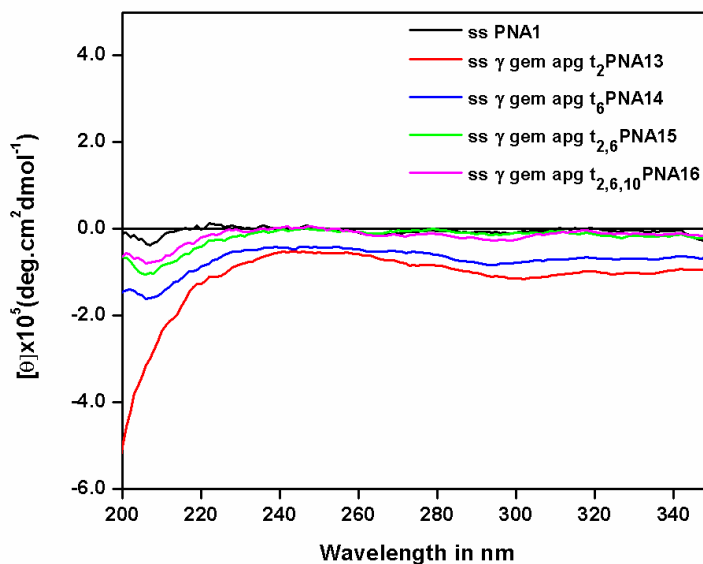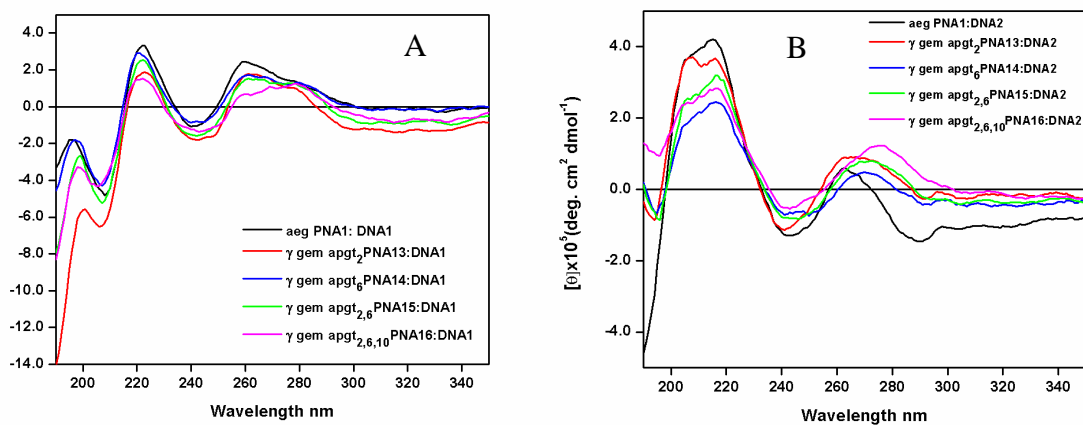**Figure 3.18:** CD spectra of *ss aeg* PNA **1,** *ss* γ-gem *apg* PNA **13-16**

Figure 3.19: (A) Duplexes of PNA **13-16** with complementary antiparallel DNA **1**

(B) Duplexes of PNA **13-16** with complementary parallel DNA **2**

From the overall results it is seen that single stranded aeg **PNA1** as well as backbone modified *ss*PNAs do not show significant CD spectral signature. However, the formation of corresponding PNA: antiparallel DNA duplexes result in a positive band at 261 nm and a low-intensity negative band at 242 nm. For PNA: parallel DNA duplex showed positive band at 264nm and a negative band at 244nm. The various modifications did not have much effect on the conformations derived PNA: DNA duplexes.

3.6 Comparative study of UV-T_m values of modified PNAs:

The temperature dependent UV-absorbance data shows variation in the stabilities of modified PNA:DNA duplexes depending on the type of modification incorporated (amine, guanidine and azide), position of modification (Figure **3.20**) and the number of modified units incorporated into *aeg* PNA sequence.

N   M   C

N-terminus   C-terminus

H-GTAGATCACT-LysNH$_2$ PNA
3'- CATCTAGTGA 5'   DNA 1
5'- CATCTAGTGA 3'   DNA 2
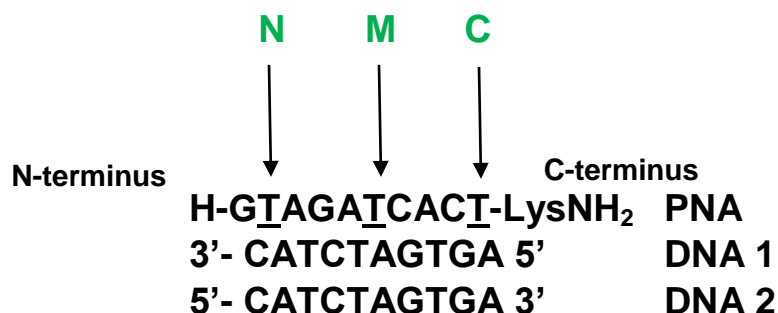
Figure 3.20: Schematic representation showing the position of modification incorporated

3.6.1 Comparative studies of γ-*gem* aeg PNA and *β*-gem aeg PNA duplexes with DNA

For both γ-*gem* aeg PNA and *β*-gem aeg PNA, the UV-*Tm* results indicate that for all modified PNAs, the stability of PNA and complementary antiparallel DNA duplex was decreased as compared to aeg PNA: DNA duplex.

The stability of modified parallel PNAs: DNA duplex was increased in both γ-*gem* aeg PNA and *β*-gem aeg PNA. The order of induced stability for γ-*gem* aeg PNA is triple

modification > double > middle > N-terminal modification. The *β*-gem aeg PNA follows middle modification > double (N, M) > N-terminal > double(C, M) (Figure **3.21** & **3.22**).

Figure 3.21: Comparative Δ*Tm* studies for PNA: antiparallel DNA duplex formed by γ-gem *aeg* PNA and β-gem *aeg* PNA modifications on *aeg* PNA backbone at various positions on mixed decamer sequence with complementary DNA (Δ*Tm* indicates the difference in *Tm* with control *aeg* PNA).

Figure 3.22: Comparative Δ*Tm* studies for PNA: parallel DNA duplex formed by γ-gem *aeg* PNA and β-gem *aeg* PNA modifications on *aeg* PNA backbone at various positions on mixed decamer sequence with complementary DNA (Δ*Tm* indicates the difference in *Tm* with control *aeg* PNA)

Possible explanation for observed trend could be the restricted rotation around **Cγ** and **Cβ** bond in PNA backbone due to incorporation of gem dimethyl group.

3.6.2 Comparative study of γ-*gem* aeg PNA and γ-*pip* aeg PNA duplexes with DNA

As discussed earlier, as the number of modifications of γ-gem aeg unit increases in PNA, the antiparallel stability of antiparallel duplex PNA:DNA decreases, whereas the stability of parallel duplexes PNA: DNA increases with the number of γ-gem aeg units in PNA.

Incorporation of γ-*pip* aeg PNA at N-terminus reduces T_m of antiparallel PNA: DNA duplex by just 0.5 °C while that of corresponding duplex with middle modified PNA is noticeably destabilized by 9.3 °C. In case of parallel duplexes γ-*pip* of PNA: DNA, both N-terminal and middle modification increases the stability of duplex by 2.2 °C and 1.5 °C (Figure **3.23** & **3.24**) respectively. Thus by fixing the position of modification and changing the functionality drastically changes the thermal stability of derived duplex.
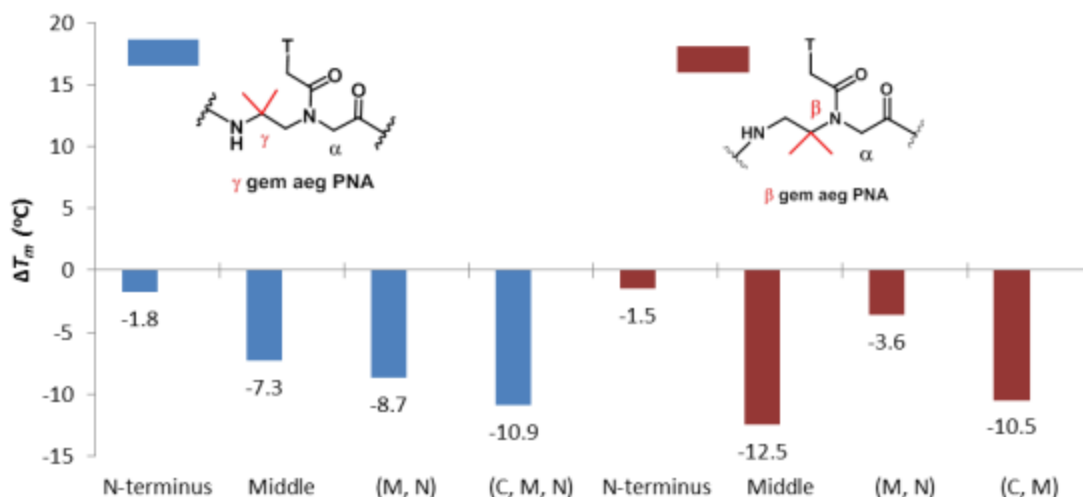

Figure 3.23: Comparative Δ*Tm* studies for PNA: antiparallel DNA duplex formed by γ-gem *aeg* PNA and γ-*pip* aeg PNA modifications on *aeg* PNA backbone at various positions on mixed decamer sequence with complementary DNA (Δ*Tm* indicates the difference in *Tm* with control *aeg* PNA)
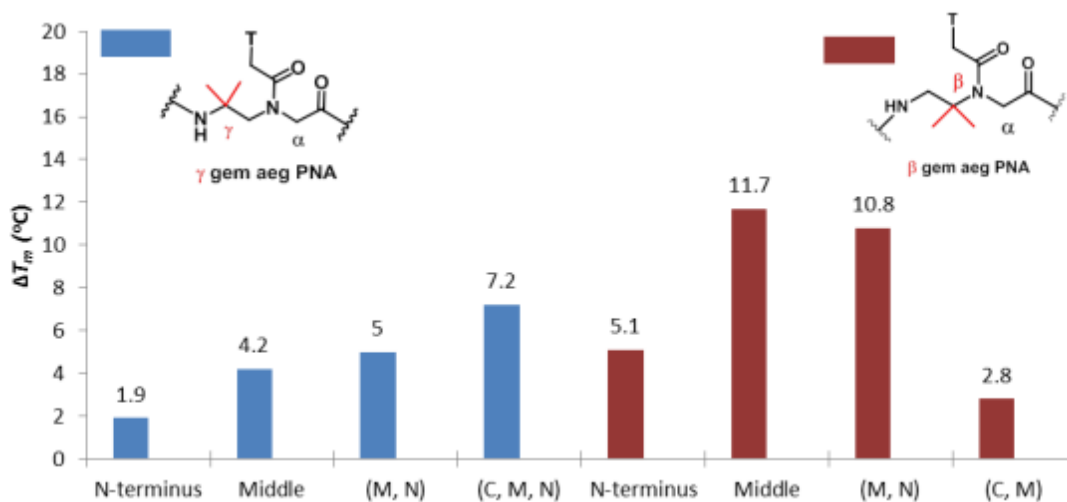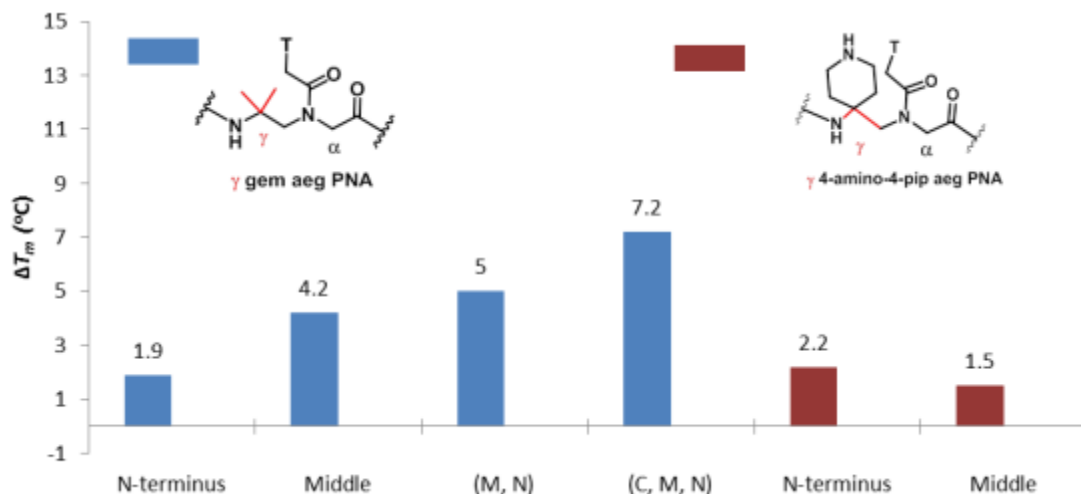
Figure 3.24: Comparative Δ*Tm* studies for PNA: parallel DNA duplex formed by γ-gem *aeg* PNA and γ-*pip* aeg PNA modifications on *aeg* PNA backbone at various positions on mixed decamer sequence with complementary DNA (Δ*Tm* indicates the difference in *Tm* with control *aeg* PNA)

3.6.3 Comparative study of γ-*gem* aeg PNA and γ- *gem* apg PNA duplexes with DNA

Though extended aeg PNA backbone is known to destabilize the derived duplex, effect of introduced rigidity in extended aeg backbone was studied by incorporating rigidity in the form of gem dimethyl group.

Like γ-gem aeg PNAs, γ gem apg PNAs also showed dependence of thermal stability on number of modifications and position of modifications. All γ gem apg PNAs destabilized the PNA: DNA duplex in both antiparallel and parallel orientation except middle modified **PNA 14**, which increases the stability of PNA: parallel DNA duplex considerably by 11.3°C (Figure **3.25** & **3.26**)
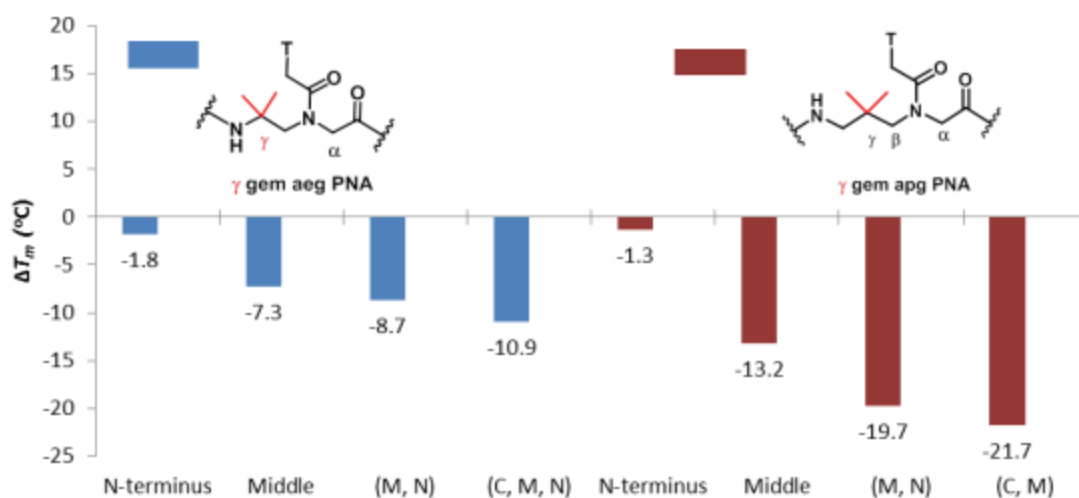
Figure 3.25: Comparative Δ*Tm* studies for PNA: antiparallel DNA duplex formed by γ-gem *aeg* PNA and γ-gem apg PNA modifications on *aeg* PNA backbone at various positions on mixed decamer sequence with complementary DNA (Δ*Tm* indicates the difference in *Tm* with control *aeg* PNA)
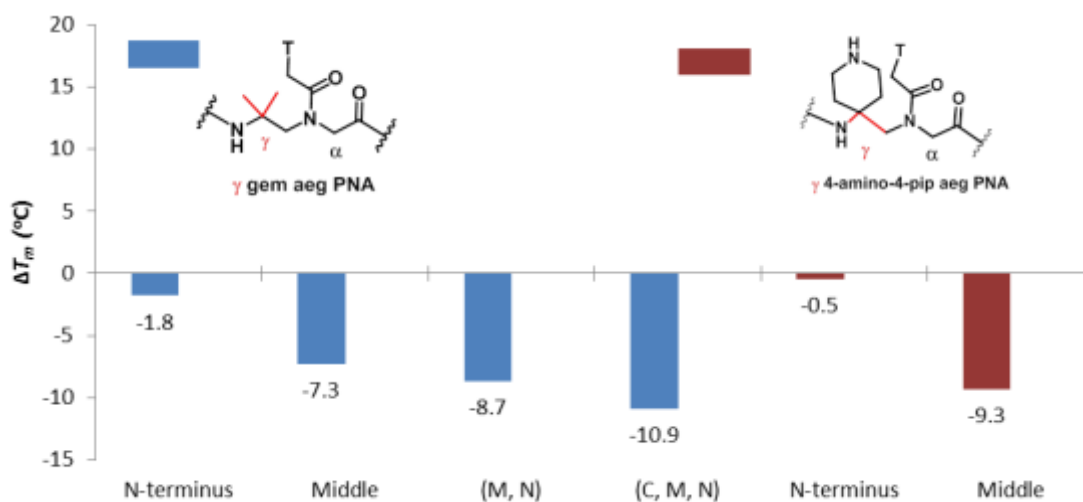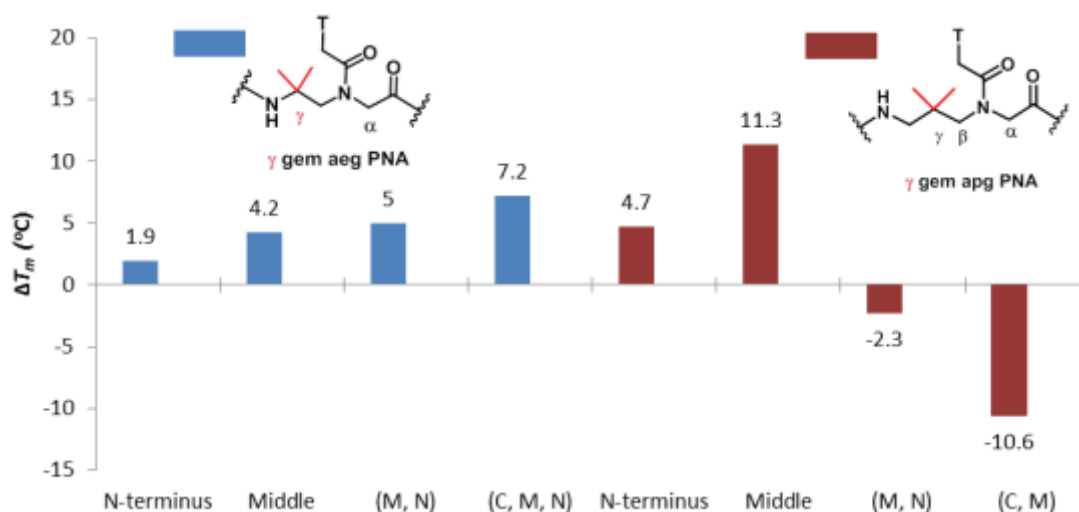

Figure 3.26: Comparative Δ*Tm* studies for PNA: parallel DNA duplex formed by γ-gem *aeg* PNA and γ-gem apg PNA modifications on *aeg* PNA backbone at various positions on mixed decamer sequence with complementary DNA (Δ*Tm* indicates the difference in *Tm* with control *aeg* PNA)

3.6.4 Comparative studies of modified PNA duplex with RNA:

All modified PNAs destabilized the the PNA: RNA duplex in both parallel and antiparallel orientation.

γ -gem aeg PNA with N-terminal modification and γ-*pip* aeg PNA with N-terminal modification, both showed T_m of antiparallel PNA: RNA duplexes same as that of aeg PNA:RNA duplex, showing preference for RNA binding than for DNA (Figure **3.28** & **3.29**)
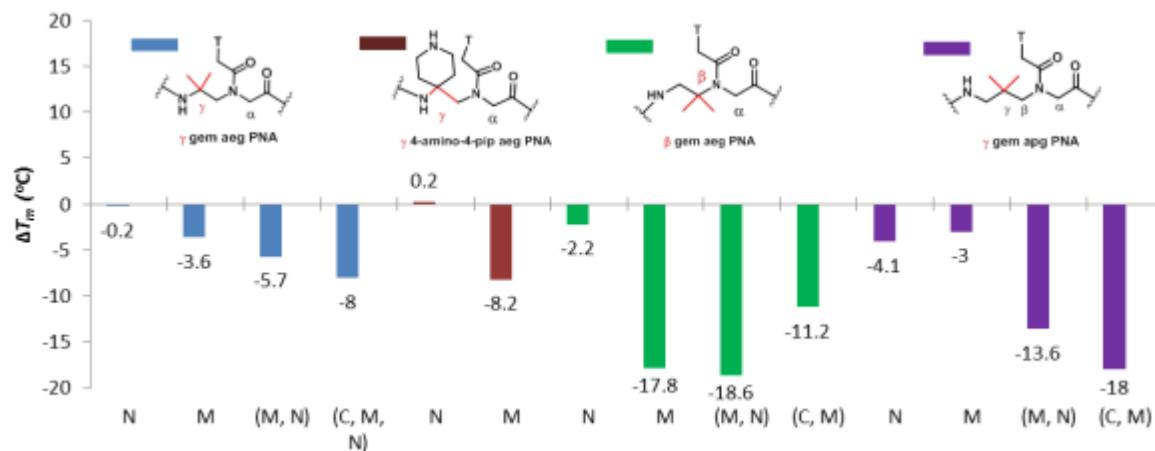
Figure 3.28: Comparative Δ*Tm* studies for PNAs (PNA 2 – PNA 16): antiparallel RNA duplex (Δ*Tm* indicates the difference in *Tm* with control *aeg* PNA)
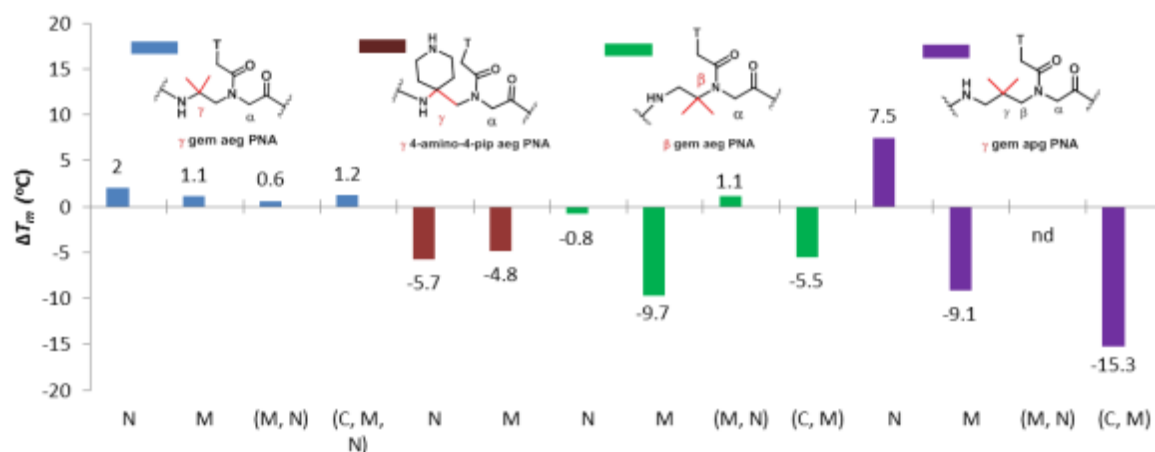
Figure 3.29: Comparative Δ*Tm* studies for parallel duplexes of PNAs (PNA **2** – PNA **16**) with RNA (Δ*Tm* indicates the difference in *Tm* with control *aeg* PNA).

3.7 Discussions:

gem dimethyl substitution introduces rigidity into conformationally flexible backbone of PNA. The extent of constrain is position dependent. Generally this leads to destabilization of antiparallel duplexes with DNA. However intensities of all gem dimethyl aeg modifications lead to satisfaction of DNA duplexes in parallel orientation. This is significant since the antiparallel PNA duplexes are always more stable than parallel duplexes, both in unmodified and modified PNA.[7] This is also true for aib-gem dimethyl PNAs.[6]

Modifications in β and γ positions show effects different than that of modification on the rotametric population amide bond. Till now there is no data which correlates the type of rotametric population with the relative orientation of chains in duplex. It has reported that the parallel duplex with (E)-OPA PNA modification is more stable than the antiparallel duplex.[8] This also with present results suggests the possibility of steric constrain around the tertiary amide bond effects the polarity (parallel / antiparallel) of duplexes.
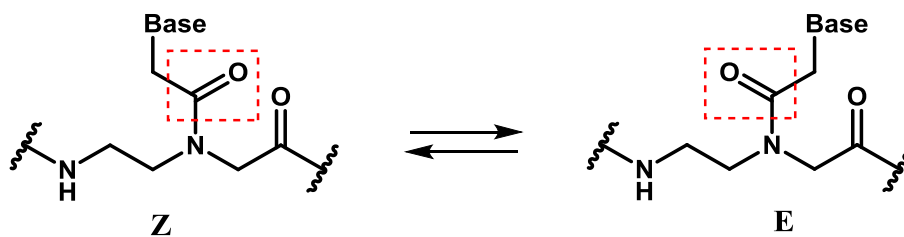
Figure 3.30: Chemical structure of the two rotameric forms of PNA

The crystal structures of many reported monomers indicate the preference of Z rotamer. However, in solution, this situation may change. Since the barrier to rotation around tertiary amide bond is high, the rotamer mixture is always observed in NMR. The ratio depends on the type of modification and perhaps the rotation of base. However, no definite correlations exist in the nature of rotamer, stability and polarity of derived duplexes.

In this context, following NMR studies have been carried out:

3.7.1 NMR Studies for β gem ester monomer:

The β gem PNA ester monomer unlikely other PNA monomers, showed predominantly presence of one rotamer which can be studied by NMR spectroscopy. Incorporation of gem dimethyl group at β-position that is next to tertiary amide can influence the rotation of tertiary amide bond carrying nucleobase which in turn may lead to fix the molecule in one particular rotamer.

^{1}H NMR and [1]H-^{1}H NOESY spectroscopy was used to investigate the conformation of the β gem PNA ester monomer (Figure **3.31**).
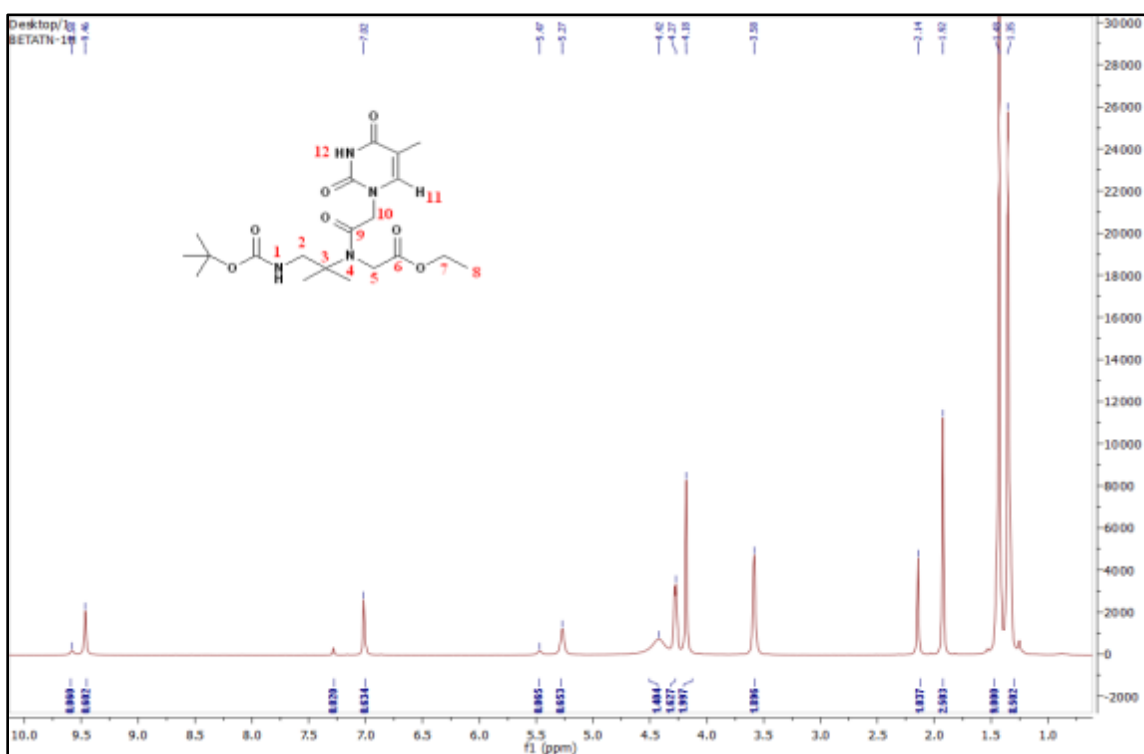
Figure 3.31: ^{1}H-NMR-assignments of β gem T ester monomer (Bruker 600MHz-CDCl$_3$)

2D 1H-1H NOESY spectra showed interaction of 2protons **H-10** with **H-5** through space. Also **H-10** protons show space interaction with **H-11.** There is no signal for space interaction of **H-10** with any proton on amino ethyl part of PNA monomer (Figure **3.32** and **3.33**)
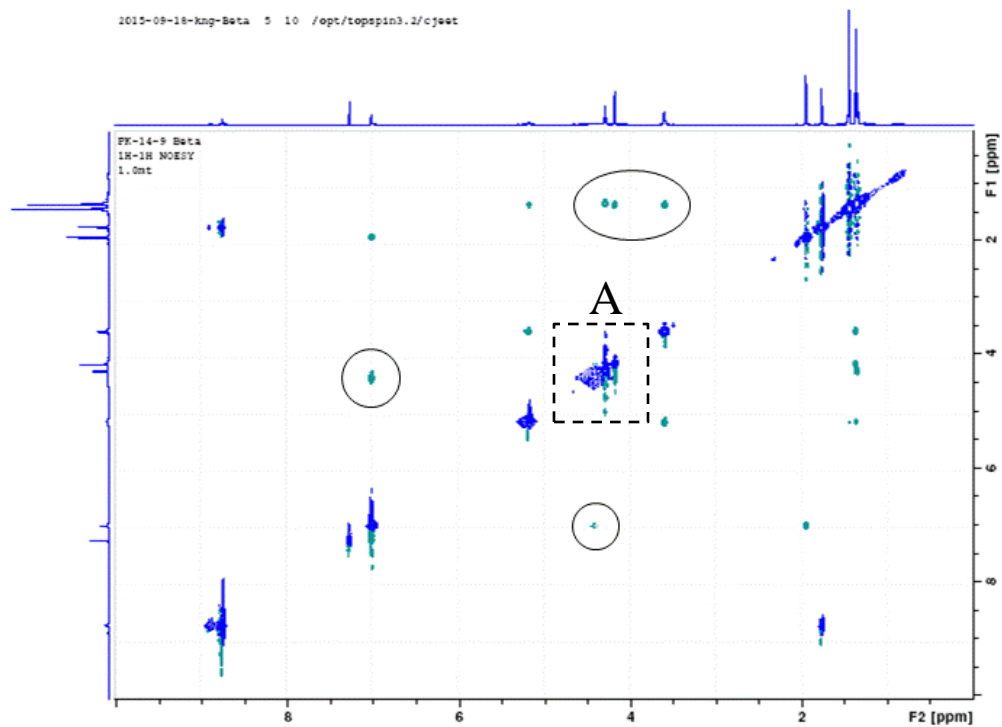
Figure: 3.32: 1H-1H NOESY for β gem T ester
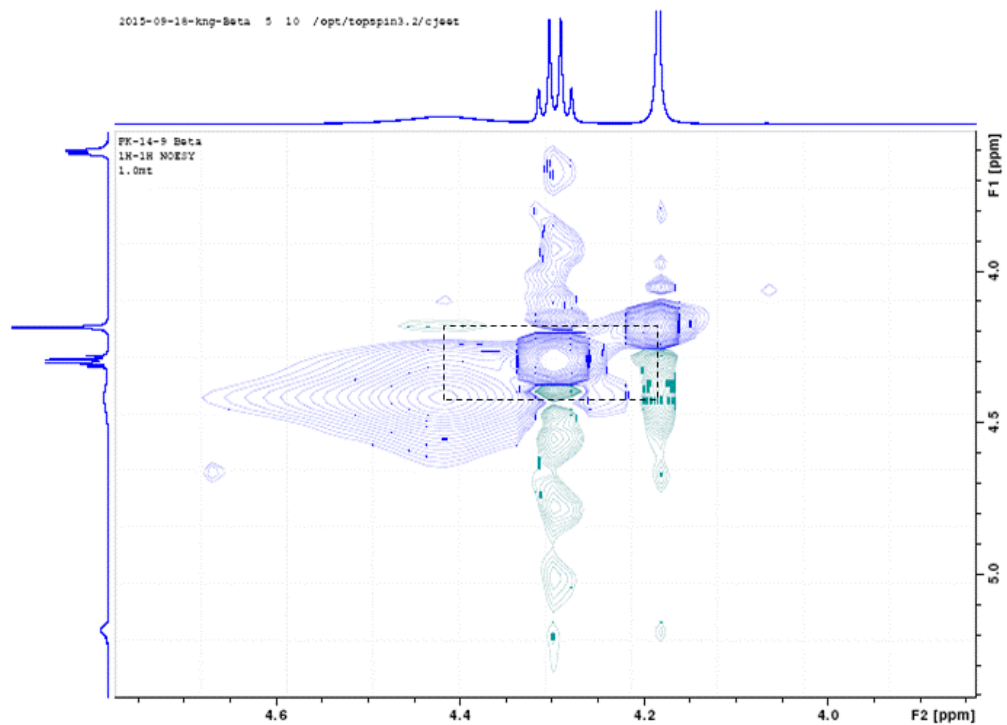
Figure: 3.33: Expanded view of section 'A' in 1H-1H NOESY for β gem T ester

The presence of **H-10** interaction with only **H-5** and absence of any signal for **H-11**with aminoethyl side protons makes the possible structure of β gem PNA ester, which is E-rotamer of PNA monomer.

3.7.2 NMR Studies for γ gem ester monomer:

The γ-gem PNA ester monomer however showed presence of two rotamers.
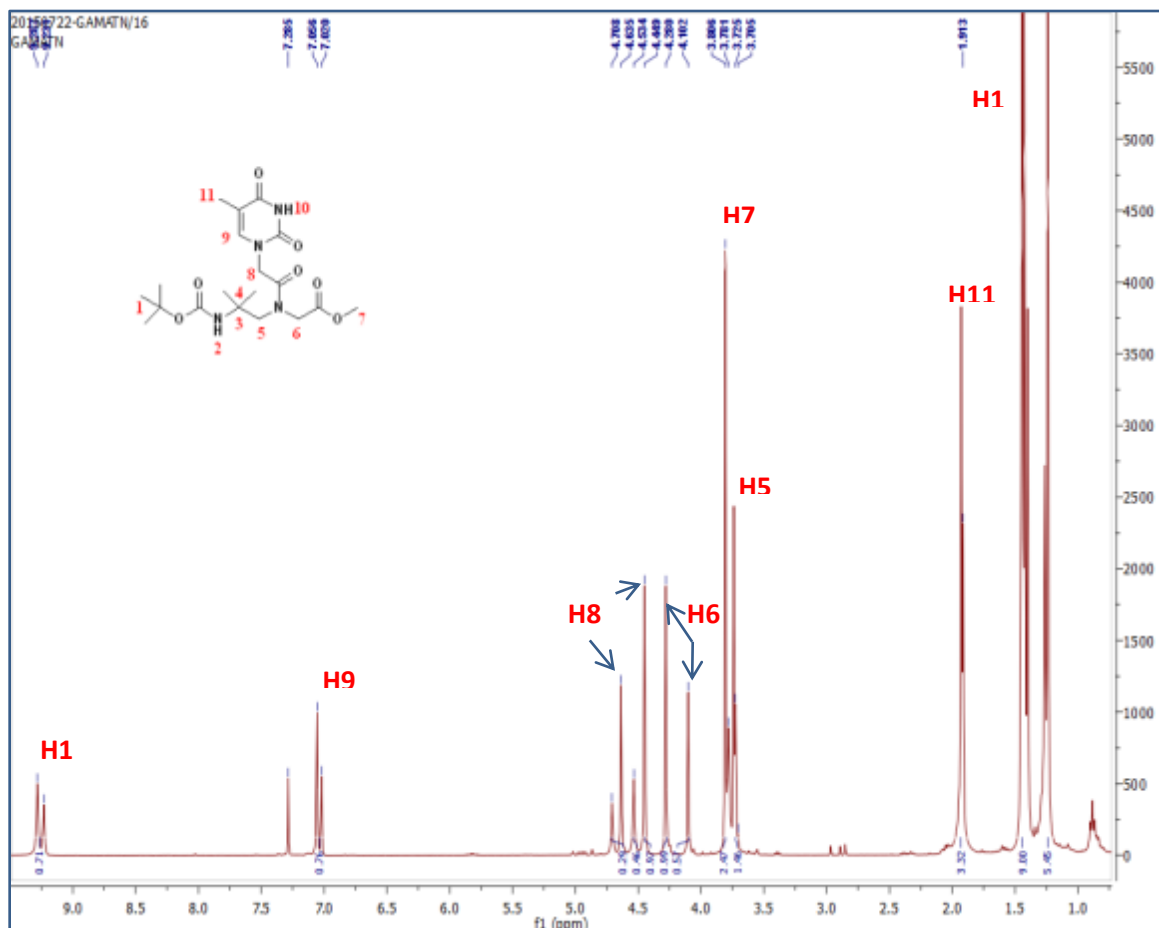
Figure: 3.34: ^{1}H-NMR-assignments of γ gem T ester monomer (Bruker 600MHz-CDCl$_3$)

The presence of two rotamers can be attributed to relatively flexible tertiary amide bond as gem dimethyl group is one carbon away from tertiary amide nitrogen.
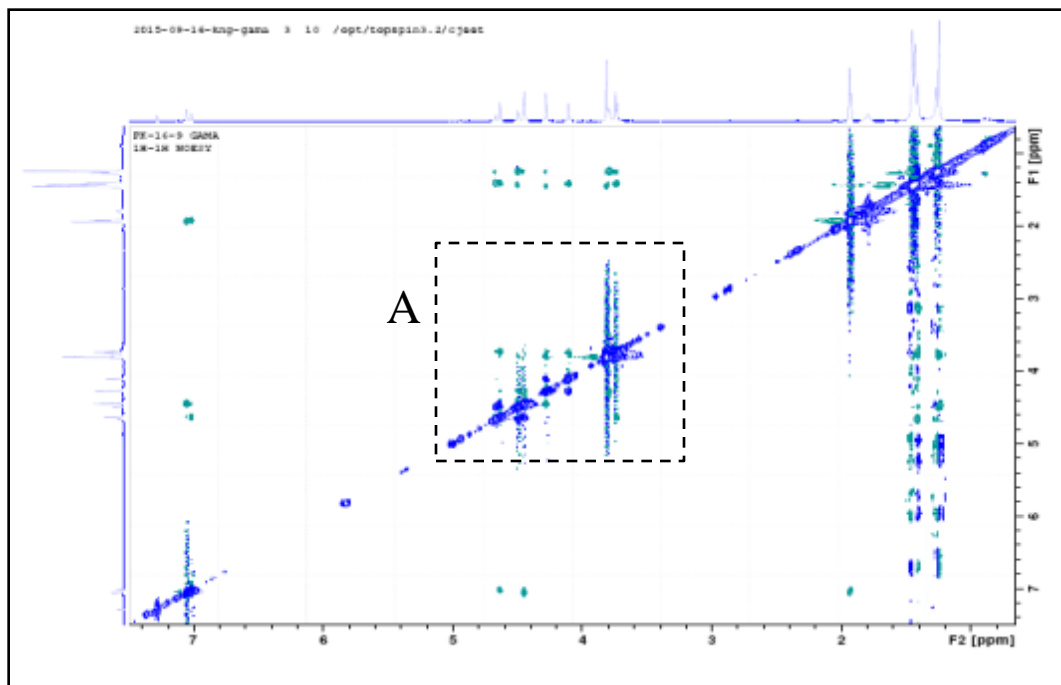
Figure: 3.35: 1H-1H NOESY for γ gem T ester
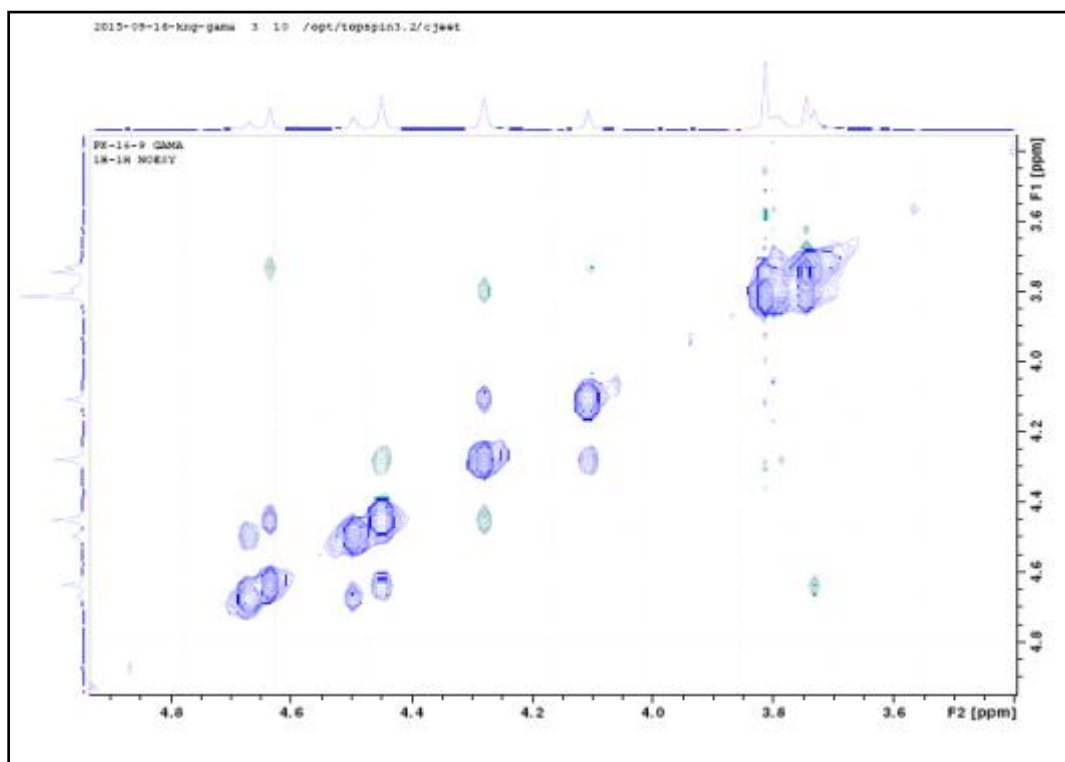
Figure: 3.36: Expanded view of section 'A' in 1H-1H NOESY for γ gem T ester

3.8 Conclusions:

Following important inferences can be drawn from the biophysical studies achiral gem dimethyl and piperidine substituted modified PNA oligomers:

➢ All modified (γ gem, β gem, *pip*) PNA oligomers showed higher binding affinity for complementary DNA when placed at any position in the sequence.

➢ γ gem *aeg* PNAs and β gem *aeg* PNAs both showed preference for complementary DNA in parallel orientation as compared to RNA.

➢ N-terminal modified γ *pip* PNA showed preference for antiparallel RNA whereas middle mofied γ *pip* PNA showed preference for parallel DNA. These findings suggest that the site of modification of cationic substitutions in the *aeg* PNA backbone is important.

CD studies showed that incorporation of various modified units in the *aeg* PNA does not alter the structure of PNA: DNA duplex which forms right handed helix.

3.9 Experimental procedures:

Chemicals: The unmodified and modified PNA oligomers were synthesized manually by general solid phase PNA synthesis protocol using *Boc*-strategy. Complementary and mismatch DNA oligonucleotides were obtained commercially from Integrated DNA Technologies (IDT). Salts and reagents used in buffer preparation such as NaCl, NaH_2PO_4, Na_2HPO_4 etc. were obtained from Sigma-Aldrich. The pH of the buffer solutions was adjusted using NaOH or HCl.

3.9.1 UV-*Tm* measurement:

UV-melting experiments were carried out on Varian Cary 300 UVspectrophotometer equipped with a peltier.

1) The samples for *Tm* measurements were prepared at 4 μM concentration of each PNA and DNA/RNA (500 μL of 10 mM phosphate buffer, pH 7.2 and 10 mM NaCl).

2) The PNA and cDNA or cRNA were mixed together in stoichiometric amounts of 1:1 and annealed at 90 ^{o}C for 3 min and cooled to room temperature slowly.

3) The samples were transferred to quartz cell, sealed with Teflon stopper and the optical density (OD) was recorded at 260 nm with a rate of 1.0 ^{o}C/min temperature increment from 16°C to 85 ^{o}C.

4) The normalized absorbance at 260 nm was plotted as a function of the temperature and the *Tm* was determined from the first derivative plots with respect to temperature and is accurate to $\pm$ 0.5 ^{o}C.

5) The data was processed using Microcal Origin8.0. The concentration of DNA, RNA and PNA were calculated on the basis of absorbance from the molar extinction coefficients of corresponding nucleobases i.e. A=15.4 cm^2/μmol, T =8.8 cm^2/μmol, C = 7.3 cm^2/μmol, G = 11.7 cm^2/μmol, U=9.9 cm^2/μmol).

3.9.2 Circular Dichroism:

CD spectra were recorded on JASCO J-715 spectro-polarimeter. The CD spectra of the PNA: DNA and PNA: RNA complexes and the relevant single strands were recorded using 4μM duplexes in 10 mM sodium phosphate buffer, 10mM NaCl at pH 7.2. The temperature of the circulating water was kept below the melting temperature of the PNA: DNA and PNA: RNA complexes, i.e., at 20°C. The CD spectra of PNA:DNA and PNA:RNA duplexes were recorded by addition of 5scans from 300to 190nm, with a 219 resolution of 0.1 nm, bandwidth of 1.0 nm, sensitivity of 2 mdeg, response of 2 sec and a scan speed of 50 nm/min.

3.10 References:

1. Cantor, C. R.; Warshaw, M. W.; Shapiro, H. *Biopolymers*, **1970**, *9*, 1059-1070.

2. Puglisi, J. D.; Tinoco, I. Jr. *Methods Enzymol*. **1989**, *180*, 304-325

3. (a) Egholm, M.; Buchardt, 0.; Nielsen, P. E.; Berg, R. H. *J. Am. Chem. Soc.* **1992**, *114*, 1895-1897. (b) Egholm, M.; Buchardt, 0.; Nielsen, P. E.; Berg, R. H. *J. Am. Chem. SOC.* **1992**, *114*, 9677-9678.

4. Egholm, M.; Buchardt, 0.; Christensen, L.; Behrens, C.; Frier, S. M.; Driver, D. A.; Berg, R. H.; Kim, S. K.; Norden, B.; Neilsen, P. E. *Nature*, **1993**, *365*, 566-568.

5. (a) Gray, D. M.; Ratliff, R. L.; Vaughan, M. R. *Methods Enzymol*. **1992**, *211*, 389-396.(b) Gray, D. M.; Hung, S. H.; Johnson, K. H. *Methods Enzymol*. **1995**, 246, 19-34.

6. Gourishankar, A.; Ganesh, K. N. *Artificial DNA: PNA & XNA* **2012**, *3*, 5-13.

7. Ganesh, K. N. *Acc. Chem. Res*. **2005**, *38*, 404-412

8. Schutz R, Cantin M, Roberts C *et* al. *Angew. Chem. Int*. Ed. Engl. **2000**, 39(7):1250-1253.

CHAPTER 4

Section A: Self assembly of PNA Analogues

Structural organization of molecules in controlled manner can be helpful for building novel structured materials. The molecules self-assembled from random to an organized state by non-covalent interactions. The self-assembling properties of Peptide Nucleic Acids have been explored using FESEM.

4.1 Introduction:

A historic address entitled "There is plenty of room at the bottom", given by physicist Richard Feynman in 1959, predicted the potential of atomic/molecular engineering. In this speech which captured the imagination of many, he prophesied the dawn of nanoengineering and nanotechnology. His vision was inspired by the activity of biological nanomachines like ribosomes and molecular motors proteins that perform an exquisite array of complex functions with high precision and excellent efficiency in the cells. His question was **can we achieve a similar feat with artificial technologies**? Decades of research has yielded several directions to fulfill this goal. The prominent and the most promising among them is the molecular self-assembly based on the key concept of bottom up approach to fabricate objects with well-defined and controllable properties.

Molecular self assembly is the process of transition from a random state to organised state via non-covalent forces. The complexity of the self-assembled state is dependent upon the chemistry of the molecules involved, specifically the spatial organization and the nature of chemical functionality within the molecule capable of intermolecular interaction. The basic pattern of self-assembly is the code inherently present within any molecule that determines its behavior within a given system. This code is governed by the physical laws of the universe. Understanding this code is essential to exploit it.

Non-covalent, intermolecular interactions such as hydrogen bonding, pi-pi stacking, hydrophobic interaction, metal coordination, and van der Waals forces drive molecular self assembly. The strength of these forces is considerably weaker than covalent bonds which allow reversibility and re-assembly.

Fundamental properties of nanomaterials are correlated with their size and shape.[1] In the context of drug delivery, size determines the surface to volume ratio of the nanoparticles, and can affect their cellular uptake as well as biodistribution.[2] Drug loaded nanomaterials can be applied for site specific drug delivery only when their uptake and blood circulation are feasible.[3] For instance, drug delivery across blood-brain barrier and blood-retina

barrier is a challenging problem that can be addressed by manipulating the size of carrier particles.[4]

Shape of the nanostructures is also a critical parameter which affects cell uptake and site specific drug delivery. Preferential interaction with specific proteins could be achieved with the appropriate shape selection of nanomaterials. The size and shape of nanomaterials have been found to play a significant role in the distribution and circulation lifetimes of these objects when delivered intravenously.[5] For example, cylindrical nanomaterials have been shown to have a 10 times longer circulation time in the bloodstream compared to their spherical counterparts.[6] The different sizes and shapes of nanomaterials certainly have an influence and hold an important place in biomedical applications.[7] Strategies to synthesise materials of biomedical importance that self-assemble into nanomaterials tunable size and shape is critical in dealing with these challenges.

Among the many self-assembly systems (DNA, protein/peptide, lipid and surfactant), peptides have drawn much attention in nanoscience and nanotechnology due to their desirable chemical/physical properties and biological functionalities

Various types of nanostructures self-assembled by peptides have been investigated and presented as biomaterials with impressive potential to be used in different applications such as biosensors,[8] drug delivery systems,[9] bioelectronics,[10] and tissue regeneration.[11] These biological nanostructures are excellent candidates for these applications due to their mild synthesis conditions, relatively simple functionalization, inexpensive and fast synthesis. Peptides have been reported to self-assemble into shape specific nanostructures, such as fibers,[12] micelles,[13] vesicles,[14] nanotubes,[15] nanospheres,[16] and many other morphologies[17] (Figure **4.1**).

The various shapes of these nanostructures arise from a series of factors including hydrophobic interactions, hydrogen bonding, aromatic stacking, crystallization, steric effects, and electrostatic interaction.[18]
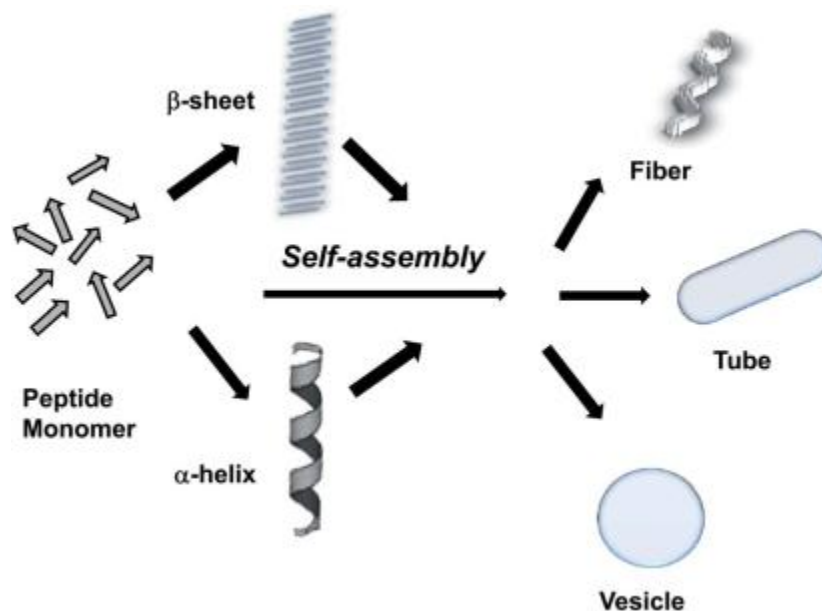
Figure 4.1: Self-assembly of peptides into different types of nanostructures[19]

Many studies have investigated the self-assembly process of peptides. However, only a few applications have been developed using the self-assembled nanostructures. This is due to the lack of understanding of the mechanisms of self-assembly and the influence of various parameters on the self-assembly process.[20] Size and shape of self-assembled peptide nanostructures are critical parameters in biomedical applications, such as biosensors or drug-delivery systems. Therefore, control of the supramolecular peptide architecture is an important subject in the field of peptide self-assembly. With respect to the nature of the self-assembly process, controlling the size and shape of peptide nanomaterials during the synthesis is difficult to achieve. However, changes in the fabrication parameters could help obtaining self-assembled nanostructures of similar dimensions.

Factors influencing peptide self assembly are amino acid sequence, salt concentration and pH, ionic strength, medium components such as solvent and substrate, presence of denaturing agents like SDS and urea, temperature, and time.

If the self-assembly of a system is well understood it allows the placement of individual atoms in three dimensions to high precision. The structures can be regulated with regards to the morphology, size, and patterning of surface chemistry. Clearly this is invaluable for designing interactions of the self-assembled structures with their environment. Hence, self-assembly is a very promising technique for producing functional materials whose properties can be designed and customized for a range of specific applications. It is known that self-assembling peptides organize into well-ordered nanostructures such as nano fibrils, nanotubes, nanospheres or vesicles, depending on the constituent peptide and environmental conditions during assembly.[21] The relatively weak non-covalent interactions act together to form intact and well-ordered supramolecular nanostructures.[22]

In contrast to peptide self-assembly, structural DNA nanotechnology is solely derived from the specificity of the hydrogen bonding interactions between complementary Watson–Crick base pairs. The use of DNA as a structural building block instead of merely a genetic material was first recognized in the early 1980s, in a theoretical work by Seeman.[23] Based on the complementary nature of nucleic acids, it is possible to predict and design DNA structures of nanoscale order. This pioneering conceptual work materialized into a vivid field of research with tremendous growth. Now, with the aid of computer design and the DNA origami method, the fabrication of any two- or even three-dimensional nanostructure shape has become considerably simpler.[24]

Peptide and DNA building blocks offer two distinct approaches for the generation of supramolecular architectures by self-assembly. Peptide-driven materials are characterized by robustness, synthetic versatility, architectural flexibility and structural complexity, whereas DNA nanostructures are based on specific molecular recognition and base-pairing complementarity. Convergence of the peptide and nucleic acid assembly strategies could be very useful for the design of novel self-organized materials.

A convergence of predictability of DNA nanotechnology and diverse functionalities of peptide nanotechnology is likely to illuminate avenues hitherto untrodden. Combining these can provide new approaches to fabricate supramolecular materials with intricate

architectures such as those created with DNA and with complex functions, afforded by the chemical versatility of aminoacids in the proteins.

Ehud Gazit *et. al.* demonstrated that dimers of peptide nucleic acids can spontaneously self-assemble to form highly organized nanostructures with unexpected optoelectronic properties. Among the 16 possible combinations of PNA dimers that were tested for self-assembly propensity in a number of conditions,some of these formed nanostructures. This illustrated therole of sequence specificity in molecular organization of these dimers. It is noteworthy that all the sequences that formed nanostructures contained guanine, G. However, depending on the neighbouring residue, the morphology of the nanostructures were found to be different. one-dimensional nanofibre structures observed for *CG* and *GC*. *GG* were spherical, rather than fibre-like. The formation of well-defined nanostructures formed by GG, which lack the Watson-Crick basepairing complementarily, suggests that other non-canonical hydrogen bonding schemes were also involved. Nanofibre morphology was observed using a 1:1 mixture of *GG* and *CC*. These findings therefore suggest that six hydrogen bonds are probably required for self-assembly of these PNA dimers. Furthermore, X-ray diffraction data for *GC* structures show that Watson–Crick base pairing and π stacking between bases plays a role in their formation, with reported distances similar to those found in Watson–Crick structures.[25]

A slightly different approach for the production of a peptide–nucleic acid hybrid is based on the conjugation of functionalized purine and pyrimidine bases to a peptide backbone.[26] The neutral peptide-like backbone replacing the negatively charged phosphodiester groups, which may limit self-association due to the repulsion of similar charges, adds structural elasticity and chemical adaptability. Another group of unnatural peptide–nucleobases hybrids (denoted nucleopeptides) have already been shown to self-assemble into nanofibres to generate supramolecular hydrogels.[27]

Despite the great potential to converge the two distinct fields of peptide self-assembly and structural DNA nanotechnology PNA has so far only been used as a template or as a conjugate to other molecules that undergo the self-assembly process, in order to gain the

hybridization properties of nucleic acids. A notable example is the work of Stupp and coworkers,[28] in which a PNA strand and a peptide sequence that promotes nanofibre formation were coupled to form a PNA–peptide amphiphile conjugate. The designed fibre-shaped nanostructures show binding of oligonucleotides with high affinity and specificity.

4.2 Objective of present work:

It was surmised that the self-assembling and hydrophobic properties of peptides and base pairing properties of nucleic acids, simultaneously present in PNA may lead to interesting nanostructures. The success of antisense therapy to regulate expression of genes associated with disease depends on successful delivery of antisense oligonucleotides and their stability in biological systems. Recently nanotechnology based delivery systems are being delivered, with synthetic lipid- and polymer-based nano-carriers as nucleic acid delivery systems.[29]

(a) γ gem aeg PNA   (b) γ 4-amino-4-pip aeg PNA   (c) β gem aeg PNA   (d) γ gem apg PNA
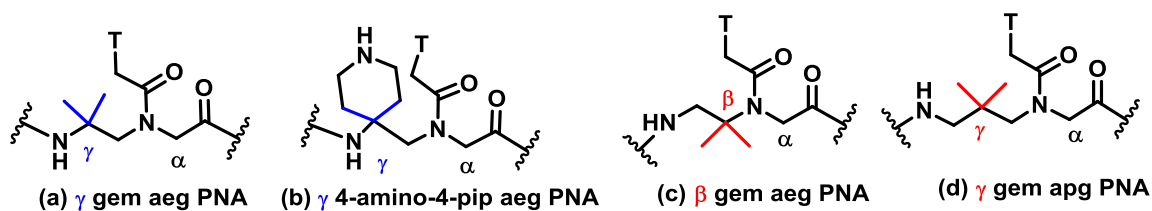
Figure 4.2: PNAs used for nanoparticle formation

The objectives are to ascertain the self-asembling properties of above single strand PNA oligomers (Figure **4.2a** to **d**) and their derived duplexes with complementary DNA, and to study the effect of back-bone modifications at different sites on aminoethyl glycyl and aminopropyl glycyl backbone on the morphology of the structures.

Among the modified PNAs, the PNAs with maximum number of modifications have been selected to check their ability to form nanostructures.

4.3 Results and discussions:

Size and morphology of nanostructure is influenced by various factors. In case of modified PNA, position and number of modifications are likely to influence the secondary structures of PNAs, which is likely to be reflected on morphology of nanostrustures they form. In addition to these factors, site (γ,β) of modification on the PNA residue also plays an important role in determining 3D structure of backbone. The effect of gem-dimethyl group and piperidine group on PNA was studied using FESEM with PNAs having maximum number of these modifications.

The nanostructure formation of ss PNAs (PNA**1**, PNA**5**, PNA**6**, PNA**10**, PNA**11**, PNA**16**) and duplexes derived with their complementary DNA was studied using Field Emission Scanning Electron Microscopy (FESEM) at different concentrations and the results are shown and discussed in following section.

All ss PNAs and their duplexes with both 5μM and 35μM concentration were studied for their nanostructure formation ability. The 5μM concentrated ssPNAs and the duplexes did not form any nanostrures.

4.3.1 Nanostructures of ss γ gem and γ gem:DNA duplex

γ **gem aeg PNA**
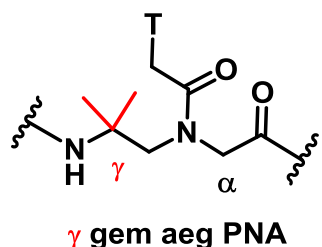
The ss γ gem PNA**5** of 35μM concentration was annealed to 90°C and cooled to room temperature and then checked for nanostructure formation. Similarly the γ gem PNA**5** and DNA were taken in 1:1 ratio and annealed to 90°C and cooled to room temperature slowly and checked for nanostructure formation.

In case of single stranded γ gem PNA**5,** sub-micrometer particles were observed (Figure **4.3A**). However, they were ill-defined in terms of their morphology. In addition to the seemingly random shapes and size of the nanostructures, larger agglomerates were also observed. The duplexes derived from γ gem PNA**5** and DNA showed larger aggregates as compared to those formed by the ssPNA. (Figure **4.3B**) The ss PNA**5** and PNA**5**: DNAduplexes with 5μM concentration did not show any nanostructure formation. Thus γ gem modification on aeg backbone was found to be unsuitable for self-assembly.
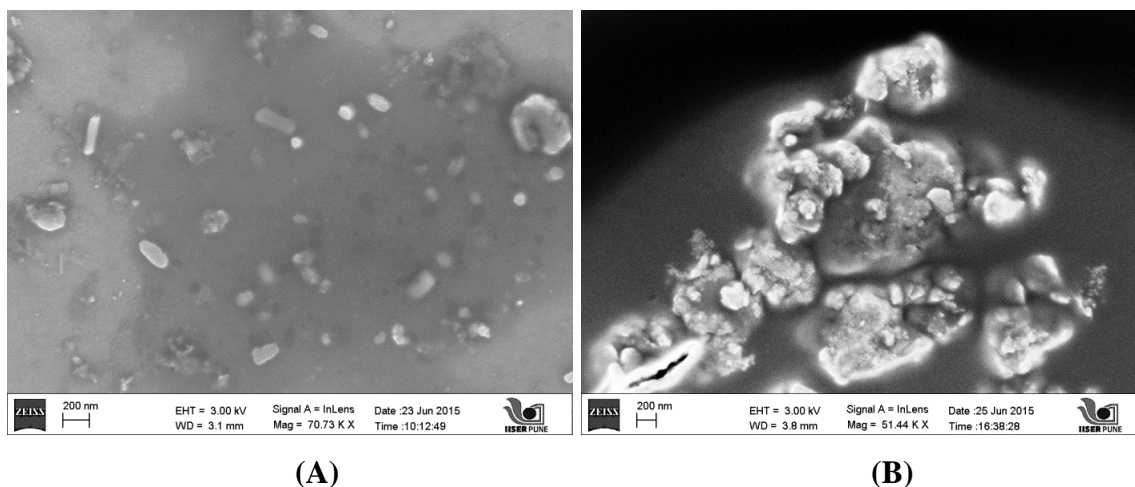

| (**A**) | (**B**) |

Figure 4.3: FESEM images of (**A**) ss γ gem PNA5 (**B**) γ gem PNA5:DNA

4.3.2 Nanostructures of ss *β* gem and *β* gem: DNA duplex

β gem aeg PNA
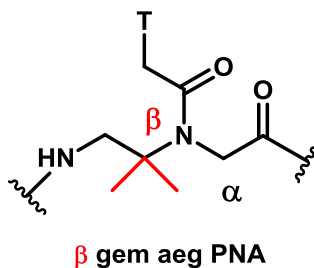
β gem modified PNA**10** and PNA **11** were found to assemble into well-defined structures. In case of PNA10, which contains a single modification at the middle of the PNA strand, well-defined nanostructures were observed only when they were taken as duplex with complementary DNA. The morphology of these PNA:DNA duplexes were distinct slender thread/needle like of a few micrometers in length and 37 nm width. PNA **11** with two modified units at middle and N-terminus were found to form isolated nano-

sheets when they occur as single strands. On complexation with its complementary DNA, PNA **11** formed clusters of vertically stacked nanosheets.
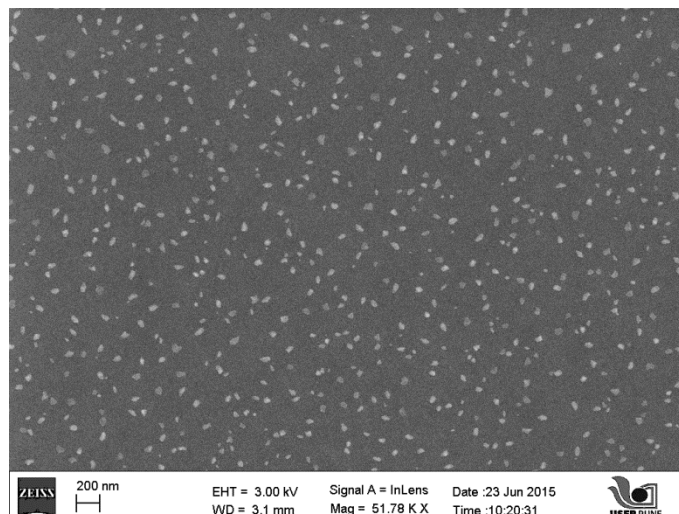
Figure 4.4: FESEM images of ss β gem PNA**11**

| A | B |
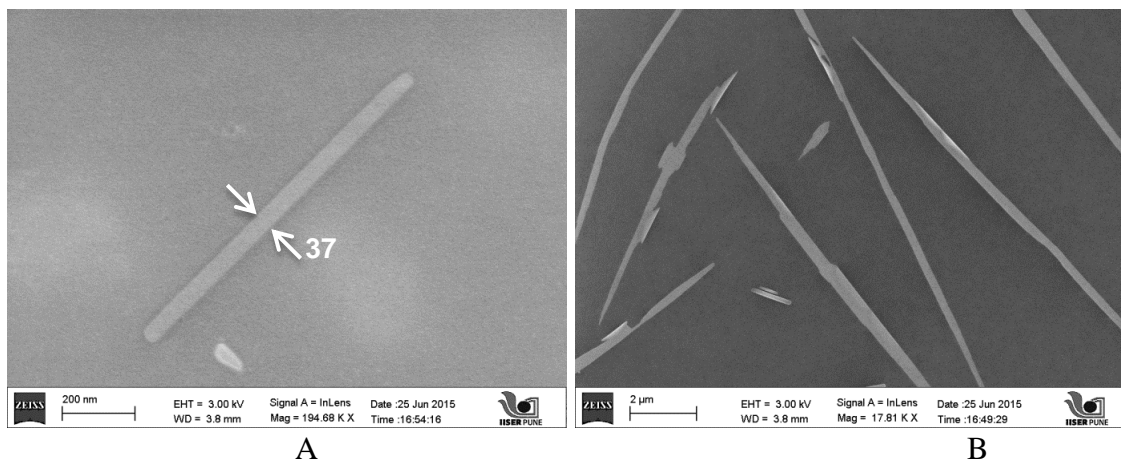
Figure 4.5: FESEM images of β gem PNA**11:**DNA

The tendency of these PNAs to form two-dimensional structures was clearly visible in the FESEM micrographs. With increase in the number of modifications this tendency was apparently enhanced as the size of the sheets were found to increase manifold

The ss PNA**12** formed small flake like nanostructures (Figure **4.6**).
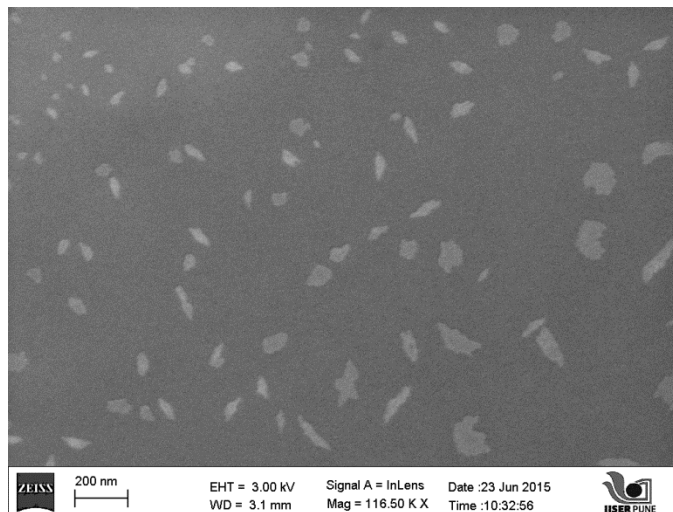
Figure 4.6: FESEM images of ss β gem PNA**12**

The small flakes of ss PNA**12** might have grown in 2dimension to show sheet like nanostructures in PNA**12**:DNA duplex (Figure **4.7**)

| **(A)** | **(B)** |
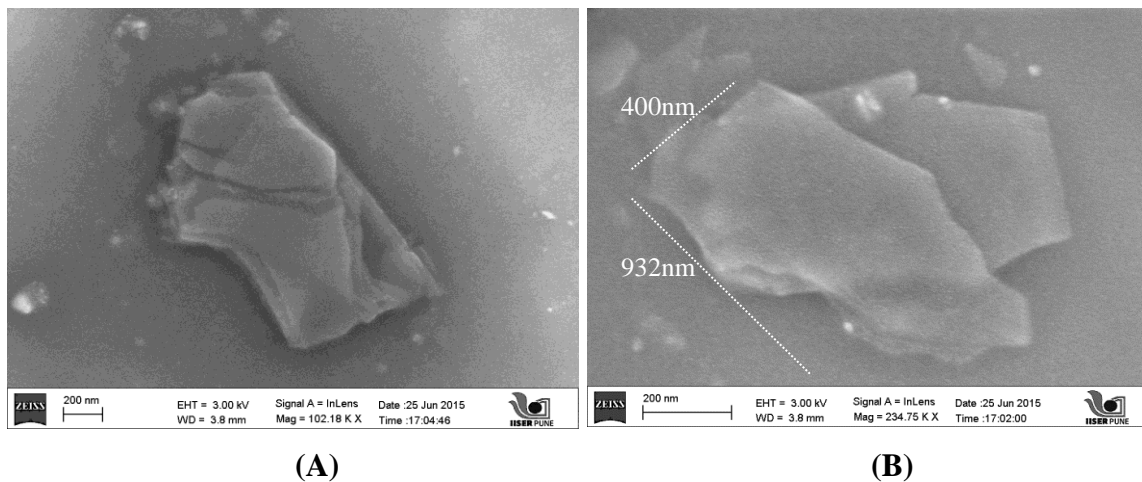
Figure 4.7: FESEM images of β gem PNA**12**:DNA

4.3.3 Nanostructures of ss γ pip gem and γ pip gem: DNA duplex

γ **4-amino-4-pip aeg PNA**
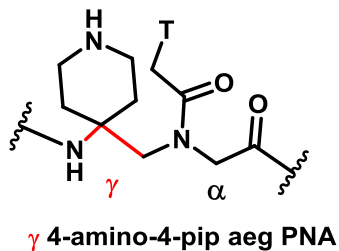
Single stranded **γ pip gem modified** PNA**7** did not show any well-defined nanostructure (Figure **4.8**). The PNA**7**:DNA duplex showed two morphologies (Figure **4.9)** on formation of PNA:DNA duplex, to assemble into concave discs with multiple edges and slender needles that were in some instances fused together to form a bow of a few micrometer in length.
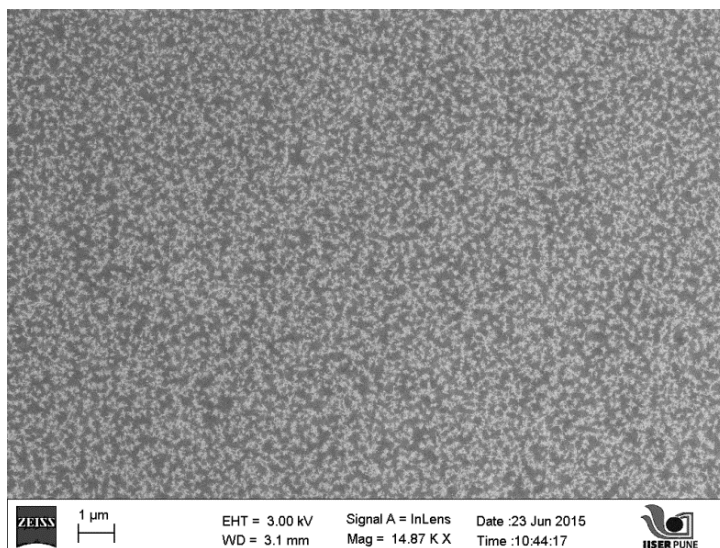
Figure 4.8: FESEM images of ss γ pip gem PNA7

These well-defined nanostructures were found to be present distributed uniformly over the substrate. The structures were found to have rough edges indicating the tendency to grow in one or two dimensions.

(A)   (B)
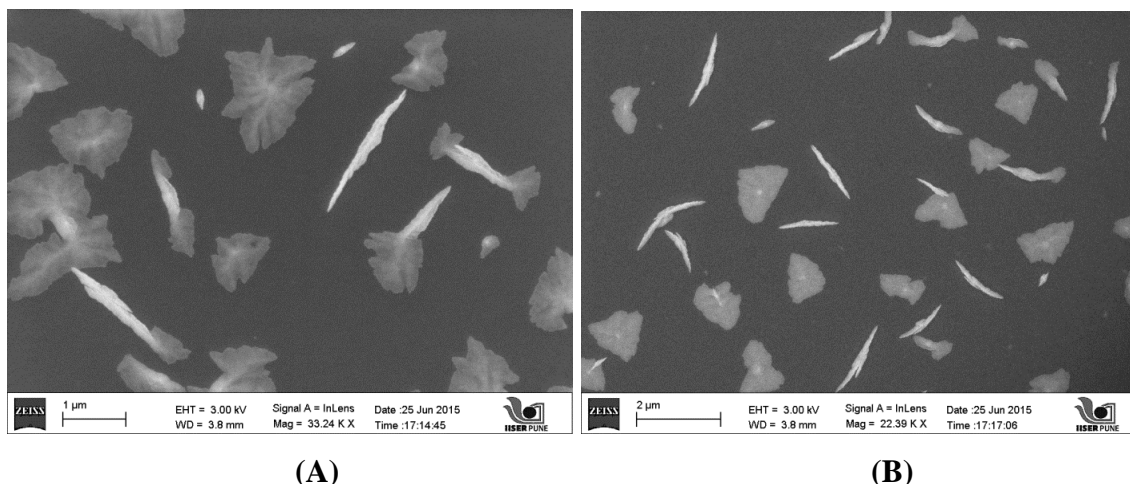
Figure 4.9: FESEM images of γ pip gem PNA**7**:DNA

4.3.4 Nanostructures of ss γ gem apg and γ gem apg PNA: DNA duplex
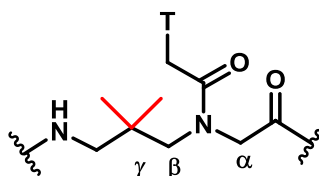
γ **gem apg PNA**

The single stranded PNA **16** showed small bunches of needle like nanostructures. (Figure **4.10**). The clusters were found isolated and were distinct unlike disordered agglomerates. In all the clusters the needles were found to be aligned longitudinally with a gentle twist at the centre of the clusters apparent in the micrographs.
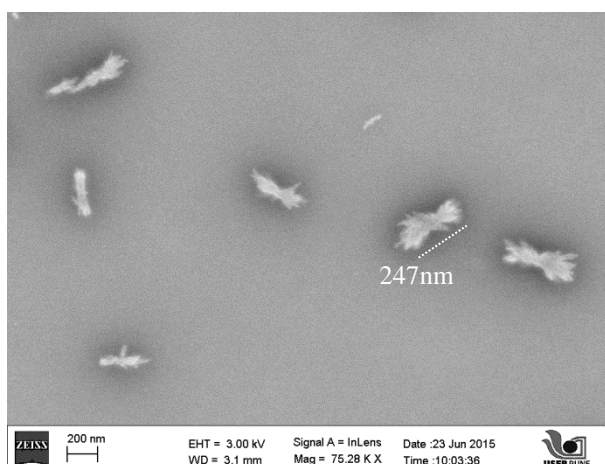
Figure 4.10: FESEM images of ss γ gem apg PNA**16**

The PNA**16**:DNA duplex showed long needle like structures (Figure **4.11**). The needles were found to be well separated unlike the ones formed by ssPNA. These one-dimensional structures were found to also have grown to longer lengths, suggesting that the self-assembling tendency of the PNA is accentuated when it is annealed with complementary DNA. Although the tips of these structures were usually pointed, along the length, they seemed to be flattened, providing a leaf like morphology.

(A)   (B)
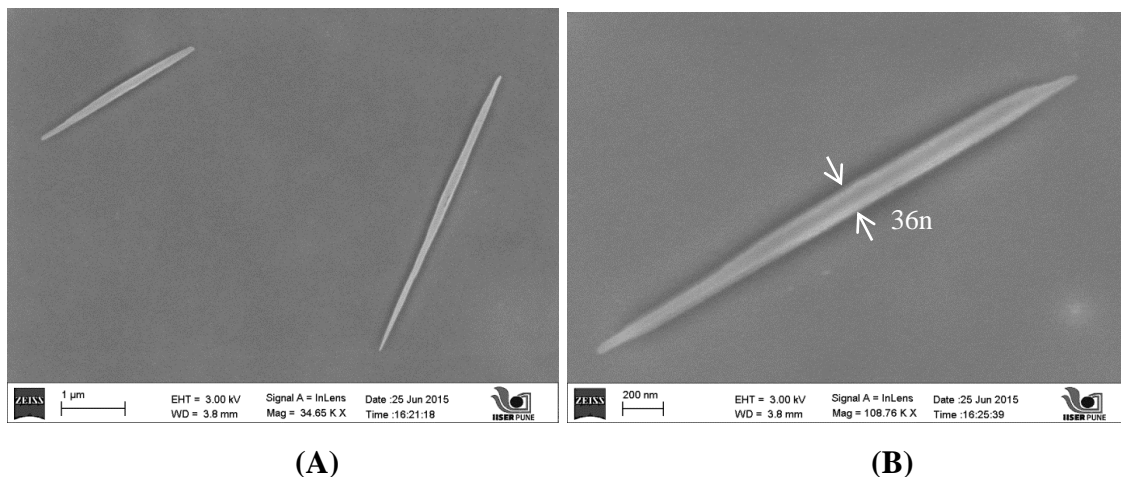
Figure 4.11: FESEM images of γ gem apg PNA**16**:DNA

4.4 Summary

- Proficiency of single stranded PNAs and their duplexes with DNA was studied using FESEM technique. The size of nanostructures varies from μm to nm.
- The morphology of duplex was more defined than the single stranded PNAs.
- Also the morphology of nanostructures got altered with the type of modification, number of modifications and site of modifications.

4.5 Experimental Procedures

4.5.1 Sample preparation for FESEM: PNA and its complementary DNA in 1:1 ratio of final concentration 35μM and heated to 90°C for 5 min and cooled to room temperature. 5μl of each sample was placed on silicon wafer; the sample was dried under vacuum. A thin coat of gold was sputtered. The sputter coated samples were then introduced into the specimen chamber and the samples were imaged for morphological analysis of the self-assembled samples using field emission scanning electron microscopy

4.6 References:

1. (a) J. Wu, N. Kamaly, J. Shi, L. Zhao, Z. Xiao, G. Hollett, R. John, S. Ray, X. Xu, X. Zhang, P. W. Kantoff and O. C. Farokhzad, Angew. *Chem., Int. Ed.*, **2014**, *53*, 8975–8979. (b) Z. Qian, S. P. Hastings, C. Li, B. Edward, C. K. McGinn, N. Engheta, Z. Fakhraai and S.-J. Park, *ACS Nano*, **2015**, *9*, 1263–1270. (c) Y. Wang, L. Sun, S. Yi, Y. Huang, S. C. Lenaghan and M. Zhang, *Adv. Funct. Mater.*, **2013**, *23*, 2175–2184

2. (a) N. Bertrand, J. Wu, X. Xu, N. Kamaly and O. C. Farokhzad, *Adv. Drug Delivery Rev.*, **2014**, *66*, 2–25. (b) L. Sun, S. Yi, Y. Wang, K. Pan, Q. Zhong and M. Zhang, *Bioinspiration Biomimetics*, **2014**, *9*, 016005.

3. Z. Popovic´, W. Liu, V. P. Chauhan, J. Lee, C. Wong, A. B. Greytak, N. Insin, D. G. Nocera, D. Fukumura, R. K. Jain and M. G. Bawendi, Angew. *Chem., Int. Ed.*, **2010**, *49*, 8649–8652.

4. R. A. Petros and J. M. DeSimone, *Nat. Rev. Drug Discovery*, **2010**, *9*, 615–627.

5. J.-W. Yoo, D. J. Irvine, D. E. Discher and S. Mitragotri, *Nat. Rev. Drug Discovery*, **2011**, *10*, 521–535.

6. Y. Geng, P. Dalhaimer, S. Cai, R. Tsai, M. Tewari, T. Minko and D. E. Discher, *Nat. Nanotechnol.*, **2007**, *2*, 249–255.

7. (a) Y. Wang, L. Sun, S. Yi, Y. Huang, S. C. Lenaghan and M. Zhang, *Adv. Funct. Mater.*, **2013**, *23*, 2175–2184.(b) S. Yi, Y. Wang, Y. Huang, L. Xia, L. Sun, S. C. Lenaghan and M. Zhang, J. *Biomed. Nanotechnol.*, **2014**, *10*, 1016–1029. (c) L. Xia, Z. Xu, L. Sun, P. Caveney and M. Zhang, J. *Nanopart. Res.*, **2013**, *15*, 1–11. (d) G. Sun, D. Wei, X. Liu, Y. Chen, M. Li, D. He and J. Zhong, *Nanomedicine*, **2013**, *9*, 829–838.

8. P. Koley and A. Pramanik, *Soft Matter*, **2012**, *8*, 5364–5374.

9. (a) Z. Yu, B. Yu, J. B. Kaye, C. Tang, S. Chen, C. Dong and B. Shen, *Nano LIFE*, **2014**, *04*, 1441016. (b) Y. Liu, M. Ji, M. K. Wong, K.-I. Joo and P. Wang, *BioMed Res. Int.*, **2013**, *2013*, 11. (c) Y. Wang, S. Yi, L. Sun, Y. Huang, S. C. Lenaghan and M. Zhang, *J. Biomed. Nanotechnol.*, **2014**, *10*, 445–454. (d)Y. Liu, Y. J. Kim, M. Ji, J. Fang, N. Siriwon, L. I. Zhang and P. Wang, *Mol. Ther. – Methods Clin. Dev.*, **2014**, *1*, 12.

10. M. Amit, G. Cheng, I. W. Hamley and N. Ashkenasy, *Soft Matter*, **2012**, *8*, 8690–8696.

11. Y. Kumada, N. A. Hammond and S. Zhang, *Soft Matter*, **2010**, *6*, 5073–5079.

12. (a) L. Zhang, J. Zhong, L. Huang, L. Wang, Y. Hong and Y. Sha, *J. Phys. Chem. B*, **2008**, *112*, 8950–8954. (b) S. Zhong, H. Cui, Z. Chen, K. L. Wooley and D. J. Pochan, *Soft Matter*, **2008**, *4*, 90–93.

13. Y. Jin, X.-D. Xu, C.-S. Chen, S.-X. Cheng, X.-Z. Zhang and R.-X. Zhuo, Macromol. *Rapid Commun.*, **2008**, *29*, 1726–1731.

14. E. K. Chung, E. Lee, Y.-b. Lim and M. Lee, *Chem. – Eur. J.*, **2010**, *16*, 5305–5309.

15. N. Kol, L. Adler-Abramovich, D. Barlam, R. Z. Shneck, E. Gazit and I. Rousso, *Nano Lett.*, **2005**, *5*, 1343–1346.

16. T. H. Han, T. Ok, J. Kim, D. O. Shin, H. Ihee, H.-S. Lee and S. O. Kim, *Small*, **2010**, *6*, 945–951.

17. (a) Z. Yu, J. Li, J. Zhu, M. Zhu, F. Jiang, J. Zhang, Z. Li, M. Zhong, J. B. Kaye, J. Du and B. Shen, *J. Mater. Chem. B*, **2014**, *2*, 3809–3818. (b) H. Cui, T. Muraoka, A. G. Cheetham and S. I. Stupp, *Nano Lett.*, **2009**, *9*, 945–951. (c) E. T. Pashuck and S. I. Stupp, *J. Am. Chem. Soc.*, **2010**, *132*, 8819–8821. (d) M. Ma, J. Zhong, W. Li, J. Zhou, Z. Yan, J. Ding and D. He, *Soft Matter*, **2013**, *9*, 11325–11333.

18. (a) Y. Zhu, Y. Chen, G. Xu, X. Ye, D. He and J. Zhong, *Mater. Sci. Eng.*, *C*, **2012**, *32*, 390–394. (b) Y. Yamamoto, T. Fukushima, Y. Suna, N. Ishii, A. Saeki, S. Seki, S. Tagawa, M. Taniguchi, T. Kawai and T. Aida, *Science*, **2006**, *314*, 1761–1764. (c) T. Shimizu, M. Masuda and H. Minamikawa, *Chem. Rev.*, **2005**, *105*, 1401–1444. (d) P. Kumaraswamy, R. Lakshmanan, S. Sethuraman and U. M. Krishnan, *Soft Matter*, **2011**, *7*, 2744–2754.

19. Chauhan V., Panda J. *Poly. Chem.,* **2014**, *5*, 4418-4436.

20. (a) P. Kumaraswamy, R. Lakshmanan, S. Sethuraman and U. M. Krishnan, Soft *Matter*, **2011**, *7*, 2744–2754. (b) S. Scanlon and A. Aggeli, *Nano Today*, **2008**, 3, 22–30.

21. (a) Zhang, S. Nat. *Biotechnol.* **2003**, *21*, 1171-1178 (b) Song, Y.; Challa, S.R.; Medforth, *et al. Chem. Commun.* **2004**, *9*, 1044-1045 (c) Reches, M.; Gazit, E. *Nat. Nanotechnol,* **2006**, *1*, 195-200 (d) Reches, M.; Gazit, E. *Phys. Biol.* **2006**, *3*, S10-S19.

22. Reches, M.; Gazit, E. *Current Nanoscience*, **2006**, *2*, 105-111.

23. Seeman, N. C. *J. Theor. Biol.* **1982**, *99*, 237–247.

24. (a) Rothemund, P. W. K. *Nature*, **2006**, *440*, 297–302 (b) Ke, Y., Ong, L. L., Shih, W. M. & Yin, P. *Science*, **2012**, *338*, 1177–1183 (c) Dietz, H., Douglas, S. M. & Shih, W. M. *Science,* **2009** *325*, 725–730.

25. Berger, O. *et al. Nature,* **2015**, *10,* 353–360.

26. Ura, Y., Beierle, J. M., Leman, L. J., Orgel, L. E. & Ghadiri, M. R. *Science,***2009**, *325*, 73–77

27. Li, X. *et al. Angew. Chem. Int. Ed.,* **2011**, *50*, 9365–9369

28. Guler, M. O., Pokorski, J. K., Appella, D. H. & Stupp, *Chem.,* **2005**, *16,* 501–503.

29. Li, J.; Wang, Y.; Zhu, Y.; Oupicky, D. *J. Control. Release* **2013**, *172*, 589-600.

CHAPTER 4

Section B: Cell Uptake Studies of PNA Oligomers

The cell penetration ability of carboxyfluorescein tagged PNA oligomers was investigated by live cell imaging in MCF-7 cell lines using confocal microscopy.

4.7 Introduction

Synthetic oligonucleotides have been proposed as a new class of potential therapeutic molecules that can interact with the messenger RNA (mRNA) of disease related protein which specifically inhibits the protein synthesis.[1,2] The fascinating approach of antisense strategy represents one of the most powerful systems for molecular recognition designed by nature.[3] Naturally occurring oligonucleotides (DNA/RNA) suffer from the various hurdles to act as potential drug candidates. Several classes of modified oligonucleotides (ONs) have been developed that can recognize and bind to target DNA/RNA with high affinity and sequence specificity. The modified oligonucleotides are resistant to degradation by cellular enzymes like proteases and nucleases, however none of them can efficiently traverse the cell membrane on their own.[4] Various ways have been attempted to improve the cell permeation properties of the antisense oligonucleotides.[5] The most important ones include the use of liposome as a carrier of antisense ONs where the therapeutic ONs are encapsulated in the liposome and specifically delivered to the target cells.[6] The use of liposomes is limited due to their short half life in the serum. The attachment of poly-L-lysine[7] and additional chemical, mechanical and electrical transduction means have been employed to improve the transport of these ONs to the cells.[8] Although these ways are useful for small-scale experimental setups, the use of such exogenous transduction reagents may lead to off-target and cytotoxic effects.[9] It is therefore desirable to modify the structures and chemical functionalities of these ONs to improve the cell permeability as well as pharmacokinetic and pharmacodynamic properties.

As discussed earlier, the attractive features in terms of binding affinity, strand invasion, resistance to degrading enzymes and high stability in cellular extracts[10] make peptide nucleic acid (PNA) a promising molecule for the development of gene-specific drugs. However, the low cellular entry of PNA limits their usefulness as an antigene/antisense drug.[11] Therefore, several different ways have been employed to increase the cellular delivery of unmodified PNAs.[12] Some of the transfection protocols for PNA are listed below:

a) Microinjection

b) Electroporation

c) Co-transfection with DNA

d) Permeabilised cells

e) Direct delivery at high concentrations

However, the faster growth of PNA development as an antisense agent depends on the finding of more efficient and general delivery protocols for PNA. To meet these demands, several modifications of PNA have been introduced and different cellular delivery protocols have been attempted. One such modification is the conjugation of PNA to lipophilic adamantyl acetic acid. But this approach was partially successful giving the cell permeability depending on the cell type and the PNA sequence used.[13]

Similarly another lipophilic moieties like triphenylphosphonium, cholesterol, bile acid etc. have been conjugated to improve the cell permeability of PNA.[14] Considerable effort has been invested in exploring the effect of 'Trojan peptides' and several other 'cell penetrating peptides' as carriers for cellular delivery of PNA. The most thoroughly studied peptides are penetratin, a 16 residue peptide derived from Drosophila homeodomain transcription factor, antenapedia and 35-amino acid basic sequence

(TAT) from the HIV tat protein.[15] PNA when conjugated to penetratin or its retroinverso derivative has shown diffusion in cytoplasm or localization in the nucleus. Transportan, a 27 amino acid long peptide and 7-residue basic nuclear localization signal (NLS) peptide have also been investigated as conjugates of PNA to improve the antisense activity.[16] The risk of adverse reactions in non-targeted cells have been tried to avoid by conjugation of PNA to cell-specific receptor ligands. Wickstrom et al. have conjugated PNA to a four residue peptide with specific binding capability to the cell surface receptor for insulin like growth factor 1 (IGF-1R). These studies showed that only IGF-1R expressing cells internalized conjugated PNA enabling specific entry to the cells. Unfortunately, the PNA was entrapped in the cytosolic compartments limiting the availability of antisense PNA to the target.[17] To explore this strategy, Corey's group has conjugated anti-telomerase PNA

to lactose which can be recognized by the hepatic asialoglycoprotein receptor (ASGP-R) where it was found that among all cell types used, only the liver derived cell type internalized the PNA conjugate.[18] The general routes taken by these PNA conjugates to get inside the cells are either direct translocation or endocytosis as shown in Figure **4.12.**[19]
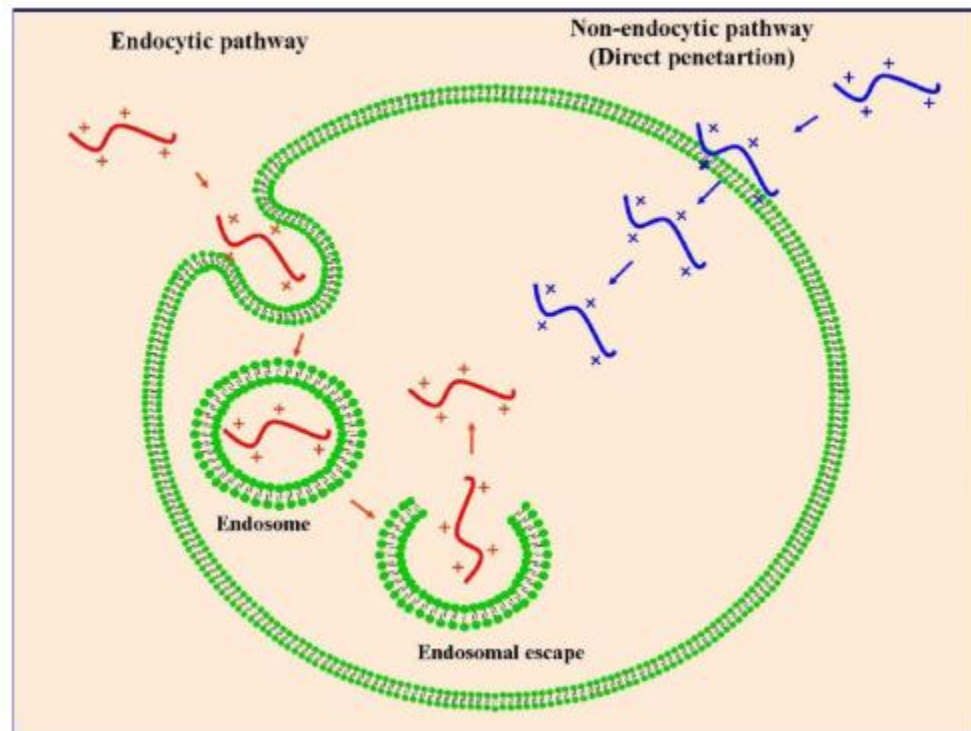

Figure 4.12: General routes for cellular entry of PNA or its conjugates[19]

The various protocols mentioned to improve the cellular uptake of PNA have suffered from the obstacles like endosomal entrapment, cytotoxicity induced by conjugating highly cationic cell penetrating peptides or polylysine and polyarginine, low plasma half-life of liposomes etc. Therefore, increasing the cell permeation ability of PNA and improvement in its use as effective antisense agent is still in progress that can help in producing more nucleic acid-based therapeutic approaches and diagnostics.

4.8 Confocal microscopy

The principal of confocal imaging was patented in 1957 by Marvin Minsky[20].In a conventional fluoresence microscop (wild-field microscope) all parts of specimen in the optical path are excited at same time and the resulting fluorescence is detected by microscop's photodetector/ camera including a large unfocused background part. In contrast aconfocal microscope uses point illumination and a pinhole in an optically conjugate plane in front of the detector to eliminate out-of-focus signal. As only light produced by fluroscence very close to focal plane can be detected, the image's optical resolution particularly in the sample depth direction, is much better than that of wild-field microscopes. However, as much of light from sample fluroscence is blocked at pinhole, this increases resolution is at the cost of decreases signal intensity. The schematic illustration of the principle of confocal microscopy is shown in the Figure **4.13.**
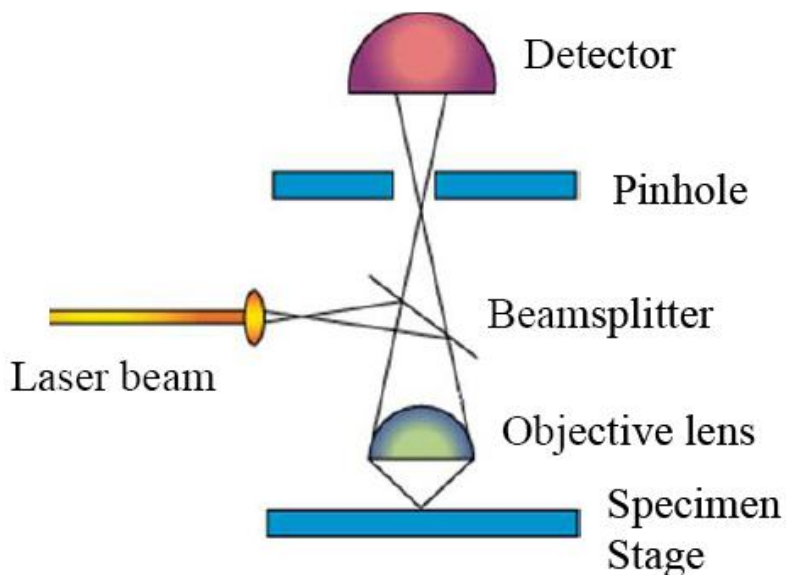
Figure 4.13: Schematic representation of confocal scanning light microscope[21]

4.9 Aim of present work

The specific objectives of this section are:

- ➢ Synthesis of 5(6)-carboxyfluorescein N-terminal-tagged PNA oligomers

> ➤ Investigation of the uptake efficiency of modified and control *aeg* PNA
>
> ➤ oligomers int MCF-7 cell lines by confocal microscopy

4.10 Results and discussion

The synthesis, purification and characterization of fluorescently tagged PNA oligomers have been discussed in this section.

4.10.1 Tagging of PNA oligomers with 5(6)-carboxyfluorescein

The modified PNA and control *aeg* PNA sequences were synthesised for studying their cell permeation properties. Using solid phase peptide synthesis protocol, each of these selected sequences were tagged with 5(6)-carboxyfluorescein [5(6)-CF] at the final step in presence of HOBt and DIC, just before their cleavage from the resin (Figure **4.14**).
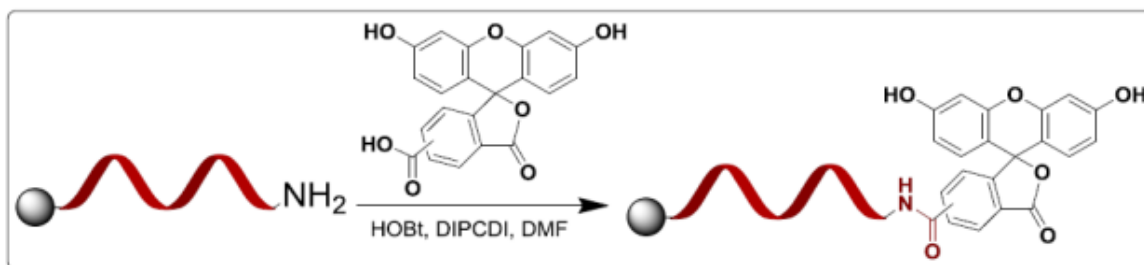

Figure 4.14 Tagging of PNA oligomers with fluorescent 5(6)-carboxyfluorescein

4.10.2 Cleavage of the fluorescent PNA oligomers from the solid Support

After coupling time was over, the resin was washed thoroughly with methanol to remove excess 5(6)-CF. The peptides were cleaved from the solid support using tifluoromethanesulfonic acid (TFMSA) in the presense of trifluoroacetic acid (TFA) (Low, High TFMSA-TFA method)[21] and thioanisole-ethanedithiol as scavengers which yielded PNA oligomers having L-lysine amide at C-terminus and carboxyfluorescein at N-terminus. After cleavage reaction was over, the PNA oligomers obtained in solution were precipitated by addition of cold diethyl ether and the PNA oligomers were dissolved

in de-ionized water. The 5(6)-carboxyfluorescein tagged PNA oligomers are listed in Table **4.1** that have been further used for cellular uptake studies.

TABLE 4.1: 5(6)-carboxyfluorescein tagged PNA oligomers

Entry	Sequence code	5(6)-CF tagged PNA oligomers	Monomers
1	aeg PNA**1-CF**	**CF**-GTAGATCACT-LysNH$_2$	
2	γ gem t^{2,6,10} PNA**5-CF**	**CF**-G**t**AGA**t**CAC**t**-LysNH$_2$	\nγ gem aeg PNA
3	γ pip t^6 PNA**7-CF**	**CF**-GTAGA**t**CACT-LysNH$_2$	\nγ 4-amino-4-pip aeg PNA
4	γ gem apg t^{2,6,10} PNA**16-CF**	**CF**-G**t**AGA**t**CAC**t**-LysNH$_2$	\nγ gem apg PNA

4.10.3 Purification and characterization of synthesized PNA oligomers

After cleavage from the solid support, fluorescently tagged PNA oligomers were purified by reverse phase high performance liquid chromatography (RP-HPLC).

The purification of PNA oligomers was carried out on a semi-preparative C18 column using a gradient system of acetonitrile and water. The purity of PNA oligomers was checked by reinjecting the sample on the same C18 semi-preparative column. All HPLC chromatograms are shown in **Appendix II**.

The integrity of these synthesized PNA oligomers was confirmed by MALDITOF mass spectrometry. 2,5-dihydroxybenzoic acid (DHB) was used as a matrix to record MALDI-TOF spectra for all synthesized PNA oligomers. The calculated and observed molecular weights for all PNAs with their molecular formulae and HPLC retention time in minutes are mentioned in Table **4.2**. The MALDI-TOF data for the confirmation of synthesis of tagged PNA oligomers are shown in **Appendix II**.

Table 4.2: Characterization of 5(6)-carboxyfluorescein tagged PNA oligomers

No.	PNA sequence code	Molecular formula	Calcd Mass	Obs. Mass	Retention Time(min)
1	aeg PNA**1-CF**	$C_{135}H_{159}N_{60}O_{37}$	3212.2405	3213.1282	28.16
2	γ gem t^{2,6,10} PNA**5-CF**	$C_{141}H_{171}N_{60}O_{37}$	3296.3344	3296.4160	30.2
3	γ pip t^6 PNA**7-CF**	$C_{139}H_{167}N_{60}O_{37}$	3282.3061	3282.1399	27.82
4	γ gem apg t^{2,6,10} PNA**16-CF**	$C_{144}H_{177}N_{60}O_{37}$	3338.3813	3339.1985	29.17

4.11 Cellular uptake studies

To gain an insight into the cell permeation abilities of these γ-C-substituted multifunctional PNA oligomers, the intracellular distribution of selected PNAs (Table **4.2**) were investigated in cell line MCF-7. The confocal microscopic technique was used to observe the cellular uptake of 5(6)- carboxyfluorescein tagged PNAs.

4.11.1 Cell lines used in study

MCF-7: MCF-7 is a human breast adenocarcinoma cell line and it was first isolated in 1970 from the breast tissue of 69 year old Caucasian woman. MCF-7 cells are useful for in vitro breast cancer studies because the cell line has retained several ideal characteristics particular to the mammary epithelium. These are estrogen receptor (ER) positive control cell lines due to the ability of these cells to process estrogen in the form of estradiol.

4.11.2 Cellular uptake experiment using confocal microscopy

1) MCF-7 cells were plated in 8-well chambered cover glass in 200μl Dulbecco's Modified Eagle Medium (DMEM) containing 10% Fetal Bovine Serum (FBS) at the concentration of $1.5X10^4$ to $2X10^4$ cells per well.

2) The cells were grown by maintaining at 37^oC in a humidified atmosphere containing 5% CO_2 for 12h. The required amounts of The required amounts of 5(6)-carboxyfluorescein tagged PNA were added to corresponding wells to achieve the desired final concentration of 2μM. The cells incubated with tagged PNA oligomers were maintained at 37^oC in a humidified atmosphere containing 5% CO_2 for 24h.

3) After 24h incubation the medium was aspirated and the cells were washed thrice with ice cold PBS. The cells were then replenished with 200μl of DMEM medium containing DAPI of 1μM concentration and incubated for 30minutes at 37^oC.

4) The excess nuclear stain DAPI was removed by washing thrice with cold PBS. Then fresh OPTIMEM medium was added to the cells and the cells were immediately visualized using 60 X objective of Zeiss LSM 710 laser scanning confocal microscope. The confocal microscopy imaging has been repeated at least twice for each PNA.

4.11.3 Observations of confocal microscopy images

Cellular permeability of tagged PNA oligomers has been monitored by confocal microscopy images using above said protocol for cell internalization. The results showed that all PNA oligomers including modified and unmodified PNAs can permeate the cell membrane. The green fluorescent signal for 5(6)-CF tagged PNA oligomers was found to be localized within the vicinity of the nucleus which was stained with DAPI giving blue color. The punctates observed for PNA oligomers in confocal images suggest that PNAs probably take the endocytotic route to get inside the cells. The pattern of all PNA oligomers getting inside the cells was almost similar irrespective of the modification incorporated in the PNA. Following are the results obtained after the incubation of PNA oligomers for 24 h in MCF-7 cell lines.

A) Cell permeation in MCF-7 cells

The relative uptake efficiency of the PNA oligomers by MCF-7 cell lines is shown in Figures **4.5-4.13**. The untreated control cells showed only the blue colored staining in the nucleus by nuclear DAPI stain and no green fluorescent signal for PNA internalization (**Figure 4.15**).
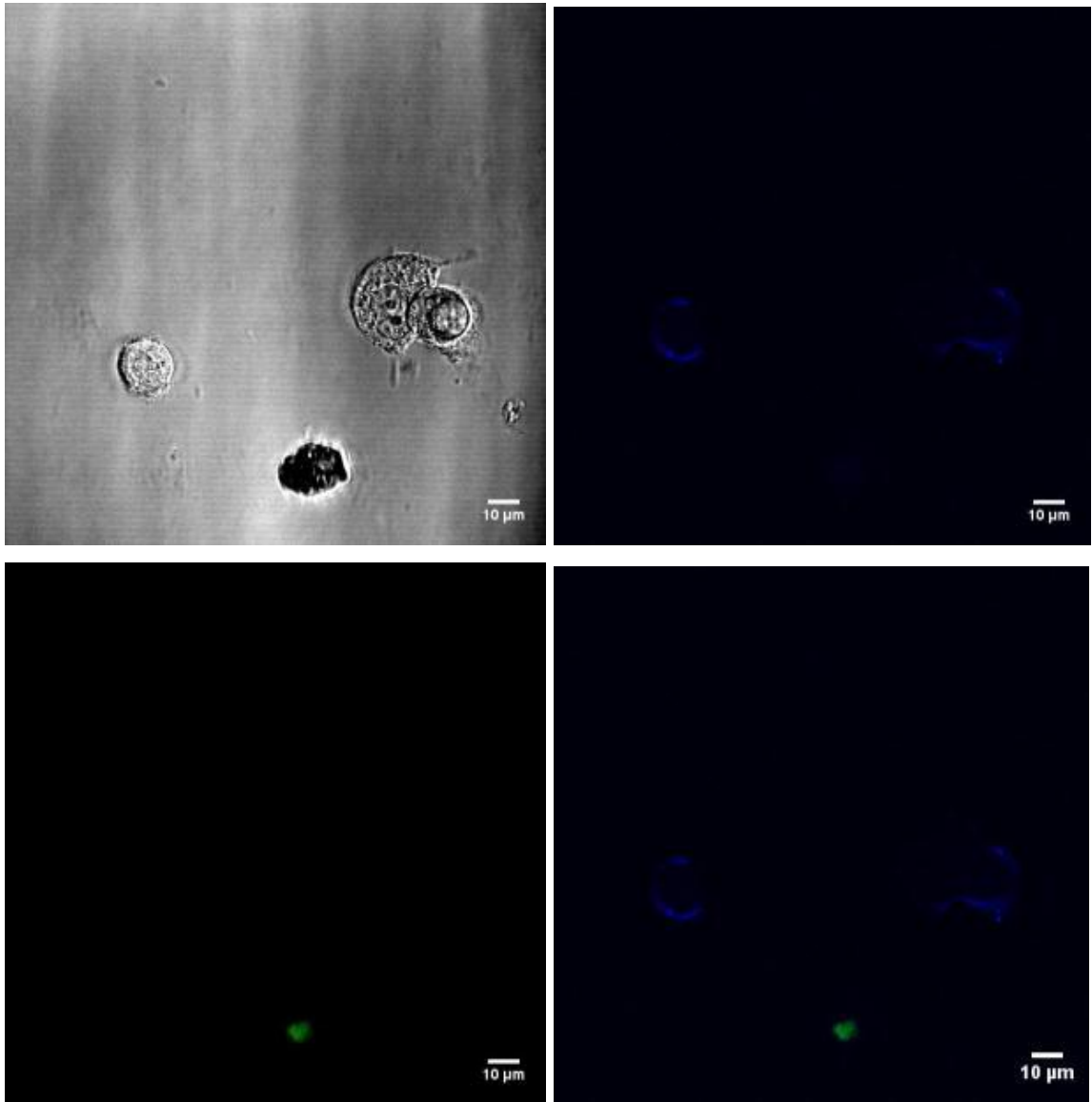

FIGURE 4.15 Confocal microscopy images for control untreated cells (a) Bright field image of MCF-7 cells (b) DAPI stained image (c) Green fluorescent image and (d) Superimposed image of images (a), (b) and (c)

The cell permeation of PNA oligomers can be confirmed by visualization of green fluorescence in the cell compartments. A more convincing evidence of the PNA uptake by cells comes from the superimposition of bright field image, fluorescent image and the DAPI stained image.
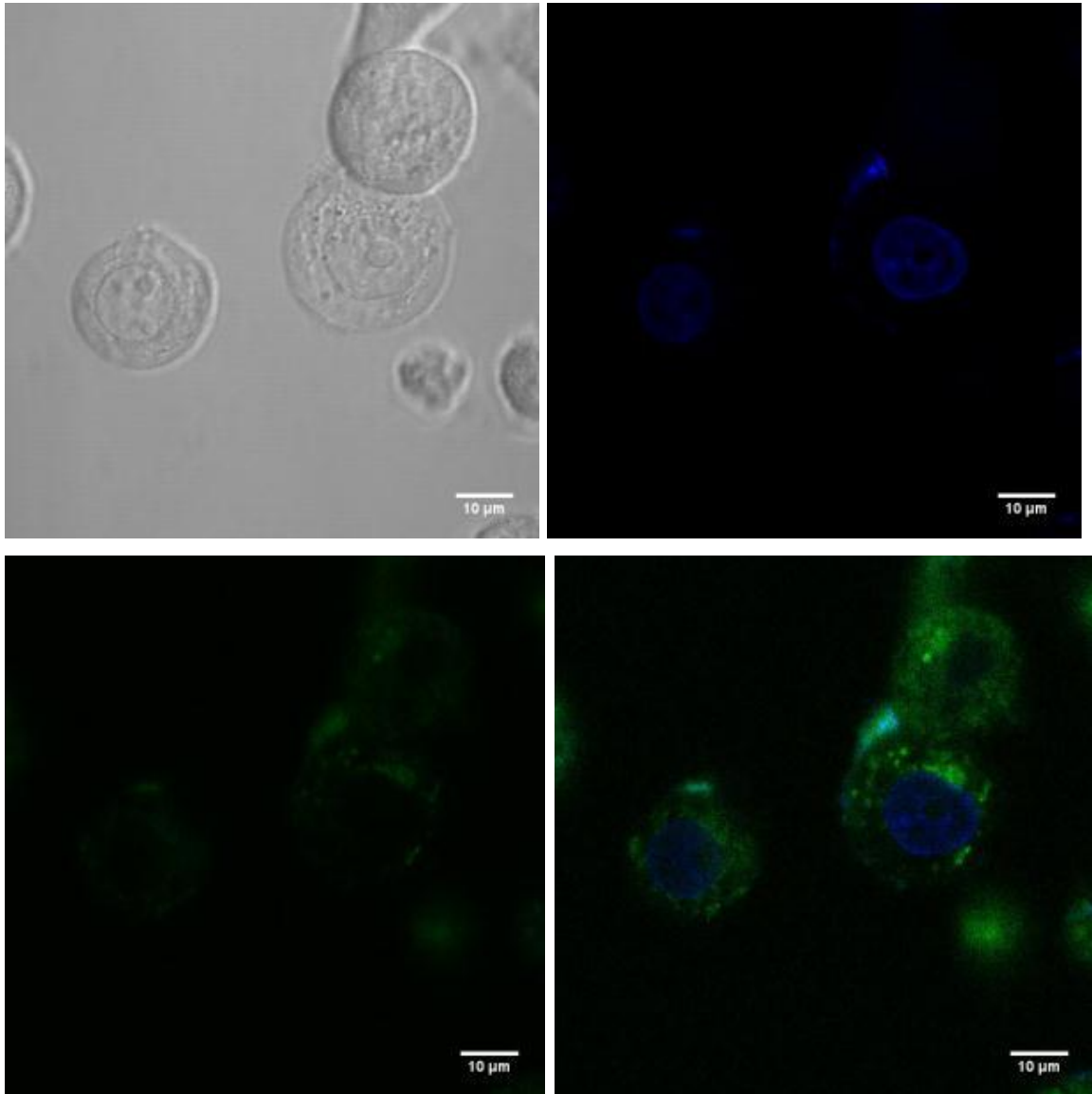

FIGURE 4.16 Confocal microscopy images for unmodified *aeg* PNA 1-CF (a) Bright field image of MCF-7 cells (b) DAPI stained image (c) Green fluorescent image and (d) Superimposed image of images (a), (b) and (c)

The cellular uptake of unmodified *aeg* PNA 1 and various amino, guanidino and azido modified PNA oligomers have been shown below (**Figures 4.16-4.19**). All images are organized in a similar way as shown in Figure **4.15 a**, **b**, **c** and **d**.
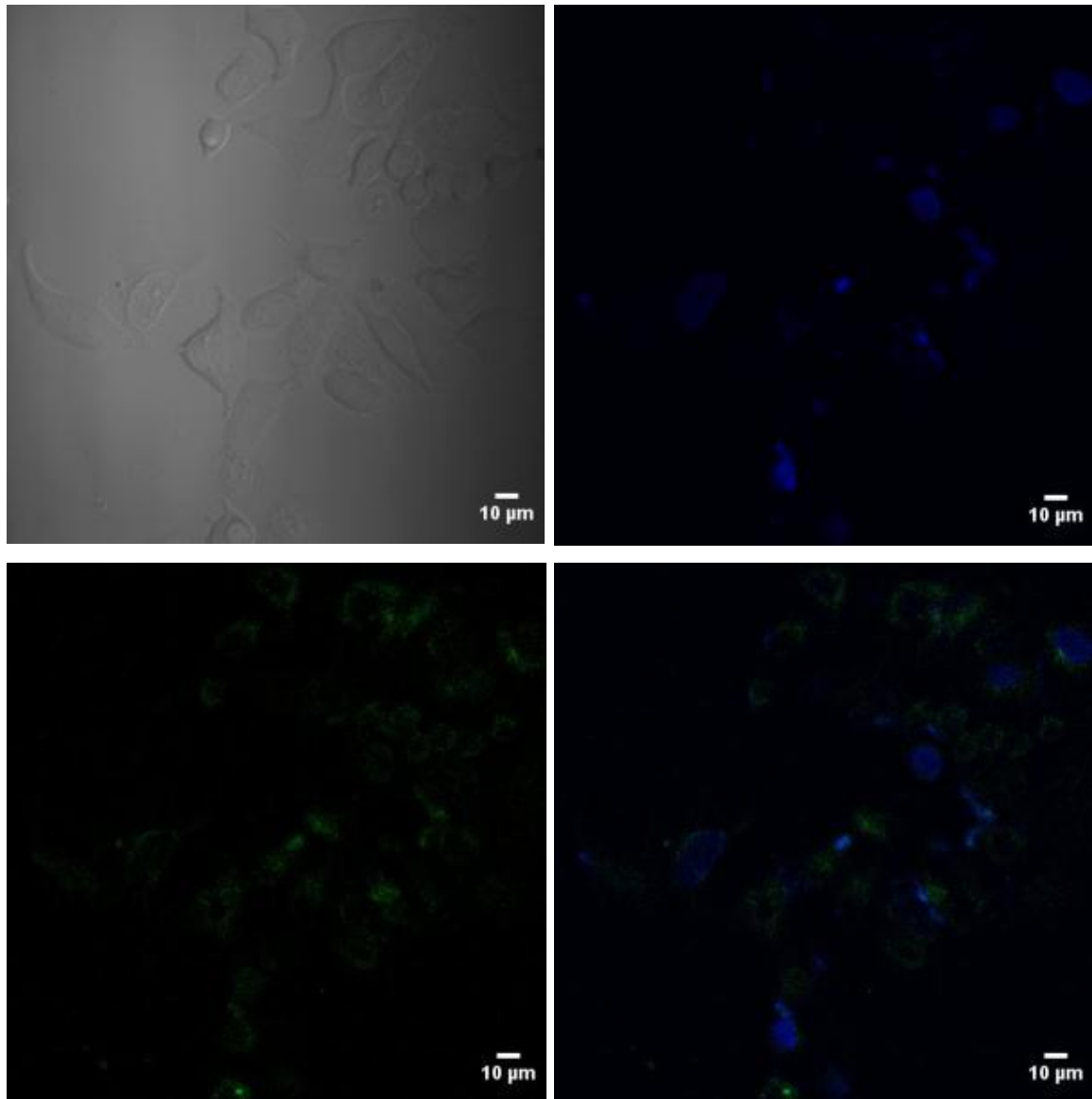

FIGURE 4.17 Confocal microscopy images for γ gem t^{2,6,10} PNA5-CF (a) Bright field image of MCF-7 cells (b) DAPI stained image (c) Green fluorescent image and (d) Superimposed image of images (b) and (c)
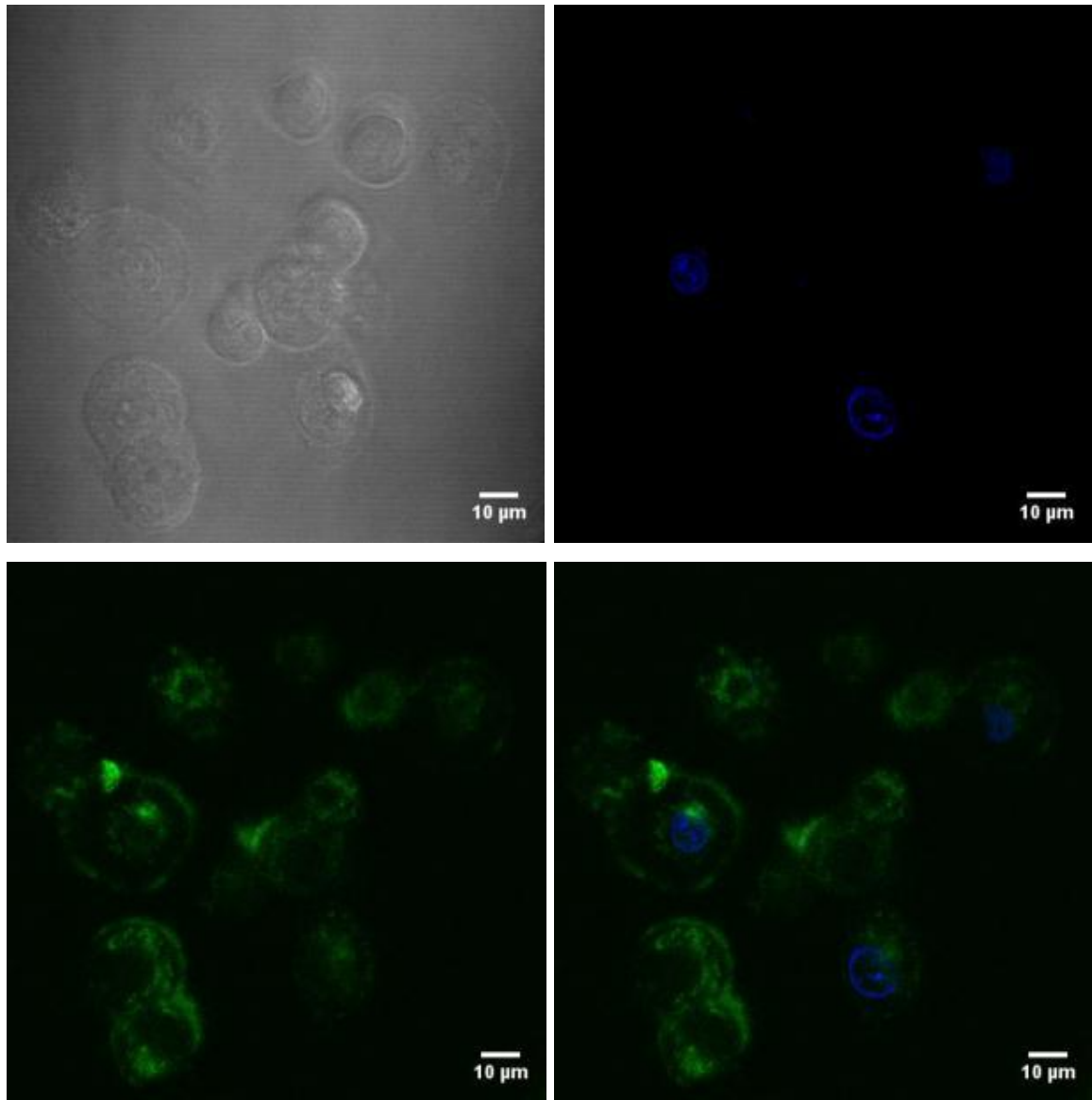
FIGURE 4.18 Confocal microscopy images for γ pip t^6 PNA7-CF (a) Bright field image of MCF-7 cells (b) DAPI stained image (c) Green fluorescent image and (d) Superimposed image of images (b) and (c)
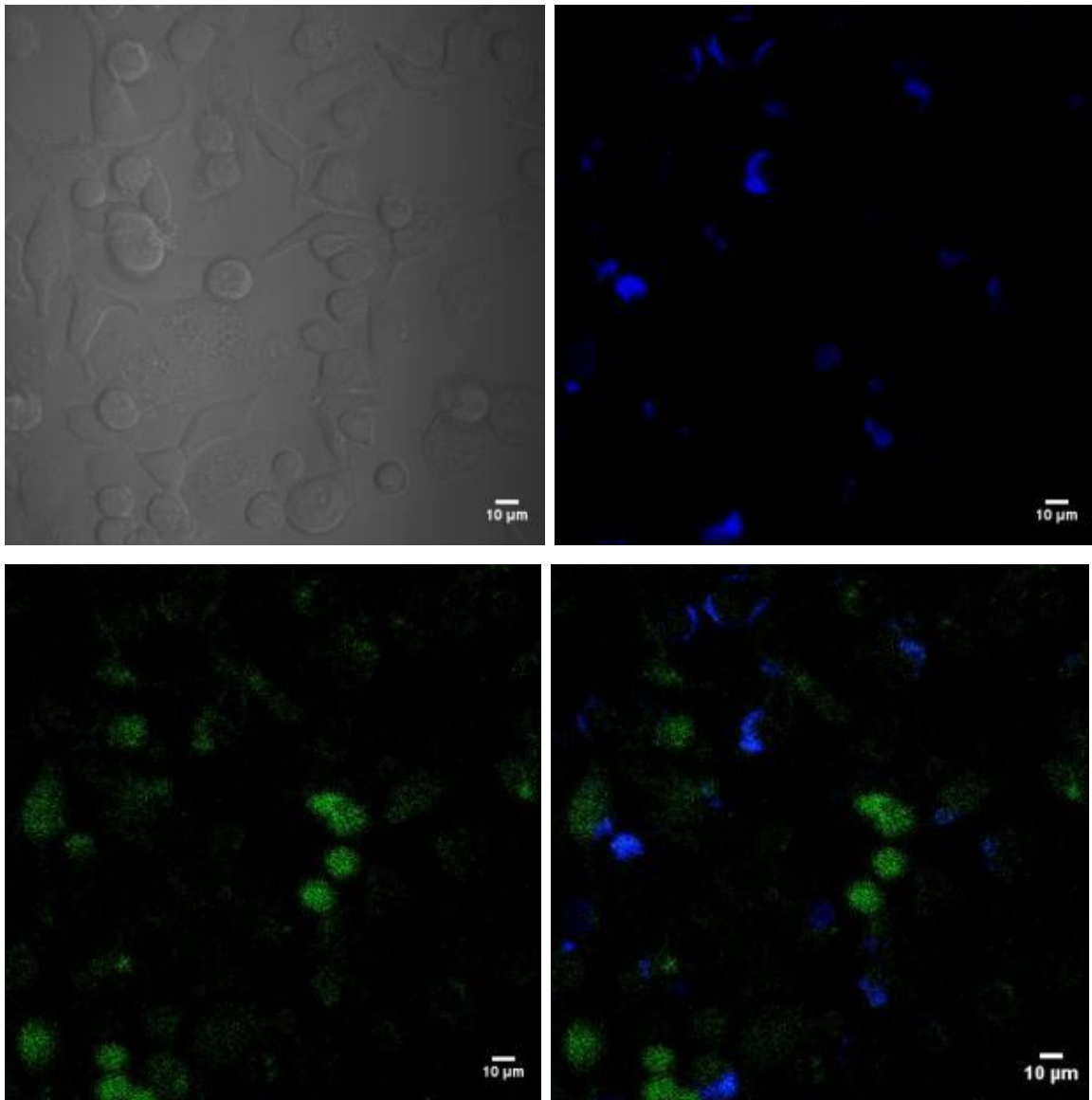
FIGURE 4.19 Confocal microscopy images for γ apg t^{2,6,10} PNA7-CF (a) Bright field image of MCF-7 cells (b) DAPI stained image (c) Green fluorescent image and (d) Superimposed image of images (b) and (c)

4.12 Quantitative estimation of cellular uptake

The confocal microscopy images showed that all PNA oligomers including modified and unmodified PNAs can penetrate the cell membrane and give fluorescent spots in the cytoplasm. It is important to quantify the cellular uptake of the different modified PNA

oligomers to differentiate their abilities of cell permeation. Quantification of cell permeation can be carried out using a Fluorescence Activated Cell Sorter (FACS) technique.

FACS is a specialized type of Flow cytometry which provides a method for sorting homogeneous as well as heterogeneous mixtures of cells based on the specific light scattering and fluorescent characteristics of each cell. FACS gives the quantitative recording of fluorescent signals from each individual cell as well as it provides important information about the positive and negative cells in terms of their fluorescent signal. The cells which give fluorescent signal are the positive cells whereas negative cells do not give any fluorescent signal. Thus, FACS data would provide quantitative estimation of cell permeability of all PNA oligomers which can be differentiated from their percent positive cells and mean fluorescence intensity.

4.13 Conclusions

➢ The confocal microsopy images clearly indicate that unmodified as well as modified PNA oligomers can penetrate into both cell lines used for the study.

➢ The PNA oligomers were observed to be localized in the vicinity of nucleus in the cytoplasm.

4.14 Experimental procedures

4.14.1 Tagging of PNA oligomers with 5(6)-carboxyfluorescein

5(6)-carboxyfluorescein, a fluorescent dye was attached to the N-terminal end of PNA oligomers. Using the solid phase peptide synthesis protocol, *Boc* group of final N-terminal amine was deprotected by 50 % TFA in DCM. The TFA salt generated after Boc-deprotection was neutralized using DIPEA as base to get free amine. The amine was coupled with 5(6) carboxyfluorescein (13.16 mg, 10 eq) using HOBt (4.72 mg, 10eq) and DIC (5.51 μL, 10 eq) in DMF as coupling reagents. The coupling reaction was completed within 12 h which was confirmed by Kaiser Test.

4.14.2 Cleavage of the PNA oligomers from the solid support

The resin beads were washed with methanol several times to remove excess 5(6)-carboxyfluorescein. The peptides were cleaved from the solid support using trifluoromethane sulfonic acid (TFMSA) in the presence of trifluoroacetic acid (TFA); (Low, High TFMSA-TFA method which is discussed in chapter 2) (section **2.2.5**). Thioanisole and ethanedithiol were used as scavengers in the cleavage protocol. This yielded PNA oligomers having L-lysine amide at C terminus and carboxyfluorescein attached at N-terminus. After cleavage reaction was over, the peptide was precipitated with cold dry ether. The peptide was isolated by centrifugation and the precipitate was dissolved in de-ionized water.

4.14.3 Purification of the fluorescently tagged PNA oligomers

PNA purification was carried out on Dionex ICS 3000 HPLC system. For the purification of peptides, semi-preparative BEH130 C18 (10X250 mm) column was used. Purification of PNA oligomers was performed with gradient elution method: A to100% B in 20 min; A= 0.1% TFA in CH3CN:H2O (5:95); B= 0.1% TFA in CH3CN:H2O (1:1) with flow rate of 3 mL/min. All the HPLC profiles were monitored at 254 and 490 nm wavelength.

4.15 References

1. Zamecnik, P. C.; Stephenson, M. L. *Proc. Natl. Acad. Sci. U.S.A.* **1978**, *75*, 1, 280-284.

2. Zamecnik, P. C.; Stephenson, M. L. *Proc. Natl. Acad. Sci. U.S.A.* **1978**, *75*, 1, 285-288.

3. Mesmaeker, A. D.; Haner, R.; Martin, P.; Moser, h. E. *Acc. Chem. Res.* **1995**, *28*, 366-374.

4. (a) Uhlmann, E.; Peyman, A. *Chem. Rev.* **1990**, *90*, 543-584. (b) Wengel, J. *Acc. Chem. Res.* **1999**, *32*, 301–310. (c) Nielsen, P. E. *Acc. Chem. Res.* **1999**, *32*, 624-630.

5. Uhlmann, E.; Peyman, A. *Chem. Rev.* **1990**, *90*, 543-584.

6. Bayard, B.; Leserman, L. D.; Bisbal, C.; Lebleu, B. *Eur. J. Biochem.* **1985**, *151*, 319-325.

7. Bisbal, C.; Silhol, M.; Lemaitre, M.; Bayard, B.; Salehzada, T.; lebleu, B. *Biochemistry* **1987**, *26*, 5172-5178.

8. (a) Juliano, R. L.; Yoon, H. *Curr. Opin. Mol. Therap.* **2000**, *2*, 297-303. (b) Lebedeva, I.; Benimetskaya, L.; Stein, C. A.; Vilenchik, M. *Eur. J. Pharm.Biopharm* **2000**, *50*, 101-119.

9. Stein, C. A. *Nat. Biotechnol.* **1999**, *17*, 209.

10. Demidov, V.; Potaman, V. N.; Franck-Kamenetskii, M. D.; Egholm, M.; Buchardt, O.; Sonnichsen, S. H.; Nielsen, P. E. *Biochem. Pharmacol.* **1994**, *48*, 1309-1313.

11. Bonham, M. A.; Brown, S.; Boyd, A. L.; Brown, P. H.; Bruckenstein, D. A.; Hanvey, J. C.; Thomson, S. A.; Pipe, A.; Hassman, F.; Bisi, J. E.; Froehler, B. C.; Matteucci, M. D.; Wagner, R. W.; Noble, S. A.; Babiss, L. E. *Nucleic Acids Res.***1995**, *23*, 1197-1203.

12. Koppelhus, U.; Nielsen, P. E. *Adv. Drug Delivery Rev.* **2003**, *55*, 267-280.

13. Ljungstrøm, T.; Knudsen, H.; Nielsen, P. E. *Bioconjugate Chem.* **1999**, *10*, 965-972.

14. (a) Muratovska, A.; Lightowlers, R. N.; Taylor, R. W.; Turnbull, D. M.; Smith, R. A. J.; Wilce, J. A.; Martin, S. W.; Murphy, M. P. *Nucleic Acids Res.* **2001**, *29*, 6, 1852-1863. (b) Geall, A.J.; Taylor, R. J.; Earll, M. E.; Eaton, M. A. W.; Blagbrough, I. S. *Bioconjugate Chem.* **2000**, *11*, 314-326. (c) Shiraishi, T.; Nielsen, P. E.; *Bioconjugate Chem.* **2012**, *23*, 196-202. (d) Zhilina, Z. V.; Ziemba, A. J.; Ebbinghaus, S. W. *Curr. Top. Med. Chem.* **2005**, *5*, 1119-1131.

15. Fisher, A. A.; Sergueev, D.; Fisher, M.; shaw, B. R.; Juliano, R. L. *Pharmaceutical Res.* **2002**, *19*, 6, 744-754.

16. (a) Pooga, M.; Soomets, U.; Hallbrink, M.; Valkna, A.; Saar, K.; Rezaei, K.; Kahl, U.; Hao, j. X.; Xu, X. J.; Hallin, Z. W.; Hokfelt, T.; Bartfai, T.; Langel, U. *Nat. Biotechnol.* **1998**, *16*, 857-861. (b) Cutrona, G.; Carpaneto, E. M.; Ulivi, M.; roncella, S.; Landt, O.; Ferrarini, M.; Boffa, L. C. *Nat. Biotechnol.* **2000**, *18*, 300-303.

17. Basu, S.; Wickstrom, E. *Bioconjugate Chem.* **1997**, *8*, 481-488.
18. Zhang, X.; Simmons, C. G.; Corey, D. R. *Bioorg. Med. Chem. Lett.* **2001**, *11*, 1269-1272.
19. CPPsite: a website for cell penetrating peptides. crdd.osdd.net/raghava/cppsite/help .php
20. (a) Minsky, M. *Scanning*, **1998**, *10*, 128-138. (b) Minsky, M. US patent 3013467, 12 Dec **1961**
21. http://emu.uct.ac.za/training/intro-to-electron-microscopy-for-biologists/confocal-laser-scanning-microscopy/
22. Morgan, D. M. L.; Larvin, V. L.; Pearson, J. D. *J. Cell Sci.* **1989**, *94*, 553-559.
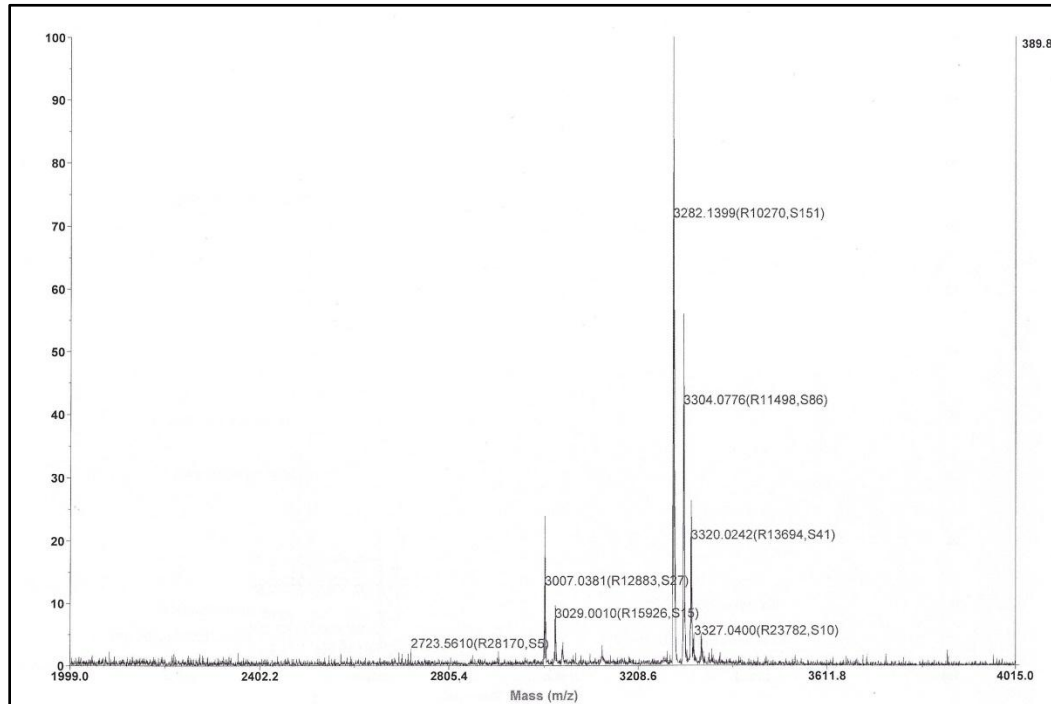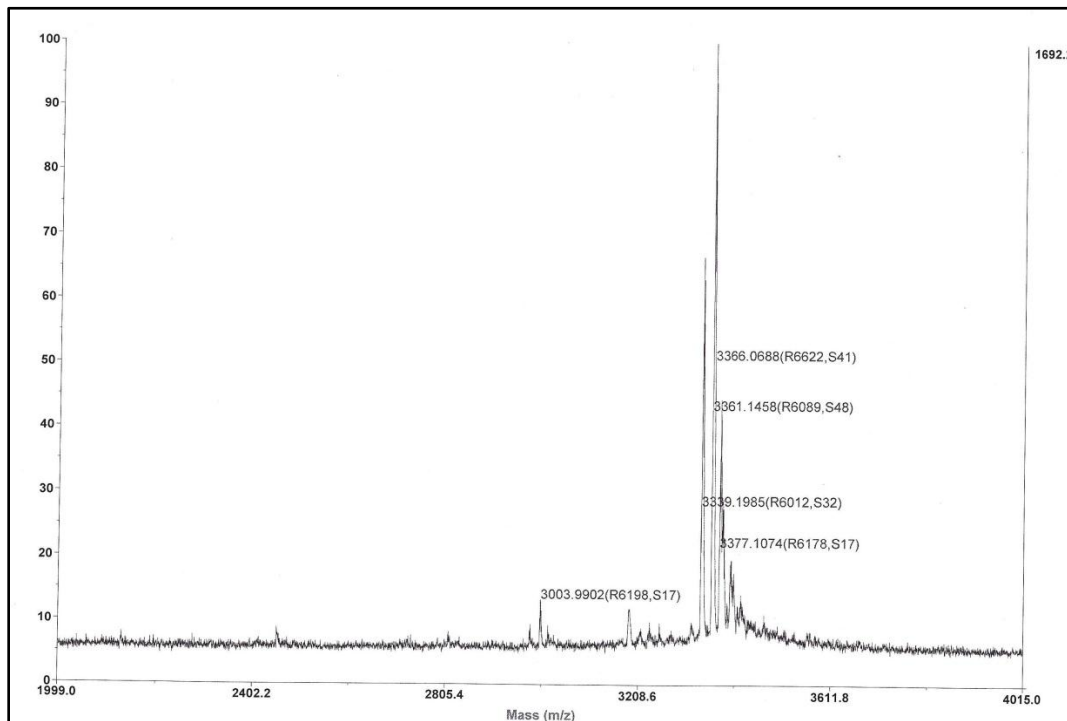
4.16 Appendix II
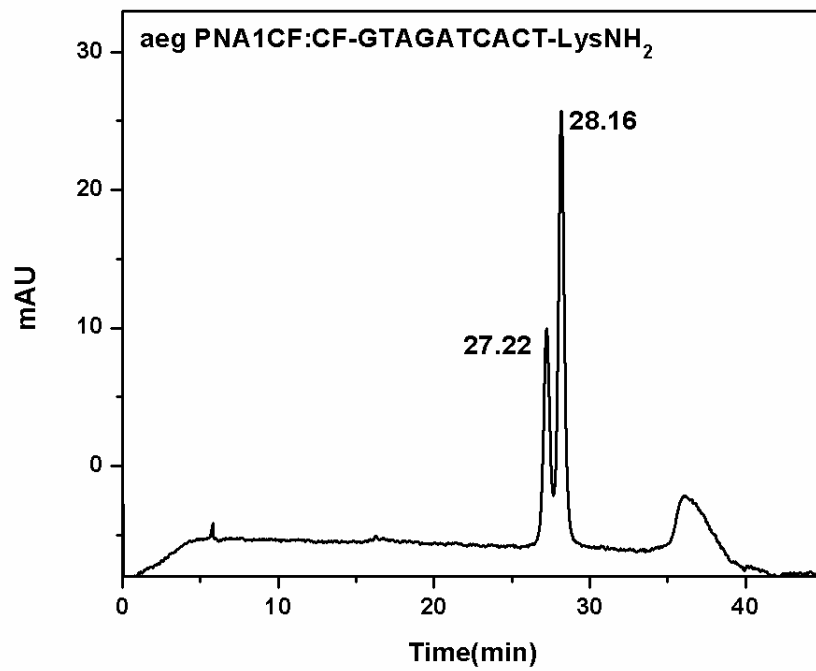
MALDI-TOF of PNA1-CF:
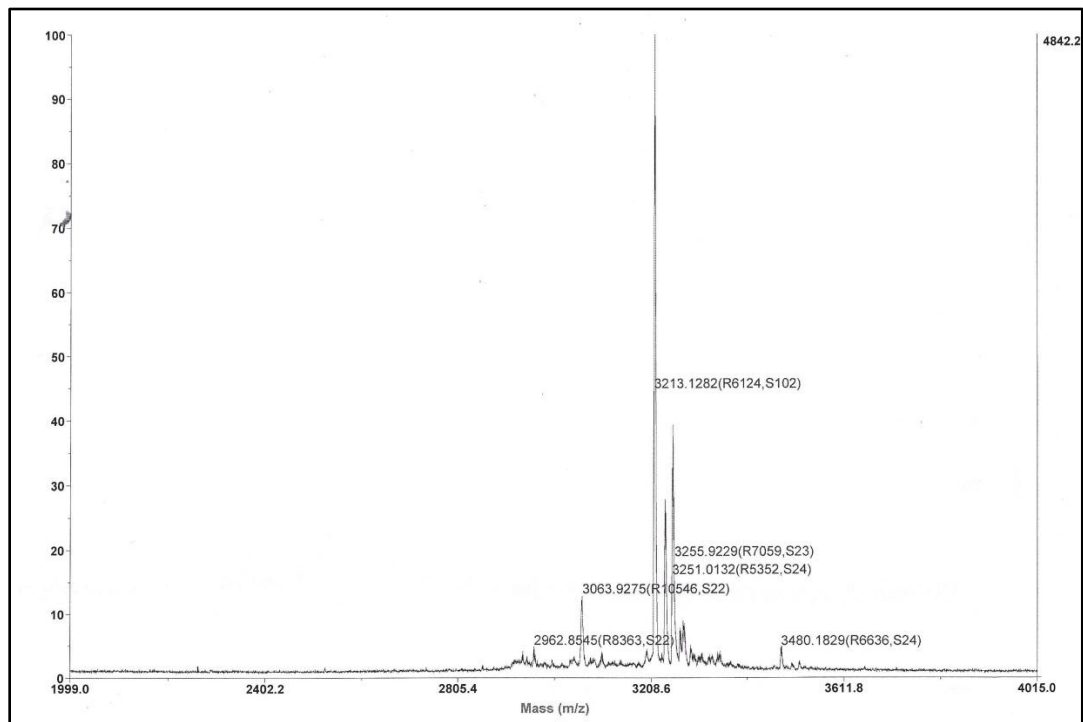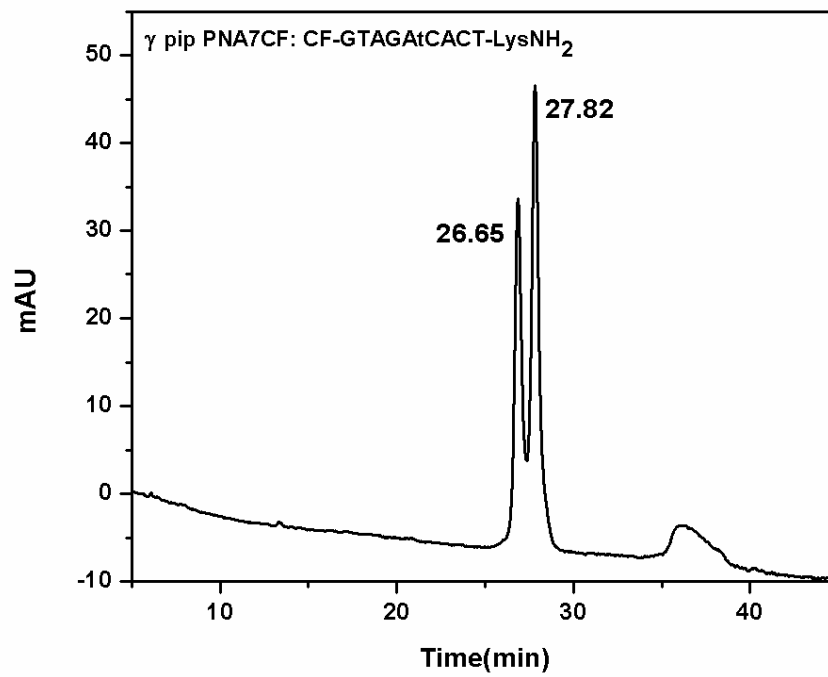

MALDI-TOF of PNA 5-CF:
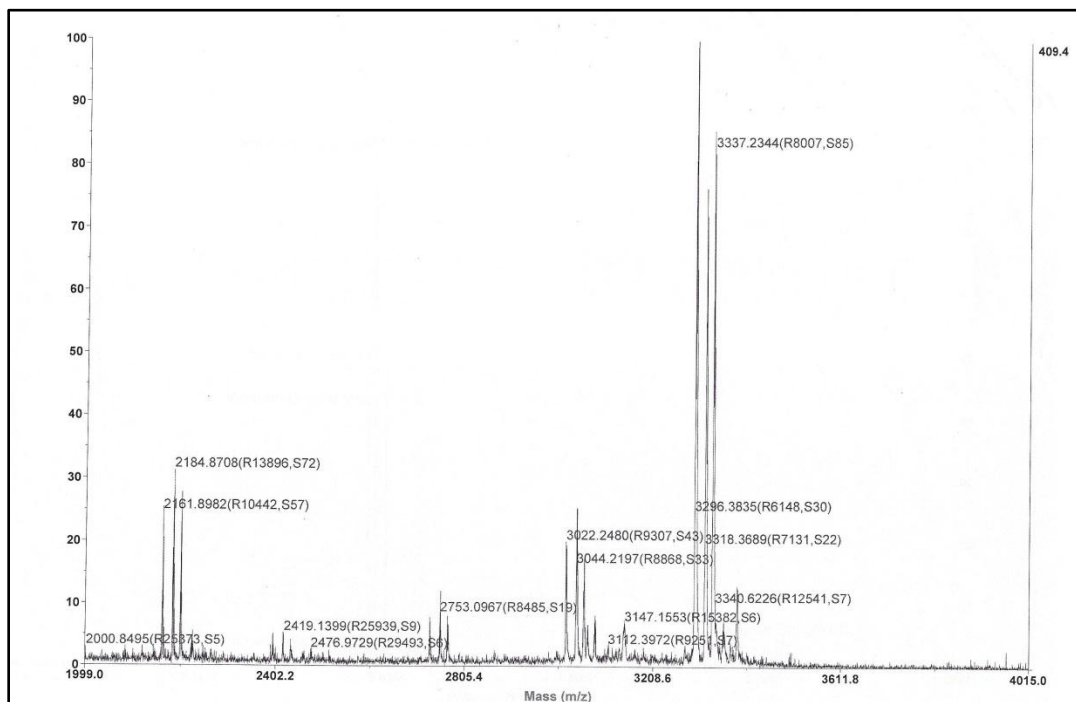
MALDI-TOF of PNA 7-CF:

MALDI-TOF of PNA 16-CF:

HPLC Trace of PNA 1-CF:

HPLC Trace of PNA 7-CF:

HPLC Trace of PNA 16-CF: